ANALYTICAL INVESTIGATIONS OF ELECTROMAGNETIC LOCATION SCHEMES RELEVANT TO MINE RESCUE

PART I - EXECUTIVE SUMMARY

Prepared by David A. Hill
Institute for Telecommunication Sciences
Office of Telecommunications
U.S. Department of Commerce
Boulder, Colorado 80302

PART II - COLLECTED REPRINTS - ANALYTICAL INVESTIGATIONS OF ELECTROMAGNETIC LOCATION SCHEMES RELEVANT TO MINE RESCUE

Prepared by James R. Wait
Cooperative Institute for Research in Environmental Sciences
University of Colorado/National Oceanic and Atmospheric Administration
Environmental Research Laboratories
U.S. Department of Commerce
Boulder, Colorado 80302

2 December 1974

Summary Report, Contract H0122061

Prepared for

Bureau of Mines
Pittsburgh Mining & Safety Research Center
U.S. Bureau of Mines
4800 Forbes Avenue
Pittsburgh, PA 15213

ANALYTICAL INVESTIGATIONS OF ELECTROMAGNETIC LOCATION SCHEMES RELEVANT TO MINE RESCUE AND EMERGENCY COMMUNICATIONS

Preface

This document consists of an executive summary and a reprinted collection of publications that have emanated from the U.S. Bureau of Mines Contract No. H0122061 with the Institute of Telecommunications Sciences of the Office of Telecommunications. Most of the material is based on preliminary reports that were submitted during this phase of the contract period (1971-1974). The Bureau of Mines contract monitors have been Howard Parkinson and Dr. James A. Powell of the Pittsburgh Mining and Safety Research Center. Valuable guidance was also received from John D. Murphy, Research Supervisor in Pittsburgh. Also, we are grateful to the National Oceanic and Atmospheric Administration and the Office of Telecommunications of the U.S. Department of Commerce who helped support this research.

It is stressed that these publications do not represent the official policy of the U.S. Bureau of Mines or any other agency of the U.S. Government.

ANALYTICAL INVESTIGATIONS OF ELECTROMAGNETIC LOCATION SCHEMES RELEVANT TO MINE RESCUE

PART I - EXECUTIVE SUMMARY

Prepared by D.A. Hill

ABSTRACT - *This volume contains a summary of the results of past analyses on U.S. Bureau of Mines Contract No. H0122061 which are relevant to electromagnetic location in mine rescue situations. The analytical results indicated that detection of a trapped miner equipped with a special transmitter is feasible in most situations. Location of the miner by surface measurements is also generally feasible within certain errors. The feasibility of miner detection and the accuracy of miner location have been examined theoretically for a wide variety of situations. Agreement with experimental results is generally good in cases where measurements are available.*

Personnel involved in the investigation include J.R. Wait (Principal Investigator), D.A. Hill (Co-Principal Investigator), K.P. Spies, A.Q. Howard, and Lana Slusher (Administrative Assistant).

TABLE OF CONTENTS

1. INTRODUCTION

The purpose of this report is to organize and summarize the results and conclusions of past analytical investigations of electromagnetic location schemes which are relevant to mine rescue. Mathematical details are included in Part II that contains a complete collection of reprints of publications which have emanated from U.S. Bureau of Mines Contract No. H0122061. References to these specific publications are identified by an asterisk whenever they appear in Part I.

For convenience, the contents of Part I have been organized according to the antenna types, sources, and geometries involved. However, the possible application of the specific configuration to electromagnetic location is discussed in each case. Also, related application of the analytical results by other investigators to electromagnetic location is included wherever appropriate. Location here is defined in the broad sense so that electromagnetic detection and through-the-earth communications are also applications which are included. A brief review of analytical techniques related to propagation in the earth was recently given by Wait (1974*).

2. CW TRANSMISSION WITH LOOP ANTENNAS

Transmitting antennas that have proved successful in location tests have consisted of either single turn or multiple turn loops usually deployed in a horizontal plane on mine floors. Normally, the loop is sufficiently small that it can be treated as a magnetic dipole. The magnetic moment is NIA where N is the number of turns, I is the loop current, and A is the loop area.

2.1 Horizontal Loop (Vertical Magnetic Dipole)

The null location method utilizes a loop antenna which is deployed by the miner in the horizontal plane and excited by a CW transmitter at a relatively low frequency. As shown in Fig. 1, a null in the horizontal magnetic field exists directly above the transmitting loops. A small loop receiving antenna can be used to search for the null at the earth's surface, and the performance of an actual system has been evaluated experimentally in both coal and hardrock mines (Large et al, 1973; Farstad, 1973a; Olsen and Farstad, 1973). Essentially the same method has also been used to survey underground quarries (Gabillard et al, 1973).

2.1.1 Homogeneous Earth

The surface magnetic fields of a small buried horizontal loop (vertical magnetic dipole) have been examined analytically by Wait (1971a*,b*) for a homogeneous half-space model of the earth. He has shown that the location of the loop can be determined from the complex ratio of the horizontal to vertical magnetic field at a point on the surface provided that the frequency is sufficiently low that the fields have a static-like behavior. Even if the usual null search were used, the information contained in the complex ratio might be useful in reducing the time required in the search for the null in the horizontal magnetic field. The above formulation and numerical results can also be applied to downlink transmission by application of reciprocity.

Although the transmitted field strength is normally computed for a specified loop current I, the power required to maintain the specified current is also of importance. In order to calculate the required power, the input impedance of the loop is required. Wait and Spies (1973a*) have calculated the input impedance of a loop above a homogeneous earth and related this impedance to the power requirements for a downlink communication system.

2.1.2 Two-Layer Earth

Wait and Spies (1971a*) have also considered the effect of earth layering on the location configuration in Fig. 1 by computing the complex magnetic field ratio at the surface when the vertical magnetic dipole is located in a two-layer earth. The null in the horizontal magnetic field is unaffected, but the structure of the fields away from the null is considerably modified unless the frequency is sufficiently low.

2.2 Vertical Loop (Horizontal Magnetic Dipole)

Wait (1972a*) has also considered the surface magnetic fields of a buried vertical loop (horizontal magnetic dipole). The primary advantage of the horizontal magnetic dipole in location is that the overhead null occurs in the vertical rather than the horizontal magnetic field as shown in Fig. 2. Consequently, the atmospheric noise which has a smaller vertical component is less of a problem. The disadvantages of a horizontal magnetic dipole are that the surface null is a line rather than a point and that a vertical loop configuration may be more difficult for a trapped miner to implement (Farstad, 1973b).

Another reason that the analytical solution for the horizontal magnetic dipole is useful is that it can be combined with the vertical magnetic dipole solution to yield the solution for a magnetic dipole at an arbitrary orientation with respect to the earth surface. Consequently, the effect of a tilted tunnel or earth surface on location can be estimated. Such effects have been examined both analytically and experimentally by Olsen and Farstad (1973).

3. CW TRANSMISSION WITH LINEAR ANTENNAS

The horizontal wire antenna has been shown experimentally to be effective for both downlink (Geyer, 1973; Olsen and Farstad, 1973) and uplink (Farstad, 1973c) transmission. One disadvantage of the horizontal wire antenna is that some type of grounding is required at the ends in order to allow sufficient current flow. However, Farstad (1973c) has successfully demonstrated the use of roof bolts for grounding in uplink transmission.

3.1 Infinite Line Source

The two-dimensional infinite line source model has analytical advantages over the more realistic finite line source considered later. The two-dimensional model is valid when the wire is sufficiently long and the observer is not located near either end.

3.1.1 Flat Homogeneous Earth

The subsurface fields of a line source on a homogeneous half space have been analyzed by Wait and Spies (1971b*), and numerical values have been computed for a wide range of parameters. The complex ratio of the vertical to horizontal magnetic field has been shown to be diagnostic of the position of the receiver relative to the source. A location scheme involving two line sources, one with variable excitation, has been described by Wait (1971c*). By changing one line current, a null in the vertical magnetic field can be swept through the earth. Where the miner detects a null in the vertical field, he signals to the surface. Such signaling could perhaps be done seismically by a hammer blow.

3.1.2 Two-Layer Earth

The subsurface fields of a line over a two-layer earth have also been analyzed by Wait and Spies (1973b). The numerical calculations reveal that the subsurface field structure can be considerably modified by the layering.

3.1.3 Curved Earth

The feature of a curved earth has been treated analytically (Wait, 1971d; Wait and Wilkerson, 1972) by treating the problem of radiation of a line source at the surface of a circular cylinder. The radius of the cylinder is chosen to match the radius of curvature of the local topography. The calculations indicate that small curvatures have little effect on the subsurface fields, but that large curvature affects both field structures and magnitudes.

3.2 Finite Length Line Source

In order to handle the finite length line source analytically, the antenna is subdivided into short pieces, and the total fields are summed numerically. The antenna is assumed to carry constant current which is normally a valid assumption for insulated antennas grounded at the ends.

3.2.1 Downlink Transmission

The formulation of the subsurface magnetic field has been simplified for efficient computation for the case of a line source located on the surface of a homogeneous half-space (Hill and Wait, 1973a*). Calculations reveal that for a cable length roughly twice the observer depth, the fields below the cable center are essentially those of an infinite line source. This has an important practical implication in that nothing is to be gained in field strength by making the cable longer. However, a longer cable will result in greater volume coverage. The subsurface electric fields of the same configurations have also been computed (Hill and Wait, 1973b*). The electric fields are important when reception is with a grounded cable rather than a loop (Geyer, 1973).

3.2.2 Uplink Transmission

The horizontal wire antenna has also been shown to be useful in uplink transmission where roof bolts can sometimes provide convenient grounding points. In order to account for possible tilts in either the tunnel or the earth surface, the case of a tilted finite line source as shown in Fig. 3 has been analyzed (Hill, 1973a*). Calculations of the magnetic field components at the surface were made for a wide variety of parameters. These are the components of interest in miner detection and location when small loops are used for reception. Measurements by Farstad (1973c) for a horizontal wire in a hardrock mine have demonstrated good signal detection for antenna depths greater than 3000 ft. In fact, the location of the overhead null in the vertical field, that may be useful in location, was also shown to be feasible in rough terrain. Calculations indicate that the infinite wire result is not reached until the cable length is several times greater than the cable depth. Thus, the cable should generally be made as long as possible to achieve maximum signal strength.

4. PULSE TRANSMISSION WITH LOOP ANTENNAS

It is also possible to pulse or shock excite a loop antenna for use in electromagnetic location. In this case the loop current is a pulse waveform rather than a CW or time-harmonic waveform. The transmitter could be a single battery-switch combination or a more sophisticated waveform generator.

4.1 Horizontal Loop

The geometry of interest in location is the same as that shown in Fig. 1 for the buried transmitting loop. An overhead null exists in the horizontal magnetic field as it did in the CW case, and a pulse system has been tested using the null technique (Sturgill, 1973). However, the waveshape distortion which occurs in propagation to the surface contains information on the loop location including the depth. No experimental attempt has yet been made to utilize the waveshape information. The remainder of this chapter summarizes the analytical results available. All the results assume a homogeneous half-space model for the earth and an earth conductivity which is independent of frequency.

4.1.1 Vertical Magnetic Dipole

As in the CW case, the solution simplifies when the loop is sufficiently small to be treated as a magnetic dipole. The case of an impulsive or delta function loop current was treated first (Wait and Hill, 1971*) because it is the most basic transient excitation. Calculations of the vertical and horizontal magnetic field waveforms at the surface were performed for a wide variety of parameters. It was shown that the waveshapes contain information on the loop location and that a knowledge of earth conductivity is an aid in interpreting the waveshape information. Similar results for step-function excitation have been obtained by integration of the impulse response (Wait and Hill, 1972a*). These waveforms contain an equal amount of location information. An exponential excitation is also of interest since it is the current waveform which results from discharge of a capacitor into a resistive loop. Responses for exponential excitation have been obtained from impulse responses by convolution (Wait and Hill, 1972b*). The waveshapes are influenced by the time constant of the exponential, but the location information is preserved.

The possibility of passive detection and location has also been analyzed for the configuration shown in Fig. 4 (Hill and Wait, 1973c*). The transmitting loop at the surface sends out a pulse which excites a current in the scattering loop which is set up by the trapped miner. This current reradiates, and the receiving loop (or loops) at the surface hopefully detects this reradiated field. Calculations reveal that the reradiated signal contains location information but is of very low strength. A more practical system might allow the miner to modulate the loop impedance in some manner while some sophisticated signal processing is employed at the surface to increase the signal to noise ratio. This idea has never been explored theoretically or experimentally, but there still appears to be some interest in passive detection (Farstad, 1973b). The obvious advantage is that no power is required by the miner.

4.1.2 Finite Size Loop

It is often desirable to make the transmitting loop quite large in order to increase signal strength, particularly in the downlink case where a large area is normally available. In such cases, the usual magnetic dipole approximation may not be valid and the finite loop must be taken into consideration. Calculations of the transient magnetic fields (both uplink and downlink configurations) have been made for various size loops by Wait and Hill (1972c*). In general, the response waveforms are more spread out and less peaked as the loop size is increased.

4.2 Vertical Loop (Horizontal Magnetic Dipole)

As in the CW case, there are two main reasons for analyzing the pulsed horizontal magnetic dipole. First, it may be a useful source for location because it has an overhead null in the vertical magnetic field for which atmospheric noise is less of a problem. Second, the solution can be combined with that of the vertical magnetic dipole to yield the solution for a magnetic dipole at an arbitrary angle to the earth-air interface. The configuration which has been analyzed (Hill, 1973b*) is that shown in Fig. 2, and the loop current was an impulse. The surface magnetic field waveforms were computed and were found to contain information on loop location.

5. PULSE TRANSMISSION WITH LINEAR ANTENNAS

As with loops, only a small amount of experimental data is available for transmission of pulses with horizontal wire antennas (Geyer, 1973). In this chapter we summarize the limited analytical results available for downlink transmission of pulses with line sources. Similar results could be obtained for uplink transmission if the information becomes necessary.

5.1 Infinite Line Source

The simplified two-dimensional model of an infinite line source on a homogeneous half-space has been analyzed by Hill and Wait (1974a*). The subsurface electric and magnetic field waveforms were computed for an impulsive source current, and the waveforms were generally found to be stretched out and attenuated as the observer moves away from the source. If desired, results for other current waveforms could be obtained by convolution.

5.2 Finite-Length Line Source

A finite-length line source on a homogeneous half-space has also been considered (Hill and Wait, 1973b*). The subsurface electric field components were calculated for a step-function current. The horizontal electric field

corresponds to the component measured by Geyer (1973) with a grounded cable receiver, and at least quantitative agreement was obtained for the waveshape.

6. SCATTERING BY OBSTACLES

Generally the overburden is not homogeneous, and inhomogeneities can distort fields and cause errors in source location. Layered earth models which were mentioned earlier mainly provide insight into field strength effects. Such models provide no prediction in source location errors because their horizontal uniformity does not produce any shift in the overhead null. To examine source location errors, models which are nonuniform in at least one horizontal direction are required.

6.1 Two-Dimensional Geometry

Even two-dimensional geometries can be quite complicated analytically because of the effect of the air-earth interface on the scattering by a cylindrical inhomogeniety. A problem which has been successfully treated by Wait (1972b*) and Howard (1972*) using different methods is illustrated in Fig. 5. A line source is located at the surface, and a circular cylindrical inhomogeniety (which could represent a pipe, rail, or elongated ore body) causes a distortion of the subsurface field. Such distortion could affect the feasibility of the location scheme outlined by Wait and Spies (1971b*) which relies on the complex ratio of the vertical to horizontal magnetic field to determine position. The solutions of Wait (1972b*) and Howard (1972*) agree quite closely in a common range of validity, and their numerical results indicate significant location errors for certain ranges of parameters.

6.2 Three-Dimensional Geometry

Three-dimensional geometries are of such complexity that either an approximate or a highly numerical treatment is required. A given configuration can be made three-dimensional by the introduction of a finite source (such as a magnetic dipole) even though the inhomogeneity may be two-dimensional (such as a long pipe). For example, Stoyer (1974) has recently treated the effect of a half-layer on the fields of a buried vertical magnetic dipole. The geometry is shown in Fig. 6, and the fields are three-dimensional even though the overburden is two-dimensional. Stoyer's calculations reveal that significant location errors can occur unless the dipole is located far away from the layer boundary. The remainder of this chapter will deal with various approximate techniques applied to a number of different inhomogenieties.

6.2.1 Cylindrical Obstacle

The effect of an infinite circular cylinder on the surface magnetic fields of a buried vertical magnetic dipole has been examined by Hill and Wait (1973, d*). The geometry is as shown in Fig. 7. The conductivity of the cylinder is arbitrary, but the frequency is assumed to be sufficiently low that currents in the overburden can be neglected. Calculations reveal that significant location errors can result if the cylinder is sufficiently close to the interface. A rather complicated treatment of the problem which considers overburden currents and the air-earth interface effect has been presented by Howard (1973).

The effect of a finite-length cylinder has also been considered in an approximate treatment. The geometry is similar to that of Fig. 7 except that the infinite cylinder is now of finite length and the small loop source is replaced by either a finite-length line source (Wait and Hill, 1973*) or a long narrow loop (Hill and Wait, 1972*). Calculations again reveal significant location errors when the cylinder is near the surface. Also, the calculations reveal that the cylinder must be extremely long before the results approach those of an infinite cylinder.

6.2.2 Spherical Obstacle

The effect of a spherical obstacle (such as an ore zone) on the surface magnetic fields of a buried vertical magnetic dipole has also been examined (Hill and Wait, 1973e*), and overburden currents are included in the treatment. The geometry is the same as that in Fig. 7 except that the cylinder is replaced by a sphere. The calculations reveal that location errors caused by small spheres are small.

The above treatment has been specifically applied to the calculation of the the shift in the null of the horizontal magnetic field when the sphere is near the surface (Hill, 1974*). Such a treatment could apply to man-made obstacles such as vehicles or machinery. The calculations reveal some secondary nulls in some cases, but the null shifts are still small for vehicle-size obstacles. Farstad (1973c) has observed experimentally that the presence of a van has only a very localized effect on the surface magnetic fields.

6.2.3 Prolate Spheroidal Obstacle

The effect of a prolate spheroidal obstacle on the surface magnetic fields of a buried vertical magnetic dipole has also been examined (Hill and Wait, 1974b*). The geometry is the same as that in Fig. 7 except that the cylinder is replaced by a prolate spheroid. The prolate spheroid is a useful shape to analyze because the axial ratio can be varied to obtain shapes ranging from a sphere to an infinite cylinder. Unfortunately, the mathematical difficulties only allow the case where overburden currents are neglected and the spheroid is perfectly conducting to be handled conveniently. Calculations indicate that the strength of the anomalous fields increases as the length of the spheroid is increased. However, the location errors are still small unless the obstacle is close to the interface and in the vicinity of the source loop.

7. CONCLUSIONS AND RECOMMENDATIONS

The conclusions and recommendations given here are generally in agreement with those of the Working Group on Electromagneti Location Techniques (Farstad, 1973b) at the Thru-the-Earth Electromagnetics Workshop, Golden, Colorado.

The homogeneous half-space earth model is well understood for both loop and horizontal wire transmitting antennas. Extensive numerical results for field strengths and profiles have been generated for a wide range of parameters as indicated in chapters 2 and 3. Some results for transient waveforms have also been generated for a few configurations as noted in chapters 4 and 5. The CW results are generally in good agreement with the available experimental results. However, there are almost no experimental pulse data for comparison with the theory since pulse location techniques have not been pursued.

The effects of terrain and conductivity anomalies pose difficult analytical problems. Some progress has been made for specific anomalies as discussed in chapter 6. Comparison with experimental results is difficult, and careful documentation of actual field environments and anomalies would be useful to theoretical investigators. One structure which merits some theoretical consideration is the hoist shaft which is normally found in hardrock mines. Farstad (1973c) has observed large location errors and large signal enhancements apparently due to a guiding effect along the hoist shaft which will generally be present in hardrock mines. Some analysis would be desirable in order to learn how to utilize the guiding effect for detection and communication and to minimize the effect on location accuracy.

REFERENCES

Farstad, A.J. (1973a), *Performance of manpack electromagnetic location equipment in trapped miner location tests*, Thru-the-Earth Electromagnetics Workshop, Golden, Colorado.

Farstad, A.J. (1973b), *Summary report of electromagnetic location techniques working group*, Thru-the-Earth Electromagnetics Workshop, Golden, Colorado.

Farstad, A.J. (1973c), *Electromagnetic location experiments in a deep hardrock mine*, Prepared by Westinghouse Georesearch Laboratory for the U.S. Bureau of Mines under USBM Contract H0242006.

Gabillard, R., J.P. Dubus, and F. Cherpereel (1973), *Electromagnetic survey method applicable to underground quarries*, Thru-the-Earth Electromagnetics Workshop, Golden, Colorado.

Geyer, R.G. (1973), *Theory and experiments relating to electromagnetic fields of buried sources with consequences to communication and location*, Thru-the-Earth Electromagnetics Workshop, Golden, Colorado.

* Hill, D.A. (1973a), *Electromagnetic surface fields of an inclined buried cable of finite length*, J. Appl. Phys., 44(12), 5275-5279.

* Hill, D.A. (1973b), *Transient signals from a buried horizontal magnetic dipole*, Pure and Appl. Geophys., 111(X), 2264-2272.

* Hill, D.A. (1974), *Effect of a spherical scatterer on EM source location*, Preliminary Report to U.S. Bureau of Mines on Contract No. H0122061.

* Hill, D.A. and J.R. Wait (1972), *Electromagnetic response of a conducting cylinder of finite length*, Geofisica Internacional, 12(4), 245-266.

* Hill, D.A. and J.R. Wait (1973a), *Subsurface electromagnetic fields of a grounded cable of finite length*, Can. J. Phys., 51(14), 1534-1540.

* Hill, D.A. and J.R. Wait (1973b), *Subsurface electric fields of a grounded cable of finite length for both frequency and time domain*, Pure and Appl. Geophys., 111(X), 2324-2332.

* Hill, D.A. and J.R. Wait (1973c), *Electromagnetic transient response of a small wire loop buried in a conducting earth*, Pure and Appl. Geophys., 105(IV), 869-878.

* Hill, D.A. and J.R. Wait (1973d), *Perturbation of magnetic dipole field by a finitely conducting circular cylinder*, Rivista Italiana di Geofisica, XXII (5/6), 421-424.

* Hill, D.A. and J.R. Wait (1973e), *The electromagnetic response of a buried sphere for buried dipole excitation*, Radio Science, 8(8,9), 813-818.

* Hill, D.A. and J.R. Wait (1974a), *Diffusion of electromagnetic pulses into the earth from a line source*, IEEE Trans. AP, 22(1), 145-146.

* Hill, D.A. and J.R. Wait (1974b), *Perturbation of magnetic dipole fields by a perfectly conducting prolate spheroid*, Radio Science, 9(1), 71-73.

* Howard, A.Q., Jr. (1972), *The electromagnetic fields of a subterranean cylindrical inhomogeneity excited by a line source*, Geophysics, 37(6), 975-984.

Howard, A.Q., Jr. (1973), *Fields of a magnetic dipole excited buried cylinder*, Thru-the-Earth Electromagnetics Workshop, Golden, Colorado.

Large, D.B., L. Ball, and A.J. Farstad (1973), *Radio transmission to and from underground coal mines - Theory and measurement*, IEEE Trans. Comm., 21(3), 194-202.

Olsen, R.G. and A.J. Farstad (1973), *Electromagnetic direction finding experiments for location of trapped miners*, IEEE Trans. Geoscience Electronics, 11, 178-185.

Stoyer, C.H. (1974), *Numerical solutions of the response of a two-dimensional earth to an oscillating magnetic dipole source with application to a groundwater field study*, Ph.D Thesis, Department of Geosciences, Pennsylvania State University.

Sturgill, C.L. (1973), *Trapped miner location and communication system development program*, Prepared by Westinghouse Electric Corporation for the U.S. Bureau of Mines under Contract H0220073.

* Wait, J.R. (1971a), *Criteria for locating an oscillating magnetic dipole buried in the earth*, Proc. IEEE, 59(6), 1033-1035.

* Wait, J.R. (1971b), *Electromagnetic induction technique for locating a buried source*, IEEE Trans. Geosci. Electronics, GE-9(2), 95-98.

* Wait, J.R. (1971c), *Array technique for electromagnetic positional determination of a buried receiving point*, Electronics Letters, 7(8), 186-187.

* Wait, J.R. (1971d), *Influence of earth curvature on the subsurface electromagnetic fields of a line source*, Electronics Letters, 7(23), 697-698.

* Wait, J.R. (1972a), *Locating an oscillating magnetic dipole in the earth,* Electronics Letters, 8(16), 404-405.

* Wait, J.R. (1972b), *The effect of a buried conductor on the subsurface fields for line source excitation,* Radio Science, 7(5), 587-591.

* Wait, J.R. (1974), *Propagation under the earth surface (a review),* Symposium on Electromagnetic Wave Theory, International Union of Radio Science, London.

* Wait, J.R. and D.A. Hill (1971), *Transient signals from a buried magnetic dipole,* J. Appl. Phys., 42(10), 3866-3869.

* Wait, J.R. and D.A. Hill (1972a), *Transient magnetic fields produced by a step function excited loop buried in the earth,* Electronics Letters, 8(11), 294-295.

* Wait, J.R. and D.A. Hill (1972b), *Electromagnetic surface fields produced by a pulse-excited loop buried in the earth,* J. Appl. Phys., 43(10), 3988-3991.

* Wait, J.R. and D.A. Hill (1972c), *Transient electromagnetic fields of a finite circular loop in the presence of a conducting half-space,* J. Appl. Phys., 43(11), 4532-4534.

* Wait, J.R. and D.A. Hill (1973), *Excitation of a homogeneous conductive cylinder of finite length by a prescribed axial current distribution,* Radio Science, 8(12), 1169-1176.

* Wait, J.R. and K.P. Spies (1971a), *Electromagnetic fields of a small loop buried in a stratified earth,* IEEE Trans. AP, 19(5), 717-718.

* Wait, J.R. and K.P. Spies (1971b), *Subsurface electromagnetic fields of a line source on a conducting half-space,* Radio Science, 6(8,9), 781-786.

* Wait, J.R. and K.P. Spies (1973a), *Low-frequency impedance of a circular loop over a conducting ground,* Electronics Letters, 9(15), 346-347.

* Wait, J.R. and K.P. Spies (1973b), *Subsurface electromagnetic fields of a line source on a two-layer earth,* Radio Science, 8(8,9), 805-810.

* Wait, J.R. and R.E. Wilkerson (1972), *The subsurface magnetic fields produced by a line current source on a non-flat earth,* Pure and Appl. Geophys., 95 (III), 150-156.

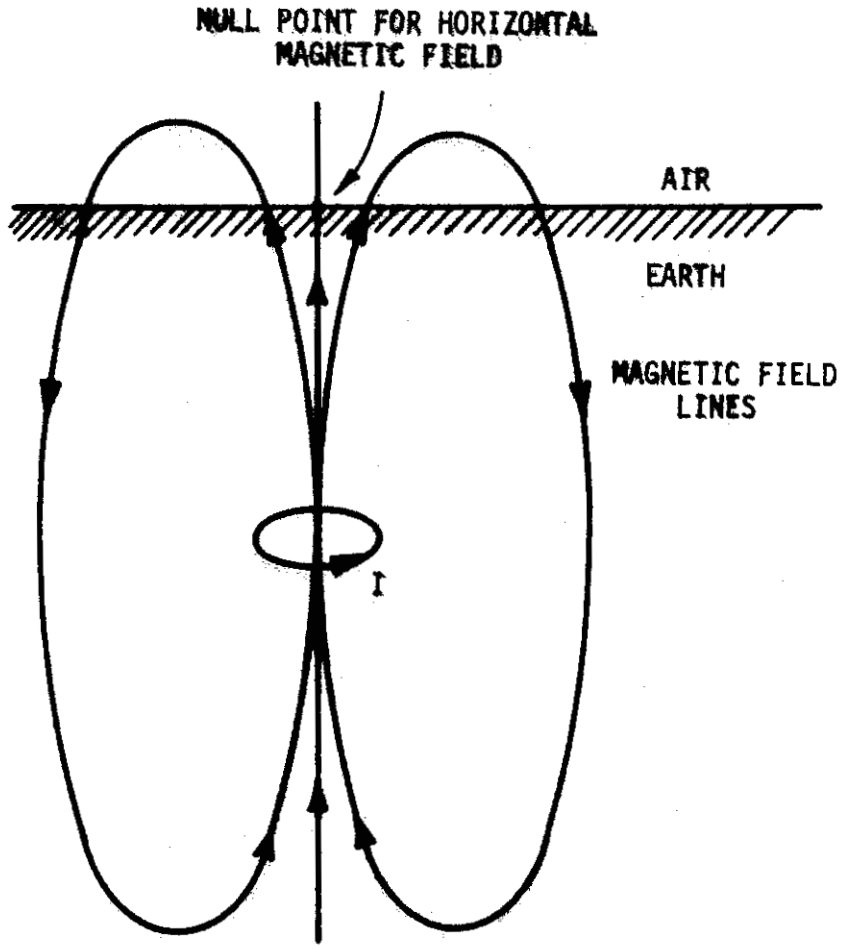

FIGURE 1 MAGNETIC FIELD LINES FOR A HORIZONTAL LOOP SOURCE (VERTICAL MAGNETIC DIPOLE)

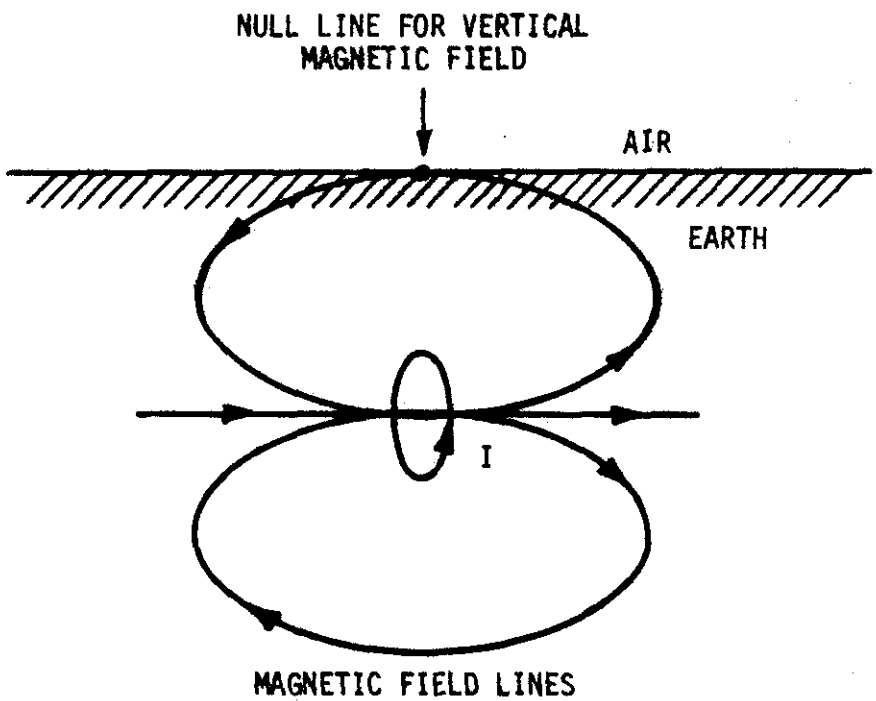

FIGURE 2 MAGNETIC FIELD LINES FOR A VERTICAL LOOP SOURCE (HORIZONTAL MAGNETIC DIPOLE)

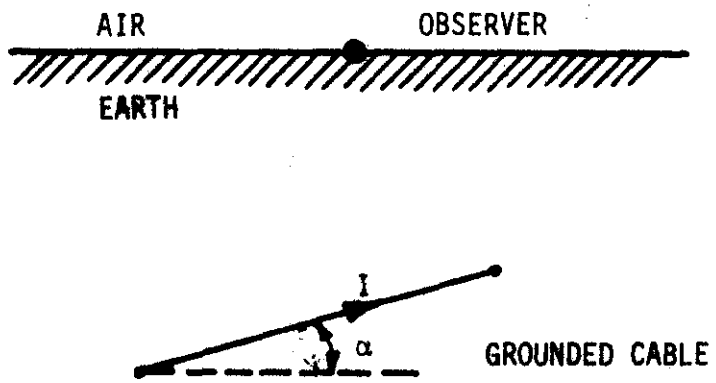

FIGURE 3 TILTED GROUNDED CABLE SOURCE FOR UPLINK TRANSMISSION

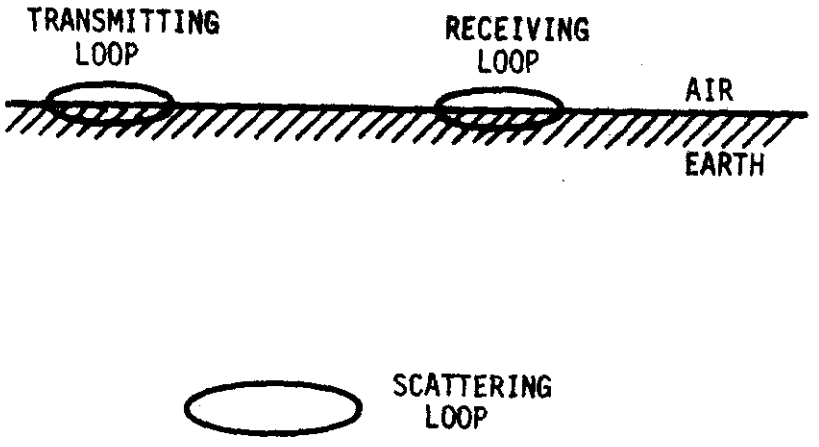

FIGURE 4 PASSIVE DETECTION CONFIGURATION

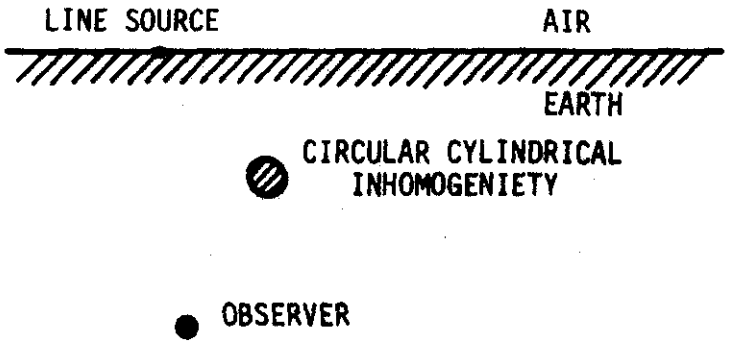

FIGURE 5 TWO-DIMENSIONAL GEOMETRY FOR A CYLINDRICAL ANOMALY

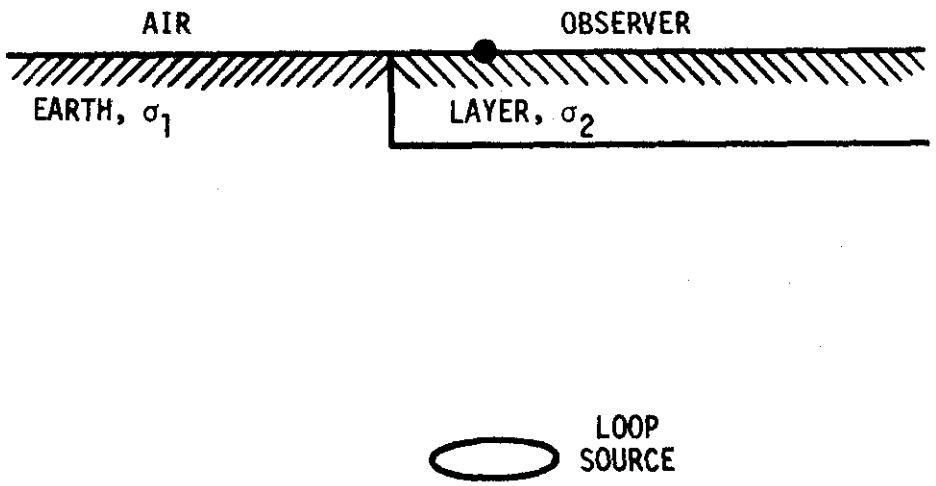

FIGURE 6 HALF-LAYER OVERBURDEN MODEL WITH A VERTICAL MAGNETIC DIPOLE SOURCE

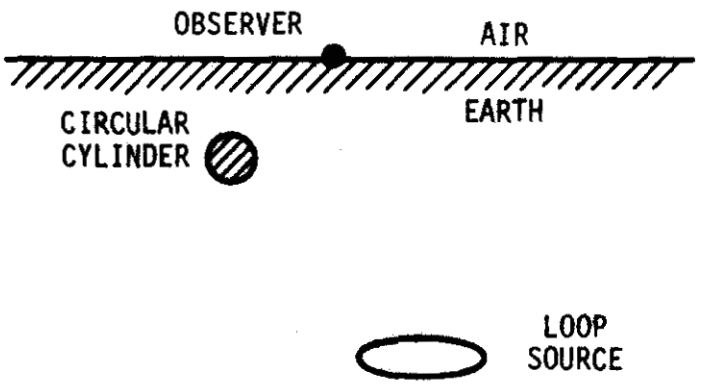

FIGURE 7 CIRCULAR CYLINDER ANOMALY WITH A VERTICAL MAGNETIC DIPOLE SOURCE

ANALYTICAL INVESTIGATIONS OF ELECTROMAGNETIC LOCATION SCHEMES RELEVANT TO MINE RESCUE

PART II - COLLECTED REPRINTS

Prepared by J.R. Wait

TABLE OF CONTENTS

TABLE OF CONTENTS (cont'd)

Proc. IEEE (Letters), Vol. 59, No. 6
1033-1035, June 1971

Criteria for Locating an Oscillating Magnetic Dipole Buried in the Earth

Abstract—The possibility is discussed of locating miners, after a disaster, by an electromagnetic technique. Specifically, it is suggested that the complex ratio of the horizontal and the vertical field components be measured. The limitation due to the finite conductivity of the overburden is also considered and shown to be a not insurmountable problem.

Following a disaster in a coal mine, there is a need to locate personnel who may be trapped or lost. The possibility that they can be found by an electromagnetic direction-finding scheme is intriguing. Unfortunately, the waves must propagate through a conductive overburden. Apart from the resulting attenuation, there is a distortion of the field vectors which can be be expected to produce errors. However, as indicated in a recent report[1] on this subject, the effect of the conductive environment can be minimized if a current-carrying loop source is used at a sufficiently low frequency. Such a method may be a useful complement to the highly promising seismic location technique being developed elsewhere.[2]

In this letter, we consider an analytical model of the direction-finding scheme and provide some quantitative criteria that may form the basis of working models. Also, hopefully, the results should provide useful information to other groups or individuals who are giving this matter their attention.

Conceptually, the simplest case is where we seek to determine the location of a small horizontal loop of area A carrying a total current I at an

Manuscript received January 22, 1971; revised February 10, 1971.

[1] *Mine Rescue and Survival Techniques*, National Academy of Engineering, Washington, D. C., 1969.

[2] D. B. Large, Westinghouse Georesearch Labs., Boulder, Colo., private communication.

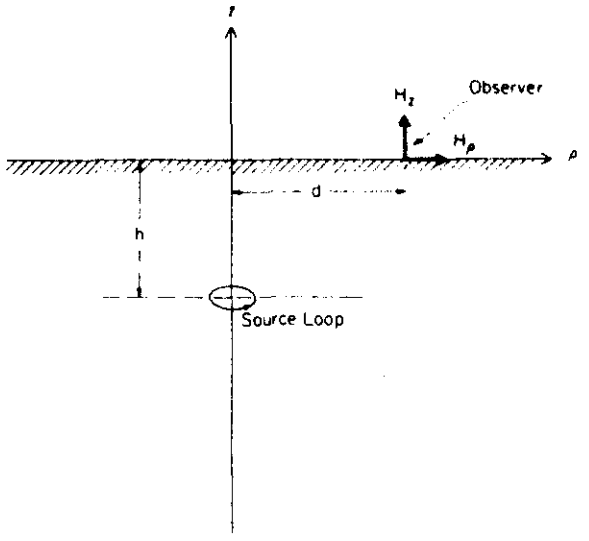

Fig. 1. Horizontal loop (i.e., vertical magnetic dipole) buried at depth h in a homogeneous half-space.

angular frequency ω. Thus we are interested in the detailed structure of the fields produced on the surface with a view to specifying meaningful measurements. To simplify the analysis, we represent the earth as a homogeneous half-space of conductivity σ and permeability μ. Here we assume $\mu = \mu_0$, where μ_0 is the permeability of free space. Also, because of the low frequencies involved, we can neglect all displacement currents in the problem. The situation is illustrated in Fig. 1 where the earth's surface is the plane $z=0$ and the loop is located at $z=-h$ on the axis of a cylindrical coordinate system (ρ, ϕ, z).

The magnetic field components H_ρ and H_z produced on the surface at $\rho = d$ can be calculated from integral expressions that have a well-known form.[3] The numerical task, however, is not trivial since the distances involved may be comparable with the effective wavelength or skin depth in the conductor. Thus the otherwise exhaustive asymptotic and near-field derivations scattered throughout the literature could not be used directly. Here we resort to a numerical evaluation of the integrals but utilize the static (i.e., $\omega \to 0$) results and other special cases as a check. Details of the analysis and computations are to be given elsewhere.

The desired field components at $\rho = d$ and $z = 0$ are given explicitly as

$$H_\rho = \frac{IA}{2\pi h^3} P \tag{1}$$

$$H_z = \frac{IA}{2\pi h^3} Q \tag{2}$$

where P and Q are convenient normalized quantities. The latter are to be obtained from

$$\left.\begin{matrix} P \\ Q \end{matrix}\right\} = \int_0^\infty \frac{x^3}{x + (x^2 + iH^2)^{\frac{1}{2}}} \exp\left[-(x^2 + iH^2)^{\frac{1}{2}}\right] \left\{\begin{matrix} J_1(xD) \\ J_0(xD) \end{matrix}\right. dx \tag{3}$$

where J_0 and J_1 are Bessel functions, $H = (\sigma\mu\omega)^{\frac{1}{2}}h$, and $D = \rho/h$.

The ratio of the magnitudes of H_ρ and H_z at the observing station is simply $|P|/|Q|$ or $|P/Q|$. This ratio is plotted in Fig. 2 as a function of the distance parameter D. Not surprisingly, this function rises from a sharp null at $D=0$ to a maximum that is near $D=1.4$ for the small H values in accordance with the expected static behavior of the dipole (i.e., a static or dc theory predicts $Q=0$ at $D=\sqrt{2}$). This pronounced maximum is blurred as H increases and, to a first order, it shifts to smaller values of D. Nevertheless, the curves in Fig. 2 indicate that, for a single measurement of $|H_\rho/H_z|$ or $|P/Q|$, two admissible values of D can be ascertained.

The phase difference between H_ρ and H_z is a quantity of interest since it can be measured at the observer station without any phase reference

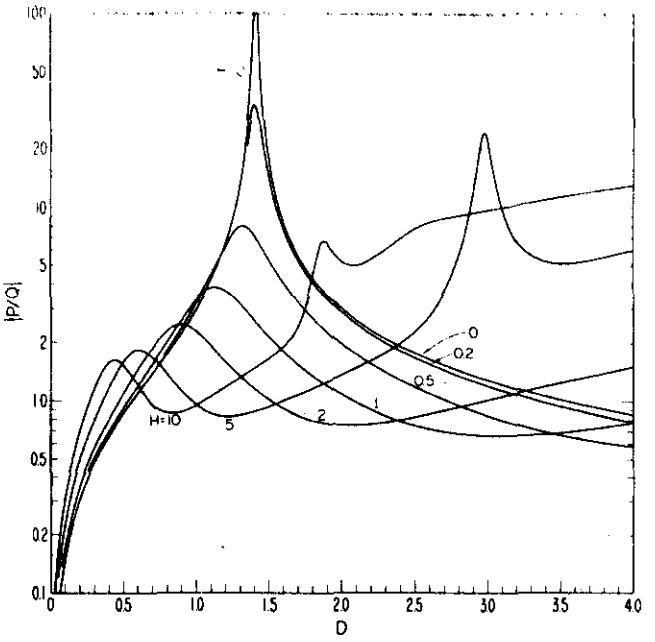

Fig. 2. The magnitude of the ratio of the horizontal and the vertical magnetic field.

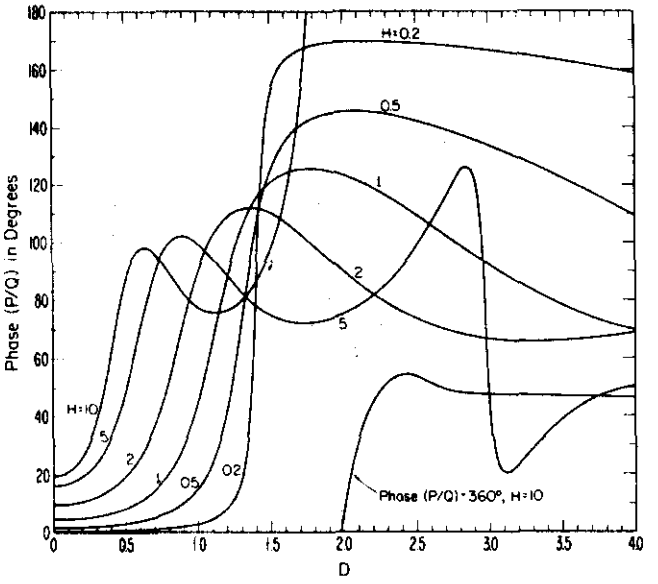

Fig. 3. The difference in phase between the horizontal and the vertical magnetic fields.

from the source. This quantity is of course equal to the argument of the ratio P/Q. It is plotted in Fig. 3 as a function of D for the same range of H. Clearly, we see that, for sufficiently small H, the phase is near either 0 or 180°, depending on whether $D<1.4$ or $D>1.4$, respectively. This fact permits us to eliminate the ambiguity from the single measurement of the amplitude ratio alluded to in the foregoing. Thus, in principle, we can deduce the appropriate value of D from the measurement of the complex P/Q. Of course, if h is known, we then can find the desired radial coordinate ρ.

In our discussion here, we have required that H be a small parameter if the conductive effects in the overburden are to be minimized. In terms of actual quantities, this can be written

$$H = 2\sqrt{2}\,\pi\sqrt{\sigma_m f}\, h_{km} \times 10^{-2} \simeq 0.086\sqrt{\sigma_m f}\, h_{km}$$

where σ_m is the earth conductivity in millimhos per meter, f is the frequency in hertz, and h_{km} is the burial depth h expressed in kilometers. For

[3] J. R. Wait, "Electromagnetic sources in lossy media," in *Antenna Theory*, pt. 2, Collin and Zucker, Ed. New York: McGraw-Hill, 1969, ch. 24.

example, if $\sigma_m = 1$, $f = 100$, and $h_{km} = 0.2$, we see that $H \simeq 0.17$ which is sufficiently small that the fields should have a static-like behavior.

The results given here, while not at all exhaustive, indicate that direction-finding possibilities definitely exist for a buried magnetic dipole source, provided the field structure can be measured at a single observation station on the surface. Conversely, we can reverse the roles of the source and the observer and locate the receiving apparatus in the earth and transmit from a grounded loop on the surface. The latter may be a more practical scheme from the operational point of view, since the to-be-rescued miners would then need only to utilize a cross-loop receiver with suitable switching provisions to measure both the field ratios and the phase differences. Also, of course, the vertical loop (i.e., horizontal axis) can be oriented to give the radial direction toward the source. For feasibility tests, however, it is recommended that the loop transmitter be buried and the field quantities be measured on the surface. From an experimental point of view, this would seem to have major advantages in the scope of the measurements and the variety of situations to be examined.

Analytical studies on this subject are continuing.[4] Among some of the problems being discussed are the effect of a stratified and nonuniform overburden, other dipole and line-source configurations, and the transient solutions for pulsed dipole sources. The work bears a close similarity to earlier investigations in geophysical exploration using electromagnetic methods.[5] The configurations are sufficiently different, however, that the previous numerical data cannot be used directly.

ACKNOWLEDGMENT

The author wishes to thank K. P. Spies for his numerical analysis and general assistance in this task.

JAMES R. WAIT
Inst. Telecommun. Sci.
Boulder, Colo. 80302

[4] These studies are being carried out under Task 5 of a contract from the U.S. Bureau of Mines to the Office of Telecommunications.

[5] G. V. Keller and F. Frischknecht, *Electrical Methods in Geophysical Prospecting*. Oxford, England: Pergamon, 1967.

IEEE Trans. Geosci. Electr., Vol. GE-9, No. 2, 95-98 (April 1971)

Electromagnetic Induction Technique for Locating a Buried Source

JAMES R. WAIT, FELLOW, IEEE

Abstract—**The field structure of a buried vertical oscillating magnetic dipole is examined. For an observer on the earth's surface, it is indicated that the finite conductivity of the earth will modify the geometrical character of the vertical and horizontal magnetic field components. However, this effect is quite small if the burial depth is less than an electrical skin depth.**

INTRODUCTION

THERE IS A possibility that electromagnetic waves can be employed to locate coal miners following a disaster. A number of studies supporting this thesis are currently being sponsored by the U. S. Bureau of Mines. In this paper, without any claim to originality, I wish to present the basic theory of a technique that may hold some promise.

The specific configuration considered is a small wire loop contained in a horizontal plane and buried at some depth h beneath the earth's surface. The objective here is to examine the structure of the electromagnetic field on the earth's surface produced by an alternating current injected into the loop. The situation is illustrated in Fig. 1 with respect to a cylindrical coordinate system (ρ, ϕ, z). The earth is represented as a homogeneous half-space of conductivity σ. All displacement currents can be neglected because we may assume that all linear

Manuscript received January 14, 1971.
The author is with the Institute for Telecommunication Sciences, Office of Telecommunications, Boulder, Colo. 80302.

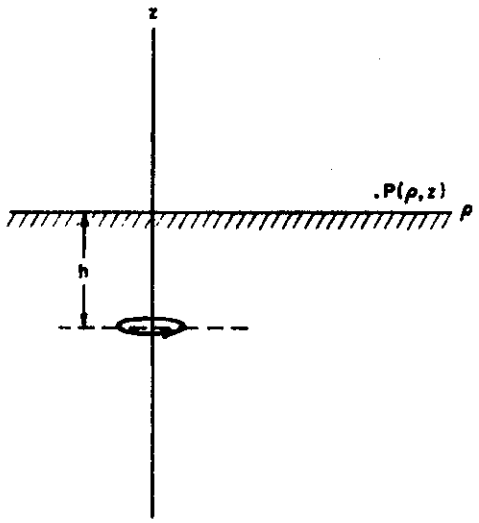

Fig. 1. Geometry of buried loop.

distances involved are small compared with the free-space wavelength.

Formulation and Solution

Considering the loop, whose area×turns product is IA, as a vertical magnetic dipole, we can derive the resultant magnetic fields in the air (i.e., $z>0$) from the following [1]:

$$i\mu_0\omega H_\rho = \partial^2 F/(\partial\rho\partial z) \tag{1}$$

and

$$i\mu_0\omega H_z = \partial^2 F/\partial z^2 \tag{2}$$

where μ_0 is the permeability of free space, ω is the angular frequency, and F is a scalar function. A straightforward boundary value analysis leads to the following integral form [1]:

$$F = \frac{i\mu_0\omega IA}{2\pi}\int_0^\infty \frac{\lambda}{u+\lambda}\left(e^{-\lambda h}\right)J_0(\lambda\rho)d\lambda \tag{3}$$

where $u=(\lambda^2+\gamma^2)^{1/2}$, $\gamma^2=i\sigma\mu_0\omega$, and J_0 is a Bessel function of order zero.

Using (1) and (2) along with (3), we find that the fields at the location (ρ, z) for $z>0$ are

$$H_\rho = b_0 P \tag{4}$$

and

$$H_z = b_0 Q \tag{5}$$

where

$$P = h^3\int_0^\infty \frac{\lambda^3}{\lambda+u}e^{-\lambda z}e^{-uh}J_1(\lambda\rho)d\lambda \tag{6}$$

and

$$Q = h^3\int_0^\infty \frac{\lambda^3}{\lambda+u}e^{-\lambda z}e^{-uh}J_0(\lambda\rho)d\lambda \tag{7}$$

and the normalizing factor is

$$b_0 = IA/(2\pi h^3). \tag{8}$$

By changing the variable of integration to $x=\lambda h$, the integrals P and Q are expressible in the form

$$P = \int_0^\infty \frac{x^3 e^{-xZ}}{x+(x^2+iH^2)^{1/2}}e^{-(x^2+iH^2)^{1/2}}J_1(xD)dx \tag{9}$$

and

$$Q = \int_0^\infty \frac{x^3 e^{-xZ}}{x+(x^2+iH^2)^{1/2}}e^{-(x^2+iH^2)^{1/2}}J_0(xD)dx \tag{10}$$

where $H=(\sigma\mu_0\omega)^{1/2}$, $D=\rho/h$, and $Z=z/h$ are dimensionless parameters. Equations (9) and (10) are in a form suitable for numerical integration, and a computer program has been prepared to accomplish this task. Before discussing the results, some special limiting cases will be mentioned.

Limiting Cases

When the conductivity σ and/or the frequency ω are sufficiently low, the parameter H is effectively zero. Then, without difficulty, the integrals P and Q are expressible in the closed forms

$$P = (3/2)D(Z+1)R^{-5} \tag{11}$$

and

$$Q = (1/2)\left[3(Z+1)^2R^{-5} - R^{-3}\right] \tag{12}$$

where $R=[D^2+(Z+1)^2]^{1/2}$. These simple results for the normalized magnetic fields P and Q correspond to static conditions.

The other limiting case of interest is when the conductivity σ and/or the frequency ω are sufficiently high that the integrals P and Q may be approximated in an asymptotic sense. Essentially, this amounts to arguing that when $|\gamma\rho|\gg 1$, the exponential factor $\exp(-uh)$ in (3), (6), and (7) may be adequately approximated by $\exp(-\gamma h)$. Then, treating both H and D as large parameters, we find that

$$P \sim -e^{i\pi/4}(3/H)D^{-4}\exp\left[-e^{i\pi/4}H\right] \tag{13}$$

and

$$Q \sim +e^{i\pi/2}(9/H^2)D^{-5}\exp\left[-e^{i\pi/4}H\right]. \tag{14}$$

A precise description of the validity of these asymptotic forms is subtle, but on comparison with numerical integration on the exact forms, it appears that they are useful when both H and HD are $\gg 1$.

Another interesting check is to let h be identically zero. Then for $z=0$, we have [1]

$$F = \frac{i\mu\omega IA}{2\pi}\int_0^\infty \frac{\lambda}{u+\lambda}J_0(\lambda\rho)d\lambda \tag{15}$$

$$= \frac{i\mu\omega IA}{2\pi}\frac{1}{\gamma^2\rho^2}\left[1-(1+\gamma\rho)e^{-\gamma\rho}\right] \tag{16}$$

where we have made use of a known identity. Then, again for $z=0$, we have

$$E_\phi = \partial F/\partial\rho = \frac{i\mu_0\omega IA}{2\pi}\cdot\frac{3}{\gamma^3\rho^4}\alpha \tag{17}$$

where

$$\alpha = 1 - [1 + \gamma\rho + (\gamma^2\rho^2/3)]e^{-\gamma\rho}. \tag{18}$$

If we now assume $|\gamma\rho| \gg 1$ and utilize the approximate (Leontovich) boundary condition [1], we have

$$H_\rho \simeq \eta E_\phi, \qquad \eta = i\mu_0\omega/\gamma \tag{19}$$

$$\simeq -\frac{IA}{2\pi}\cdot\frac{3}{\gamma\rho^4}\cdot \tag{20}$$

This is consistent with (13) given above if we note that the right-hand side of (20) is $\lim_{h\to 0} b_0 P$. Also, we can obtain an exact expression for H_z at $z=0$ by using $i\mu_0\omega H_z = -(1/\rho)/(\partial/\partial\rho)\rho E_\phi$ and (17); thus $H_z = -IA\rho/(2\pi\gamma^3\rho^5)\beta$ where

$$\beta = 1 - [1 + \gamma\rho + (4/9)\gamma^2\rho^2 + (1/9)\gamma^3\rho^3]e^{-\gamma\rho}. \tag{21}$$

Again, if $|\gamma\rho| \gg 1$, $\beta \simeq 1$, and (21) is consistent with (14).

As a matter of theoretical interest, we have one final special case which deserves mention. Specifically, we take $\rho=0$, which means the observer is directly above the source loop. Then, of course, $P=0$, but Q is finite. If, in fact $z=0$, we have

$$Q = Q_e = h^3\int_0^\infty \lambda^3(u+\lambda)^{-1}e^{-uh}d\lambda. \tag{22}$$

Now,

$$(u+\lambda)^{-1} = (u-\lambda)(u^2-\lambda^2)^{-1} = \gamma^{-2}(u-\lambda),$$

and therefore

$$Q_e = \frac{h^3}{\gamma^2}\left[\int_0^\infty u\lambda^3 e^{-uh}d\lambda - \int_0^\infty \lambda^4 e^{-uh}d\lambda\right]. \tag{23}$$

We can now verify that

$$Q_e = \frac{h^3}{\gamma^2}\left[\frac{\partial^4 p}{\partial h^4} - \gamma^2\frac{\partial^2 p}{\partial h^2} + \frac{\partial^5 q}{\partial h^5} - 2\gamma^2\frac{\partial^3 q}{\partial h^3} + \gamma^4\frac{\partial q}{\partial h}\right] \tag{24}$$

where

$$p = \int_0^\infty e^{-uh}\frac{\lambda}{u}d\lambda \tag{25}$$

and

$$q = \int_0^\infty \frac{e^{-uh}}{u}d\lambda. \tag{26}$$

These latter two integrals are known to be

$$p = e^{-\gamma h}/h \tag{27}$$

and

$$q = K_0(\gamma h) \tag{28}$$

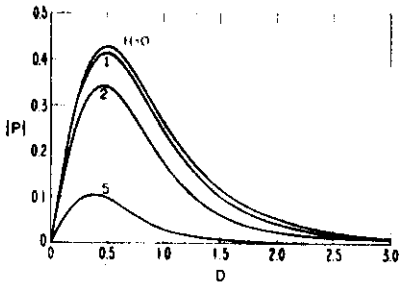

Fig. 2. Horizontal component of normalized magnetic field on surface as function of distance parameter D.

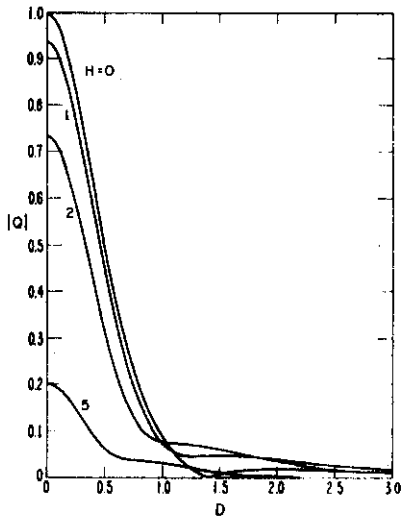

Fig. 3. Vertical component of normalized magnetic field on surface as function of distance parameter D.

where K_0 is a modified Bessel function of order zero. Using only the well-known identities $K_0'(Z) = -K_1(Z)$ and $K_1'(Z) = -[K_0(Z) + Z^{-1}K_1(Z)]$, it turns out that (24) can be reduced to the compact form

$$Q_e = 2e^{-x}x^{-2}[(12 + 12x + 5x^2 + x^3)] - 3[(x + (8/x))K_1(x) + 4K_0(x)]$$

where $x = \gamma h = \sqrt{i}H$. This provides an alternative method to compute the field directly above the source dipole.

Discussion of Results and Final Remarks

As indicated above, P and Q are the normalized components of the horizontal and the vertical magnetic field on the surface for the buried loop source. The magnitudes $|P|$ and $|Q|$ plotted as a function of the normalized distance D (or ρ/h) are illustrated in Figs. 2 and 3, respectively. The parameter on the curve is the normalized depth parameter H (or $(\sigma\mu_0\omega)^{1/2}h$). This can be calculated from the simple formula $H = 0.086(\sigma_{\text{mmho}}f)^{1/2}h_{\text{km}}$ where σ_{mmho} is the earth conductivity in millimhos per meter, f is the frequency in hertz, and h_{km} is the burial depth in kilometers. For example, if $\sigma_{\text{mmho}}=1$, $f=10^2$, and $h_{\text{km}}=0.2$, we have $H=0.17$. In this case, we can make the rather important observation that the character of the $|P|$ versus D curves in Fig. 2 are essentially

the same as for the case $H=0$. Thus, the conductivities of the overburden are probably negligible for this configuration of the receiving loop provided the burial depths are not more than 0.5 km and the operating frequencies are in the low audio range. It is significant, however, that the vertical magnetic field component as indicated by the $|Q|$ versus D curve in Fig. 3 has a significant modification in the region near $D=\sqrt{2}$. Here, the static field (i.e., for $H=0$) has a null which is smeared out even for small values of the parameter H. This effect, however, is still not detrimental to the operation of a detection scheme.

While there are many other aspects of a practical scheme for using the induction field for source location, we feel that this approach is worthy of critical examination. Furthermore, by applying some simple notions of reciprocity, we can adapt the present results to the situation when the source loop is located on the surface and the receiving loop is located at depth. Other factors receiving our attention are the influence of an inhomogeneous overburden and the effect of irregular terrain.

Acknowledgment

The author wishes to thank K. P. Spies for his assistance with the numerical calculations and Dr. D. B. Large for several stimulating discussions.

References

[1] J. R. Wait, "Electromagnetic fields of sources in lossy media," in *Antenna Theory*, pt. II, R. E. Collin and F. J. Zucker, Eds. New York: McGraw-Hill, 1969, ch. 24, pp. 468–471.

IEEE Trans. Antennas and Propagation, vol. AP-19, No. 5, (Communications) 717-718 (Sept. 1971)

Electromagnetic Fields of a Small Loop Buried in a Stratified Earth

Abstract—The field structure of a buried vertical oscillating magnetic dipole is examined. The earth is represented as a two-layer half-space, and the source is located in the bottom semi-infinite region. Using numerical integration, the magnitude of the ratio of the horizontal to the vertical magnetic field is examined for an observer on the earth's surface. It is shown that at sufficiently low frequencies, the field ratio is not appreciably modified by the finite conductivity and the geometry of the layers.

Communication to the earth's surface from a buried transmitter may be useful in emergency situations such as after a mine disaster [1]. Unfortunately, the conductive losses in the intervening rock will severely attenuate the signal unless extremely low frequencies are employed. Also, direction finding of the buried source, from the surface observer, is inhibited by the conductive overburden. In this communication, we wish to consider an analytical model which may shed some light on this problem.

As indicated in Fig. 1, we consider a vertical magnetic dipole or small loop (with vertical axis) located at a depth h beneath the surface of a flat earth. The current in the loop is taken to vary as $\exp(i\omega t)$. To simulate the effect of an inhomogeneous earth, we adopt a two-layer model. The upper layer has a conductivity σ_1 and a thickness b. The semi-infinite lower layer, which contains the source dipole, has a conductivity σ_2. A cylindrical coordinate system (ρ,ϕ,z) is chosen as illustrated in Fig. 1 with the observer located at $P(\rho,z)$ on or above the earth's surface at $z = 0$. It is our objective to evaluate the magnetic field components H_ρ and H_z at $P(\rho,z)$ for a specified total current I in the small loop of area A located at $z = -h$.

The formal solution for the problem as stated was given some time ago [2], although in the original derivation, it was assumed that the magnetic dipole was in the air above a two-layer stratified earth. Clearly, the solution has the same form as for the problem posed here. Also, as indicated before, all displacement currents can be neglected if the free-space wavelength is much greater than the significant dimensions of the problem. We assume this is the case here. Also, to simplify matters, we assume that both of the conductive layers have magnetic permeabilities which are the same as for free space. Thus, without difficulty, we find that

$$H_\rho = b_0 P \tag{1}$$

and

$$H_z = b_0 Q \tag{2}$$

where $b_0 = IA/(2\pi h^3)$ is a suitable normalizing factor, while P and Q are the dimensionless field quantities. Under the assumptions stated previously, we have the integral formulas

$$P = \frac{h^3}{2}\int_0^\infty \lambda^2 T(\lambda)\exp(-\lambda z)J_1(\lambda\rho)\,d\lambda \tag{3}$$

and

$$Q = \frac{h^3}{2}\int_0^\infty \lambda^2 T(\lambda)\exp(-\lambda z)J_0(\lambda\rho)\,d\lambda \tag{4}$$

where

$$T(\lambda) = \frac{\left(\frac{2\lambda}{u_1+\lambda}\right)\left(\frac{2u_1}{u_1+u_2}\right)\exp\left[-u_2(h-b)-u_1 b\right]}{\left[1-\left(\frac{u_1-\lambda}{u_1+\lambda}\right)\left(\frac{u_1-u_2}{u_1+u_2}\right)\exp(-2u_1 b)\right]} \tag{5}$$

$u_1 = (\lambda^2 + i\sigma_1\mu_0\omega)^{1/2}$, and $u_2 = (\lambda^2 + i\sigma_2\mu_0\omega)^{1/2}$.

Manuscript received January 28, 1971.

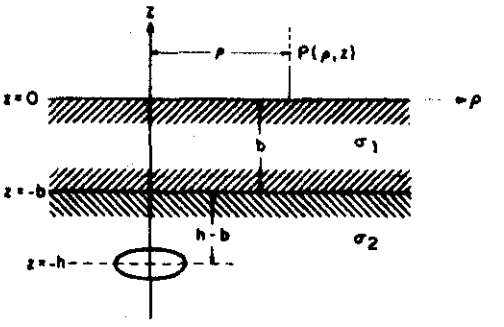

Fig. 1. Magnetic dipole located within two-layer stratified earth.

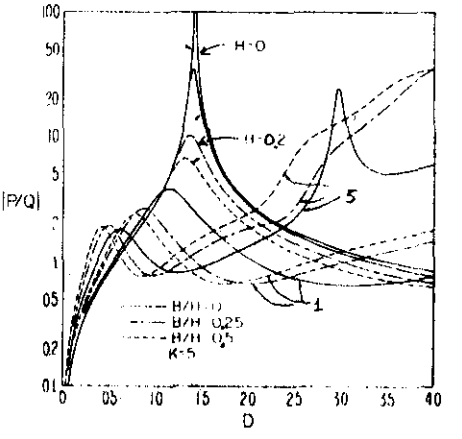

Fig. 2. Field ratio on surface for various values of $H = (\sigma_2\mu_0\omega)^{1/2}h$ and $B/H = b/h$ for fixed $K = (\sigma_1/\sigma_2)^{1/2} = 5$.

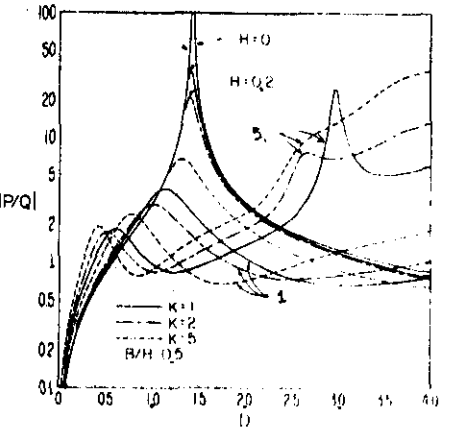

Fig. 3. Field ratio for various values of H and K for fixed $B/H = b/h = 0.5$.

While (3) and (4) can be evaluated analytically in certain limiting cases, the most direct approach is numerical integration. Convergence of the integrals is assured by the exponential factor in the numerator of the right-hand side of (5). Also, we note that P and Q are functions of the dimensionless parameters $B = (\sigma_1\mu_0\omega)^{1/2}b$, $H = (\sigma_2\mu_0\omega)^{1/2}h$, $D = \rho/h$, $Z = z/h$, and $K = (\sigma_1/\sigma_2)^{1/2}$. A digital computer program has been written for evaluating P and Q, and results have been obtained for a wide range of the parameters [3].

A quantity of special interest is the magnitude of the ratio H_ρ/H_z at $z = 0$ on the earth's surface. The magnitude of this ratio is $|P/Q|$ and typical plots are indicated in Figs. 2–4 for selected values of the parameters. The abscissa in each case is the distance parameter D or ρ/h. The limiting case designated $H = 0$ corresponds to purely static conditions (i.e., $\omega \to 0$). In this case, it is not diffi-

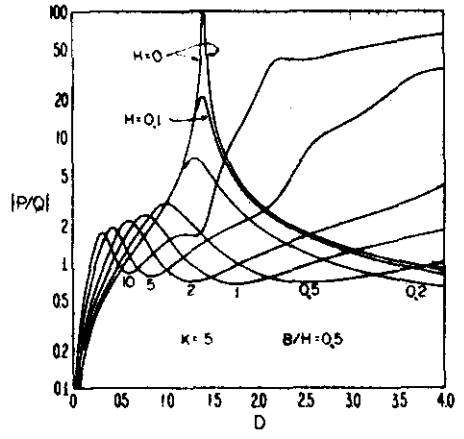

Fig. 4. Field ratio for various values of H for fixed $K = (\sigma_1/\sigma_2)^{1/2} = 5$ and $B/H = b/h = 0.5$.

cult to verify that, for $z = 0$, (3) and (4) reduce to

$$P = (3/2)DR^{-5}$$

and

$$Q = (1/2)[3R^{-5} - R^{-3}]$$

where $R = (D^2 + 1)^{1/2}$. The curves in Figs. 2–4 are consistent with these static field formulas for the small values of H. In particular, we see that the null for Q at $D = \sqrt{2}$ leads to an infinity for $|P/Q|$. This pronounced peak, however, is somewhat blurred when H is different from zero. In fact, the behavior of the ratio $|P/Q|$ becomes modified drastically for the larger values of H.

To consider a specific example, we choose $f = \omega/2\pi = 10^3$ Hz, $\sigma_2 = 10^{-3}$ mho/m, and $h = 200$ m; thus, $H = 0.17$. In this case, the upper layer of thickness $(B/H) \times 200$ m, has a conductivity $K^2 \times 10^{-3}$ mho/m. As indicated in Figs. 2 and 3, the presence of this masking layer deteriorates the ideal static-like behavior of the field ratio $|P/Q|$.

Using the analytical results from this study, it is possible to elucidate the effect of the stratification in the overburden and to provide improved criteria for direction finding techniques. The results given here are considered only as an example of the many possibilities that exist.

James R. Wait
Kenneth P. Spies
Inst. Telecommun. Sci.
Office of Telecommun.
U. S. Dep. Commerce
Boulder, Colorado 80302

References

[1] G. Meloy, G. V. Keller, *et al.*, "Mine rescue and survival," Nat. Acad. Eng., Washington, D. C., Tech. Rep. 1969.
[2] J. R. Wait, "The magnetic dipole over the horizontally stratified earth," *Can. J. Phys.*, vol. 29, 1951, pp. 577–592.
[3] J. R. Wait and K. P. Spies, "Evaluation of the surface EM fields," AFCRL Rep. 52, Feb. 1971, (available from Federal Clearinghouse. NTIS, Springfield, Va. 22151).

Electronics Letters, Vol. 8,
No. 16, 10th August 1972

LOCATING AN OSCILLATING MAGNETIC DIPOLE IN THE EARTH

Indexing terms: Magnetic fields, Mining

The merits of a horizontal magnetic dipole in a source-location scheme are considered. The results have possible applications in locating trapped miners following disasters.

In a previous communication,[1] we pointed out the possibility that, following a disaster, miners could be located by an electromagnetic technique. The basis of the method was to observe the structure of the vector magnetic field on the surface produced by a buried magnetic dipole whose location was to be determined. Specifically, we considered the source to be a vertically oriented magnetic dipole (i.e. a small horizontal loop) buried at a depth h in the conducting halfspace. It was indicated that the radial co-ordinate of the observer, relative to the source, could be ascertained from measurements of the horizontal and vertical magnetic fields at the surface. In such a scheme, it is necessary that the trapped miner(s) have available a means to excite a loop of wire with sufficient audio-frequency current to be detected on the surface.

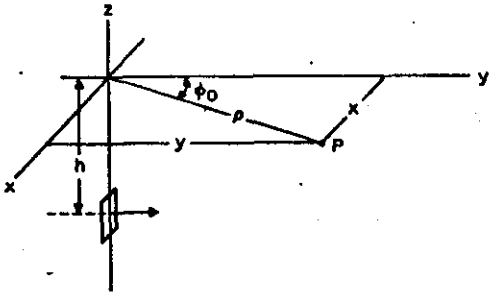

Fig. 1 *Horizontal magnetic dipole located at depth h in a conducting halfspace*

Current field investigations of the e.m. location scheme have shown that the null of the horizontal magnetic field directly over a buried vertical magnetic dipole is a relatively simple and useful criterion that may have promise in a practical scheme.*† Unfortunately, in this case, the received magnetic field must compete with atmospheric noise that always has significant horizontal components of magnetic field. This immediately suggests that a better scheme would be to employ a horizontal magnetic-dipole source, in which case the null over the source occurs in the vertical magnetic-field component. The received atmospheric noise is then much reduced. With this motivation, we consider here the structure of the surface fields produced by a buried horizontal magnetic dipole (i.e. a small loop contained in a vertical plane). Also, as we shall indicate, there are other features of this configuration that may have some use.

The analytical model is indicated in Fig. 1, where we choose a Cartesian co-ordinate system (x, y, z), with the space $z < 0$ corresponding to a homogeneous nonmagnetic earth of conductivity σ. The source is a small loop or frame of area A carrying a total current I at an angular frequency ω. The equivalent magnetic-dipole source is located at $z = -h$ on the z axis and is oriented in the y direction. As before,[1] we can neglect all displacement currents because of the low frequencies involved.

The resultant magnetic field components H_x, H_y and H_z at a point P on the surface $z = 0$ can be calculated from integral expressions that are well known.[2] The latter are evaluated numerically, even though certain special cases can be expressed in closed form.[2]

First of all, we note that the fields in the region $z > 0$ can be derived from a scalar potential Φ via

$$\vec{H} = -\nabla\Phi \qquad (1)$$

where

$$\Phi = -\frac{IA}{2\pi}\frac{\partial}{\partial y}\int_0^\infty \frac{u}{\lambda+u} J_0(\lambda\rho)\exp(-uh-\lambda z)\,d\lambda \qquad (2)$$

where $\rho = (x^2+y^2)^{\frac{1}{2}}$ and $u = (\lambda^2 + i\sigma\mu_0\omega)^{\frac{1}{2}}$. If the conductivity σ and/or the frequency ω are sufficiently low, eqn. 1 is reduced to the simple static form

$$\Phi_s = -\frac{IA}{4\pi}\frac{\partial}{\partial y}\int_0^\infty J_0(\lambda\rho)\exp\{-\lambda(h+z)\}\,d\lambda$$

$$= -\frac{IA}{4\pi}\frac{\partial}{\partial y}\{\rho^2+(h+z)^2\}^{-\frac{1}{2}} \qquad (3)$$

On carrying out the differentiations in eqns. 1 and 2 and changing the integration variable to dimensionless form, we readily obtain convenient explicit forms for the fields for $z > 0$. Thus

$$H_x = \{IA/(2\pi h^3)\}\,CS\{(T/D)-M\} \qquad (4)$$

$$H_y = -\{IA/(2\pi h^3)\}\{(S^2/D)T + C^2 M\} \qquad (5)$$

$$H_z = \{IA/(2\pi h^3)\}\,CN \qquad (6)$$

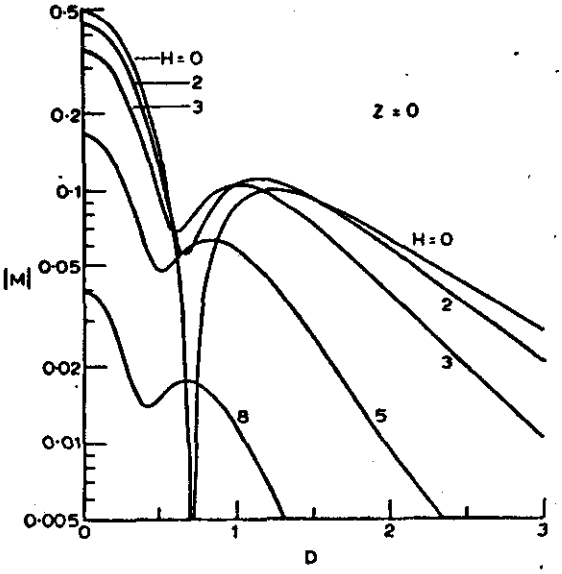

Fig. 2 *Function |M|, proportional to $|H_x|$, for observer at (0, y, 0) as a function of D = y/h for various values of $H = (\sigma\mu_0\omega)^{\frac{1}{2}}h$*

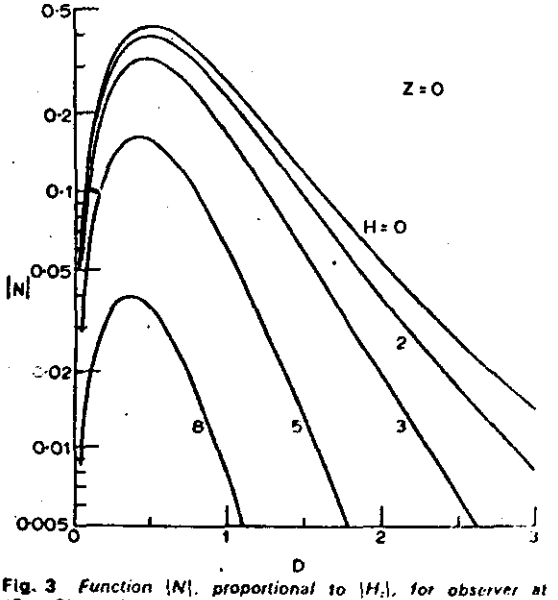

Fig. 3 *Function |N|, proportional to $|H_z|$, for observer at (0, y, 0) as a function of D = y/h*

* FARSTAD, A. J. (Personal communication, April 1972)
† GEYER, R. G. (Personal communication, April 1972)

where

$$C = (y/\rho) = \cos\phi_0$$

$$S = (x/\rho) = \sin\phi_0$$

and

$$D = (x^2+y^2)^{\frac{1}{2}}/h = \rho/h$$

The dimensionless integral functions M, N and T are defined by

$$M = \int_0^\infty gF(g, H, Z)(J_0(gD) - \frac{1}{gD} J_1(gD))dg \quad . \quad . \quad (7)$$

$$N = \int_0^\infty gF(g, H, Z) J_1(gD)\, dg \quad . \quad . \quad . \quad . \quad . \quad . \quad (8)$$

$$T = \int_0^\infty F(g, H, Z) J_1(gD)\, dg \quad . \quad . \quad . \quad . \quad . \quad . \quad (9)$$

where

$$F(g, H, Z) = \frac{g(g^2+iH^2)^{\frac{1}{2}}}{g+(g^2+iH^2)^{\frac{1}{2}}} \exp\{-(g^2+iH^2)^{\frac{1}{2}} - gZ\} \quad (10)$$

where $H = (\sigma\mu_0\omega)^{\frac{1}{2}} h$ and $Z = z/h$.

The corresponding static forms for the basic integrals M, N, and T are the elementary functions

$$M_s = \tfrac{1}{2}\left[\frac{1}{\{D^2+(Z+1)^2\}^{3/2}} - \frac{3D^2}{\{D^2+(Z+1)^2\}^{5/2}}\right] \quad (11)$$

$$N_s = \tfrac{1}{2}\frac{3D(Z+1)}{\{D^2+(Z+1)^2\}^{5/2}} \quad . \quad . \quad . \quad . \quad . \quad . \quad . \quad (12)$$

and

$$T_s = \tfrac{1}{2}\frac{D}{\{D^2+(Z+1)^2\}^{3/2}} \quad . \quad . \quad . \quad . \quad . \quad . \quad . \quad (13)$$

The following cases are of special interest. If $x = 0$ (i.e. $S = 0$ or $\phi_0 = \pi/2$), we find that

$$\left.\begin{aligned} H_x &= 0 \\ H_y &= -\{IA/(2\pi h^3)\}\, M \\ H_z &= IA/(2\pi h^3)\, N \end{aligned}\right\} \quad . \quad . \quad . \quad . \quad . \quad . \quad (14)$$

On the other hand, if $y = 0$ (i.e. $C = 0$ or $\phi_0 = 0$), we see that

$$\left.\begin{aligned} H_x &= 0 \\ H_y &= -\{IA/(2\pi h^3)\}(T/D) \\ H_z &= 0 \end{aligned}\right\} \quad . \quad . \quad . \quad . \quad . \quad (15)$$

A general computer program has been written for the integrals M, N, and T/D that will yield numerical results for any value of the parameters D, H and Z. To illustrate the situation here, we plot $|M|$, $|N|$ and $|T/D|$ as functions of D in Figs. 2, 3 and 4, respectively, for the case $Z = 0$ and various values of H. The appropriate static behaviour is evident for the case $H = 0$. In general, we note that $H \simeq 0{\cdot}086(\sigma_m f)^{\frac{1}{2}} h_{km}$, where σ_m is the earth conductivity in millisiemens per metre, f is the frequency in hertz and h_{km} is the burial depth in kilometres. For example, if $\sigma_m = 1$, $f = 100$ and $h_{km} = 0{\cdot}2$, we see that $H = 0{\cdot}17$.

The functional behaviour of $|N|$ indicated in Fig. 3 shows that, in general, the vertical component H_z has a null directly over the source. This would appear to be a useful diagnostic property. On the other hand, the functional dependences of M and T provide secondary criteria that could also be exploited.

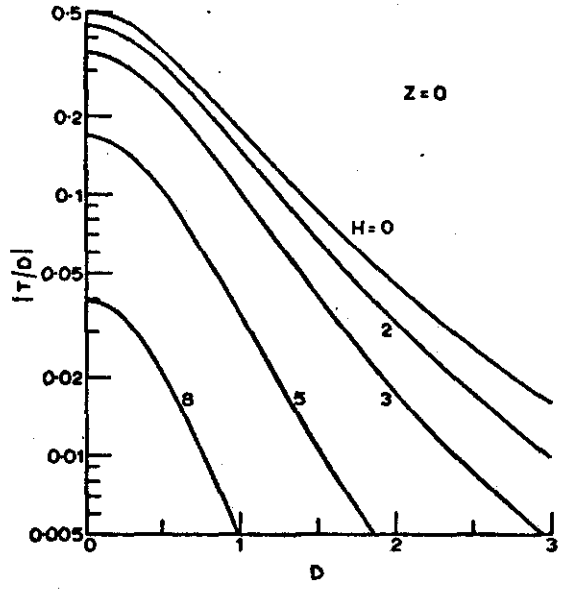

Fig. 4 *Function $|T/D|$, proportional to $|H_z|$ for observer at (x, 0, 0) as a function of $D = x/h$*

The results described here are part of analytical study supported by the US Bureau of Mines under a contract monitored by H. E. Parkinson. I am grateful to K. P. Spies for performing the calculations.

JAMES R. WAIT

Environmental Research Laboratories
National Oceanic & Atmospheric Administration
US Department of Commerce
Boulder, Colo. 80302, USA

30th June 1972

References

1 WAIT, J. R.: 'Criteria for locating an oscillating magnetic dipole buried in the earth', *Proc. Inst. Elec. Electron. Eng.*, 1971, 59, pp. 1033–1035

2 WAIT, J. R., and CAMPBELL, L. L.: 'The fields of an oscillating magnetic dipole immersed in a semi-infinite conducting medium', *J. Geophys. Res.*, 1953, 58, pp. 167–178 (In eqn. 22, $2\gamma_0^2$ in the numerator should be $2\gamma_1^2$.)

Radio Science, Volume 8, Numbers 8, 9, pages 813–818, August-September 1973

The electromagnetic response of a buried sphere for buried-dipole excitation

David A. Hill

Institute for Telecommunication Sciences, Office of Telecommunications, US Department of Commerce, Boulder, Colorado 80302

James R. Wait

Cooperative Institute for Research in Environmental Sciences, University of Colorado, Boulder, Colorado 80302 and National Oceanic and Atmospheric Administration, Environmental Research Laboratories, US Department of Commerce, Boulder, Colorado 80302

(Received April 4, 1973.)

The effect of a spherical inhomogeneity on the surface fields of a buried magnetic dipole source is determined from the reradiated fields of induced electric and magnetic dipole moments. For small spheres where the theory is valid, the errors introduced in source location are shown to be small. The results have possible application to rescue operations following coal mine disasters.

INTRODUCTION

The feasibility of locating a buried horizontal-loop source from surface measurements of the vertical and horizontal magnetic-field components has been investigated by *Wait* [1971]. For sufficiently low frequencies, the magnetic fields have a static-like behavior, and a single observation of the ratio and relative phases of the vertical and horizontal components is sufficient for location when the earth is homogeneous. However, when inhomogeneities are present, the surface fields will be modified, and source location may be more difficult.

In order to obtain a quantitative idea of the surface field modifications, we consider a spherical conducting ore zone as a perturbation to the homogeneous half-space. The corresponding rigorous problem of scattering by a buried sphere has been treated by *D'Yakanov* [1959]. Unfortunately, his solution is restricted to azimuthally symmetric excitation, and even then the solution is not in a convenient computational form. However, if the sphere is electrically small and is located at a sufficient distance from both the loop source and the interface, the scattered fields can be identified as the secondary fields of induced dipole moments. The latter are equal to the product of the incident fields and the polarizabilities of the sphere.

Wait [1968] has used this induced dipole approach for scattering by a small sphere above a conducting half-space. The method has the advantage that it is easily generalized to scatterers of other shapes for which both the electric and magnetic polarizabilities are known, such as spheroids [*van de Hulst*, 1957]. This concept has also been considered by *Ward* [1967] in the context of electromagnetic detection of massive sulphide-ore bodies from airborne platforms. In his applications, however, the induced electric dipole moments for his spheres and disk models were not used. This was justified for the low audio frequencies used in exploration systems such as AFMAG.

FORMULATION

The geometry is illustrated in Figure 1, which shows both the Cartesian coordinate system (x, y, z) and the cylindrical coordinate system (ρ, ϕ, z). The half-space $z < 0$ is free space, and, except for the sphere, the lower half-space $z > 0$ has conductivity σ, permittivity ϵ, and free-space permeability μ_0. The sphere of radius a is located at $(x_0, 0, z_0)$, and has conductivity σ_s, permittivity ϵ_s, and permeability μ_s.

The small source loop of area A is located at

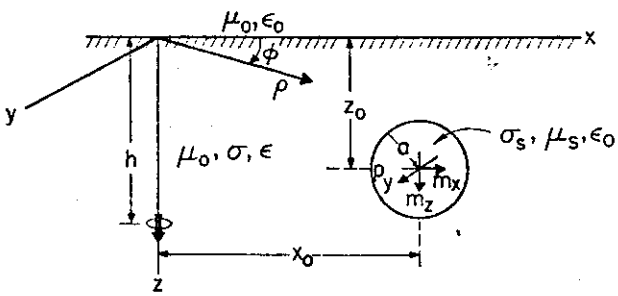

Fig. 1. Geometry for source loop and buried sphere with induced dipole moment.

$(0, 0, h)$ and carries a current I which varies as $\exp(i\omega t)$, where ω is the angular frequency. Since A is small, the source is equivalent to a vertical magnetic dipole. For an observer at the surface ($z = 0$), the vertical and horizontal components in the absence of the scattering sphere, H_ρ^i and H_z^i, have been given by *Wait* [1971]:

$$H_\rho^i = (-IA/2\pi h^3)P$$
$$H_z^i = (IA/2\pi h^3)Q \tag{1}$$

Here, P and Q are the dimensionless quantities:

$$\begin{matrix} P \\ Q \end{matrix} = \int_0^\infty \{[s^3 \exp(-u)]/(s+u)\} \begin{matrix} J_1(sD) \\ J_0(sD) \end{matrix} ds \tag{2}$$

where $u = (s^2 + iH^2)^{1/2}$, J_0 and J_1 are zero- and first-order Bessel functions, $H = (\sigma\mu_0\omega)^{1/2}h$, and $D = \rho/h$. The result in (2) assumes that displacement currents are negligible, and we retain this assumption throughout since we are interested in low frequencies. *Wait* [1971] has shown that for H sufficiently small, a single measurement of the complex ratio H_ρ^i/H_z^i is adequate to determine D and consequently ρ if h is known.

INDUCED DIPOLE MOMENTS

Although the distances involved here are much less than a free-space wavelength, they are not necessarily small compared to a wavelength in the lower half-space. Consequently, the induced electric dipole moment must be considered as well as the induced magnetic dipole moment. This is in contrast to the case in which the source and the scatterer are above ground [*Wait*, 1968].

Since both types of dipole moments are induced, both the unperturbed electric and magnetic fields at the sphere center $(x_0, 0, z_0)$ must be calculated. The unperturbed magnetic field has both z and x components, H_z^0 and H_x^0, and the unperturbed electric field has only a y component, E_y^0. These components can be obtained from *Wait* [1951; 1971], *Baños* [1966], or *Ward* [1967], and written in the following form which is similar to (1):

$$H_x^0 = (IA/2\pi h^3)Q^0$$
$$H_z^0 = (-IA/2\pi h^3)P^0 \tag{3}$$
$$E_y^0 = (-iH^2IA/4\pi\sigma h^4)Y^0$$

where

$$Q^0 = (1/2)\int_0^\infty \{\exp[-u|1-Z|] + [(u-s)/(u+s)]\exp[-u(1+Z)]\} \cdot \{[s^3 J_0(sX)]/u\}\, ds$$

$$P^0 = (1/2)\int_0^\infty \{\exp[-u|1-Z|] - [(u-s)/(u+s)]\exp[-u(1+Z)]\} \cdot s^2 J_1(sX)\, ds$$

$$Y^0 = \int_0^\infty \{\exp[-u|1-Z|] + [(u-s)/(u+s)]\exp[-u(1+Z)]\} \cdot \{[s^2 J_1(sX)]'/u\}\, ds$$

$$Z = z_0/h$$

$$X = x_0/h$$

Note that Z must be positive, but X can be either positive or negative. The evaluation of the integrals will be discussed later.

The induced magnetic dipole moments, m_z and m_x, are given by the product of the magnetic polarizability and the incident magnetic field [*Wait*, 1960; 1968]

$$m_z = -2\pi a^3[3(M+iN)]H_z^0$$
$$m_x = -2\pi a^3[3(M+iN)]H_x^0 \tag{4}$$

where

$$3(M+iN) = -\frac{2\mu_s(\sinh\alpha - \alpha\cosh\alpha) + \mu_0(\sinh\alpha - \alpha\cosh\alpha + \alpha^2\sinh\alpha)}{\mu_s(\sinh\alpha - \alpha\cosh\alpha) - \mu_0(\sinh\alpha - \alpha\cosh\alpha + \alpha^2\sinh\alpha)}$$

where

$$\alpha = (i\omega\mu_s\sigma_s)^{1/2}a$$

We observe that the function $3(M + iN)$ has the following high-frequency limit

$$\lim_{|\alpha|\to\infty} [3(M + iN)] = 1 \tag{5}$$

If me assume that $\sigma_s \gg \sigma$, then the y-directed induced electric-current moment $(Ids)_y$ is given by [*van de Hulst*, 1957]

$$(Ids)_y = 4\pi\sigma a^3 E_y^0 \tag{6}$$

which is valid even if $|\alpha|$ is not large [*Wait*, 1960]. This electric-current moment has dimensions of current times length and differs by a factor of $i\omega$ from the electric-dipole moment which has dimensions of charge times length.

Several assumptions are implicit in the induced dipole-moment method used here to calculate the reradiated fields. First, the sphere radius a must be small in comparison to a wavelength in the lower half-space [*Stratton*, 1941]. Second, the sphere radius must be small compared to the geometric mean of the source and observer distances [*Wait*, 1960]. These conditions insure that higher-order multipoles are not important. Third, the sphere radius must be small compared to the distance between the sphere and the interface so that interactions between the sphere and the interface are not important. Actually, it is possible to compute correction terms which take into account interactions with the interface, and it has been done for a buried cylinder [*Wait*, 1972]. However, the correction terms are more complicated for a sphere because of coupling between the electric and magnetic modes [*Hill*, 1970]. At any rate, the interaction in the static limit has been shown to be unimportant for a sphere-interface separation of at least two sphere radii [*Hill and Wait*, 1972].

SCATTERED FIELDS

From the induced dipole moments in (4) and (6), it is possible to compute the scattered fields at any point on the surface by superposition. However, to simplify the discussion, we restrict our observation point to the x axis. This, of course, includes the point directly above the sphere ($x = x_0$) where the distortion of the surface fields is expected to be greatest. The scattered magnetic field on the x axis has only z and x components, H_z^s and H_x^s, which can be written as the sum of three contributions.

$$\begin{aligned} H_z^s &= H_z^v + H_z^h + H_z^e \\ H_x^s &= H_x^v + H_x^h + H_x^e \end{aligned} \tag{7}$$

H_z^v and H_x^v are the reradiated fields of the vertical magnetic moment m_z, H_z^h and H_x^h are the reradiated fields of the horizontal magnetic moment m_x, and H_z^e and H_x^e are the reradiated fields of the electric moment $(Ids)_y$.

The fields of the vertical magnetic moment can be written in the following form [*Wait*, 1971]

$$\begin{aligned} H_z^v &= (m_z/2\pi h^3)Q^r \\ H_x^v &= (-m_z/2\pi h^3)P^r \end{aligned} \tag{8}$$

where

$$\begin{matrix} P^r \\ Q^r \end{matrix} = \int_0^\infty \{[s^3 \exp(-uZ)]/(s + u)\} \begin{matrix} J_1[s(D - X)] \\ J_0[s(D - X)] \end{matrix} ds$$

Since we are observing the fields on the x axis, we redefine D to be x/h and let it be either positive or negative.

The fields of a horizontal magnetic moment have been given by *Wait* [1972], and for this geometry are given by

$$\begin{aligned} H_z^h &= (-m_x/2\pi h^3)N^r \\ H_x^h &= (-m_x/2\pi h^3)M^r \end{aligned} \tag{9}$$

where

$$N^r = \int_0^\infty \{[s^2 u \exp(-uZ)]/(s + u)\} \cdot J_1[s(D - X)]\, ds$$

$$M^r = \int_0^\infty \{[s^2 u \exp(-uZ)]/(s + u)\} \cdot \{J_0[s(D - X)] - \{J_1[s(D - X)]\}/[s(D - X)]\}\, ds$$

The fields of the electric moment are given by *Wait* [1961] and *Baños* [1966], and can be written in the following form

$$\begin{aligned} H_z^e &= \{[-(Ids)_y]/2\pi h^2\} S^r \\ H_x^e &= \{[-(Ids)_y]/2\pi h^2\} T^r \end{aligned} \tag{10}$$

where

$$S^r = \int_0^\infty \{[s^2 \exp(-uZ)]/(s+u)\} J_1[s(D-X)]\, ds$$

$$T^r = \int_0^\infty \{[\exp(-uZ)]/(s+u)\}((s^2 J_0[s(D-X)] - \{s J_1[s(D-X)]\}/(D-X))\, ds$$

By substituting (3), (4), (6), (8), (9), and (10) into (7), the final expressions for the scattered field are obtained

$$H_z^s = \{[-IA(a/h)^3]/2\pi h^3\} \cdot [3(M+iN)(Q^0Q^r + P^0N^r) - iH^2(Y^0S^r)]$$
$$H_x^s = \{[IA(a/h)^3]/2\pi h^3\} \cdot [3(M+iN)(Q^0P^r - P^0M^r) + iH^2(Y^0T^r)] \quad (11)$$

Note that the contribution from the electric moment goes to 0 as the frequency goes to 0 because H^2 vanishes. However, the contribution from the magnetic moment goes to 0 in the static limit only if the sphere is nonmagnetic ($\mu_s = \mu_0$). This can be seen by examining the behavior of $3(M + iN)$ in (4). This point has also been emphasized by *Ward* [1959].

The total fields observed on the surface are the sum of the incident and scattered fields

$$H_z^t = H_z^i + H_z^s$$
$$H_x^t = H_x^i + H_x^s \quad (12)$$

where H_z^i and H_x^i are given by (1), and H_z^s and H_x^s are given by (11).

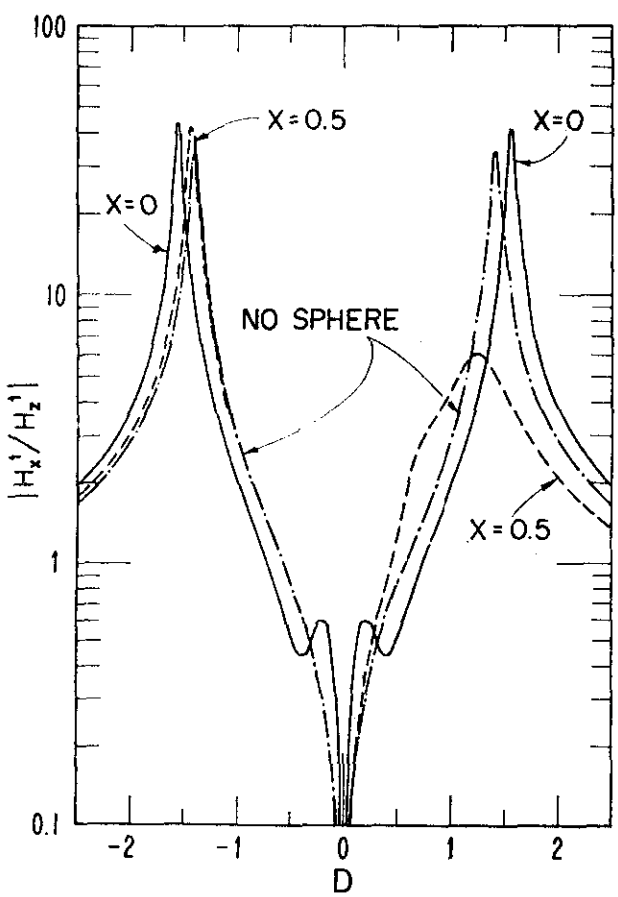

Fig. 2. Effect of sphere location on $|H_z^t/H_z^t|$. $H = 0.2$, $a/h = 0.3$, $Z = 0.5$, $|\alpha| = 5.0$, and $\mu_s = \mu_0$.

NUMERICAL RESULTS

Before performing a numerical evaluation of the integrals required for the magnetic components in (1) and (11), it is useful to obtain the static limits of the integrals by letting H approach 0. These limits are useful because they serve as a check on the general formulation and because H is sometimes quite small in realistic situations. By setting $H = 0$, the following static limits denoted by subscript s are obtained [*Wheelon*, 1968]:

$$P_s = 3D/[2(1+D^2)^{5/2}]$$
$$Q_s = (2-D^2)/[2(1+D^2)^{5/2}]$$
$$Q_s^0 = [2(1-Z)^2 - X^2]/\{2[X^2+(1-Z)^2]^{5/2}\}$$
$$P_s^0 = [3X(1-Z)]/\{2[X^2+(1-Z)^2]^{5/2}\}$$
$$Y_s^0 = X/[X^2+(1-Z)^2]^{5/2}$$
$$P_s^r = [3(D-X)Z]/\{2[(D-X)^2+Z^2]^{5/2}\}$$
$$Q_s^r = [2Z^2 - (D-X)^2]/\{2[(D-X)^2+Z^2]^{5/2}\}$$
$$N_s^r = [3(D-X)Z]/\{2[(D-X)^2+Z^2]^{5/2}\}$$
$$M_s^r = [Z^2 - 2(D-X)^2]/\{2[(D-X)^2+Z^2]^{5/2}\}$$
$$S_s^r = (D-X)/\{2[(D-X)^2+Z^2]^{3/2}\}$$
$$T_s^r = -Z/\{2[Z^2+(D-X)^2]^{3/2}\} \quad (13)$$

If these static results are subtracted from the general integral forms given earlier, then the convergence of the remaining numerical integral is improved if H is not too large. Of course, for $H = 0$, the integrands vanish and only the static terms remain. Computer programs were written for the numerical integrals, and the resultant quantities of

interest, $|H_z^t/H_x^t|$ and arg (H_z^t/H_x^t), were examined as a function of the various parameters.

Results for a nonmagnetic sphere ($\mu_s = \mu_0$) are shown in Figures 2 and 3. Parameter values are $H = 0.2$, $Z = 0.5$, $a/h = 0.3$, $|\alpha| = 5$, and $X = 0$ and 0.5. In a typical example where $f = 100$ Hz and $\sigma = 10^{-3}$ mhos m^{-1}, h would be 225 m. The amplitude curve in Figure 2 with no sphere present agrees with the previous result of *Wait* [1971]. With the sphere directly above the source ($X = 0$), the curve is still symmetrical about $D = 0$. The peak magnitudes are increased somewhat, but the peak locations are only slightly shifted. When the sphere is no longer above the source ($X = 0.5$), symmetry is lost and the peak for negative D increases while the peak for positive D decreases. The peak locations are again only slightly shifted. The phase curves in Figure 3 indicate that the greatest phase deviations occur close to the sphere location (D small for $X = 0$ and $D > 0$ for $X = 0.5$).

Results for smaller spheres and spheres farther from the source indicate smaller deviations. Another interesting result is that deviations were smaller for larger values of $|\alpha|$ due to the fact that the scattered field becomes more nearly real. Results were not obtained for larger spheres because the simplified treatment used here is not expected to be valid if a/h becomes too large.

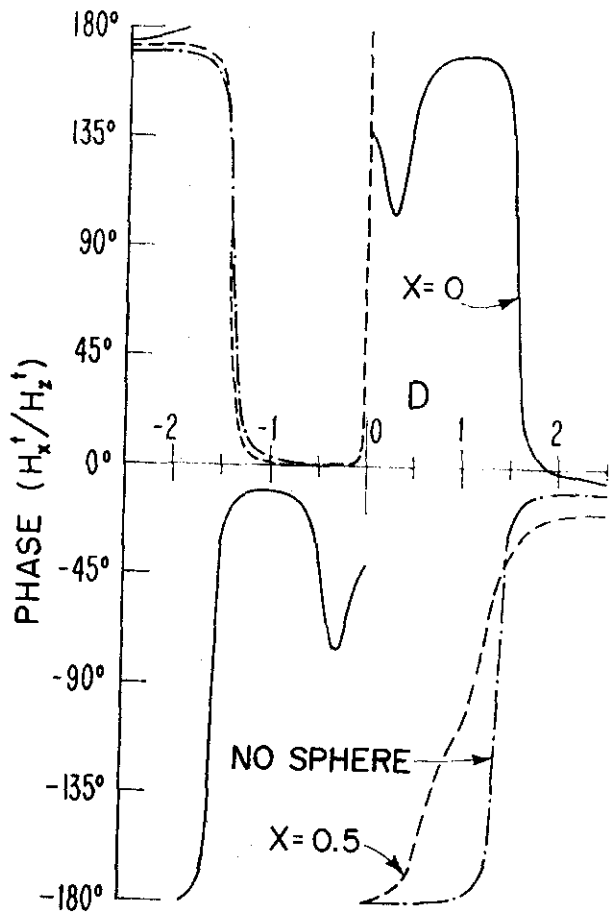

Fig. 3. Effect of sphere location on arg (H_z^t/H_x^t).

CONCLUDING REMARKS

A method for calculating the perturbation of the surface fields of a buried magnetic dipole has been developed. The method utilizes the reradiated fields of induced electric and magnetic dipole moments and is valid when the sphere radius is small compared with the source distance, the interface distance, and the wavelength in the earth.

A typical example shows that the magnitude and phase of the ratio of horizontal to vertical magnetic field can be noticeably altered by the presence of a sphere which is located at half the source depth and has a radius of 0.3 times the source depth. However, the variation of the surface fields as a function of position remains quite similar, and only small errors in source location should result.

Larger deviations can be expected when the sphere is larger or closer to the source or the interface, but the simplified theory presented here is not valid under such conditions. The study of this case is a worthwhile extension.

REFERENCES

Baños, A. (1966), *Dipole Radiation in the Presence of a Conducting Half-space*, pp. 195–230, Pergamon, New York.

D'Yakonov, B. P. (1959), The diffraction of electromagnetic waves by a sphere located in a half-space, *Bull. Acad. Sci. USSR, Geophys. Ser., 11*, 1120–1125.

Hill, D. A. (1970), Electromagnetic scattering concepts applied to the detection of targets near the ground, Ph.D. dissertation, pp. 90–100, Ohio State University, Columbus, Ohio.

Hill, D. A., and J. R. Wait (1972), Electromagnetic scattering of a small spherical obstacle near the ground, *Can. J. Phys., 50*(3), 237–243.

Stratton, J. A. (1941), *Electromagnetic Theory*, pp 563 573, McGraw-Hill, New York.

van de Hulst, H. C. (1957), *Light Scattering by Small Particles*, pp. xxx–xxx, John Wiley, New York.

Wait, J. R. (1951), The magnetic dipole over the horizontally stratified earth, *Can. J. Phys., 29*(6), 577–592.

Wait, J. R. (1960), On the electromagnetic response of a conducting sphere to a dipole field, *Geophysics, 25*(3), 649–658.

Wait, J. R. (1961), The electromagnetic fields of a horizontal dipole in the presence of a conducting half-space, *Can. J. Phys., 39*(7), 1017–1028.

Wait, J. R. (1968), Electromagnetic induction in a small conducting sphere above a resistive half-space, *Radio Sci., 3*(10), 1030–1034.

Wait, J. R. (1971), Criteria for locating an oscillating magnetic dipole buried in the earth, *Proc. IEEE, 59*(6), 1033–1035.

Wait, J. R. (1972), The effect of a buried conductor on the subsurface fields for line source excitation, *Radio Sci., 7*(5), 587–591.

Ward, S. H. (1959), Unique determination of conductivity, susceptibility, size, and depth in multifrequency electromagnetic exploration, *Geophysics, 24*, 531–546.

Ward, S. H. (1967), Electromagnetic theory for geophysical applications, in *Mining Geophysics*, vol. 2, edited by D. A. Hansen, W. R. Heinricks, Jr., R. C. Holmen, R. E. MacDougall, G. R. Rogers, J. S. S. Sumner, and S. H. Ward, pp. 10–196, Society of Exploration Geophysicists, Tulsa, Okla.

Wheelon, A. D. (1968), *Tables of Summable Series and Integrals Involving Bessel Function*, pp. 68–92, Holden-Day, San Francisco, Calif.

Preliminary Report to U.S. Bureau of Mines on Contract No. H0122061, with the Institute for Telecommunication Sciences, Office of Telecommunications, U.S. Department of Commerce, Boulder, CO, monitored by Dr. James A. Powell
Principal Investigator - Dr. James R. Wait 14 January 1974

Effect of a Spherical Scatterer on EM Source Location

by
David A. Hill
Institute for Telecommunication Sciences
Office of Telecommunications
U.S. Department of Commerce
Boulder, Colorado 80302

ABSTRACT

Calculations are made to determine the shift in the overhead null of a buried vertical magnetic dipole caused by a spherical scatterer located near the earth surface. A table of results is given to illustrate the effect of various parameters, and a closed form expression is given for a special case.

INTRODUCTION

The distortion of surface fields of a buried vertical magnetic dipole (horizontal loop) has been examined for several scattering bodies: spheres [Hill and Wait, 1973a], prolate spheroids [Hill and Wait, 1973b], and infinite cylinders [Hill and Wait, 1973c]. Although the entire magnetic field profile is of interest in source location, the shift in the null of the horizontal magnetic field is a limiting factor in location accuracy. Consequently, we examine here the null shift caused by a highly conducting body near the earth surface. The conducting body could be natural or man-made (vehicle, machinery, etc.).

Since the past treatments of the prolate spheroid and infinite cylinder have a more restricted realm of validity, we choose to utilize the previous work on the conducting sphere [Hill and Wait, 1973a]. The previously developed computer program is applicable with only minor modifications, and the specific numerical parameters of interest have been furnished by Dr. James A. Powell (private communication, September 7, 1973).

GEOMETRY AND PARAMETERS

The geometry of the source and scatterer are shown in Fig. 1. The sphere is centered at $x = x_o$ and $y = 0$. Although the general analysis is for an arbitrary sphere depth z_o, here we set $z_o = a$ so that the sphere is tangent to the surface. This is as high as we can position the sphere since the previous analysis is for a buried sphere. We omit the analysis and assumptions here since they have been covered previously [Hill and Wait, 1973a]. Some error will result from positioning the sphere close to the interface (since interaction between the sphere and the interface have been neglected), but this error will be small for sufficiently low frequencies. The permeability of both the half-space and the sphere are taken to be that of free space.

The frequency of use is taken to be 2000 Hz. Several sphere masses and densities have been suggested, but only the largest resultant sphere radius of 11.7' is used here. This corresponds to a mass of 100 tons and a density of 30 lbs/ft^3. We present results in English units as requested, but all calculations are actually performed in MKS units. The sphere conductivity is taken to be 10^6mhos/m which corresponds to that of cast iron. The resultant electrical size of the sphere $|\alpha|$ is given by

$$|\alpha| = \sqrt{2\pi f \mu_o \sigma_s}\, a = 448.$$

Consequently, the sphere appears to be almost a perfect conductor at 2000 Hz.

Two depths, h = 500' and 1000', are assumed for the transmitter depth. Two values of the horizontal displacement of the sphere, x_o = 10' and 100', are also assumed. For earth conductivity σ, 10^{-2}mhos/m and 10^{-3}mhos/m are assumed. Consequently, we are considering a total of eight cases. Other values of parameters have been examined, but the resultant null shifts are too small to be of interest.

NUMERICAL RESULTS

In order to locate the null in the horizontal magnetic field, the x - component H_x was computed along the x - axis. Although the primary field H_x^p has a null at $x = 0$, the total field is complex and in general there is no value of x for which $H_x = 0$. Consequently, we are actually searching for local minima of H_x which occur at $x = x_m$. The values of x_m for eight cases discussed earlier are given in Table 1.

Note that for $x_o = 10'$, there are actually three minima, and one of them occurs for negative x_m. Of course, the largest error in source location would occur for the maximum $|x_m|$ which in these cases is on the order of 30'. Results are not shown for larger values of x_o and smaller values of a because the resultant values of $|x_m|$ are extremely small.

SPECIAL LOW-FREQUENCY CASE

Since a partial profile of H_x is required to obtain the resultant null shift for each set of parameters, a great many calculations are required to determine the effect of various parameters on the null shift. Consequently, it is desirable to obtain an expression which gives the dependence on some of the parameters explicitly. This can be done if the frequency is sufficiently low to neglect currents in the overburden and if the sphere conductivity is sufficiently high to appear perfectly conducting. Mathematically, these conditions are equivalent to the followng inequalities

$$(\omega \mu_o \sigma)^{1/2} h \ll 1 \quad \text{and} \quad (\omega \mu_o \sigma_s)^{1/2} a \gg 1.$$

Under these conditions, the magnetic fields take on a static behavior, and the fields scattered by the sphere are essentially those of an induced magnetic dipole. To simplify even further, we let $z_o = 0$ in Fig. 1. Consequently only the horizontal induced magnetic dipole moment p_x contributes to

the horizontal magnetic field H_x on the x axis. The horizontal magnetic field incident at the sphere center H_x^o is given by

$$H_x^o = \frac{-IA}{2\pi h^3} \frac{3(x_o/h)}{2[1 + (x_o/h)^2]^{5/2}} \tag{1}$$

where IA is the magnetic moment of the transmitting loop. The magnetic polarizability of the sphere is $-2\pi a^3$. Consequently, the x component of the induced magnetic dipole moment is given by

$$p_x = \frac{IA\, a^3}{h^3} \frac{3(x_o/h)}{2[1 + (x_o/h)^2]^{5/2}} \tag{2}$$

On the x axis, H_x can now be written as the sum of the primary and secondary fields:

$$H_x = \frac{IA}{2\pi h^3} \left\{ \frac{-3(x/h)}{2[1 + (x/h)^2]^{5/2}} + \frac{a^3}{|x - x_o|^3} \frac{3(x_o/h)}{2[1 + (x_o/h)^2]^{5/2}} \right\} \tag{3}$$

In order to find the null shift x_m, we set $H_x = 0$:

$$\frac{(x_m/h)}{[1 + (x_m/h)^2]^{5/2}} - \frac{a^3}{|x_m - x_o|^3} \frac{(x_o/h)}{[1 + (x_o/h)^2]^{5/2}} = 0 \tag{4}$$

In general, (4) can be solved by plotting the function versus x_m. However, if x_o is sufficiently large, then the following two approximations are valid:

$$\frac{x_m}{x_o} << 1 \quad \text{and} \quad \frac{x_m}{h} << 1 \tag{5}$$

If (5) is applied to (4), we have a closed form solution for x_m:

$$x_m = \frac{a^3\, \mathrm{sgn}(x_o)}{x_o^2[1 + (x_o/h)^2]^{5/2}} \tag{6}$$

Note that the null is moved toward the sphere due to the $\mathrm{sgn}(x_o)$ factor. This approximate expression has been found to check with the computer solution in appropriate test cases.

CONCLUSIONS

From the results in Table 1 and Eqn. 6, we can draw some conclusions about null shifts caused by scatterers near the surface. First, the null shift is only weakly dependent on the transmitting antenna depth and the overburden conductivity. Second, the null shift is roughly proportional to the volume of the scattering body (proportional to a^3). The null shift decreases rapidly as the horizontal displacement x_o increases. Consequently, even a moderate size scatter (11.7' radius sphere) has a significant effect only when it is close to the null point. This is consistent with measurements by Farstad (1973) on the effect of a vehicle on the surrounding magnetic field.

REFERENCES

Farstad, A.J. (1973), Electromagnetic location experiments in a deep hardrock mine", prepared by Westinghouse Georesearch Laboratory, for the U.S. Bureau of Mines.

Hill, D.A. and J.R. Wait (1973a), "The electromagnetic response of a buried sphere for buried dipole excitation", Radio Science, 8, (8,9), 813-818.

Hill, D.A. and J.R. Wait (1973b), "Perturbation of magnetic dipole fields by a perfectly conducting prolate spheroid", Preliminary report to U.S. Bureau of Mines.

Hill, D.A. and J.R. Wait (1973c), "Perturbation of magnetic dipole fields by a finitely conducting circular cylinder", Preliminary report to U.S. Bureau of Mines.

TABLE AND FIGURE CAPTIONS

Figure 1 Geometry for the source loop and a spherical scatterer.

Table 1 Effect of various parameters on the null shift.

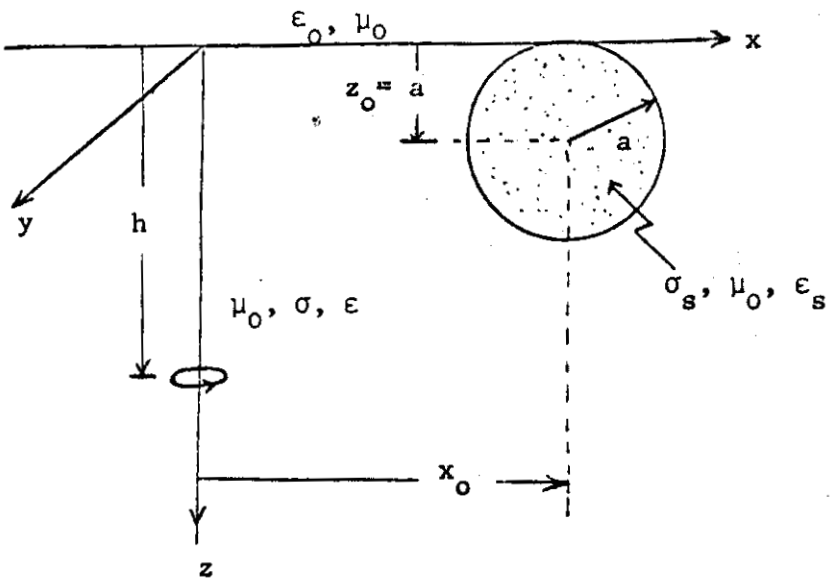

Figure 1

TABLE 1

a = 11.7', f = 2000 Hz

h	σ	x_o	x_m
500'	10^{-3} mhos/m	10'	-14.4', 11.1', 30.7'
500'	10^{-3} "	100'	.07'
500'	10^{-2} "	10'	-13.9', 11.1', 30.2'
500'	10^{-2} "	100'	.085'
1000'	10^{-3} "	10'	-18.0', 11.0', 34.4'
1000'	10^{-3} "	100'	.01'
1000'	10^{-2} "	10'	-16.5', 11.0', 30.0'
1000'	10^{-2} "	100'	.05'

Journal of Applied Physics, Vol. 42,
No. 10, 3866-3869, September 1971

Transient Signals from a Buried Magnetic Dipole

James R. Wait and David A. Hill
Cooperative Institute for Research in the Environmental Sciences, University of Colorado, Boulder, Colorado 80302
(Received 28 January 1971)

The solution for a pulse-excited magnetic dipole is carried through for a conducting half-space model of the earth. All displacement currents are neglected so the solution is not valid at very small times in the transient response. It is shown that the waveforms of the magnetic field components on the surface depend both on the conductivity of the earth and the geometrical parameters of the problem. The results have possible application to electromagnetic signaling and direction finding for a buried source.

I. INTRODUCTION

One method of signaling to the surface from a terminal buried in the earth is to shock excite an underground loop of wire. Because of the Ohmic conduction in the overburden, we can expect only that the low-frequency spectral components will reach the surface. Also, because of the dispersion, the radiated transient signal will undergo considerable distortion in waveform. It is of interest to examine this situation in a quantitative fashion. To facilitate the analysis, we shall adopt a homogeneous half-space model for the earth. The unground loop buried at depth h is represented by a magnetic dipole with a vertical axis. The situation is illustrated in Fig. 1.

The time-harmonic problem of a magnetic dipole in the presence of a half-space is very well known. A great deal of attention has been given to the numerical evaluation of the integrals for the range of parameters of interest in geophysical prospecting.[1] In such cases, the linear distances involved are very small compared with the wavelength in air, but not necessarily with the wavelength in the conductor. Except for certain second-order effects, this means that all displacement currents can be neglected at the outset. In spite of this simplification, the integrals in the time-harmonic problem are nonelementary and numerical integration is the order of the day.[1,2] However, we wish to point out that the pulse solution of the problem can be carried through in a relatively simple fashion. This fact was demonstrated earlier for a buried electric dipole,[3] but the method we adopt here for the magnetic dipole seems more straightforward.

II. TIME-HARMONIC FORMULATION

As indicated above, the formal integral solution of the time-harmonic problem is well known.[1] Thus, if the time factor is $e^{i\omega t}$, the magnetic field components H_ρ and H_z in the air (i.e., $z>0$) are given by

$$H_\rho = b_0(i\omega)\ P(i\omega) \tag{1}$$

and

$$H_z = b_0(i\omega)\ Q(i\omega), \tag{2}$$

where $b_0(i\omega)$ is a normalizing quantity which is proportional to the current in the small loop, while

$$\begin{aligned} P(i\omega) &= h^3 \int_0^\infty F(i\omega, \lambda, h)\lambda^3 e^{-\lambda z} J_1(\lambda\rho)\ d\lambda, \\ Q(i\omega) &= h^3 \int_0^\infty F(i\omega, \lambda, h)\lambda^3 e^{-\lambda z} J_0(\lambda\rho)\ d\lambda, \end{aligned} \tag{3}$$

where J_0 and J_1 are Bessel functions of order zero and order one, respectively. The function of $i\omega$, λ, and h in the integrand of (3) is

$$F(i\omega, \lambda, h) = [(\lambda^2 + i\sigma\mu\omega)^{1/2} + \lambda]^{-1} \exp[-(\lambda^2 + i\sigma\mu\omega)^{1/2} h]. \tag{4}$$

For a loop of area A, turns N, and current $I(i\omega)$, we have

$$b_0(i\omega) = AN(2\pi h^3)^{-1} I(i\omega). \tag{5}$$

III. TRANSIENT FORMULATION

We now consider the fact that the loop current (assumed uniform) is $I_0\delta(t)$, where $\delta(t)$ is the unit impulse function. We then wish to calculate the time-dependent voltages $v_\rho(t)$ and $v_z(t)$ induced in a small receiving loop oriented in the ρ and z directions, respectively. If the receiving loop has area A_r and turns N_r, these voltages are obtained as follows:

$$v_\rho(t) = A_r N_r \mu \frac{\partial}{\partial t} h_\rho(t),$$

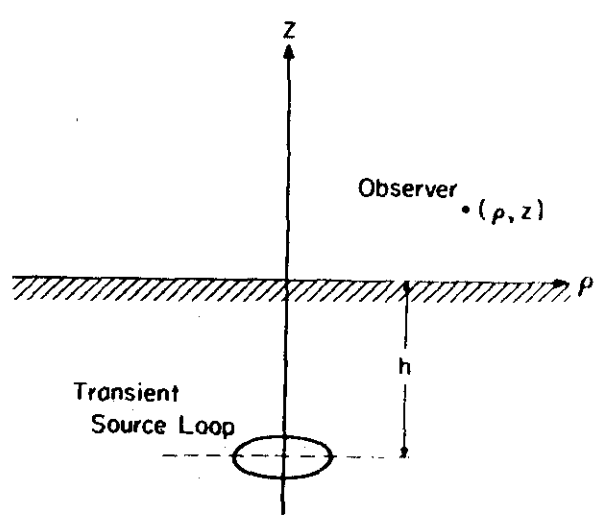

FIG. 1. Geometry for the situation.

$$v_\rho(t) = A_r N_r \mu \frac{\partial}{\partial t} h_\rho(t), \tag{6}$$

where

$$h_\rho(t) = \mathcal{L}^{-1} b_0(s) P(s),$$
$$h_z(t) = \mathcal{L}^{-1} b_0(s) Q(s), \tag{7}$$

and

$$b_0(s) = AN(2\pi h^3)^{-1} I_0. \tag{8}$$

Here μ is the magnetic permeability of the whole space. $\mathcal{L}^{-1}$ denotes the inverse Laplace transform operator and s is the transform variable which can be identified formally with $i\omega$ in the time-harmonic problem. Thus, consolidating the above developments, we have

$$v_\rho(t) = \frac{ANA_r N_r \mu I_0}{2\pi h^3} p(t),$$
$$v_z(t) = \frac{ANA_r N_r \mu I_0}{2\pi h^3} q(t), \tag{9}$$

where

$$p(t) = \mathcal{L}^{-1} s P(s), \tag{10}$$
$$q(t) = \mathcal{L}^{-1} s Q(s), \tag{11}$$

or, equivalently,

$$p(t) = h^3 \int_0^\infty [\mathcal{L}^{-1} sF(s, \lambda, h)] \lambda^3 e^{-\lambda z} J_1(\lambda\rho)\, d\lambda,$$
$$q(t) = h^3 \int_0^\infty [\mathcal{L}^{-1} sF(s, \lambda, h)] \lambda^3 e^{-\lambda z} J_0(\lambda\rho)\, d\lambda, \tag{12}$$

and

$$\mathcal{L}^{-1} sF(s, \lambda, h) = \mathcal{L}^{-1} s[(\lambda^2 + \sigma\mu s)^{1/2} + \lambda]^{-1} \times \exp[-(\lambda^2 + \sigma\mu s)^{1/2} h]. \tag{13}$$

The inverse transform can be evaluated by performing the following sequences of operations:

$$\begin{aligned}
\mathcal{L}^{-1} sF(s, \lambda, h) &= (\sigma\mu)^{-1} \mathcal{L}^{-1} [(\lambda^2 + \sigma\mu s)^{1/2} - \lambda] \\
&\quad \times \exp[-(\lambda^2 + \sigma\mu s)^{1/2} h] \\
&= -\frac{1}{\sigma\mu} \left(\lambda + \frac{\partial}{\partial h}\right) \mathcal{L}^{-1} \\
&\quad \times \exp[-(\lambda^2 + \sigma\mu s)^{1/2} h] \\
&= -\frac{1}{\sigma\mu} \left[\left(\lambda + \frac{\partial}{\partial h}\right) \frac{(\sigma\mu)^{1/2} h}{2\pi^{1/2} t^{3/2}}\right] \\
&\quad \times \exp\left(-\frac{\sigma\mu h^2}{4t} - \frac{\lambda^2 t}{\sigma\mu}\right) \\
&= \frac{1}{2(\pi\sigma\mu)^{1/2} t^{3/2}} \left(1 - \frac{\sigma\mu h^2}{2t} + \lambda h\right) \\
&\quad \times \exp\left(-\frac{\sigma\mu h^2}{4t} - \frac{\lambda^2 t}{\sigma\mu}\right).
\end{aligned} \tag{14}$$

Here, we have used a standard Laplace transform relation[4] to perform the inversion before applying the derivative operation.

Combining (12) and (14), we see that the desired time-dependent waveforms are

$$p(t) = -\frac{h^3 \exp(-\sigma\mu h^2/4t)}{2(\pi\sigma\mu)^{1/2} t^{3/2}} \int_0^\infty \lambda^3 \left(1 - \frac{\sigma\mu h^2}{2t} + \lambda h\right) e^{-\lambda z} \times \exp\left(-\frac{\lambda^2 t}{\sigma\mu}\right) J_1(\lambda\rho)\, d\lambda, \tag{15}$$

$$q(t) = -\frac{h^3 \exp(-\sigma\mu h^2/4t)}{2(\pi\sigma\mu)^{1/2} t^{3/2}} \int_0^\infty \lambda^3 \left(1 - \frac{\sigma\mu h^2}{2t} + \lambda h\right) e^{-\lambda z} \times \exp\left(-\frac{\lambda^2 t}{\sigma\mu}\right) J_0(\lambda\rho)\, d\lambda,$$

where it is understood that the right-hand side is zero if $t < 0$. For a general location (ρ, z) of the observer in the air, the integrals are of a form which can be evaluated numerically without undue difficulty. In particular, we note that for $t > 0$, the integrands are highly damped as λ approaches infinity along the real axis. Also, the convergence is improved if $z > 0$, corresponding to an observer in the air *above* the ground.

IV. REDUCTION TO WORKING FORM

For the important special case $z = 0$, the integrals in (15) can be treated analytically. The integrals to contend with are all of the form

$$A_{m,n} = \int_0^\infty \lambda^m e^{-\alpha\lambda^2} J_n(\lambda\rho)\, d\lambda, \tag{16}$$

where $\alpha = t/\sigma\mu$, $m = 3, 4$, and $n = 0, 1$. Using the ascending series definition of the Bessel function $J_n(\lambda\rho)$, we can deduce without difficulty that

$$A_{3,0} = \frac{1}{2\alpha^2} \left(1 - \frac{\rho^2}{4\alpha}\right) \exp\left(-\frac{\rho^2}{4\alpha}\right), \tag{17}$$

$$A_{4,1} = \frac{\rho}{2\alpha^3} \left(1 - \frac{\rho^2}{8\alpha}\right) \exp\left(-\frac{\rho^2}{4\alpha}\right), \tag{18}$$

$$A_{4,0} = \frac{1}{2\alpha^{5/2}} \sum_{n=0}^{\infty} \frac{\Gamma(n + \frac{5}{2})}{(n!)^2} \left(-\frac{\rho^2}{4\alpha}\right)^n, \tag{19}$$

$$A_{3,1} = \frac{\rho}{4\alpha^{5/2}} \sum_{n=0}^{\infty} \frac{\Gamma(n + \frac{5}{2})}{(n+1)(n!)^2} \left(-\frac{\rho^2}{4\alpha}\right)^n. \tag{20}$$

Actually, the latter two relations can be expressed in terms of derivatives of the modified Bessel function I_0. For example, if we start with the known form[5]

$$A_{0,0} = \tfrac{1}{2}(\pi/\alpha)^{1/2} \exp(-\rho^2/8\alpha) I_0(\rho^2/8\alpha), \tag{21}$$

we see that

$$A_{4,0} = \frac{\partial^2 A_{0,0}}{\partial \alpha^2} \tag{22}$$

and

$$A_{3,1} = \frac{\partial^2 A_{0,0}}{\partial \alpha \partial \rho}. \tag{23}$$

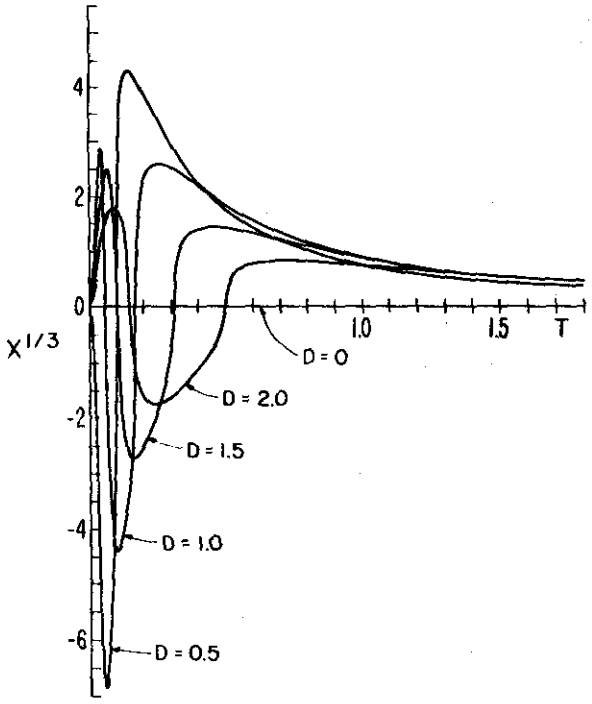

FIG. 2. Waveform of the time derivative of the horizontal magnetic field on the surface for an impulsive current in the buried source loop.

These can be further reduced to a complicated combination of exponential factors and modified Bessel functions I_0 and I_1. Thus, we have

$$A_{4,0}=\frac{\pi^{1/2}}{8\alpha^{5/2}}\exp\left(-\frac{\rho^2}{8\alpha}\right)\left[\left(3-\frac{3}{2}\frac{\rho^2}{\alpha}+\frac{\rho^4}{8\alpha^2}\right)I_0+\left(\frac{\rho^2}{\alpha^2}-\frac{5\rho^4}{16\alpha^2}\right)I_1\right] \tag{22'}$$

and

$$A_{3,1}=\frac{\pi^{1/2}\rho}{8\alpha^{5/2}}\exp\left(-\frac{\rho^2}{8\alpha}\right)\left[\left(\frac{3}{2}-\frac{\rho^2}{4\alpha}\right)I_0+\left(\frac{\rho^2}{4\alpha}-\frac{1}{2}\right)I_1\right], \tag{23'}$$

where the arguments of the modified Bessel functions are $\rho^2/8\alpha$.

Using the results (17)–(20), the waveform functions defined by (15) are given by

$$p(t)=-[4\pi^{1/2}(\sigma\mu h^2)^2]^{-1}X(D,T) \tag{24}$$

and

$$q(t)=-[4\pi^{1/2}(\sigma\mu h^2)^2]^{-1}Y(D,T), \tag{25}$$

where

$$X(D,T)=\exp\left(-\frac{1}{4T}\right)\frac{1}{T^{7/2}}\left[\left(1-\frac{1}{2T}\right)\frac{D}{T^{1/2}}\times\sum_{n=0}^{\infty}\frac{\Gamma(n+\frac{5}{2})}{(n+1)(n!)^2}\left(-\frac{D^2}{4T}\right)^n+\frac{D}{T}\left(1-\frac{D^2}{8T}\right)\exp\left(-\frac{D^2}{4T}\right)\right] \tag{26}$$

and

$$Y(D,T)=\exp\left(-\frac{1}{4T}\right)\frac{1}{T^{7/2}}\left[\left(1-\frac{1}{2T}\right)\left(1-\frac{D^2}{2T}\right)\exp\left(-\frac{D^2}{4T}\right)+\frac{1}{T^{1/2}}\sum_{n=0}^{\infty}\frac{\Gamma(n+\frac{5}{2})}{(n!)^2}\left(-\frac{D^2}{4T}\right)^n\right], \tag{27}$$

where $T=\alpha/h^2=t/\sigma\mu h^2$ and $D=\rho/h$. Here, we note that X and Y are dimensionless functions of the time parameter T and the distance parameter D. As a consequence, $p(t)$ and $q(t)$ have dimensions of $\sec^{-2}$ which is consistent with our formulation.

The series expansions indicated in (26) and (27) are rapidly convergent provided T is not zero and D is not too large compared with unity. In fact, if $D=0$ (corresponding to locating the observer right over the source loop), we see that $X(0,T)=0$ and

$$Y(0,t)=\exp\left(-\frac{1}{4T}\right)\frac{1}{T^{7/2}}\left[\left(1-\frac{1}{2T}\right)+\frac{3\pi^{1/2}}{4}\frac{1}{T^{1/2}}\right]. \tag{28}$$

Equivalent forms of (26) and (27) involving modified Bessel functions are found, from (22b) and (23b), to be

$$X(D,T)=\frac{1}{T^{7/2}}\exp\left(-\frac{1}{4T}\right)\left(\frac{D}{T}\left(1-\frac{D^2}{8T}\right)\exp\left(-\frac{D^2}{4T}\right)+\left(1-\frac{1}{2T}\right)\left\{\frac{D}{4}\left(\frac{\pi}{T}\right)^{1/2}\exp\left(-\frac{D^2}{8T}\right)\times\left[\left(\frac{3}{2}-\frac{D^2}{4T}\right)I_0+\left(\frac{D^2}{4T}-\frac{1}{2}\right)I_1\right]\right\}\right) \tag{29}$$

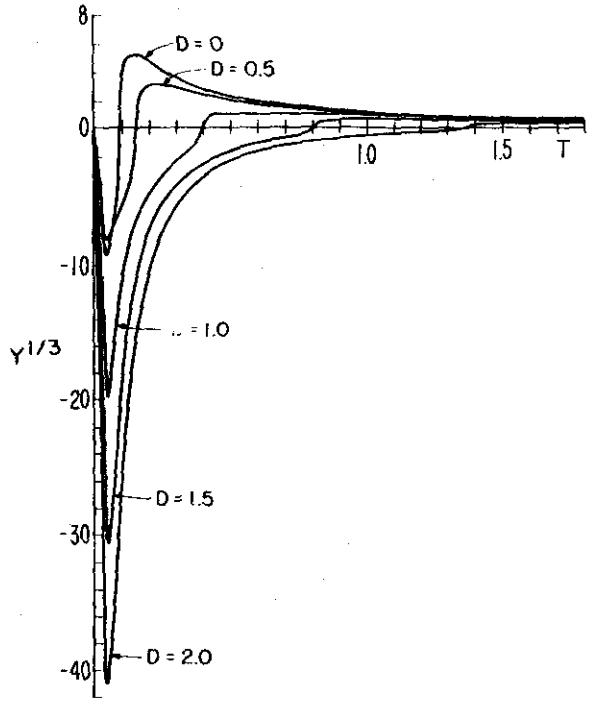

FIG. 3. Waveform of the time derivative of the vertical magnetic field on the surface.

and

$$Y(D,T)=\frac{1}{T^{7/2}}\exp\left(-\frac{1}{4T}\right)\left\{\left(1-\frac{1}{2T}\right)\left(1-\frac{D^2}{4T}\right)\right.$$
$$\times\exp\left(-\frac{D^2}{4T}\right)+\frac{1}{4}\left(\frac{\pi}{T}\right)^{1/2}\exp\left(-\frac{D^2}{8T}\right)\left[\left(3-\frac{3D^2}{2T}+\frac{D^4}{8T^2}\right)I_0\right.$$
$$\left.\left.+\left(\frac{D^2}{T}-\frac{5D^4}{16T^2}\right)I_1\right]\right\}, \qquad (30)$$

where the arguments of I_0 and I_1 are $D^2/8T$. The functions X and Y are plotted in Figs. 2 and 3 vs the time parameter. To facilitate the presentation, the cube roots of X and Y are shown as a function of T on a linear scale. Various values of the parameter $D(=\rho/h)$ are chosen, including the value $D=0$, which corresponds to the observer directly underneath the source loop.

We may observe that the waveforms shown in Figs. 2 and 3 have a characteristic shape which is significantly dependent upon D. Thus, it is not inconceivable that the shape can be used as a criterion to locate the source from an observer on the surface. We note that the normalized time axis T may be read directly in msec, if $4\pi\sigma h^2=10^4$; if, for example, $\sigma=10^{-2}$ mhos/m, we find that $h=283$ m.

We stress that in our formulation, all displacement currents have been neglected. This means that our results are only valid when t is somewhat greater than ϵ/σ sec.[3] If, for example, $\sigma=10^{-2}$ and $\epsilon/\epsilon_0=10$ for the half-space, we have $\epsilon/\sigma=8.85\times10^{-9}$ sec.

Further work on this subject should allow for the inhomogeneity and possible layering of the conducting half-space. Also, without additional difficulty, we can allow for the finite duration of the current pulse in the source loop and the transient response of the loop receiving antennas.

---

[1] J. R. Wait, J. Geophys. 20, 630 (1955).
[2] J. H. Coggon and H. F. Morrison, J. Geophys. 35, 476 (1970).
[3] J. R. Wait, Appl. Sci. Res. (Sec. B) 8, 213 (1960).
[4] Here, we use the classical result

$$\mathcal{L}^{-1}\exp(-s^{1/2})=\tfrac{1}{2}(\pi t^3)^{-1/2}\exp(-1/4t)$$

along with a simple change of variable.
[5] A. D. Wheelon, *Tables of Summable Series and Integrals Involving Bessel Functions* (Holden-Day, Los Angeles, 1968), p. 81, No. 1.704.

Electronics Letters, Vol. 8, No. 11,
1 June 1972

TRANSIENT MAGNETIC FIELDS PRODUCED BY A STEP-FUNCTION-EXCITED LOOP BURIED IN THE EARTH

Indexing terms: Magnetic fields, Transients

Using a previously developed formalism, we obtain explicit results for the field waveforms observed on the Earth's surface for a small horizontal loop buried in a conducting halfspace. It is shown that the shape of the waveforms is diagnostic of the relative location of the buried source. The results have possible application in mine rescue operations.

In a previous paper,[1] we derived expressions for the transient electromagnetic fields of a small wire loop buried in the Earth and excited by an impulsive current. Here we use this formalism to calculate the fields on the surface of the Earth when the current in the loop varies with time as a step function.

The model used before is described briefly here. As indicated in Fig. 1, we adopt a homogeneous halfspace model for the Earth with conductivity σ. The loop buried at depth h is represented by a magnetic dipole with a vertical axis. In terms of a cylindrical co-ordinate system (ρ, ϕ, z), the Earth's surface is $z = 0$ and the homogeneous Earth of conductivity σ occupies the region $z < 0$. The loop is located at $z = -h$ on the z axis. The quantities of interest are the voltages $v_\rho(t)$ and $v_z(t)$ induced in small receiving loops oriented in the radial and vertical directions, respectively. In the previous paper, we derived closed-form expressions for these voltage waveforms when the current was $I_0\,\delta(t)$ Amperes, where $\delta(t)$ is the unit impulse and I_0 is a constant. Numerical results for the impulse-response waveforms $p(t)$ and $q(t)$ were given for the special case where the observer was located at the Earth's surface $z = 0$. The results have also been generalised for a source loop of finite size.[2] In this case, the inverse transforms required numerical integration. In what follows here, we will restrict attention to the magnetic-dipole

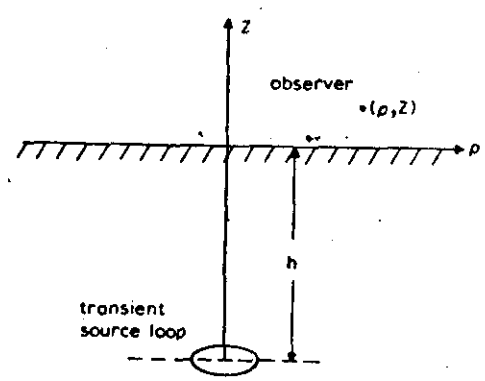

Fig. 1 *Geometry of the situation*

approximation, so that the dimensions h and ρ should be at least five times the radius a of the source loop. As before, we neglect all displacement currents.

We now consider that the current in the source loop is $I(t)\,u(t)$ amperes, where $u(t) = 1$ for $t > 0$ and 0 for $t < 0$. Then, by an application of the convolution theorem, the corresponding voltage responses are

$$\left.\begin{matrix} v_\rho(t) \\ v_z(t) \end{matrix}\right\} = \frac{ANA_r N_r \mu_0}{2\pi h^3} \int_0^t \left\{\begin{matrix} p(\tau) \\ q(\tau) \end{matrix}\right. I(t-\tau)\,d\tau \quad . \quad . \quad (1)$$

where $\mu_0 = 4\pi \times 10^{-7}$ H/m, $A = \pi a^2$ = area of source loop (i.e. magnetic dipole) of radius a, N = number of turns in source loop, A_r = area of receiving loop (of infinitesimal size) and N_r = number of turns of receiving loops. Explicit expressions were given before[1] for the functions $p(\tau)$ and $q(\tau)$. For what follows, it is convenient to rewrite eqn. 1 as follows:

$$\left.\begin{matrix} v_\rho(t) \\ v_z(t) \end{matrix}\right\} = \underbrace{\frac{ANA_r N_r \mu_0}{2\pi h^3}}_{\text{henrys}} \underbrace{\left\{\frac{1}{\frac{1}{2}\pi^2(\sigma\mu_0)^2 h^4}\right\}}_{(\text{seconds})^{-2}} \int_0^t \underbrace{\left\{\begin{matrix} X(D,\hat{T}) \\ Y(D,\hat{T}) \end{matrix}\right.}_{\text{ampere-seconds}} I(t-\tau)\,d\tau \quad . \quad (2)$$

where we have indicated the physical dimensions of the various factors. Here, X and Y are dimensionless functions defined by[1]

$$\left.\begin{matrix} X(D,\hat{T}) \\ Y(D,\hat{T}) \end{matrix}\right\} \quad \frac{2}{\hat{T}^4} \exp\left(-\frac{1}{4\hat{T}}\right) \int_0^\infty \left(1 + x - \frac{1}{2\hat{T}}\right) x^3 \times \exp(-x^2\hat{T}) \left\{\begin{matrix} J_1(xD) \\ J_0(xD) \end{matrix}\right. dx \quad (3)$$

where $\hat{T} = t/(\sigma\mu_0 h^2)$ and $D = \rho/h$. As mentioned above, the functions X and Y were evaluated by both analytical and numerical integration for this situation. Thus for a specified form for $I(t)$, we need to perform a further integration as indicated by eqn. 2.

When the source current is a step function, $I(t) = I_s\,u(t)$, we see that

$$\left.\begin{matrix} v_\rho(t) \\ v_z(t) \end{matrix}\right\} = \frac{ANA_r N_r \mu_0}{2\pi h^3} \left(\frac{-1}{4\pi^4 \sigma\mu_0 h^2}\right) I_s \left\{\begin{matrix} X_s(D,T) \\ Y_s(D,T) \end{matrix}\right. \quad . \quad . \quad (4)$$

where

$$\left.\begin{matrix} X_s(D,T) \\ Y_s(D,T) \end{matrix}\right\} = \int_0^T \left\{\begin{matrix} X(D,\hat{T}) \\ Y(D,\hat{T}) \end{matrix}\right. d\hat{T} \quad . \quad . \quad . \quad . \quad . \quad (5)$$

where $T = t/(\sigma\mu_0 h^2)$.

Using numerical integration, the dimensionless functions X_s and Y_s are plotted in Figs. 2A and 2B as functions of T for

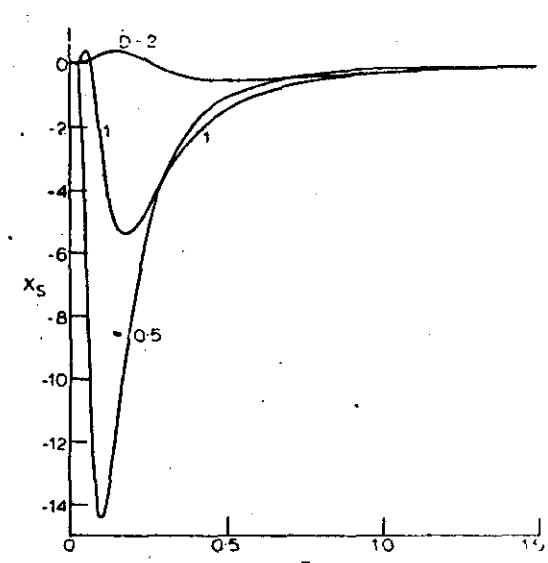

Fig. 2A *Waveform of the voltage in the receiving loop with radially oriented axis*

several values of D. As indicated, these step function responses approach zero for large values of the time parameter T. This can easily be demonstrated analytically, and thus it is a check on the accuracy of the numerical integration.

We stress that, in our formulation, all displacement currents have been neglected. This means that our results are only valid when t is somewhat greater than ε/σ seconds. If, for example, $\sigma = 10^{-2}$ and $\varepsilon/\varepsilon_0 = 10$ for the half-space, we have $\varepsilon/\sigma = 8{\cdot}85 \times 10^{-9}$ s.

It is believed that these waveform functions X_s and Y_s can be useful to interpret signals received on the surface for a pulse-excited buried loop. The latter could be any unearthed wire lying more or less in a horizontal plane. The power source could be a battery connected to the loop by a simple on/off toggle switch.

It is evident that the waveform shape depends on D. Thus

Reprinted from ELECTRONICS LETTERS Vol. 8 No. 11

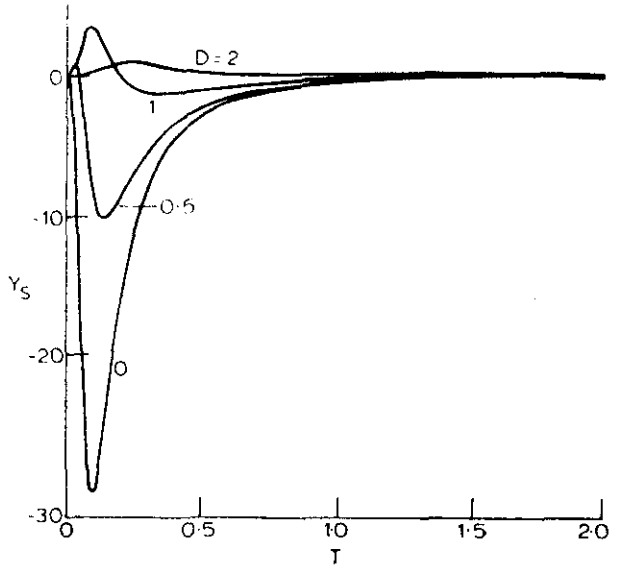

Fig. 2B *Waveform of the voltage in the receiving loop with vertically oriented axis*

it is possible that the waveform can be used as a readily detected criterion of source location for a single observation point on the surface. We note that the time parameter T can be read directly in milliseconds if $4\pi\sigma h^2 \quad 10^3$; if, for example, $\sigma = 10^{-2}$ S/m, we see that $h = 283$ m. The feasibility of such a scheme in mine rescue operations needs to be examined.

JAMES R. WAIT

Environmental Research Laboratories
National Oceanic & Atmospheric Administration
US Department of Commerce
Boulder, Colo. 80302, USA

DAVID A. HILL

Institute for Telecommunication Sciences
Office of Telecommunications
US Department of Commerce
Boulder, Colo. 80302, USA

5th May 1972

References

1 WAIT, J. R., and HILL, D. A.: 'Transient signals from a buried magnetic dipole', *J. Appl. Phys.*, 1971, **42**, pp. 3866–3869
2 WAIT, J. R., and HILL, D. A.: 'Transient electromagnetic fields of a finite circular loop in the presence of a conducting half-space', *ibid.*, 1972, **43** (to be published)

Journal of Applied Physics, Vol. 43, No. 11,
4532-4534, November 1972

Transient electromagnetic fields of a finite circular loop in the presence of a conducting half-space

James R. Wait and David A. Hill
Cooperative Institute for Research in Environmental Sciences, University of Colorado, Boulder, Colorado 80302
(Received 27 December 1971)

A previous solution for a pulse-excited dipole is extended to allow for the finite size of the buried source loop. Numerical results for the above surface fields are presented. We also consider the situation when the finite source loop is located on the surface and the observer is buried. It is suggested that the waveform of the received pulse signals can be used for direction-finding and source location.

I. INTRODUCTION

In a previous paper[1] we presented a theoretical analysis for the transient magnetic fields produced by a pulse-excited magnetic dipole buried in the earth. All displacement currents were neglected, so the solution was not valid at very small times in the transient response. It was shown that the magnetic field waveforms on the surface depended on the conducitivity of the earth and the geometrical parameters of the problem. The results have possible application to mine rescue operations. We consider here a number of new aspects of this problem.

II. FORMULATION

An important extension of the theory pertains to the use of a source loop of finite size.[2] The situation is indicated in Fig. 1(a) where we have located a horizontal single-turn loop of radius a at depth h. For an impulsive uniform current $I_0\delta(t)$, we then wish to calculate the waveform of the field at an observer point P, at a radial coordinate ρ on the surface. The theory given before is almost directly applicable to this situation. In particular, we again consider the time-dependent voltages $v_\rho(t)$ and $v_z(t)$ induced in small receiving loops, of area A_r and N_r turns, oriented in the ρ (radial) and the z (vertical) loops, respectively. Then it follows that

$$v_\rho(t) = [AA_rN_r\mu I_0/(2\pi h^3)]p(t), \tag{1}$$

$$v_z(t) = [AA_rN_r\mu I_0/(2\pi h^3)]q(t), \tag{2}$$

where $A = \pi a^2$,

$$p(t) = h^3\int_0^\infty [\mathcal{L}^{-1}sF(s,\lambda,h)]\lambda^3 e^{-\lambda u}J_1(\lambda\rho)f(\lambda)\,d\lambda, \tag{3}$$

$$q(t) = h^3\int_0^\infty [\mathcal{L}^{-1}sF(s,\lambda,h)]\lambda^3 e^{-\lambda u}J_0(\lambda\rho)f(\lambda)\,d\lambda, \tag{4}$$

with

$$f(\lambda a) = 2J_1(\lambda a)/(\lambda a) \tag{5}$$

and

$$\mathcal{L}^{-1}sF(s,\lambda,h) = \mathcal{L}^{-1}s[(\lambda^2+\sigma\mu s)^{1/2}+\lambda]^{-1} \times \exp[-(\lambda^2+\sigma\mu s)^{1/2}h]. \tag{6}$$

The inverse Laplace transform indicated above was treated explicitly before.[1] But now the added complication[2] is the function $f(\lambda a)$ that can only be replaced by 1 if a becomes vanishingly small (i.e., the magnetic dipole limit).

Following the normalization used before, we write

$$p(t) = -[4\pi^{1/2}(\sigma\mu)^2h^4]^{-1}X(D,\ T,\ Z,\ A), \tag{7}$$

$$q(t) = -[4\pi^{1/2}(\sigma\mu)^2h^4]^{-1}Y(D,\ T,\ Z,\ A), \tag{8}$$

where X and Y are functions of the dimensionless parameters $D=\rho/h$, $T=t/(\sigma\mu h^2)$, $Z=z/h$, and $A=a/h$. From (7) and (8) in the earlier paper[1] it follows that

$$\frac{X}{Y} = \frac{2}{T^{3/2}}\exp\left(-\frac{1}{4T}\right)\int_0^\infty\left(1+x-\frac{1}{2T}\right)x^3 \times \exp(-x^2T)\begin{Bmatrix}J_1(xD)\\J_0(xD)\end{Bmatrix}f(xA)\exp(-xZ)\,dx, \tag{9}$$

where $f(xA) = 2J_1(xA)/(xA)$.

III. SOME RESULTS FOR BURIED SOURCE LOOPS

The case of immediate practical interest is when the observer is located at the earth's surface (i.e., $Z=0$). The waveform functions X and Y have been calculated using numerical integration for this case and for a range of values of T, D, and A. These results for X are shown in Figs. 2(a) and 2(b) where the abscissa is the time parameter T. The curves in Fig. 2(a) are for $A=0$, and the results are in agreement with those given before[1] for the magnetic dipole case. The influence of having a nonzero value of A is seen in Fig. 2(b). While the curves have a qualitative similarity, there is a sig-

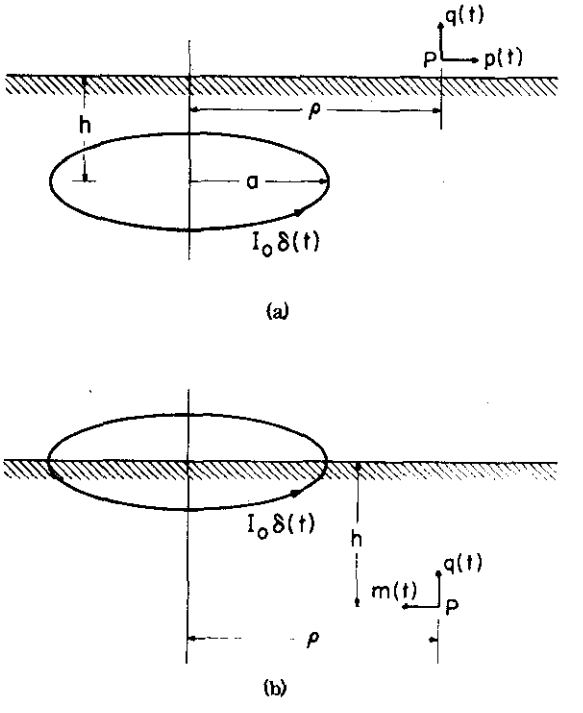

FIG. 1. (a) Buried circular loop excited by an impulsive current. (b) Circular source loop on surface.

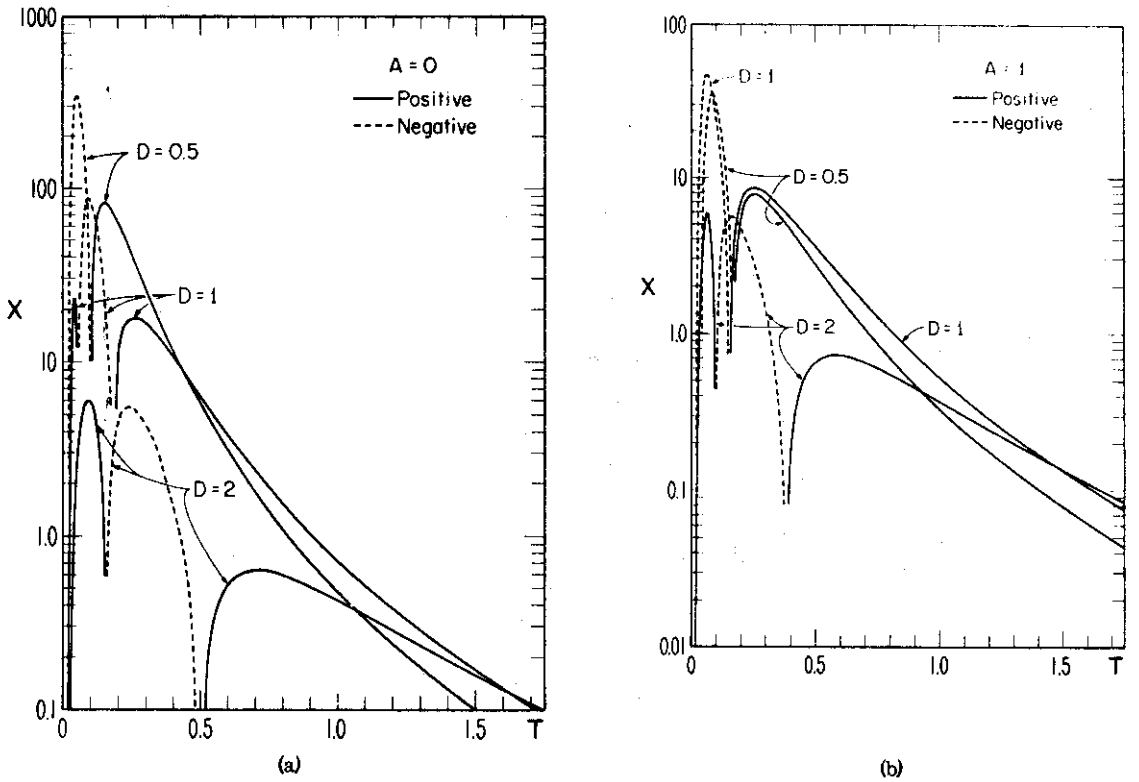

FIG. 2. Normalized impulse response of voltage in small vertical loop on surface (with axis oriented in radial direction) for buried source loop.

nificant difference between the two cases. The agreement between the results based on the analytical formula for X (for $A=0$) and the numerical integration results (for $A=0$) gives confidence to the curves.

The corresponding waveform functions Y for $Z=0$ are shown in Figs. 3(a)–3(c) for the same range of the parameters. The case for $A=0$ here disagreed with the numerical results given before,[1] but this was traced to an algebraic error in the derivation of the working formula. To correct the earlier development,[1] we note that the factor multiplying I_1 in (22′) should be

$$\rho^2/\alpha - \rho^4/8\alpha^2$$

and the factor multiplying I_1 in (30) should be

$$D^2/T - D^4/8T^2.$$

The earlier numerical results[1] for Y, when corrected for $D>0$, agreed to within five digit accuracy with the

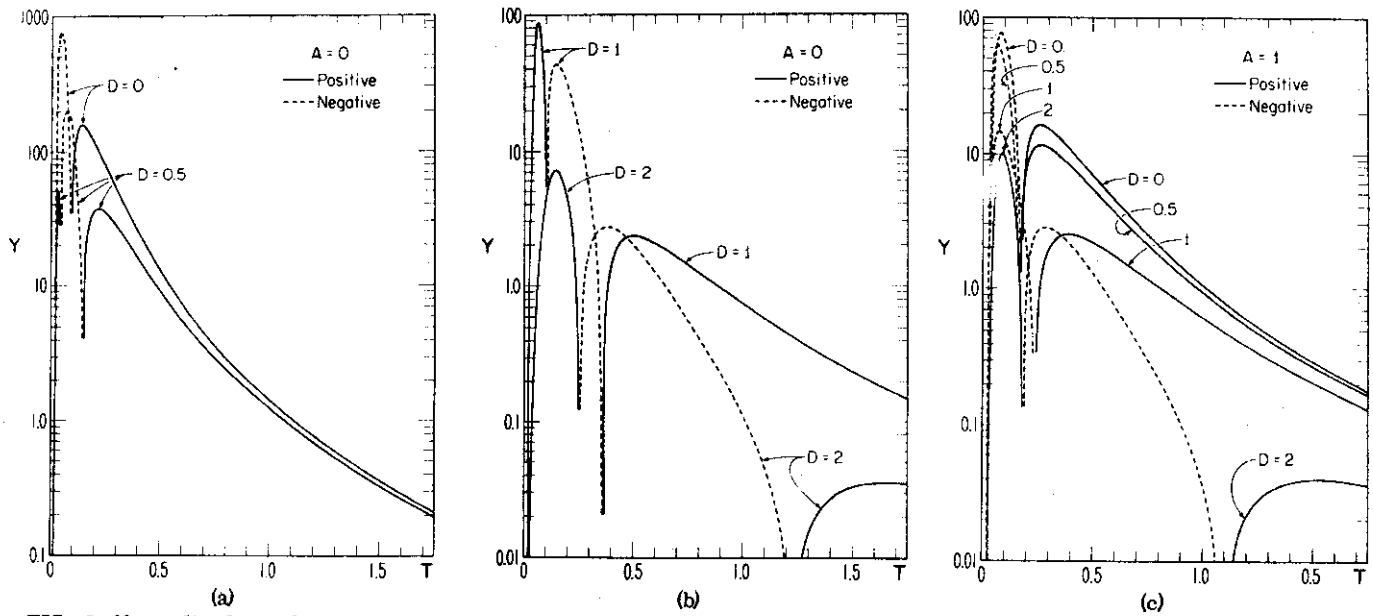

FIG. 3. Normalized impulse response of voltage in small horizontal loop on surface (with axis vertical) for buried source loop. Also applicable to small buried horizontal loop and source loop on surface (see text).

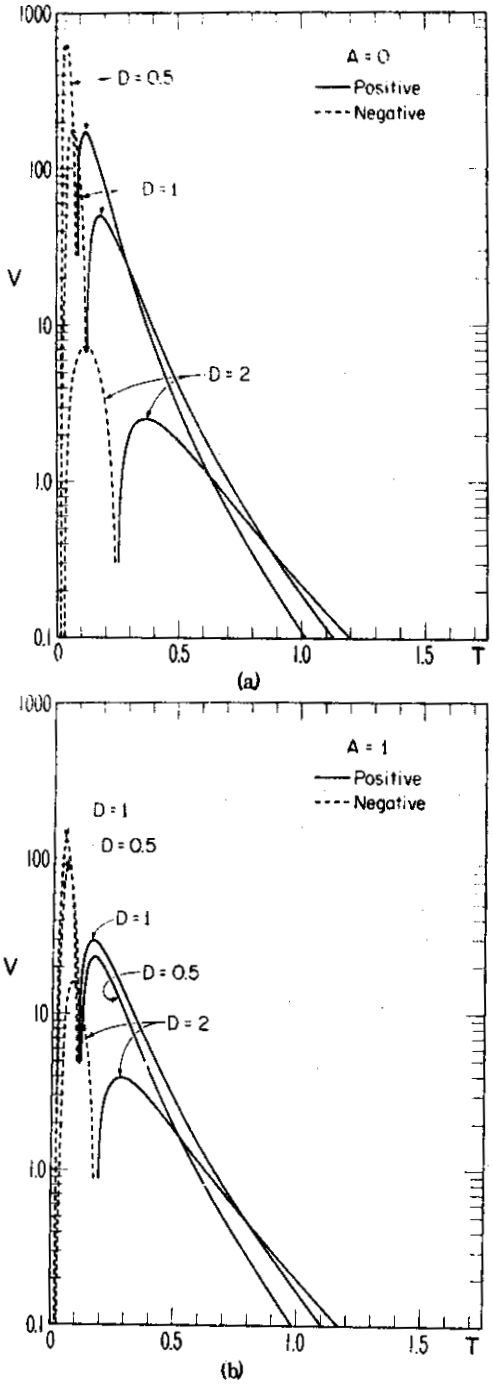

FIG. 4. Normalized impulse response of voltage in small buried vertical loop (with axis oriented in radial direction) for source loop on surface.

numerical integration data shown in Figs. 3(a) and 3(b).

IV. SOURCE LOOP ON SURFACE

A situation of even more practical interest is when the source loop of radius a is located on the surface and the fields are to be observed within the earth. The situation is indicated in Fig. 1(b). We again consider that the source current is $I_0\delta(t)$, and then the time-dependent voltages $v_\rho(t)$ and $v_z(t)$ induced in small receiving loops at P are given by

$$v_\rho(t) = -[AA_r N_r \mu I_0/(2\pi h^3)]m(t), \tag{10}$$

$$v_z(t) = [AA_r N_r \mu I_0/(2\pi h^3)]q(t). \tag{11}$$

The waveform $v_z(t)$ is the same here as in the reciprocal situation mentioned above. Thus, $q(t)$ is again defined by (4). On the other hand, $m(t)$ is to be obtained from

$$m(t) = -h^3 \frac{\partial}{\partial h} \int_0^\infty \mathcal{L}^{-1}[sF(s,\lambda,h)]\lambda^2 J_1(\lambda\rho)e^{-\lambda z_0} f(a\lambda)\, d\lambda, \tag{12}$$

where now z_0 corresponds to the elevation of the source loop above ground and h is the depth of the observer.

Evaluating the inverse transform, as indicated before,[1] we get

$$m(t) = -h^3 \frac{\partial}{\partial h} \frac{1}{2(\sigma\mu\pi)^{1/2}t^{3/2}} \int_0^\infty \left(\lambda h + 1 - \frac{\sigma\mu h^2}{2t}\right) \times \exp\left(-\frac{\sigma\mu h^2}{4t}\right) \exp\left(-\frac{\lambda^2 t}{\sigma\mu}\right)\lambda^2 J_1(\lambda\rho) f(\lambda a)\, d\lambda$$

$$= \frac{h^3}{2(\sigma\mu\pi)^{1/2}t^{3/2}} \exp\left(-\frac{\sigma\mu h^2}{4t}\right) \times \int_0^\infty \left[\lambda^2\left(\frac{(\sigma\mu)^2 h^3}{4t^2} - \frac{3\sigma\mu h}{2t}\right) + \lambda^3\left(1 - \frac{\sigma\mu h^2}{2t}\right)\right] \times \exp -(\lambda^2/\sigma\mu)t\, J_1(\lambda\rho) f(\lambda a)\, d\lambda.$$

Putting this in dimensionless form, we find that

$$m(t) = -[4\pi^{1/2}(\sigma\mu)^2 h^4]^{-1} V(D, T, Z, A),$$

where

$$V = \frac{2}{T^{3/2}} \exp\left(-\frac{1}{4T}\right) \int_0^\infty \left[x^2\left(\frac{3}{2T} - \frac{1}{4T^2}\right) - x^3\left(1 - \frac{1}{2T}\right)\right] \times \exp(-x^2 T) J_1(xD) f(xA)\, dx,$$

where $D = \rho/h$, $A = a/h$, $T = t/(\sigma\mu h^2)$, and $Z = z_0/h$.

Using numerical integration, the waveform function V for $Z = 0$ is shown plotted in Figs. 4(a) and 4(b) for the same range of the parameters.

V. CONCLUDING REMARKS

The waveforms $p(t)$, $q(t)$, and $m(t)$ shown here all depend significantly on the parameter D, which is the ratio of the observer's radial coordinate ρ to the depth h. This is true for both finite and infinitesimal loops. Also, we note that the transient coupling between a finite horizontal source loop on the surface and an infinitesimal buried receiving horizontal loop is the same as for the reciprocal situation where the finite source loop is buried. On the other hand, the transient coupling between the horizontal finite source loop and a small vertical receiving loop depends on whether the source loop is on the surface or buried. In the latter case, there is a difference between the up-link and the down-link situation. We stress, however, that this is not inconsistent with the principle of electromagnetic reciprocity, since the mutual impedance for a given configuration does not depend on which loop transmits.

[1] J. R. Wait and D. A. Hill, J. Appl. Phys. **42**, 3866 (1971).
[2] J. R. Wait, Geophysics **19**, 290 (1954).

Pure and Applied Geophysics (PAGEOPH), Vol. 111,
2264-2272, (1973/X)

Transient Signals From a Buried Horizontal Magnetic Dipole

By D. A. HILL[1])

Summary – The impulse response for a horizontal magnetic dipole buried in a conducting half-space is obtained in closed form by an inverse Fourier transform of the known time harmonic solution. Since displacement currents are neglected, the response is not valid for very short times. The waveforms of the magnetic field components at the surface have geometrical dependences which may have application to source location.

1. Introduction

In a previous communication (WAIT and HILL [1]) it was pointed out that a method of signaling to the surface was to shock excite an underground horizontal loop of wire (vertical magnetic dipole). It was indicated that the source location could be determined either by searching for the null in the vertical magnetic field or by observing the waveshapes, which contain sufficient information, at arbitrary locations. However, if the loop is not quite horizontal, then the effective magnetic dipole moment has an additional horizontal component which changes both the null location and waveshapes. Consequently, it is of interest to obtain the pulse solution for a horizontal magnetic dipole so that the solution for arbitrary orientation can be obtained by superposition. Also, the horizontal dipole itself may be useful in source location since it has a null in the vertical field directly overhead.

The time harmonic solution is well known, but even in the quasi-static case where displacement currents are negligible the solution requires a numerical integration. However, for the pulse solution we are able to evaluate the required integrals analytically and obtain a closed-form solution. This has also been done earlier for the buried electric dipole (WAIT [2]).

2. Formulation

The starting point is the well-known time harmonic solution (WAIT and CAMPBELL [3] and WAIT [4]), and the geometry is shown in Fig. 1. The half-space ($z \leq 0$) is homogeneous, isotropic, and nonmagnetic, and has conductivity σ. The source is a small loop

[1]) Department of Commerce, OT/ITS, Boulder, Colorado 80302, USA.

of area A and N turns carrying a current I which varies as $\exp(i\omega t)$. The equivalent magnetic dipole source is located at $z = -h$ on the z-axis and is oriented in the positive y direction. Displacement currents are negligible at the low frequencies of interest here.

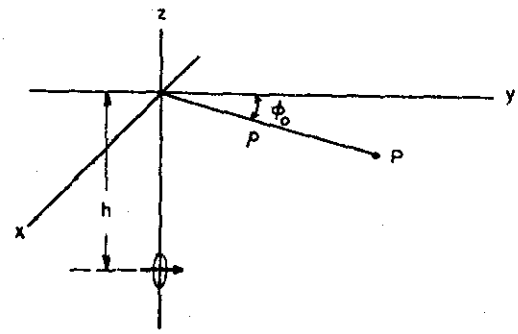

Figure 1
Horizontal magnetic dipole in a conducting half-space

If the observation point is located at the interface, then the magnetic field components (H_x, H_y, H_z) are given by

$$H_x(\omega) = \frac{IAN}{2\pi h^3} CS\left[\frac{Q(\omega)}{D} - M(\omega)\right], \tag{1}$$

$$H_y(\omega) = \frac{-IAN}{2\pi h^3}\left[\frac{S^2}{D} Q(\omega) + C^2 M(\omega)\right],$$

$$H_z(\omega) = \frac{IAN}{2\pi h^3} CN(\omega),$$

where $C = (y/\rho) = \cos\phi_0$, $S = (x/\rho) = \sin\phi_0$, and $D = \rho/h$. The dimensionless integral functions M, N, and Q are defined by

$$M(\omega) = h^3 \int_0^\infty F(\lambda, \omega)\left[J_0(\lambda\rho) - \frac{J_1(\lambda\rho)}{\lambda\rho}\right]\lambda^2\, d\lambda, \tag{2}$$

$$N(\omega) = h^3 \int_0^\infty F(\lambda, \omega) J_1(\lambda\rho)\, \lambda^2\, d\lambda,$$

$$Q(\omega) = h^2 \int_0^\infty F(\lambda, \omega) J_1(\lambda\rho)\, \lambda\, d\lambda,$$

where

$$F(\lambda, \omega) = \frac{(\lambda^2 + i\omega\sigma\mu_0)^{1/2} \exp[-(\lambda^2 + i\omega\sigma\mu_0)^{1/2} h]}{\lambda + (\lambda^2 + i\omega\sigma\mu_0)^{1/2}},$$

μ_0 is the permeability of free space, and J_0 and J_1 are the zero-order and first-order Bessel functions.

In order to obtain the impulse response, let the loop current equal $Q_0\delta(t)$, where Q_0 is a constant with dimensions of charge. The transient voltages induced in small receiving loops at the surface (v_x, v_y, v_z), where the subscript refers to the direction of the loop axis, are given by the following

$$v_x(t) = A_r N_r \mu_0 \frac{\partial h_x(t)}{\partial t}, \tag{3}$$

$$v_y(t) = A_r N_r \mu_0 \frac{\partial h_y(t)}{\partial t},$$

$$v_z(t) = A_r N_r \mu_0 \frac{\partial h_z(t)}{\partial t},$$

where h_x, h_y, and h_z are the time-dependent magnetic field components which can be obtained from the inverse Fourier transform of the time harmonic magnetic field components given by (1). Consequently, the time-dependent voltages can be written:

$$v_x(t) = \frac{Q_0 ANA_r N_r \mu_0}{2\pi h^3} CS\left[\frac{\tilde{Q}'(t)}{D} - \tilde{M}'(t)\right], \tag{4}$$

$$v_y(t) = \frac{Q_0 ANA_r N_r \mu_0}{2\pi h^3}\left[\frac{S^2}{D}\tilde{Q}'(t) + C^2\tilde{M}'(t)\right],$$

$$v_z(t) = \frac{Q_0 ANA_r N_r \mu_0}{2\pi h^3} C\tilde{N}'(t),$$

where $\tilde{M}'$, $\tilde{N}'$, and $\tilde{Q}'$ are the time derivatives of the inverse Fourier transforms of M, N, and Q. By the differentiation rule they are given by

$$\tilde{M}'(t) = F^{-1}[i\omega M(\omega)], \tag{5}$$

$$\tilde{N}'(t) = F^{-1}[i\omega N(\omega)],$$

$$\tilde{Q}'(t) = F^{-1}[i\omega Q(\omega)],$$

where F^{-1} denotes inverse Fourier transform.

Since the only frequency dependence in M, N, and Q is contained in the function $F(\lambda, \omega)$, the inverse Fourier transforms in (5) can be rewritten

$$\tilde{M}'(t) = h^3 \int_0^\infty \tilde{F}'(\lambda, t)\left[J_0(\lambda\rho) - \frac{J_1(\lambda\rho)}{\lambda\rho}\right]\lambda^2\, d\lambda, \tag{6}$$

$$\tilde{N}'(t) = h^3 \int_0^\infty \tilde{F}'(\lambda, t) J_1(\lambda\rho)\lambda^2\, d\lambda,$$

$$\tilde{Q}'(t) = h^2 \int_0^\infty \tilde{F}'(\lambda, t) J_1(\lambda\rho)\lambda\, d\lambda,$$

where

$$\tilde{F}'(\lambda, t) = F^{-1}[i\omega F(\lambda, \omega)].$$

Consequently, the remaining problem is to evaluate $\tilde{F}'(\lambda, t)$. By rationalizing the denominator of $F(\lambda, \omega)$ and applying the differentiation rule, we arrive at the following:

$$\tilde{F}'(\lambda, t) = (\sigma\mu_0)^{-1}\left[\lambda^2 + \sigma\mu_0\frac{\partial}{\partial t} + \lambda\frac{\partial}{\partial h}\right] \tag{7}$$

$$F^{-1}\{\exp[-(\lambda^2 + i\omega\sigma\mu_0)^{1/2}h]\}.$$

The following transform pair can be derived from classical results plus the shifting theorem:

$$F^{-1}\{\exp[-(\lambda^2 + i\omega\mu_0\sigma)^{1/2}h]\} = \frac{\sqrt{\sigma\mu_0}\,h\exp\left(-\dfrac{\sigma\mu_0 h^2}{4t} - \dfrac{\lambda^2 t}{\sigma\mu_0}\right)}{2\sqrt{\pi t^3}}, \tag{8}$$

where the time function is zero for negative t. Since this will always be the case, all following time-dependent quantities will apply only for positive t. By combining (7) and (8) and carrying out the derivative operations, we obtain the following

$$\tilde{F}'(\lambda, t) = \frac{\exp\left(-\dfrac{\sigma\mu_0 h^2}{4t} - \dfrac{\lambda^2 t}{\sigma\mu_0}\right)}{2\sqrt{\pi\sigma\mu_0}\,t^{3/2}}\left[\frac{\sigma^2\mu_0^2 h^3}{4t^2} - \frac{3\sigma\mu_0 h}{2t} + \lambda\left(1 - \frac{\sigma\mu_0 h^2}{2t}\right)\right]. \tag{9}$$

Thus, the received voltages are now given by (4), (6) and (9). Only the λ integrations remain to be carried out, and this will be done in the following section.

3. *Reduction to working form*

In order to evaluate the functions in (6), we need to evaluate integrals which are all of the form:

$$A_{m,n} = \int_0^\infty \lambda^m e^{-\alpha\lambda^2} J_n(\lambda\rho)\, d\lambda, \tag{10}$$

where $\alpha = t/(\sigma\mu_0)$; $m = 1, 2, 3$; and $n = 0, 1$. The following integrals have known forms (WHEELON [5]):

$$A_{0,0} = \frac{1}{2}\sqrt{\frac{\pi}{\alpha}}\exp\left(\frac{-\rho^2}{8\alpha}\right) I_0\left(\frac{\rho^2}{8\alpha}\right), \tag{11}$$

$$A_{1,0} = \frac{\exp\left(\dfrac{-\rho^2}{4\alpha}\right)}{2\alpha},$$

$$A_{2,1} = \frac{\rho \exp\left(\frac{-\rho^2}{4\alpha}\right)}{4\alpha^2},$$

where I_0 is the zero-order modified Bessel function. The remaining integrals can be derived by differentiation:

$$A_{1,1} = -\frac{\partial A_{0,0}}{\partial \rho} \tag{12}$$

$$= \frac{\sqrt{\pi}\rho \exp\left(-\frac{\rho^2}{8\alpha}\right)}{8\alpha^{3/2}}(I_0 - I_1),$$

$$A_{2,0} = -\frac{\partial A_{0,0}}{\partial \alpha}$$

$$= \frac{\sqrt{\pi}\exp\left(\frac{-\rho^2}{8\alpha}\right)}{4\alpha^{3/2}}\left[\frac{\rho^2}{4\alpha}I_1 + \left(1 - \frac{\rho^2}{4\alpha}\right)I_0\right],$$

$$A_{3,0} = -\frac{\partial A_{1,0}}{\partial \alpha}$$

$$= \frac{\exp\left(\frac{-\rho^2}{4\alpha}\right)}{2\alpha^2}\left(1 - \frac{\rho^2}{4\alpha}\right),$$

$$A_{3,1} = \frac{\partial^2 A_{0,0}}{\partial \alpha \partial \rho}$$

$$= \frac{\sqrt{\pi}\rho \exp\left(\frac{-\rho^2}{8\alpha}\right)}{8\alpha^{5/2}}\left[\left(\frac{3}{2} - \frac{\rho^2}{4\alpha}\right)I_0 + \left(\frac{\rho^2}{4\alpha} - \frac{1}{2}\right)I_1\right],$$

where I_0 and I_1 are zero- and first-order modified Bessel functions of argument $\rho^2/(8\alpha)$.

It is now possible to substitute the results of (9), (11), and (12) into (6) to obtain the required time responses. However, it is first convenient to introduce a normalized time, $T = t/(\sigma\mu_0 h^2)$. By also using the earlier parameter, $D = \rho/h$; we can now write the time responses in their following normalized forms:

$$\tilde{M}'(t) = \frac{\exp\left(-\frac{1}{4T} - \frac{D^2}{8T}\right)}{8\sqrt{\pi}(\sigma\mu_0 h^2)^2 T^{7/2}}\left[\frac{\sqrt{\pi}}{T^{1/2}}\left(\frac{1}{4T} - \frac{3}{2}\right)\left(\frac{1}{2} - \frac{D^2}{4T}\right)\right. \tag{13}$$

$$\left.(I_0 - I_1) + \exp\left(\frac{-D^2}{8T}\right)\left(1 - \frac{1}{2T}\right)\left(1 - \frac{D^2}{2T}\right)\right],$$

$$\tilde{N}'(t) = \frac{D\exp\left(-\frac{1}{4T}-\frac{D^2}{8T}\right)}{8\sqrt{\pi}(\sigma\mu_0 h^2)^2 T^4}\left\{\frac{\exp\left(-\frac{D^2}{8T}\right)}{T^{1/2}}\left(\frac{1}{4T}-\frac{3}{2}\right)\right.$$
$$\left.+\frac{\sqrt{\pi}}{2}\left(1-\frac{1}{2T}\right)\left[\left(\frac{3}{2}-\frac{D^2}{4T}\right)I_0+\left(\frac{D^2}{4T}-\frac{1}{2}\right)I_1\right]\right\},$$

$$\tilde{Q}'(t) = \frac{D\exp\left(-\frac{1}{4T}-\frac{D^2}{8T}\right)}{8\sqrt{\pi}(\sigma\mu_0 h^2)^2 T^{7/2}}\left[\frac{\sqrt{\pi}}{2T^{1/2}}\left(\frac{1}{4T}-\frac{3}{2}\right)(I_0-I_1)+\exp\left(\frac{-D^2}{8T}\right)\left(1-\frac{1}{2T}\right)\right].$$

In order to express the received voltage in (4) in the simplest form, we can substitute (13) into (4) and rewrite the result in the final form:

$$\left.\begin{matrix} v_x(t) \\ v_y(t) \\ v_z(t) \end{matrix}\right\} = K\cdot\begin{cases} CS[Q_n(T)-M_n(T)] \\ -[S^2 Q_n(T)+C^2 M_n(T)] \\ CN_n(T) \end{cases} \tag{14}$$

where

$$K = \frac{Q_0 ANA_r N_r \mu_0}{2\pi h^3(\sigma\mu_0 h^2)^2},$$

$$M_n(T) = \frac{\exp\left(\frac{-1}{4T}-\frac{D^2}{8T}\right)}{8\sqrt{\pi}T^{7/2}}\left[\frac{\sqrt{\pi}}{T^{1/2}}\left(\frac{1}{4T}-\frac{3}{2}\right)\left(\frac{1}{2}-\frac{D^2}{4T}\right)(I_0-I_1)\right.$$
$$\left.+\exp\left(\frac{-D^2}{8T}\right)\left(1-\frac{1}{2T}\right)\left(1-\frac{D^2}{2T}\right)\right],$$

$$N_n(T) = \frac{D\exp\left(\frac{-1}{4T}-\frac{D^2}{8T}\right)}{8\sqrt{\pi}T^4}\left\{\frac{\exp\left(\frac{-D^2}{8T}\right)}{T^{1/2}}\left(\frac{1}{4T}-\frac{3}{2}\right)\right.$$
$$\left.+\frac{\sqrt{\pi}}{2}\left(1-\frac{1}{2T}\right)\left[\left(\frac{3}{2}-\frac{D^2}{4T}\right)I_0+\left(\frac{D^2}{4T}-\frac{1}{2}\right)I_1\right]\right\},$$

$$Q_n(T) = \frac{\exp\left(-\frac{1}{4T}-\frac{D^2}{8T}\right)}{8\sqrt{\pi}T^{7/2}}\left[\frac{\sqrt{\pi}}{2T^{1/2}}\left(\frac{1}{4T}-\frac{3}{2}\right)(I_0-I_1)+\exp\left(\frac{-D^2}{8T}\right)\left(1-\frac{1}{2T}\right)\right.$$

Note that K has units of volts and the normalized functions M_n, N_n, Q_n are dimensionless. The form of (14) is especially convenient because the response magnitude is determined by K, the waveshapes are determined by the normalized functions, and the effective time constant is $\sigma\mu_0 h^2$.

4. Numerical results

For a general observation point on the surface, the three received voltages are functions of the three normalized waveforms, M_n, N_n, and Q_n. However, for special cases on the x- and y-axes, the results simplify. For instance, on the positive y-axis, we have

$$\left.\begin{matrix} v_x(t) \\ v_y(t) \\ v_z(t) \end{matrix}\right\} = K \begin{cases} 0 \\ -M_n(T) \\ N_n(T) \end{cases} \tag{15}$$

A plot of M_n which is proportional to v_y in this case is shown in Fig. 2 for various values of D. Note that the waveform stretches out and changes sign as D increases. This sign

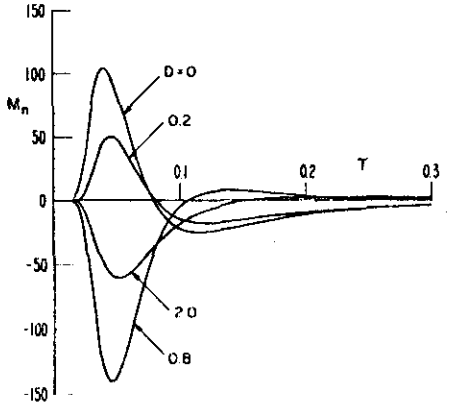

Figure 2
Normalized waveform, $M_n(T)$, for various values of D

change is not surprising since it also occurs in the static case. A plot of N_n which is proportional to v_z is shown in Fig. 3 for various values of D. The waveform is zero for $D = 0$ because of the overhead null in the vertical magnetic field. The waveform increases in magnitude for small D to a maximum value and then begins to fall off and stretch out for larger D.

On the x-axis, we have the following result:

$$\left.\begin{matrix} v_x(t) \\ v_y(t) \\ v_z(t) \end{matrix}\right\} = K \begin{cases} 0 \\ -Q_n(T) \\ 0 \end{cases}$$

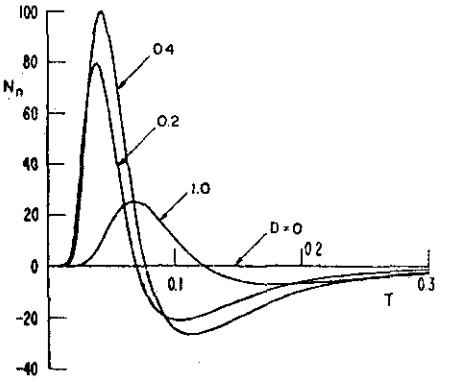

Figure 3
Normalized waveform, $N_n(T)$, for various values of D

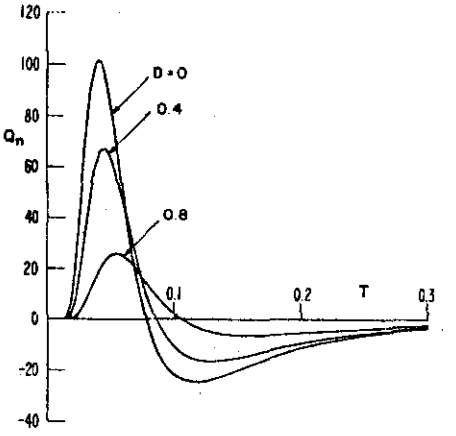

Figure 4
Normalized waveform, $Q_n(T)$, for various values of D

A plot of Q_n which is proportional to v_y in this case is shown in Fig. 4 for various values of D. As D increases, Q_n is seen to decrease in magnitude and stretch out.

5. Concluding remarks

A closed form solution has been obtained for the impulse response of a buried horizontal magnetic dipole with the restriction that displacement currents are negligible. This means that the results are valid only for t somewhat greater than ε/σ. However, this restriction is not serious since such times are orders of magnitude smaller than those of interest here.

Although the prime motivation for obtaining the horizontal dipole solution is to allow a solution for arbitrary dipole orientation, the horizontal dipole (vertical loop) has possibilities of use in direction finding. For instance, it may be possible to search for the null in the vertical magnetic field or to deduce the location from the waveshapes which depend on the source-receiver geometry as shown in Figs. 2–4. Although only the impulse response waveforms are given here it is possible to obtain responses to arbitrary current pulses by convolution as was done for the vertical magnetic dipole case (WAIT and HILL [6], and WAIT and HILL [7].

Acknowledgement

The author would like to thank Dr. J. R. WAIT for his useful comments.

REFERENCES

[1] J. R. WAIT and D. A. HILL, *Transient signals from a buried magnetic dipole*, J. Appl. Phys. *42* (10) (1971), 3866–3869.

[2] J. R. WAIT, *Propagation of electromagnetic pulses in a homogeneous conducting earth*, Appl. Sci. Res. *8* (B) (1960), 213–253.

[3] J. R. WAIT and L. L. CAMPBELL, *The fields of an oscillating magnetic dipole immersed in a semi-infinite conducting medium*, J. Geophys. Res. *58* (2) (1953), 167–178.

[4] J. R. WAIT, *Locating an oscillating magnetic dipole in the earth*, Electronics Letters *8* (16) (1972), 404.

[5] A. D. WHEELON, *Tables of Summable Series and Integrals Involving Bessel Functions* (Holden-Day, San Francisco 1968), pp. 80–81.

[6] J. R. WAIT and D. A. HILL, *Transient magnetic fields produced by a step function excited loop buried in the earth*, Electronics Letters *8* (11) (1972a), 294–295.

[7] J. R. WAIT and D. A. HILL, *Electromagnetic surface fields produced by a pulse-excited loop buried in the earth*, J. Appl. Phys. *43* (10) (1972), 3988–3991.

(Received 19th December 1972)

Radio Science, Volume 6, Numbers 8, 9, pages 781–786, August-September 1971

Subsurface electromagnetic fields of a line source on a conducting half-space

James R. Wait and Kenneth P. Spies

Institute for Telecommunication Sciences
Office of Telecommunications, Boulder, Colorado 80302

(Received January 15, 1971.)

An infinite line source or current-carrying cable on the surface of a flat homogeneous earth is considered. The integral formula, for the case of negligible displacement currents, is reduced either to tabulated functions or to a form suitable for numerical integration. A table of numerical values of these basic integrals is presented. We also show that, in principle, the relative location of the line source can be deduced from measurements of the subsurface field The results have possible application to mine rescue operations.

INTRODUCTION

In certain aspects of applied geophysics [*Grant and West*, 1966], one is interested in the nature of the electromagnetic fields within the earth for a source on the surface. For example, if a communication link is to be established from a sender on the earth's surface to a receiving point in a mine or other subterranean terminal, it is necessary to choose a transmitting antenna and an operating frequency that are appropriate for the task. With this objective in mind, we shall consider a two-dimensional model which hopefully provides insight to this problem. The earth is regarded as a homogeneous conducting half-space in this formulation. We also consider the possibility that the structure of the measured subsurface field can be employed to deduce the relative location of the line source on the surface.

FORMULATION OF THE GREEN'S FUNCTION

We begin with the fields of a uniform line current I at (x', y') in a nonmagnetic homogeneous half-space ($y < 0$) of conductivity σ as indicated in Figure 1. Everything is considered to be invariant in the z direction, so the posed problem is entirely two-dimensional. The fields are taken to vary with time as $\exp(i\omega t)$, and the (angular) frequency ω is sufficiently low that all displacement currents are negligible compared with the conduction currents. The electric field at $P(x, y)$ has only a z component $E(x, y)$ and it can be conveniently written as follows [*Wait*, 1962]:

$$E = (-i\mu_0\omega I/2\pi)G(x, y; x', y') \tag{1}$$

where $\mu_0 = 4\pi \times 10^{-7}$ is the permeability of free space. Then the 'Green's function,' for $y \geq 0$, is

$$G(x, y; x', y') = K_0[\gamma[(x - x')^2 + (y - y')^2]^{1/2}] - K_0[\gamma[(x - x')^2 + (y + y')^2]^{1/2}] + 2\int_0^\infty \frac{e^{-u(y+y')}}{u + \lambda} \cos[\lambda(x - x')]\, d\lambda \tag{2}$$

where $u = (\lambda^2 + \gamma^2)^{1/2}$ and $\gamma^2 = i\sigma\mu_0\omega$. The first modified Bessel function on the right-hand side of (2) can be identified as the Green's function of the line source for an infinite medium, while the second term is associated with an 'image' of the line source at $x = x'$ and $y = -y'$. For the region $y < 0$, we have

$$G(x, y; x', y') = 2\int_0^\infty \frac{e^{-uy'}e^{\lambda y}}{u + \lambda} \cos[\lambda(x - x')]\, d\lambda \tag{3}$$

It is not difficult to verify that G has the proper singularity at the source, and that G and $\partial G/\partial y$ are continuous at the interface $y = 0$. Also, we see that $(\nabla^2 - \gamma^2)\, G = 0$ for $y > 0$, while $\nabla^2 G = 0$ for $y < 0$. Furthermore, if $\mathrm{Re}\, u > 0$, and noting that λ is also real, the solutions for G behave properly as $|y| \to \infty$. In establishing the correctness of (2) and (3), one makes use of the integral representation

$$K_0[\gamma(x^2 + y^2)^{1/2}] = \int_0^\infty \frac{e^{-u|y|}}{u} \cos \lambda x\, d\lambda \tag{4}$$

This key formula is also used in the developments which follow.

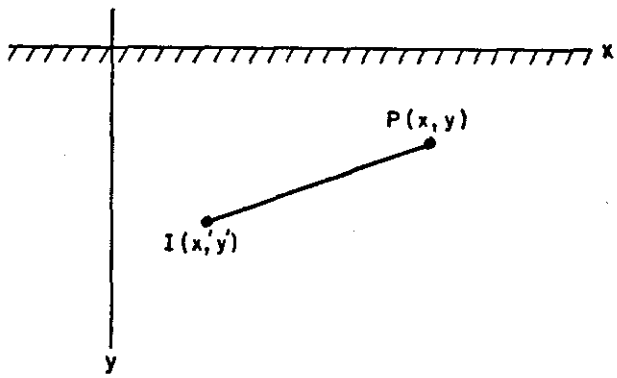

Fig. 1. Current line source in the presence of a homogeneous half-space.

SUBSURFACE MAGNETIC FIELDS FOR LINE CURRENT ON SURFACE

A situation of special interest is when the line source is on the earth's surface and we observe the resultant magnetic field **H** at a subsurface point $P(x, h)$, as indicated in Figure 2. Thus, in (1), we take $x' = y' = 0$ and use $i\mu_0\omega H_x = -\partial E/\partial y$ and $i\mu_0\omega H_y = \partial E/\partial x$ to obtain

$$H_x = -\frac{I}{\pi}\int_0^\infty \frac{u}{u+\lambda} e^{-uh} \cos \lambda x \, d\lambda \tag{5}$$

$$H_y = +\frac{I}{\pi}\int_0^\infty \frac{\lambda}{u+\lambda} e^{-uh} \sin \lambda x \, d\lambda \tag{6}$$

while, of course, $H_z \equiv 0$. While the evaluation of (5) and (6) for the general case requires numerical integration, the important special case for $x = 0$ is amenable to analytical treatment. Then the magnetic field is purely horizontal, (i.e., $H_y = 0$) and is reduced as follows:

$$\begin{aligned} H_x = H_x^0 &= -\frac{I}{\pi}\int_0^\infty \frac{u}{u+\lambda} e^{-uh} \, d\lambda \\ &= +\frac{I}{\pi}\frac{\partial}{\partial h}\int_0^\infty \frac{e^{-uh}}{u+\lambda} d\lambda \\ &= +\frac{I}{\pi\gamma^2}\frac{\partial}{\partial h}\int_0^\infty (u-\lambda)e^{-uh} \, d\lambda \end{aligned} \tag{7}$$

where we note that $(u - \lambda)(u + \lambda) = \gamma^2$. Now a special case of (4) is

$$\int_0^\infty \frac{e^{-uh}}{u} d\lambda = K_0(\gamma h) \tag{8}$$

thus

$$\int_0^\infty u e^{-uh} \, d\lambda = \frac{d^2}{dh^2} K_0(\gamma h) \tag{9}$$

Similarly, if we use the standard form

$$\int_0^\infty \lambda \frac{e^{-uh}}{u} d\lambda = \frac{e^{-\gamma h}}{h} \tag{10}$$

we have

$$\int_0^\infty \lambda e^{-uh} \, d\lambda = -\frac{\partial}{\partial h}\frac{e^{-\gamma h}}{h} \tag{11}$$

Thus, making use of (9) and (11), we see that (7) is equivalent to

$$H_x^0 = +\frac{I}{\pi\gamma^2}\left[\frac{\partial^3}{\partial h^3} K_0(\gamma h) + \frac{\partial^2}{\partial h^2}\frac{e^{-\gamma h}}{h}\right] \tag{12}$$

By utilizing the Bessel function relations

$$d K_0(\alpha)/d\alpha = -K_1(\alpha) \tag{13}$$

$$d K_1(\alpha)/d\alpha = -[K_0(\alpha) + \alpha^{-1} K_1(\alpha)] \tag{14}$$

we can express (12) in the form

$$H_x^0 = -[I/(2\pi h)] A_0(\alpha) \tag{15}$$

where

$$\begin{aligned} A_0(\alpha) = 2K_0(\alpha) + 2\left(\alpha + \frac{2}{\alpha}\right) K_1(\alpha) \\ - \alpha^{-2}(2 + 2\alpha + \alpha^2)e^{-\alpha} \end{aligned} \tag{16}$$

where $\alpha = \gamma h = (i\sigma\mu_0\omega)^{1/2}h$. At sufficiently low frequencies (i.e., $\alpha \to 0$), we see that $A_0(\alpha)$ approaches 1, and we recover the expected static form. On the other hand, the high-frequency limit (i.e., $\alpha \to \infty$) leads to

$$A_0(\alpha) \sim (2\pi\alpha)^{1/2} e^{-\alpha} \tag{17}$$

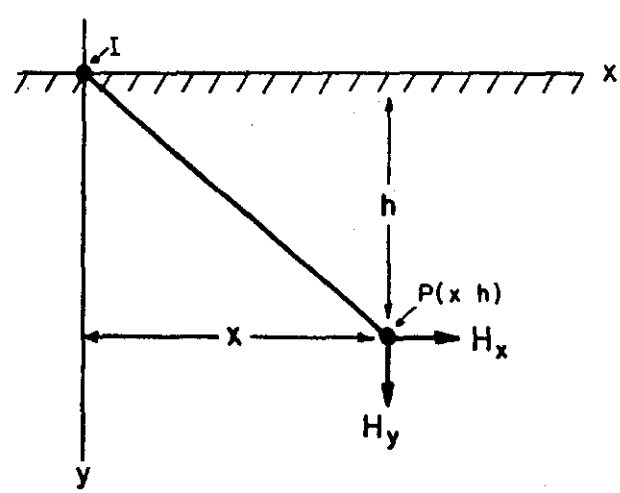

Fig. 2. Line source on surface and field components to be observed at subsurface point.

which is a factor of 2 greater than the corresponding result for an infinite medium. In this asymptotic limit, the air-ground interface has the effect of doubling the field of the line source.

In the general case, for numerical work, it is convenient to express (15) and (16) in terms of dimensionless parameters $H = (\sigma\mu_0\omega)^{1/2}h$ and $X = x/h$. Thus, on changing the integration variable to $s = \lambda h$, we have

$$H_z = -\frac{I}{2\pi h} A(H, X)$$

$$H_y = +\frac{I}{2\pi h} B(H, X)$$

where

$$A(H, X) = 2\int_0^\infty \frac{(s^2 + iH^2)^{1/2}}{(s^2 + iH^2)^{1/2} + s} \cdot \exp\left[-(s^2 + iH^2)^{1/2}\right] \cos(sX)\, ds \qquad (18)$$

$$B(H, X) = 2\int_0^\infty \frac{s}{(s^2 + iH^2)^{1/2} + s} \cdot \exp\left[-(s^2 + iH^2)^{1/2}\right] \sin(sX)\, ds \qquad (19)$$

The corresponding form for the electric field is

$$E = (-i\mu\omega I/2\pi)F(H, X)$$

where

$$F(H, X) = G(x, y; 0, 0) = 2\int_0^\infty \frac{1}{(s^2 + iH^2)^{1/2} + s} \cdot \exp\left[-(s^2 + iH^2)^{1/2}\right] \cos sX\, ds \qquad (20)$$

Because these integrals recur frequently in electromagnetic induction problems involving buried terminals, tables of the integrals A, B, and F have been prepared. Except for the case $X = 0$, numerical integration is necessary. First of all, however, we discuss some limiting situations which are useful for checking the numerical work.

LIMITING FORMS

A very simple limiting form is when the frequency tends to zero. Then $\gamma^2 \to 0$ and then (5) and (6) reduce to

$$H_z = H_{0z} = -\frac{I}{2\pi}\int_0^\infty e^{-\lambda h}\cos\lambda x\, d\lambda = \frac{-I}{2\pi h}\frac{h^2}{h^2 + x^2} \qquad (21)$$

$$H_y = H_{0y} = \frac{I}{2\pi}\int_0^\infty e^{-\lambda h}\sin\lambda x\, d\lambda = \frac{I}{2\pi h}\frac{xh}{h^2 + x^2} \qquad (22)$$

Then, the corresponding forms of (18) and (19) are simply

$$A(0, X) = A_0 = (1 + X^2)^{-1} \qquad (23)$$

$$B(0, X) = B_0 = X(1 + X^2)^{-1} \qquad (24)$$

Another useful limiting case is to allow the conductivity or frequency or both to be sufficiently high that $|\gamma x|$ can be regarded as a large parameter. Some consideration shows that this justifies the replacement of $\exp(-uh)$ by $\exp(-\gamma h)$ in the integrands of (5) and (6). Then also

$$F = 2\int_0^\infty \frac{\cos\lambda x}{u + \lambda} e^{-uh}\, d\lambda \sim 2e^{-\gamma h}\int_0^\infty \frac{\cos\lambda x}{u + \lambda}\, d\lambda \sim \frac{2}{\gamma^2 x^2} e^{-\gamma h} \qquad (25)$$

where we have used previously developed results

TABLE 1. Field calculations for a line source on a conducting half-space at zero frequency limit ($H = 0$)

X	A_0	B_0	A_0/X
0.0	1.000 + 0	0.000 + 0	
0.1	9.901 - 1	9.901 - 2	1.000 + 1
0.2	9.615 - 1	1.923 - 1	5.000 + 0
0.3	9.174 - 1	2.752 - 1	3.333 + 0
0.4	8.621 - 1	3.448 - 1	2.500 + 0
0.5	8.000 - 1	4.000 - 1	2.000 + 0
0.6	7.353 - 1	4.412 - 1	1.667 + 0
0.7	6.711 - 1	4.698 - 1	1.429 + 0
0.8	6.098 - 1	4.878 - 1	1.250 + 0
0.9	5.525 - 1	4.972 - 1	1.111 + 0
1.0	5.000 - 1	5.000 - 1	1.000 + 0
1.1	4.525 - 1	4.977 - 1	9.091 - 1
1.2	4.098 - 1	4.918 - 1	8.333 - 1
1.3	3.717 - 1	4.833 - 1	7.692 - 1
1.4	3.378 - 1	4.730 - 1	7.143 - 1
1.5	3.077 - 1	4.615 - 1	6.667 - 1
1.6	2.809 - 1	4.494 - 1	6.250 - 1
1.7	2.571 - 1	4.370 - 1	5.882 - 1
1.8	2.358 - 1	4.245 - 1	5.556 - 1
1.9	2.169 - 1	4.121 - 1	5.263 - 1
2.0	2.000 - 1	4.000 - 1	5.000 - 1
2.1	1.848 - 1	3.882 - 1	4.762 - 1
2.2	1.712 - 1	3.767 - 1	4.545 - 1
2.3	1.590 - 1	3.657 - 1	4.348 - 1
2.4	1.479 - 1	3.550 - 1	4.167 - 1
2.5	1.379 - 1	3.448 - 1	4.000 - 1
2.6	1.289 - 1	3.351 - 1	3.846 - 1
2.7	1.206 - 1	3.257 - 1	3.704 - 1
2.8	1.131 - 1	3.167 - 1	3.571 - 1
2.9	1.063 - 1	3.082 - 1	3.448 - 1
3.0	1.000 - 1	3.000 - 1	3.333 - 1
3.1	9.424 - 2	2.923 - 1	3.226 - 1
3.2	8.897 - 2	2.847 - 1	3.125 - 1
3.3	8.410 - 2	2.775 - 1	3.030 - 1
3.4	7.962 - 2	2.707 - 1	2.941 - 1
3.5	7.547 - 2	2.642 - 1	2.857 - 1
3.6	7.163 - 2	2.579 - 1	2.778 - 1
3.7	6.807 - 2	2.519 - 1	2.703 - 1
3.8	6.477 - 2	2.461 - 1	2.632 - 1
3.9	6.169 - 2	2.406 - 1	2.564 - 1
4.0	5.882 - 2	2.353 - 1	2.500 - 1
4.1	5.615 - 2	2.302 - 1	2.439 - 1
4.2	5.364 - 2	2.253 - 1	2.381 - 1
4.3	5.131 - 2	2.206 - 1	2.326 - 1
4.4	4.914 - 2	2.163 - 1	2.273 - 1
4.5	4.706 - 2	2.118 - 1	2.222 - 1
4.6	4.511 - 2	2.076 - 1	2.174 - 1
4.7	4.331 - 2	2.036 - 1	2.128 - 1
4.8	4.160 - 2	1.997 - 1	2.083 - 1
4.9	3.998 - 2	1.959 - 1	2.041 - 1
5.0	3.846 - 2	1.923 - 1	2.000 - 1

[*Wait*, 1962]. Thus, for the asymptotic limit $HX \to \infty$,

$$F \sim \left(\frac{2}{iH^2}\right) \frac{1}{X^2} \exp\left[-(i)^{1/2}H\right] \tag{26}$$

$$A \sim \left(\frac{2}{(i)^{1/2}H}\right) \frac{1}{X^2} \exp\left[-(i)^{1/2}H\right] \tag{27}$$

$$B \sim \left(\frac{4}{iH^2}\right) \frac{1}{X^3} \exp\left[-(i)^{1/2}H\right] \tag{28}$$

In a similar fashion, we readily find the corrsponding asymptotic forms

In particular, we see that

$$A/B \sim (i)^{1/2} H X/2 \tag{29}$$

TABLE 2. Field calculations for a line source on a conducting half-space

H = 0.10

X	A	PHASE(A) IN DEGREES	B	PHASE(B) IN DEGREES	A/B	PHASE(A/B) IN DEGREES	F	PHASE(F) IN DEGREES
0.00	1.041+000	3.14	0.000+000				2.986+000	-15.79
0.02	1.041+000	3.14	1.995-002	-0.59	5.215+001	1.73	2.986+000	-15.79
0.04	1.039+000	3.14	3.986-002	-0.59	2.606+001	1.73	2.985+000	-15.79
0.06	1.037+000	3.14	5.966-002	-0.59	1.739+001	1.73	2.984+000	-15.80
0.08	1.035+000	3.14	7.933-002	-0.59	1.304+001	1.74	2.983+000	-15.80
0.10	1.031+000	3.15	9.881-002	-0.59	1.043+001	1.74	2.981+000	-15.81
0.15	1.019+000	3.16	1.466-001	-0.60	6.956+000	1.76	2.975+000	-15.84
0.20	1.003+000	3.18	1.919-001	-0.61	5.224+000	1.79	2.967+000	-15.89
0.25	9.834-001	3.24	2.346-001	-0.63	3.490+000	1.87	2.944+000	-16.01
0.30	9.631-001	3.32	3.440-001	-0.66	2.625+000	1.98	2.914+000	-16.17
0.35	9.410-001	3.43	3.690-001	-0.70	2.104+000	2.13	2.879+000	-16.37
0.40	9.176-001	3.55	4.400-001	-0.75	1.764+000	2.30	2.839+000	-16.59
0.45	8.931-001	3.70	4.684-001	-0.81	1.526+000	2.51	2.794+000	-16.85
0.50	8.678-001	3.87	4.962-001	-0.87	1.339+000	2.74	2.748+000	-17.12
0.55	8.419-001	4.06	5.233-001	-0.94	1.198+000	3.00	2.701+000	-17.41
0.60	8.156-001	4.26	5.496-001	-1.02	1.087+000	3.28	2.654+000	-17.72
0.65	7.891-001	4.49	5.751-001	-1.10	9.961-001	3.59	2.606+000	-18.03
0.70	7.625-001	4.73	5.996-001	-1.19	9.215-001	3.92	2.559+000	-18.35
0.75	7.360-001	4.99	6.231-001	-1.28	8.590-001	4.27	2.513+000	-18.68
0.80	7.096-001	5.26	6.455-001	-1.38	8.061-001	4.64	2.467+000	-19.01
0.85	6.835-001	5.54	6.668-001	-1.49	7.606-001	5.03	2.423+000	-19.34
0.90	6.577-001	5.84	6.869-001	-1.55	7.219-001	5.43	2.380+000	-19.67
0.95	6.324-001	6.14	7.057-001	-1.71	6.880-001	5.85	2.338+000	-20.01
1.00	6.077-001	6.46	7.231-001	-1.82	6.584-001	6.28	2.298+000	-20.34
1.05	5.836-001	6.78	7.393-001	-1.94	6.324-001	6.72	2.259+000	-20.67
1.10	5.602-001	7.11	7.542-001	-2.07	6.094-001	7.17	2.220+000	-21.00
1.15	5.376-001	7.44	7.677-001	-2.19	5.891-001	7.63	2.183+000	-21.34
1.20	5.157-001	7.77	7.799-001	-2.32	5.710-001	8.09	2.146+000	-21.67
1.25	4.947-001	8.10	7.909-001	-2.46	5.550-001	8.56	2.113+000	-21.99
1.30	4.745-001	8.44	8.006-001	-2.59	5.406-001	9.03	2.079+000	-22.32
1.35	4.552-001	8.77	8.092-001	-2.73	5.278-001	9.50	2.047+000	-22.65
1.40	4.367-001	9.10	8.167-001	-2.87	5.163-001	9.98	2.016+000	-22.97
1.45	4.191-001	9.43	8.231-001	-3.02	5.060-001	10.45	1.986+000	-23.29
1.50	4.024-001	9.76	8.286-001	-3.17	4.967-001	10.92	1.956+000	-23.61
1.55	3.866-001	10.08	8.331-001	-3.32	4.884-001	11.39	1.927+000	-23.93
1.60	3.717-001	10.39	8.367-001	-3.47	4.810-001	11.86	1.899+000	-24.25
1.65	3.577-001	10.70	8.396-001	-3.62	4.744-001	12.33	1.871+000	-24.56
1.70	3.447-001	11.01	8.417-001	-3.78	4.684-001	12.81	1.844+000	-24.87
1.75	3.325-001	11.31	8.431-001	-3.94	4.630-001	13.28	1.817+000	-25.18
1.80	3.213-001	11.60	8.440-001	-4.11	4.581-001	13.75	1.791+000	-25.49
1.85	3.109-001	11.89	8.443-001	-4.27	4.536-001	14.22	1.765+000	-25.80
1.90	3.013-001	12.17	8.441-001	-4.44	4.495-001	14.69	1.740+000	-26.12
1.95	2.926-001	12.45	8.435-001	-4.60	4.457-001	15.16	1.715+000	-26.44
2.00	2.846-001	12.72	8.425-001	-4.77	4.422-001	15.66	1.690+000	-26.75
2.05	2.774-001	12.99	8.412-001	-4.94	4.390-001	16.09	1.666+000	-27.07
2.10	2.709-001	13.25	8.396-001	-5.11	4.361-001	16.56	1.642+000	-27.38
2.15	2.650-001	13.50	8.378-001	-5.28	4.335-001	17.03	1.622+000	-27.70
2.20	2.597-001	13.74	8.358-001	-5.45	4.311-001	17.50	1.602+000	-28.02
2.25	2.550-001	13.98	8.336-001	-5.63	4.290-001	17.97	1.583+000	-28.34
2.30	2.508-001	14.21	8.313-001	-5.80	4.270-001	18.44	1.565+000	-28.66
2.35	2.470-001	14.43	8.289-001	-5.98	4.253-001	18.91	1.548+000	-28.98
2.40	2.437-001	14.64	8.264-001	-6.16	4.237-001	19.38	1.532+000	-29.30
2.45	2.407-001	14.85	8.239-001	-6.34	4.223-001	19.85	1.516+000	-29.62
2.50	2.381-001	15.05	8.213-001	-6.51	4.210-001	20.32	1.501+000	-29.94
2.55	2.358-001	15.25	8.187-001	-6.69	4.198-001	20.79	1.487+000	-30.26
2.60	2.338-001	15.44	8.161-001	-6.87	4.187-001	21.26	1.473+000	-30.58
2.65	2.321-001	15.63	8.134-001	-7.05	4.178-001	21.73	1.460+000	-30.90
2.70	2.307-001	15.81	8.107-001	-7.23	4.170-001	22.20	1.447+000	-31.22
2.75	2.295-001	15.99	8.080-001	-7.41	4.163-001	22.67	1.435+000	-31.54
2.80	2.286-001	16.16	8.053-001	-7.59	4.157-001	23.14	1.424+000	-31.86
2.85	2.279-001	16.33	8.026-001	-7.77	4.152-001	23.61	1.413+000	-32.18
2.90	2.274-001	16.50	7.999-001	-7.95	4.148-001	24.08	1.403+000	-32.50
2.95	2.271-001	16.66	7.972-001	-8.13	4.145-001	24.55	1.393+000	-32.82
3.00	2.270-001	16.82	7.945-001	-8.31	4.143-001	25.02	1.384+000	-33.14

H = 0.50

X	A	PHASE(A) IN DEGREES	B	PHASE(B) IN DEGREES	A/B	PHASE(A/B) IN DEGREES	F	PHASE(F) IN DEGREES
0.00	1.092+000	-5.60	0.000+000				1.400+000	-34.91
0.02	1.092+000	-5.60	1.899-002	-6.46	5.751+001	2.86	1.400+000	-34.91
0.04	1.091+000	-5.61	3.793-002	-8.47	2.876+001	2.86	1.400+000	-34.92
0.06	1.089+000	-5.61	5.678-002	-8.48	1.918+001	2.87	1.399+000	-34.94
0.08	1.086+000	-5.62	7.549-002	-8.49	1.439+001	2.87	1.398+000	-34.97
0.10	1.083+000	-5.63	9.401-002	-8.51	1.152+001	2.88	1.396+000	-35.00
0.15	1.070+000	-5.67	1.392-001	-8.59	7.689+000	2.92	1.391+000	-35.10
0.20	1.054+000	-5.72	1.823-001	-8.69	5.780+000	2.97	1.384+000	-35.25
0.25	1.034+000	-5.81	2.604-001	-8.87	3.976+000	3.10	1.364+000	-35.67
0.30	1.011+000	-5.87	2.604-001	-8.87	3.876+000	3.10	1.364+000	-35.67
0.40	9.544-001	-6.07	3.262-001	-9.36	2.934+000	3.29	1.338+000	-36.23
0.50	8.922-001	-6.31	3.758-001	-9.85	2.374+000	3.53	1.336+000	-36.92
0.60	8.273-001	-6.60	4.125-001	-10.42	2.006+000	3.82	1.271+000	-37.72
0.70	7.630-001	-6.91	4.369-001	-11.08	1.746+000	4.16	1.233+000	-38.62
0.80	7.014-001	-7.26	4.508-001	-11.81	1.556+000	4.55	1.194+000	-39.60
0.90	6.438-001	-7.63	4.564-001	-12.60	1.411+000	4.97	1.154+000	-40.63
1.00	5.910-001	-8.01	4.564-001	-13.45	1.298+000	5.44	1.114+000	-41.72
1.10	5.431-001	-8.41	4.497-001	-14.35	1.208+000	5.94	1.074+000	-42.85
1.20	5.000-001	-8.82	4.405-001	-15.30	1.135+000	6.47	1.035+000	-44.01
1.30	4.615-001	-9.24	4.288-001	-16.28	1.076+000	7.04	9.965-001	-45.19
1.40	4.273-001	-9.67	4.156-001	-17.30	1.028+000	7.62	9.596-001	-46.39
1.50	3.963-001	-10.11	4.014-001	-18.34	9.874-001	8.23	9.239-001	-47.60
1.60	3.689-001	-10.56	3.866-001	-19.42	9.541-001	8.86	8.896-001	-48.82
1.70	3.444-001	-11.01	3.718-001	-20.51	9.264-001	9.50	8.569-001	-50.05
1.80	3.226-001	-11.47	3.573-001	-21.63	9.034-001	10.16	8.245-001	-51.27
1.90	3.029-001	-11.94	3.434-001	-22.76	8.844-001	10.82	7.945-001	-52.50
2.00	2.851-001	-12.41	3.302-001	-23.90	8.687-001	11.49	7.664-001	-53.72
2.10	2.692-001	-12.89	3.176-001	-25.04	8.560-001	12.17	7.395-001	-54.94
2.20	2.547-001	-13.38	3.061-001	-26.19	8.457-001	12.85	7.139-001	-56.16
2.30	2.416-001	-13.87	2.955-001	-27.34	8.376-001	13.53	6.893-001	-57.37
2.40	2.297-001	-14.37	2.857-001	-28.49	8.314-001	14.22	6.659-001	-58.57
2.50	2.189-001	-14.89	2.766-001	-29.64	8.270-001	14.90	6.434-001	-59.76
2.60	2.090-001	-15.40	2.684-001	-30.78	8.240-001	15.59	6.219-001	-60.94
2.70	1.998-001	-15.93	2.608-001	-31.92	8.223-001	16.28	6.012-001	-62.10
2.80	1.913-001	-16.46	2.539-001	-33.05	8.217-001	16.97	5.813-001	-63.25
2.90	1.834-001	-17.00	2.477-001	-34.17	8.220-001	17.66	5.621-001	-64.39
3.00	1.761-001	-17.55	2.419-001	-35.29	8.232-001	18.36	5.436-001	-65.51
3.10	1.693-001	-18.10	2.366-001	-36.40	8.253-001	19.06	5.258-001	-66.61
3.20	1.630-001	-18.65	2.317-001	-37.50	8.282-001	19.76	5.086-001	-67.70
3.30	1.571-001	-19.21	2.272-001	-38.59	8.317-001	20.46	4.920-001	-68.77
3.40	1.516-001	-19.78	2.230-001	-39.67	8.359-001	21.16	4.760-001	-69.83
3.50	1.465-001	-20.34	2.192-001	-40.74	8.407-001	21.86	4.605-001	-70.87
3.60	1.418-001	-20.91	2.157-001	-41.80	8.460-001	22.56	4.455-001	-71.89
3.70	1.374-001	-21.48	2.125-001	-42.85	8.519-001	23.26	4.310-001	-72.90
3.80	1.333-001	-22.13	2.096-001	-43.89	8.582-001	23.96	4.170-001	-73.89
3.90	1.295-001	-22.73	2.070-001	-44.92	8.650-001	24.66	4.034-001	-74.87
4.00	1.260-001	-23.33	2.046-001	-45.94	8.722-001	25.36	3.903-001	-75.83
4.20	1.197-001	-24.53	2.005-001	-47.98	8.874-001	26.77	3.651-001	-77.72
4.40	1.142-001	-25.74	1.969-001	-49.99	9.035-001	28.18	3.413-001	-79.56
4.60	1.093-001	-26.96	1.938-001	-51.98	9.203-001	29.59	3.189-001	-81.34
4.80	1.049-001	-28.18	1.913-001	-53.94	9.378-001	30.99	2.979-001	-83.07
5.00	1.009-001	-29.40	1.892-001	-55.88	9.559-001	32.40	2.782-001	-84.74

H = 0.70

X	A	PHASE(A) IN DEGREES	B	PHASE(B) IN DEGREES	A/B	PHASE(A/B) IN DEGREES	F	PHASE(F) IN DEGREES
0.00	1.070+000	0.59	0.000+000				2.298+000	-21.19
0.02	1.070+000	0.59	1.982-002	-1.93	5.397+001	2.51	2.298+000	-21.19
0.04	1.069+000	0.59	3.960-002	-1.93	2.699+001	2.52	2.297+000	-21.20
0.06	1.067+000	0.59	5.928-002	-1.93	1.799+001	2.52	2.296+000	-21.20
0.08	1.064+000	0.59	7.882-002	-1.93	1.350+001	2.53	2.295+000	-21.22
0.10	1.062+000	0.60	9.817-002	-1.94	1.080+001	2.54	2.293+000	-21.23
0.15	1.054+000	0.61	1.464-001	-1.96	7.206+000	2.57	2.288+000	-21.26
0.20	1.042+000	0.62	1.936-001	-1.98	5.413+000	2.61	2.280+000	-21.31
0.25	1.027+000	0.64	2.387-001	-2.01	3.622+000	2.72	2.258+000	-21.45
0.30	1.009+000	0.67	2.727-001	-2.05	3.622+000	2.72	2.258+000	-21.55
0.40	9.623-001	0.73	3.415-001	-2.15	2.730+000	2.88	2.224+000	-21.81
0.50	8.702-001	0.88	3.559-001	-2.28	2.198+000	3.08	2.194+000	-22.13
0.60	8.055-001	0.90	4.362-001	-2.43	1.847+000	3.32	2.155+000	-22.51
0.70	7.613-001	1.01	4.691-001	-2.60	1.597+000	3.61	2.112+000	-22.93
0.80	6.798-001	1.13	4.813-001	-2.79	1.413+000	3.92	2.068+000	-23.38
0.90	6.226-001	1.27	4.899-001	-3.00	1.271+000	4.25	2.023+000	-23.86
1.00	5.780-001	1.43	4.819-001	-3.23	1.159+000	4.66	1.977+000	-24.37
1.10	5.225-001	1.59	4.889-001	-3.48	1.069+000	5.07	1.931+000	-24.89
1.20	4.797-001	1.77	4.823-001	-3.74	9.947-001	5.51	1.886+000	-25.43
1.30	4.416-001	1.96	4.738-001	-4.01	9.335-001	5.97	1.841+000	-25.97
1.40	4.075-001	2.15	4.620-001	-4.30	8.821-001	6.45	1.798+000	-26.53
1.50	3.773-001	2.35	4.479-001	-4.60	8.387-001	6.94	1.756+000	-27.09
1.60	3.505-001	2.54	4.372-001	-4.91	8.017-001	7.45	1.715+000	-27.65
1.70	3.265-001	2.75	4.241-001	-5.22	7.699-001	7.97	1.675+000	-28.21
1.80	3.052-001	2.95	4.110-001	-5.55	7.426-001	8.50	1.637+000	-28.78
1.90	2.861-001	3.14	3.980-001	-5.89	7.190-001	9.03	1.600+000	-29.35
2.00	2.691-001	3.34	3.852-001	-6.23	6.986-001	9.57	1.564+000	-29.92
2.10	2.538-001	3.53	3.728-001	-6.59	6.809-001	10.11	1.529+000	-30.48
2.20	2.400-001	3.71	3.607-001	-6.95	6.654-001	10.65	1.496+000	-31.05
2.30	2.276-001	3.88	3.491-001	-7.31	6.521-001	11.19	1.463+000	-31.61
2.40	2.164-001	4.05	3.379-001	-7.68	6.405-001	11.73	1.432+000	-32.17
2.50	2.062-001	4.20	3.272-001	-8.06	6.304-001	12.26	1.402+000	-32.73
2.60	1.970-001	4.35	3.169-001	-8.44	6.217-001	12.79	1.373+000	-33.29
2.70	1.886-001	4.48	3.070-001	-8.83	6.143-001	13.31	1.345+000	-33.84
2.80	1.808-001	4.61	2.975-001	-9.22	6.079-001	13.83	1.317+000	-34.40
2.90	1.738-001	4.72	2.884-001	-9.62	6.025-001	14.33	1.290+000	-34.94
3.00	1.673-001	4.81	2.798-001	-10.02	5.980-001	14.83	1.265+000	-35.49
3.10	1.613-001	4.90	2.715-001	-10.42	5.943-001	15.32	1.240+000	-36.04
3.20	1.558-001	4.97	2.635-001	-10.83	5.912-001	15.80	1.216+000	-36.57
3.30	1.507-001	5.02	2.559-001	-11.24	5.887-001	16.27	1.192+000	-37.14
3.40	1.459-001	5.07	2.486-001	-11.66	5.868-001	16.73	1.170+000	-37.64
3.50	1.415-001	5.10	2.417-001	-12.08	5.854-001	17.18	1.147+000	-38.17
3.60	1.374-001	5.12	2.350-001	-12.50	5.846-001	17.62	1.126+000	-38.69
3.70	1.335-001	5.13	2.286-001	-12.92	5.842-001	18.05	1.105+000	-39.21
3.80	1.299-001	5.13	2.224-001	-13.35	5.842-001	18.48	1.085+000	-39.73
3.90	1.265-001	5.12	2.165-001	-13.78	5.846-001	18.90	1.065+000	-40.25
4.00	1.234-001	5.10	2.108-001	-14.21	5.853-001	19.31	1.046+000	-40.77
4.20	1.176-001	5.01	2.001-001	-15.08	5.878-001	20.09	1.010+000	-41.79
4.40	1.124-001	4.89	1.901-001	-15.95	5.914-001	20.84	9.750-001	-42.81
4.60	1.078-001	4.73	1.809-001	-16.83	5.959-001	21.56	9.420-001	-43.81
4.80	1.036-001	4.52	1.723-001	-17.72	6.013-001	22.24	9.105-001	-44.80
5.00	9.982-002	4.28	1.644-001	-18.60	6.073-001	22.89	8.806-001	-45.76

H = 1.00

X	A	PHASE(A) IN DEGREES	B	PHASE(B) IN DEGREES	A/B	PHASE(A/B) IN DEGREES	F	PHASE(F) IN DEGREES
0.00	1.000+000	-21.52	0.000+000				7.775-001	-56.23
0.02	9.998-001	-21.52	1.863-002	-23.52	6.013+001	1.99	7.774-001	-56.24
0.04	9.995-001	-21.54	3.721-002	-23.53	3.007+001	2.00	7.770-001	-56.26
0.06	9.987-001	-21.56	5.569-002	-23.56	2.006+001	2.02	7.763-001	-56.29
0.08	9.940-001	-21.59	7.405-002	-23.60	1.505+001	2.01	7.753-001	-56.34
0.10	9.905-001	-21.64	9.222-002	-23.66	1.204+001	2.05	7.741-001	-56.40
0.15	9.787-001	-21.78	1.216-001	-23.84	8.048+000	2.05	7.698-001	-56.60
0.20	9.627-001	-21.99	1.590-001	-24.09	6.054+000	2.18	7.635-001	-56.89
0.25	9.198-001	-22.55	2.260-001	-24.80	4.071+000	2.25	7.476-001	-57.64
0.30	8.659-001	-23.32	2.803-001	-25.77	3.089+000	2.44	7.263-001	-58.76
0.40	8.056-001	-24.26	3.212-001	-26.97	2.508+000	2.72	7.018-001	-60.06
0.50	7.428-001	-25.35	3.490-001	-28.39	2.128+000	3.04	6.728-001	-61.61
0.60	6.807-001	-26.55	3.654-001	-29.99	1.863+000	3.44	6.429-001	-63.32
0.70	6.212-001	-27.86	3.722-001	-31.76	1.669+000	3.91	6.120-001	-65.18
0.80	5.658-001	-29.24	3.716-001	-33.66	1.523+000	4.43	5.810-001	-67.15
0.90	5.151-001	-30.67	3.652-001	-35.69	1.410+000	5.00	5.502-001	-69.22
1.00	4.692-001	-32.14	3.548-001	-37.81	1.322+000	5.62	5.202-001	-71.35
1.10	4.279-001	-33.63	3.417-001	-40.02	1.252+000	6.25	4.911-001	-73.53
1.20	3.911-001	-35.12	3.268-001	-42.29	1.197+000	7.17	4.633-001	-75.75
1.30	3.582-001	-36.62	3.109-001	-44.62	1.152+000	8.09	4.366-001	-77.98
1.40	3.289-001	-38.11	2.945-001	-46.99	1.117+000	8.84	4.113-001	-80.23
1.50	3.028-001	-39.60	2.782-001	-49.40	1.089+000	9.84	3.874-001	-82.48
1.60	2.796-001	-41.08	2.621-001	-51.84	1.067+000	10.78	3.647-001	-84.72
1.70	2.587-001	-42.51	2.465-001	-54.3	1.050+000	11.79	3.433-001	-86.94
1.80	2.400-001	-43.93	2.314-001	-56.	1.037+000	12.84	3.232-001	-89.15
2.00	2.232-001	-45.33	2.171-001	-59.24	1.028+000	13.91	3.042-001	-91.34
2.10	2.081-001	-46.71	2.034-001	-61.72	1.023+000	15.01	2.864-001	-93.50
2.20	1.944-001	-48.07	1.905-001	-64.18	1.020+000	16.13	2.698-001	-95.62
2.30	1.820-001	-49.41	1.783-001	-66.64	1.020+000	17.27	2.539-001	-97.72
2.40	1.707-001	-50.72	1.669-001	-69.14	1.023+000	18.43	2.390-001	-99.77
2.50	1.604-001	-52.00	1.561-001	-71.60	1.027+000	19.60	2.251-001	-101.79
2.60	1.509-001	-53.27	1.460-001	-74.04	1.034+000	20.77	2.120-001	-103.77
2.70	1.422-001	-54.51	1.366-001	-76.47	1.042+000	21.98	1.997-001	-105.70
2.80	1.343-001	-55.73	1.277-001	-78.87	1.051+000	23.15	1.882-001	-107.59
2.90	1.269-001	-56.92	1.194-001	-81.26	1.063+000	24.34	1.773-001	-109.44
3.00	1.201-001	-58.09	1.116-001	-83.62	1.076+000	25.53	1.671-001	-111.24
3.10	1.138-001	-59.24	1.044-001	-85.96	1.090+000	26.72	1.575-001	-112.99
3.20	1.079-001	-60.37	9.761-002	-88.28	1.105+000	27.91	1.485-001	-114.69
3.30	1.024-001	-61.47	9.127-002	-90.57	1.122+000	29.10	1.400-001	-116.34
3.40	9.732-002	-62.55	8.534-002	-92.83	1.140+000	30.28	1.321-001	-117.93
3.50	9.255-002	-63.60	7.981-002	-95.06	1.160+000	31.46	1.246-001	-119.48
3.60	8.809-002	-64.64	7.463-002	-97.26	1.180+000	32.62	1.175-001	-120.97
3.70	8.390-002	-65.64	6.979-002	-99.43	1.202+000	33.78	1.108-001	-122.40
3.80	7.997-002	-66.63	6.527-002	-101.56	1.225+000	34.93	1.047-001	-123.78
3.90	7.627-002	-67.59	6.104-002	-103.66	1.249+000	36.07	9.881-002	-125.11
4.00	7.278-002	-68.52	5.709-002	-105.72	1.274+000	37.20	9.330-002	-126.37
4.20	6.640-002	-70.32	4.993-002	-109.74	1.330+000	39.42	8.305-002	-128.73
4.40	6.071-002	-72.02	4.368-002	-113.60	1.390+000	41.58	7.427-002	-130.84
4.60	5.561-002	-73.61	3.821-002	-117.29	1.456+000	43.69	6.652-002	-132.72
4.80	5.104-002	-75.09	3.342-002	-120.81	1.527+000	45.72	5.966-002	-134.34
5.00	4.692-002	-76.47	2.924-002	-124.15	1.605+000	47.68	5.365-002	-135.72

TABLE 2. (continued)

H = 2.00

X	A	PHASE(A) IN DEGREES	B	PHASE(B) IN DEGREES	A/B	PHASE(A/B) IN DEGREES	F	PHASE(F) IN DEGREES
0.00	6.847-001	-58.87	0.000+000				2.985-001	-97.71
0.02	6.840-001	-58.89	1.114-002	-59.33	6.141+001	0.45	2.984-001	-97.73
0.04	6.830-001	-58.92	2.224-002	-59.37	3.071+001	0.45	2.982-001	-97.77
0.06	6.814-001	-58.98	3.327-002	-59.44	2.048+001	0.46	2.977-001	-97.83
0.08	6.792-001	-59.05	4.418-002	-59.53	1.537+001	0.47	2.971-001	-97.93
0.10	6.765-001	-59.17	5.495-002	-59.65	1.231+001	0.48	2.964-001	-98.04
0.15	6.664-001	-59.54	8.101-002	-60.07	8.227+000	0.52	2.937-001	-98.45
0.20	6.531-001	-60.06	1.055-001	-60.64	6.193+000	0.58	2.900-001	-99.02
0.30	6.174-001	-61.49	1.480-001	-62.25	4.173+000	0.76	2.800-001	-100.62
0.40	5.731-001	-63.43	1.804-001	-64.44	3.176+000	1.02	2.671-001	-102.76
0.50	5.234-001	-65.78	2.023-001	-67.16	2.589+000	1.38	2.520-001	-105.39
0.60	4.732-001	-68.48	2.144-001	-70.32	2.207+000	1.84	2.356-001	-108.43
0.70	4.237-001	-71.46	2.181-001	-73.88	1.943+000	2.43	2.185-001	-111.80
0.80	3.771-001	-74.63	2.152-001	-77.77	1.752+000	3.14	2.017-001	-115.44
0.90	3.343-001	-77.35	2.075-001	-81.35	1.611+000	4.00	1.849-001	-119.27
1.00	2.957-001	-81.30	1.866-001	-86.31	1.584+000	5.02	1.684-001	-123.25
1.10	2.614-001	-84.64	1.838-001	-90.87	1.423+000	6.18	1.531-001	-127.29
1.20	2.311-001	-88.05	1.695-001	-95.55	1.361+000	7.50	1.388-001	-131.38
1.30	2.046-001	-91.35	1.557-001	-100.32	1.314+000	8.97	1.256-001	-135.48
1.40	1.813-001	-94.56	1.418-001	-105.15	1.279+000	10.59	1.134-001	-139.56
1.50	1.610-001	-97.66	1.284-001	-110.02	1.254+000	12.36	1.022-001	-143.57
1.60	1.432-001	-100.64	1.157-001	-114.90	1.237+000	14.27	9.197-002	-147.50
1.70	1.276-001	-103.47	1.040-001	-119.77	1.228+000	16.30	8.267-002	-151.33
1.80	1.140-001	-106.16	9.308-002	-124.62	1.225+000	18.45	7.423-002	-155.04
1.90	1.021-001	-108.70	8.314-002	-129.41	1.228+000	20.71	6.660-002	-158.60
2.00	9.163-002	-111.07	7.409-002	-134.14	1.237+000	23.07	5.970-002	-162.01
2.10	8.241-002	-113.29	6.590-002	-138.81	1.251+000	25.52	5.348-002	-165.24
2.20	7.428-002	-115.34	5.851-002	-143.38	1.270+000	28.04	4.798-002	-168.29
2.30	6.710-002	-117.24	5.186-002	-147.85	1.294+000	30.62	4.285-002	-171.14
2.40	6.076-002	-118.95	4.590-002	-152.22	1.323+000	33.26	3.833-002	-173.77
2.50	5.512-002	-120.56	4.057-002	-156.47	1.359+000	35.91	3.429-002	-176.17
2.60	5.012-002	-121.98	3.581-002	-160.58	1.400+000	38.59	3.068-002	-178.34
2.70	4.568-002	-123.26	3.157-002	-164.55	1.447+000	41.29	2.746-002	179.75
2.80	4.172-002	-124.43	2.779-002	-168.36	1.501+000	43.97	2.459-002	178.10
2.90	3.820-002	-125.39	2.444-002	-172.01	1.563+000	46.62	2.204-002	176.77
3.00	3.506-002	-126.25	2.140-002	-175.48	1.638+000	49.23	1.979-002	175.62
3.10	3.224-002	-126.98	1.883-002	-178.75	1.712+000	51.77	1.780-002	174.80
3.20	2.972-002	-127.59	1.650-002	178.16	1.801+000	-305.78	1.604-002	174.25
3.30	2.746-002	-128.09	1.444-002	176.35	1.902+000	-303.44	1.450-002	173.99
3.40	2.544-002	-128.49	1.263-002	172.75	2.014+000	-301.24	1.314-002	173.98
3.50	2.363-002	-128.79	1.104-002	170.42	2.141+000	-299.21	1.196-002	174.21
3.60	2.199-002	-129.00	9.637-003	168.37	2.282+000	-297.37	1.094-002	174.67
3.70	2.052-002	-129.14	8.413-003	166.63	2.439+000	-295.77	1.004-002	175.31
3.80	1.920-002	-129.21	7.345-003	165.21	2.614+000	-294.42	9.267-003	176.11
3.90	1.800-002	-129.21	6.415-003	164.15	2.806+000	-293.36	8.595-003	177.01
4.00	1.692-002	-129.18	5.609-003	163.46	3.016+000	-292.63	8.012-003	178.00
4.20	1.504-002	-128.98	4.314-003	163.24	3.487+000	-292.22	7.063-003	-179.96
4.40	1.349-002	-128.69	3.367-003	164.59	4.006+000	-293.28	6.334-003	-178.03
4.60	1.219-002	-128.35	2.689-003	167.34	4.533+000	-295.69	5.759-003	-176.36
4.80	1.109-002	-128.09	2.213-003	171.05	5.011+000	-299.14	5.285-003	-175.03
5.00	1.015-002	-127.58	1.882-003	175.10	5.392+000	-302.68	4.831-003	-174.05

H = 10.00

X	A	PHASE(A) IN DEGREES	B	PHASE(B) IN DEGREES	A/B	PHASE(A/B) IN DEGREES	F	PHASE(F) IN DEGREES
0.00	5.701-003	-20.45	0.000+000				5.527-004	[illegible]
0.02	5.693-003	-20.52	9.685-005	-18.67	5.878+001	-1.90	5.520-004	-63.97
0.04	5.669-003	-20.74	1.928-004	-18.85	2.940+001	-1.89	5.500-004	[illegible]
0.06	5.629-003	-21.09	2.870-004	-19.22	1.961+001	-1.87	5.466-004	[illegible]
0.08	5.575-003	-21.59	3.785-004	-19.74	1.473+001	-1.85	5.415-004	[illegible]
0.10	5.505-003	-22.23	4.666-004	-20.41	1.180+001	-1.82	5.260-004	[illegible]
0.15	5.272-003	-24.43	6.671-004	-22.72	7.904+000	-1.71	5.159-004	[illegible]
0.20	4.966-003	-27.46	8.321-004	-25.92	5.568+000	-1.55	4.813-004	[illegible]
0.30	4.204-003	-35.84	1.036-003	-34.85	4.058+000	-0.99	[illegible]	[illegible]
0.40	3.360-003	-46.87	1.074-003	-46.87	3.130+000	-0.00	3.453-004	-90.44
0.50	2.554-003	-59.87	9.841-004	-61.52	2.595+000	1.65	2.693-004	-103.67
0.60	1.857-003	-74.06	8.225-004	-78.31	2.258+000	4.25	2.010-004	-118.29
0.70	1.296-003	-88.53	6.387-004	-96.69	2.030+000	8.16	1.419-004	-133.51
0.75	1.068-003	-95.55	5.496-004	-106.29	1.942+000	10.74	1.198-004	-141.08
0.80	8.708-004	-102.25	4.662-004	-116.08	1.868+000	13.83	9.872-005	-148.46
0.85	7.036-004	-108.46	3.849-004	-125.98	1.804+000	17.51	8.042-005	-155.52
0.90	5.631-004	-114.02	3.218-004	-135.92	1.750+000	21.90	6.473-005	-162.11
0.95	4.468-004	-118.60	2.620-004	-145.83	1.706+000	27.14	5.147-005	-168.02
1.00	3.518-004	-122.25	2.104-004	-155.64	1.673+000	33.39	4.041-005	-173.09
1.05	2.758-004	-124.40	1.665-004	-165.26	1.656+000	40.85	3.133-005	-176.82
1.10	2.162-004	-124.85	1.297-004	-174.60	1.667+000	49.75	2.403-005	-178.98
1.15	1.722-004	-123.38	9.933-005	176.44	1.723+000	-299.82	1.834-005	-179.01
1.20	1.383-004	-120.00	7.457-005	168.00	1.855+000	-288.00	1.408-005	-176.37
1.25	1.157-004	-115.15	5.468-005	160.28	2.115+000	-275.43	1.110-005	-170.86
1.30	1.008-004	-109.69	3.896-005	153.59	2.587+000	-263.28	9.716-006	-163.16
1.32	9.647-005	-107.58	3.370-005	151.32	2.863+000	-258.87	8.713-006	-159.82
1.34	9.286-005	-105.53	2.896-005	149.34	3.207+000	-254.87	8.323-006	[illegible]
1.36	8.982-005	-103.65	2.471-005	147.74	3.635+000	-251.39	8.027-006	-153.39
1.38	8.724-005	-101.95	2.092-005	146.60	4.170+000	-248.54	7.806-006	-150.51
1.40	8.501-005	-100.43	1.756-005	146.05	4.840+000	-246.48	7.640-006	-147.94
1.42	8.305-005	-99.19	1.461-005	146.28	5.683+000	-245.35	7.515-006	-145.70
1.44	8.128-005	-97.95	1.205-005	147.64	6.746+000	-245.48	7.418-006	-143.80
1.46	7.965-005	-96.97	9.858-006	150.17	8.080+000	-247.14	7.337-006	-142.22
1.48	7.812-005	-96.16	8.040-006	154.63	9.716+000	-250.79	[illegible]	-140.94
1.50	7.665-005	-95.48	6.604-006	161.41	1.161+001	-256.89	7.196-006	-139.93
1.52	7.527-005	-94.93	5.564-006	170.73	[illegible]	-265.66	7.127-006	[illegible]
1.54	7.381-005	-94.49	[illegible]	-177.97	[illegible]	83.42	[illegible]	[illegible]
1.56	7.241-005	-94.15	4.653-006	-166.07	1.556+001	71.93	6.974-006	[illegible]
1.58	7.102-005	-93.88	4.659-006	-155.55	1.524+001	61.67	6.888-006	-137.82
1.60	6.967-005	-93.68	4.837-006	-147.32	1.440+001	53.64	6.796-006	-137.63
1.62	6.823-005	-93.53	5.092-006	-141.41	1.340+001	47.88	6.698-006	[illegible]
1.64	6.684-005	-93.43	5.363-006	-137.40	1.246+001	43.97	6.593-006	-137.51
1.66	6.545-005	-93.36	5.616-006	-134.81	1.165+001	41.45	6.483-006	-137.53
1.68	6.407-005	-93.32	5.832-006	-133.23	1.099+001	39.91	6.369-006	-137.60
1.70	6.270-005	-93.30	6.003-006	-132.38	1.044+001	39.08	6.251-006	-137.69
1.75	5.932-005	-93.29	6.231-006	-132.19	9.520+000	38.90	5.946-006	-137.98
1.80	5.608-005	-93.31	6.214-006	-133.43	9.025+000	40.12	5.635-006	-138.27
1.85	5.299-005	-93.31	6.018-006	-135.18	8.807+000	41.86	5.329-006	-138.50
1.90	5.010-005	-93.29	5.787-006	-136.98	8.778+000	43.69	5.036-006	-138.64
1.95	4.740-005	-93.22	5.335-006	-138.59	8.865+000	45.37	4.760-006	-138.69
2.00	4.490-005	-93.13	4.940-006	-139.89	9.090+000	46.76	4.503-006	-138.65

H = 5.00

X	A	PHASE(A) IN DEGREES	B	PHASE(B) IN DEGREES	A/B	PHASE(A/B) IN DEGREES	F	PHASE(F) IN DEGREES
0.00	1.334-001	-178.33	0.000+000				2.516-002	139.64
0.02	1.333-001	-178.36	2.202-003	-177.06	6.053+001	-1.30	2.514-002	139.51
0.04	1.330-001	-178.46	4.393-003	-177.17	3.028+001	-1.29	2.509-002	139.41
0.06	1.325-001	-178.63	6.559-003	-177.35	2.020+001	-1.28	2.501-002	139.23
0.08	1.317-001	-178.87	8.699-003	-177.60	1.516+001	-1.27	2.490-002	[illegible]
0.10	1.308-001	-179.17	1.077-002	-177.93	1.214+001	-1.25	2.476-002	138.68
0.15	1.276-001	179.77	1.571-002	-179.05	8.123+000	358.82	2.428-002	137.62
0.20	1.233-001	178.32	2.013-002	179.40	6.123+000	-1.08	2.363-002	[illegible]
0.30	1.120-001	173.97	2.705-002	175.05	4.142+000	-0.77	[illegible]	132.04
0.40	9.862-002	168.91	3.110-002	169.17	3.171+000	-0.26	1.974-002	125.59
0.50	8.444-002	162.43	3.241-002	161.94	2.605+000	0.49	[illegible]	119.90
0.60	7.069-002	155.13	3.152-002	153.56	2.243+000	1.57	1.498-002	112.32
0.70	5.809-002	147.33	2.909-002	144.25	1.997+000	3.04	1.267-002	104.09
0.80	4.706-002	139.21	2.579-002	134.21	1.824+000	5.00	[illegible]	95.44
0.90	3.769-002	131.16	2.215-002	123.64	1.701+000	7.52	8.660-003	86.62
1.00	2.990-002	123.39	1.853-002	112.71	1.614+000	10.68	7.015-003	77.87
1.10	2.356-002	116.16	1.517-002	101.61	1.553+000	14.54	5.615-003	69.40
1.20	1.846-002	109.67	1.218-002	90.48	1.515+000	19.19	4.443-003	61.45
1.30	1.441-002	104.16	9.624-003	79.48	1.497+000	24.68	3.477-003	[illegible]
1.40	1.124-002	99.81	7.485-003	68.74	1.502+000	31.06	[illegible]	48.00
1.50	8.792-003	96.78	5.734-003	58.41	1.532+000	38.37	2.069-003	43.04
1.55	7.795-003	95.80	4.990-003	53.45	1.562+000	42.35	1.809-003	[illegible]
1.60	6.929-003	95.18	4.320-003	48.64	1.602+000	46.54	1.581-003	39.70
1.65	6.180-003	94.92	3.726-003	44.03	1.654+000	50.90	1.381-003	38.73
1.70	5.536-003	95.00	3.213-003	39.62	1.723+000	55.38	1.208-003	[illegible]
1.75	4.982-003	95.40	2.751-003	35.44	1.811+000	59.94	1.055-003	38.32
1.80	4.510-003	96.07	2.345-003	31.57	1.923+000	64.50	9.324-004	39.04
1.85	4.107-003	96.97	1.990-003	28.01	2.064+000	68.96	[illegible]	[illegible]
1.90	3.766-003	98.06	1.681-003	24.82	2.241+000	73.22	[illegible]	41.95
1.95	3.476-003	99.22	1.413-003	22.07	2.460+000	77.15	6.645-004	44.06
2.00	3.229-003	100.46	1.182-003	19.84	2.732+000	80.61	[illegible]	46.47
2.05	3.018-003	101.69	9.843-004	18.24	3.066+000	83.46	5.551-004	49.03
2.10	2.836-003	102.89	8.165-004	17.37	3.473+000	85.52	[illegible]	51.60
2.15	2.679-003	104.01	6.757-004	17.39	3.964+000	86.63	4.900-004	54.05
2.20	2.540-003	105.04	5.590-004	18.44	4.545+000	86.59	4.659-004	56.29
2.25	2.418-003	105.95	4.643-004	20.68	5.208+000	85.27	4.494-004	58.26
2.30	2.308-003	106.75	3.893-004	24.19	5.929+000	82.56	4.284-004	59.93
2.35	2.208-003	107.44	3.320-004	28.91	6.651+000	78.52	4.135-004	61.30
2.40	2.117-003	108.02	2.901-004	34.57	7.295+000	73.44	4.001-004	62.40
2.45	2.032-003	108.50	2.611-004	40.68	7.781+000	67.63	3.877-004	63.25
2.50	1.953-003	108.90	2.421-004	46.62	8.068+000	62.28	3.759-004	63.89
2.55	1.878-003	109.23	2.299-004	51.92	8.169+000	57.32	3.646-004	64.36
2.60	1.808-003	109.49	2.222-004	56.28	8.136+000	53.22	3.534-004	64.58
2.65	1.742-003	109.71	2.170-004	59.66	8.027+000	50.05	3.426-004	64.99
2.70	1.679-003	109.88	2.128-004	62.14	7.888+000	47.74	3.319-004	65.02
2.75	1.618-003	110.01	2.088-004	63.86	7.751+000	46.16	3.213-004	65.09
2.80	1.561-003	110.12	2.046-004	64.97	7.631+000	45.15	3.110-004	65.11
2.85	1.507-003	110.21	1.999-004	65.63	7.538+000	44.59	3.009-004	65.10
2.90	1.454-003	110.29	1.946-004	65.94	7.473+000	44.35	2.910-004	65.07
2.95	1.405-003	110.35	1.899-004	65.99	7.436+000	44.36	2.814-004	65.04
3.00	1.357-003	110.41	1.827-004	65.88	7.427+000	44.53	2.721-004	65.01

NUMERICAL RESULTS

The numerical values of A, B, and A/B for the zero frequency limit (i.e., $H = 0$) are listed in Table 1 for X ranging from 0 to 5. Of course, in this static limit, both A and B are purely real.

The numerical results for the complex values of A, B, and A/B are given in Table 2 for H ranging from 0.1 to 10. Here, the amplitudes of the quantities and their phases are given. For the smaller H values, it is immediately evident that the results are consistent with the zero-frequency values in Table 1. Also, if HX is sufficiently large, the complex values of A, B, and A/B do appear to approach their respective asymptotic limits. On a point of theoretical interest, we note that the asymptotic results are really only valid at quite large values of the parameters X and H. Nevertheless, they do serve as a good check on the numerical integration, since this is just when the integrands have the greatest number of oscillations over the range of integration.

A key parameter in the above formulation is H. This can be expressed in a fairly simple form as follows:

$$H = (\sigma\mu\omega)^{1/2}h = 0.086(\sigma_m f)^{1/2}h_{km}$$

if σ_m is the conductivity expressed in mmho m^{-1}, f is the frequency in Hz, and h_{km} is the burial depth in km. Thus, for example, if $\sigma_m = 1$, $f = 100$, and $h_{km} = 0.2$, we have H = 0.17. As we can see from the tables, this value of H is sufficiently small that the behavior of the functions A and B is very similar to that for the static case (i.e., zero frequency) where $H = 0$.

We stress that the present analysis and results are applicable only to a homogeneous half-space model

for the earth. Nevertheless, this should serve as a guide for further work on the subject.

FINAL REMARKS

A graphical presentation of the ratio $|A/B|$ is given in Figure 3. As is indicated, the ordinate is the magnitude of the ratio between the horizontal and the vertical magnetic field at the observer for a line source on the surface. The abscissa X or x/h is the normalized horizontal coordinate (i.e., $x = 0$ for the observer at a distance h directly beneath the source). The phase of the quantity A/B is shown in Figure 4. In each case, the H values range from 0 to 10.

Both the amplitude and phase of the quantity A/B are measurable quantities if the observer is equipped with a crossed loop receiving antenna and suitable switching facility. If the value of H is known (or if it can be assumed to be effectively zero), the value of X should, in principle, be estimated from the measured ratio $|A/B|$. Even if H is not known,

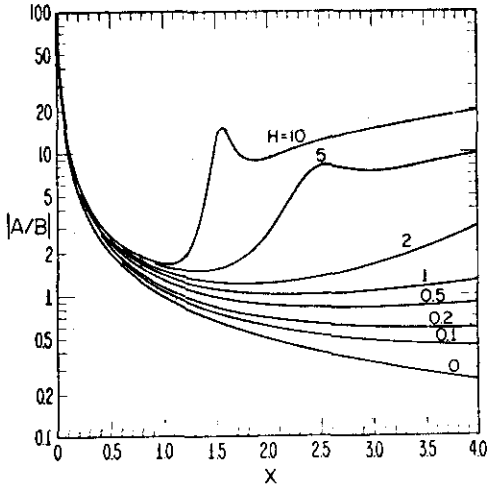

Fig. 3. Ratio of the magnitudes of the horizontal and vertical magnetic field components plotted as a function of the horizontal coordinate.

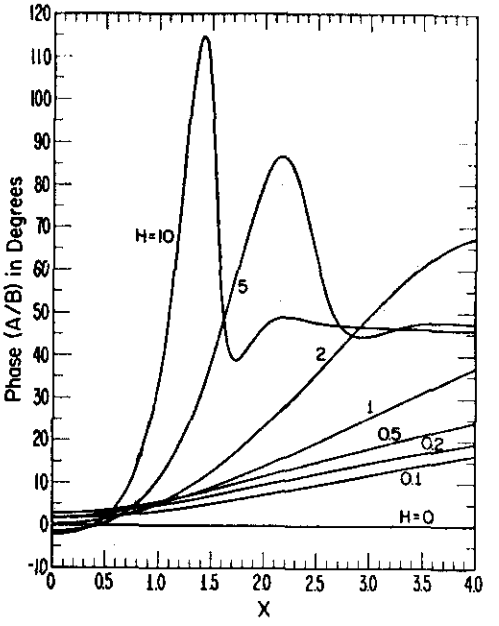

Fig. 4. Phase difference between the horizontal and the vertical magnetic field components plotted as a function of the horizontal coordinate.

the combined use of Figure 3 and Figure 4 should permit an unambiguous choice for X. Though operational procedures for carrying out this step have not been worked out, the approach seems promising.

The possibility of using an array of line sources on the surface is also being considered. At the expense of a more complicated source configuration with scanning capabilities, the observer would need only to signal the occurrence of a null. The up-link communication in this case could well be a seismically propagating impulse generated by a hammer blow.

REFERENCES

Grant, F. S., and G. F. West (1966), *Interpretation Theory in Applied Geophysics*, McGraw-Hill, New York.

Wait, J. R. (1962), *Electromagnetic Waves in Stratified Media*, chap. 2, Pergamon, New York.

Radio Science, Volume 7, Number 5, pages 587–591, May 1972

The effect of a buried conductor on the subsurface fields for line source excitation

James R. Wait[1]

Cooperative Institute for Research in the Environmental Sciences, University of Colorado, Boulder, Colorado 80302

(Received November 12, 1971.)

An approximate analytical method is presented for treating electromagnetic scattering from a slender cylindrical conductor buried in a homogeneous conducting half-space. The excitation is by a uniform line source of current located on the surface. The solution is achieved by an iterative method that accounts for the interaction of the induced current in the cylinder and the air-earth interface. It is shown that the cylindrical inhomogeneity will distort the profile of the subsurface magnetic field as the horizontal displacement is varied.

INTRODUCTION

In a previous paper [*Wait and Spies*, 1971] we considered an infinite line source or current-carrying cable on the surface of a flat homogeneous earth. The integral representation for the subsurface fields was reduced to tabulated functions. The results were of interest in mine communication problems, particularly during emergency conditions, for transmission paths through the overburden. The possibility that an array of such line sources could be used in direction-finding should not be overlooked [*Wait* 1971]. In the present paper, we wish to consider an inhomogeneous earth model that provides insight to the general problem. Specifically, we assume that the uniform half-space model adopted earlier [*Wait and Spies*, 1971] has a cylindrical conductor embedded within it. This is a possible means to account for the presence of conductive rails, pipes, or ore veins that would modify the total field at the subsurface observing point. In order to simplify the problem, we consider a two-dimensional model in which the buried cylindrical inhomogeneity is taken to be parallel to the surface line source.

Electromagnetic scattering from buried cylinders has been considered by *Parry and Ward* [1971] and *Hohmann* [1971] using integral equation formulations that require elaborate numerical techniques to achieve usable results. A modified integral equation technique for such problems has recently been developed (A. Q. Howard, Jr., personal communication, 1971). Also, we should point out that *D'Yakonov* [1959] has actually published a formally exact solution to the case for a buried cylinder of circular cross section. Unfortunately, his results are not in a form to obtain numerical data. Instead, we shall adopt an approximate analytical method that is particularly suitable when the buried conductor has a small cross section which is the case for a buried metallic pipe or rail.

FORMULATION

We refer the reader to the previous paper [*Wait and Spies*, 1971] for the formulation of the necessary two-dimensional Green's function $G(x', y'; x, y)$ for the homogeneous nonmagnetic half-space of conductivity σ. As before, we neglect all displacement currents, and the time factor is exp $(i\omega t)$. Thus, the propagation constant in the half-space is $\gamma = (i\sigma\mu_0\omega)^{1/2}$.

We now consider the influence of an idealized inhomogeneity in the half-space for a current I on the surface. As indicated in Figure 1, the half-space is homogeneous for $y > 0$ except for a cylindrical region of conductivity δ, radius a, centered at (x', y'). In order to simplify the analysis, we now consider the radius a to be sufficiently small that the currents induced in the cylinder are effectively symmetrical. As indicated in the Appendix, this is an adequate approximation provided $|\gamma a| \ll 1$ even though the exciting field is nonuniform. We note this does not place a restriction on the parameter γa where $\gamma = (i\delta\mu_0\omega)^{1/2}$. In fact, we wish to allow for the possibility

[1] Consultant, Office of Telecommunications, Boulder, Colorado.

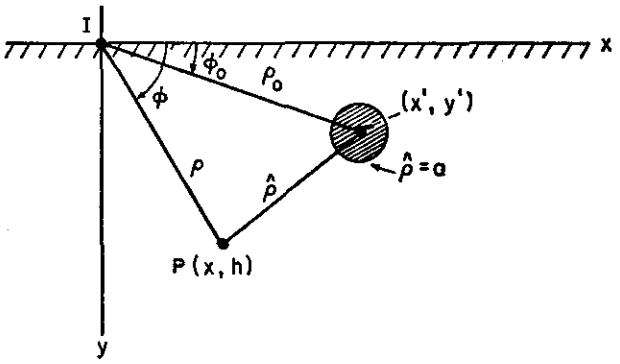

Fig. 1. Geometry for the buried cylinder in a conducting half-space.

that the cylindrical region has a high conductivity such as might exist for a metallic pipe or track buried in the earth.

In the first approximation, we argue that the field $E(x', y')$, which excites axial currents in the cylinder, is given by

$$E(x', y') = (-i\mu\omega I/2\pi)G(x', y'; 0, 0) \qquad (1)$$

Then the corresponding axial current $I_c^{(1)}$ is given by

$$I_c^{(1)} \simeq (Z)^{-1}E(x', y') \qquad (2)$$

where Z is the effective series impedance per unit length for excitation by a uniform axial field. In analogy to the development in the Appendix, we see that $Z = Z_i + Z_e$ which is the sum of the internal and external impedances, Z_i and Z_e, respectively. Without difficulty, we find that

$$Z_i = [\hat{\eta} I_0(\hat{\gamma}a)]/[2\pi a I_1(\hat{\gamma}a)] \qquad (3)$$

where I_0 and I_1 are modified Bessel functions of order zero and one, respectively, and $\hat{\eta} = i\mu_0\omega/\hat{\gamma}$ is the intrinsic impedance of the material inside the cylinder. Here, we note that in the low-frequency limit (i.e., $\omega \to 0$), Z_i approaches $(\pi a^2\delta)^{-1}$, which is the direct-current resistance per unit length of the cylinder. On the other hand, at high frequencies where $|\hat{\gamma}a| \gg 1$, Z_i is well approximated by $Z_i \simeq \hat{\eta}/(2\pi a) = i\mu_0\omega/(2\pi\hat{\gamma}a)$ which, of course, vanishes in the perfect conductivity limit. Eddy current losses within the cylinder are accounted for by (3), and the numerical calculations can be facilitated by expressing I_0 and I_1 in terms of Thomson's ber and bei functions and their derivatives:

$$I_0[(i)^{1/2}Z] = \text{ber } Z + i \text{ bei } Z$$

and

$$i^{1/2}I_1[(i)^{1/2}Z] = \text{ber}' Z + i \text{ bei}' Z$$

An adequate form for the external impedance is

$$Z_e \simeq \frac{\eta K_0(\gamma a)}{2\pi a K_1(\gamma a)} \simeq \frac{i\mu_0\omega}{2\pi}\left(\log\frac{1}{\gamma a} + 0.116\right) \qquad (4)$$

since we have already adopted the premise that $|\gamma a| \ll 1$ (see Appendix).

The total field E_T at $P(x, h)$ is now regarded as the sum of the direct field due to the line source I at (0, 0) and the secondary or scattered field from the cylinder at (x', y'). Thus, to within the first-order approximation

$$E_T^{(1)}(x, h) = \frac{-i\mu\omega I}{2\pi} G(x, y; 0, 0) - \frac{i\mu\omega I_c^{(1)}}{2\pi} G(x, y; x', y') \qquad (5)$$

which automatically satisfies the boundary condition at the air-ground interface if we employ the form of the Green's function given in *Wait and Spies* [1971].

To obtain a second order approximation $I_c^{(2)}$, we correct $I_c^{(1)}$ in (5) to account for the interaction with the interface. Thus

$$I_c^{(2)} \simeq Z^{-1}E^{(1)} \qquad (6)$$

where

$$E^{(1)} \simeq -\frac{i\mu\omega I}{2\pi} G(x', y'; 0, 0)(1 - \Gamma^2 a^2 \hat{G})$$

where $\Gamma^2 a^2 = i\mu_0\omega/(2\pi Z)$ and $\hat{G}$ is the appropriate Green's function. Using $h \gg a$, we find that

$$\hat{G} \cong -K_0(2\gamma y') + 2\int_0^\infty \frac{\exp(-2uy')}{u + \lambda}\, d\lambda \qquad (7)$$

$$= -K_0(\beta) + 2\left[\frac{d^2}{d\beta^2} K_0(\beta) + \frac{d}{d\beta}\frac{\exp(-\beta)}{\beta}\right] \qquad (8)$$

where $\beta = 2\gamma y'$. Carrying out the derivative operations leads to

$$\hat{G} = +K_0(\beta) + (2/\beta)K_1(\beta) - (2/\beta)(1 + \beta)\exp(-\beta) \qquad (9)$$

The corresponding second-order approximated field at $P(x, h)$ is thus

$$E_T^{(2)}(x, h) = \frac{-i\mu\omega I}{2\pi} G(x, y; 0, 0) - \frac{i\mu\omega I_c^{(2)}}{2\pi} G(x, y; x', y') \qquad (10)$$

This in turn can be employed to calculate the third-order approximated current $I_c^{(3)}$. When the inter-

active process is continued indefinitely, we arrive at

$$I_c \simeq Z^{-1}E'(x', y') \tag{11}$$

where

$$E'(x', y') \simeq -\frac{i\mu_0\omega I}{2\pi} G(x', y'; 0, 0)$$
$$\cdot[1 - \Gamma^2a^2\hat{G} + (\Gamma^2a^2\hat{G})^2 - (\Gamma^2a^2\hat{G})^3 + \cdots] \tag{12}$$

which is formally summed to give

$$E'(x', y') \simeq -\frac{i\mu_0\omega I}{2\pi} G(x', y'; 0, 0)(1 + \Gamma^2a^2\hat{G})^{-1} \tag{13}$$

Using (11), we now obtain the final form of the perturbed total field at $P(x, h)$:

$$E_T(x, h) \simeq -\frac{i\mu_0\omega I}{2\pi}[G(x, h; 0, 0)$$
$$- \Omega G(x', y'; 0, 0)G(x, h; x', y')] \tag{14}$$

where

$$\Omega = \Gamma^2a^2/(1 + \Gamma^2a^2\hat{G}) \tag{15}$$

The corresponding magnetic field components are

$$H_{T_x}(x, h) \simeq \frac{I}{2\pi}\left[\frac{\partial G(x, y; 0, 0)}{\partial y}\right.$$
$$\left. - \Omega G(x', y'; 0, 0)\frac{\partial G(x, y; x', y')}{\partial y}\right]_{y=h} \tag{16}$$

$$H_{T_y}(x, h) \simeq -\frac{I}{2\pi}\left[\frac{\partial G(x, y; 0, 0)}{\partial x}\right.$$
$$\left. - \Omega G(x', y'; 0, 0)\frac{\partial G(x, y; x', y')}{\partial x}\right]_{y=h} \tag{17}$$

Using the integral forms $A(H, X)$, $B(H, X)$, and $F(H, X)$ defined in *Wait and Spies* [1971], we can express (14), (16), and (17) as follows:

$$E_T = \frac{-i\mu_0\omega I}{2\pi}[F(H, X)$$
$$- \Omega F(H', X')\{F(H + H', X - X')$$
$$+ K_0[\exp(i\pi/4)R_1] - K_0[\exp(i\pi/4)R_2]\}] \tag{18}$$

$$H_{T_x} = \frac{-I}{2\pi h}[A(H, X)$$
$$- \Omega F(H', X')\{K_1[\exp(i\pi/4)R_1]\exp(i\pi/4)HS_1$$
$$- K_1[\exp(i\pi/4)R_2]\exp(i\pi/4)HS_2$$
$$+ A(H + H', X - X')\}] \tag{19}$$

and

$$H_{T_y} = \frac{I}{2\pi h}[B(H, X)$$
$$- \Omega F(H', X')\{K_1[\exp(i\pi/4)R_1]\exp(i\pi/4)HC_1$$
$$- K_1[\exp(i\pi/4)R_2]\exp(i\pi/4)HC_2$$
$$+ B(H + H', X - X')\}] \tag{20}$$

where

$$H = (\sigma\mu_0\omega)^{1/2}h \qquad H' = (\sigma\mu_0\omega)^{1/2}y'$$
$$X = x/h \qquad X' = x'/h$$
$$R_1 = [H^2(X - X')^2 + (H - H')^2]^{1/2}$$
$$R_2 = [H^2(X - X')^2 + (H + H')^2]^{1/2}$$
$$C_1 = \frac{(x - x')}{[(x - x')^2 + (h - y')^2]^{1/2}}$$
$$C_2 = \frac{(x - x')}{[(x - x')^2 + (h + y')^2]^{1/2}}$$
$$S_1 = \frac{(h - y')}{[(x - x')^2 + (h - y')^2]^{1/2}}$$
$$S_2 = \frac{(h - y')}{[(x - x')^2 + (h + y')^2]^{1/2}}$$

AN ILLUSTRATIVE EXAMPLE

The explicit forms given by (18), (19), and (20) can be used to calculate the resultant fields at the subsurface observation point at depth x for any specified location of the cylindrical conductor. Of particular interest is the vertical component H_{T_y} of the magnetic field since this is readily detected by a rudimentary loop contained in the horizontal plane. In Figures 2 and 3, we illustrate the normalized field magnitude

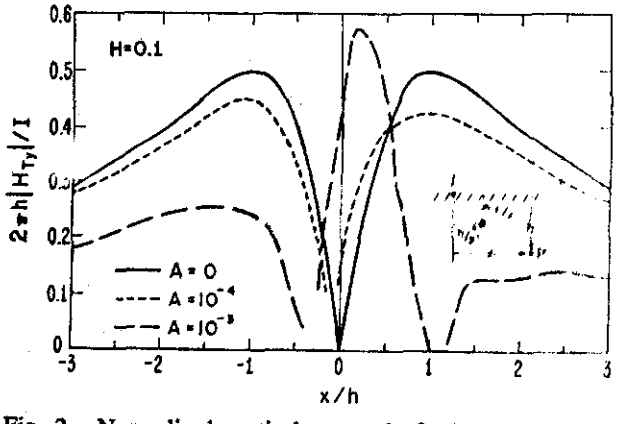

Fig. 2. Normalized vertical magnetic field at a depth h for $H = 0.1$.

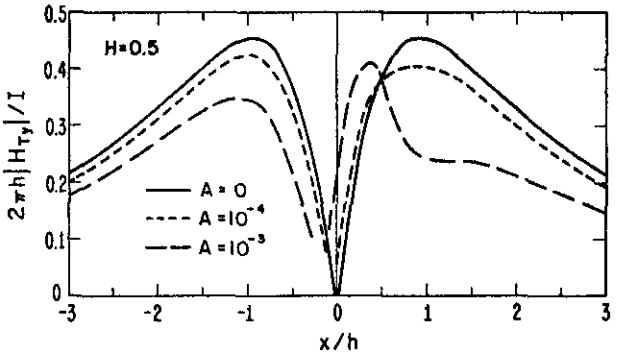

Fig. 3. Normalized vertical magnetic field at a depth h for $H = 0.5$.

$2\pi h\ |H_y|/I$ as a function of the relative horizontal displacement, x/h, of the observer. For this example, we located the buried metallic cylinder at $x = h/2$ and $y = h/2$. In Figures 2 and 3, we choose $H = (\sigma\mu_0\omega)^{1/2}h$ to be 0.1 and 0.5 respectively, while $A = |\gamma a| = (\sigma\mu_0\omega)^{1/2}a$ is 0.0, 10^{-4}, and 10^{-3} for each figure. Also, we assume that $\hat{\sigma}/\sigma = 10^7$.

First of all, we note the curves for $A = 0$ in Figures 2 and 3, corresponding to a homogeneous half-space, are perfectly symmetrical with the expected null of the vertical magnetic field directly beneath the line source. However, when $A > 0$, the asymmetry becomes evident, and the null is shifted. In this sense, the buried conductor distorts the subsurface field.

In order to attach a more physical meaning to the curves in Figures 2 and 3, we note first of all that the parameter $H = (\sigma_m f)^{1/2}h_{km} \times 8.6 \times 10^{-2}$, when σ_m is the overburden conductivity expressed in mmhos/m, f is the frequency in Hz and h_{km} is the depth of the observer expressed in km. Thus, if $\sigma_m = 1$ and $f = 100$, we see that $H = 0.1$ and 0.5 corresponds to $h_{km} = 0.116$ and 0.58, respectively. Then the parameter values $A = 10^{-4}$ and 10^{-3} correspond to a buried cylinder radius of 0.116 and 1.16 m, respectively, with a conductivity of 10^4 mhos/m. Of course, by a suitable scaling of the parameters, other possibilities exist. Also, with limited numerical effort, many other cases can be treated.

CONCLUDING REMARKS

The analytical method given in this paper permits quantitative estimates to be made of the effect of an idealized inhomogeneity in the conducting half-space. The method is admittedly not usable if the buried cylinder is very near the air-earth interface. Also, it is restricted to cylinder radii that are electrically small in terms of the wavelength in the external media. In other words, the parameter A should be small compared with 1. Recent numerical comparisons with integral equation formulations indicate, however, that the method works well for A as large as 0.1 (A. Q. Howard, Jr., personal communication, 1971).

APPENDIX

The method used to estimate the scattered field from a cylinder buried in the half-space employs certain concepts which can be clearly illustrated in the problem [*Wait*, 1959] of scattering from a cylinder of electrical constants $\hat{\sigma}$, $\hat{\epsilon}$, and μ_0, located in an infinite medium of electrical constants σ, ϵ, and μ_0.

The situation is illustrated in Figure 4, in which we take the line current I at (ρ_0, ϕ_0) to be parallel to the axis of the cylinder. Without repeating any details of the derivation, we can write down an exact expression for the electric field E_z external to the cylinder in the following form:

$$E_z = (-i\mu_0\omega I/2\pi)K_0(\gamma R) + E_z^s \tag{21}$$

where

$$R = [\rho^2 + \rho_0^2 - 2\rho\rho_0 \cos(\phi - \phi_0)]^{1/2}$$

$$\gamma = [i(\sigma + i\epsilon\omega)\mu_0\omega]^{1/2}$$

and E_z^s is the scattered or secondary field. We know that

$$E_z^s = -i\mu_0\omega I/2\pi \cdot \sum_{n=0}^{\infty} \epsilon_n A_n K_n(\gamma\rho_0) K_n(\gamma\rho) \cos n(\phi - \phi_0) \tag{22}$$

where

$$A_n = \frac{I_n'(\gamma a)}{K_n'(\gamma a)} \cdot \frac{\eta[I_n(\gamma a)]/[I_n'(\gamma a)] - \hat{\eta}[I_n(\hat{\gamma} a)]/[I_n'(\hat{\gamma} a)]}{Z_{e,n} + Z_{i,n}} \tag{23}$$

where

$$Z_{e,n} = [-\eta K_n(\gamma a)]/[K_n'(\gamma a)]$$

$$Z_{i,n} = [\hat{\eta} I_n(\hat{\gamma} a)]/[I_n'(\hat{\gamma} a)]$$

and where $\eta = i\mu_0\omega/\gamma$, $\hat{\eta} = i\mu_0\omega/\hat{\gamma}$, and $\hat{\gamma} = [i(\hat{\sigma} + i\hat{\epsilon}\omega)\mu_0\omega]^{1/2}$.

If we now insist that $|\gamma a| \ll 1$ (without any restriction on $\hat{\gamma} a$), we can approximate the Bessel functions of argument γa by the leading term of their series expansions. Also, if additionally, we allow $\rho \gg a$, only

the $n = 0$ term in (22) need be retained. For this dominant term, we see that

$$A_0 \simeq \frac{-i\mu_0\omega}{2\pi(Z_e + Z_i)}\,[1 - (Z_i/2)(\sigma + i\epsilon\omega)a]$$

$$\simeq \frac{-i\mu_0\omega}{2\pi(Z_e + Z_i)} \tag{24}$$

where

$$Z_e = Z_{e,0}/2\pi a$$

$$Z_i = Z_{i,0}/2\pi a$$

are the external and the internal impedances of the cylinder as employed in the context of the previous derivation. Thus, (22) is expressible in the meaningful form

$$E_z^s \simeq \frac{-i\mu_0\omega I_e}{2\pi} K_0(\gamma\rho) \tag{25}$$

where

$$I_e = \frac{-i\mu_0\omega I}{2\pi} K_0(\gamma\rho_0)[Z_e + Z_i]^{-1} \tag{26}$$

is the total *induced* current in the cylinder. These results are consistent with the analysis for the half-space configuration provided we recognize that the appropriate Green's function here is simply the modified Bessel function $K_0(\gamma\rho)$.

Acknowledgments. I am indebted to Dr. David A. Hill for his cogent comments on an earlier version of this paper. Also, I wish to thank Allen Q. Howard, Jr., for carrying out the numerical calculations and for his collaboration on related integral equation approaches to the problem. The research was supported by the U. S. Bureau of Mines.

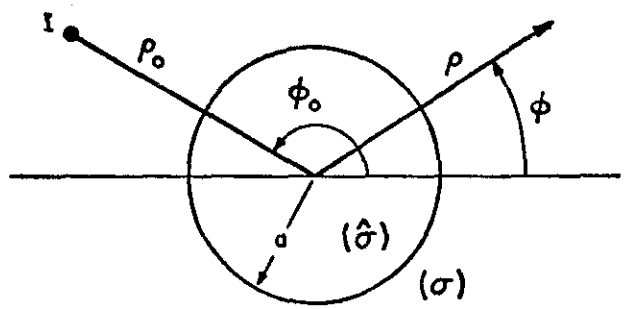

Fig. 4. Prototype problem of line source in presence of cylinder in an infinite medium.

REFERENCES

D'Yakonov, B. P. (1959), The diffraction of electromagnetic waves by a circular cylinder in a homogeneous half-space, *Bul. Acad. Scl. USSR, Geophys. Ser.*, no. 9, 950–955.

Hohmann, G. W. (1971), Electromagnetic scattering by conductors in the earth near a line source of current, *Geophysics, 36,* 101–131.

Parry, J. R., and S. H. Ward (1971), EM scattering from cylinders of arbitrary cross section in a conductive half-space, *Geophysics, 36,* 67–100.

Wait, J. R. (1959), *Electromagnetic Radiation from Cylindrical Structures,* Pergamon, Oxford, England.

Wait, J. R. (1971), Array technique for electromagnetic positional determination of a buried receiving point. *Elect. Lett. 7*(8), 186–187.

Wait, J. R., and K. P. Spies (1971), Subsurface electromagnetic fields of a line source on a conducting half-space, *Radio Sci. 6*(8/9), 781–786.

GEOPHYSICS, VOL. 37, NO. 6 (DECEMBER 1972), P. 975–984, 8 FIGS.

THE ELECTROMAGNETIC FIELDS OF A SUBTERRANEAN CYLINDRICAL INHOMOGENEITY EXCITED BY A LINE SOURCE†

ALLEN Q. HOWARD, JR.*

The anomalous fields from a buried cylindrical inhomogeneity in an otherwise uniform half-space are analyzed. The problem is rendered two-dimensional by assuming that the uniform line source of current is parallel to the subsurface cylinder. The multipole scattered field coefficients are obtained from the numerical solution to the associated singular Fredholm integral equation of the second kind. The horizontal magnetic field amplitude, the vertical magnetic field phase, and the amplitude and phase of the ratio of horizontal to vertical magnetic fields are shown to be diagnostic of the location of the inhomogeneity. The results have possible applications to electromagnetic location in mine rescue operations and to geophysical prospecting.

INTRODUCTION

In a number of situations in applied geophysics we are interested in the electromagnetic response of an inhomogeneous half-space. A recent special issue of GEOPHYSICS (Ward and Morrison, 1971) was devoted to this general problem. In particular, papers by Parry and Ward (1971) and Hohmann (1971) considered the effect of a buried inhomogeneity. We extend Hohmann's analysis here using a similar formulation. However, our technique is more analytical, and thereby we avoid the difficulties associated with the point-matching method. Of course, in doing so, we must pay with some loss in generality; namely, the inhomogeneity must be describable in a separable coordinate system. In the point-matching technique, used by Hohmann and others, poorly conditioned large matrices must be inverted to solve for the coefficients of the scattered field.

Actually, D'Yakonov (1959) rather ingeniously found a solution to the problem we pose as a limiting case of a boundary value problem involving two nonconcentric cylinders. His final results, however, appear difficult to treat numerically. An approximate perturbation method, accounting for interactions between the induced monopoles and the air interface, has been proposed recently (Wait 1970). It is useful for treating cylindrical scatterers of small cross-section. As indicated below, this technique (described as "Wait's method") serves as a good check of the numerical method.

THE INTEGRAL EQUATION, GREEN'S FUNCTION, AND UNPERTURBED FIELDS

In the analysis to follow, we give a complete but concise description of the mode-match solution to the two-dimensional Fredholm integral equation of the second kind for our problem. The interested reader is referred to Howard (1972) for background material and more detail on the application of this technique to problems of geophysical interest.

We refer to Figure 1a for the geometry. In the following, a polar coordinate system (ρ, ϕ) and a cartesian system (x, y) will be used interchangeably. In either case the coordinate origin is at the center of the cylinder. The total unknown electric field, denoted by E_2, can be expressed in terms of an integral equation (Howard, 1972). For the case of TE polarization and assuming a time variation $e^{-i\omega t}$, the relation is given by

$$E_2(\bar{x}) = E_1(\bar{x}) + i\omega(\epsilon_1' - \epsilon_2')(i\omega\mu \cdot \int_0^{2\pi} d\phi' \int_0^a d\rho' \rho' E_2(\bar{x}') G(\bar{x}, \bar{x}'), \quad (1)$$

† Manuscript received by the Editor February 7, 1972; revised manuscript received July 14, 1972.

* Institute for Telecommunication Sciences, Office of Telecommunications, U. S. Department of Commerce, Boulder, Colorado 80302.

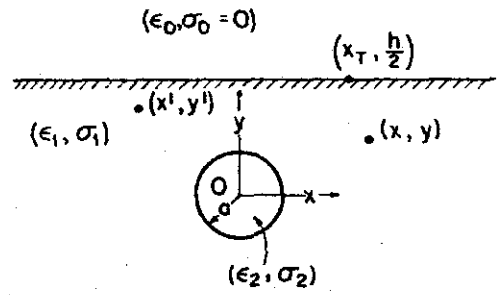

FIG. 1a. Buried cylinder geometry.

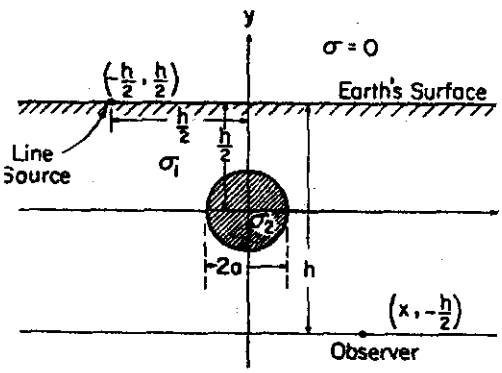

FIG. 1b. Special geometry for numerical examples.

where the Green's function $G(\bar{x}, \bar{x}')$ is given by (Wait and Spies, 1971)

$$G(\bar{x}, \bar{x}') = \frac{i}{4} H_0^{(1)}(k_1 | \bar{x} - \bar{x}'|) + \frac{i}{4\pi} \cdot \int_{-\infty}^{+\infty} h(l) e^{i(x-x')l - i\beta_1(y+y')} dl, \tag{2}$$

$$h(l) = \frac{\beta_1 - \beta_0}{\beta_1 + \beta_0} e^{i\beta_1 h}, \quad \beta_0 = (k_0^2 - l^2)^{\frac{1}{2}}, \text{ and}$$

$$\beta_1 = (k_1^2 - l^2)^{\frac{1}{2}},$$

for

$$\epsilon_j' = \epsilon_j + i\sigma_j/\omega, \quad j = 0, 1, 2, \quad k_j^2 = \omega^2 \mu_0 \epsilon_j',$$

$$\text{Im}\, \beta_0 \geq 0, \quad \text{Im}\, \beta_1 \geq 0,$$

and $E_1(\bar{x})$ is the field due to an electric line source at $(x_T, h/2)$ and in the absence of the cylinder; for $y < h/2$, we know that (Wait and Spies, 1971)

$$E_1(\bar{x}) = \frac{i}{2\pi} \int_{-\infty}^{+\infty} \frac{e^{i(x_T - x)l + i\beta_1(l)[(h/2) - y]}}{\beta_0 + \beta_1} dl. \tag{3}$$

Equation (1) can be solved by introducing a complete representation for $E_2(\bar{x})$ that is valid for $|\bar{x}| \leq a$. Thus,

$$E_2(\bar{x}) = \sum_{m=-\infty}^{+\infty} a_m J_m(k_2 \rho) e^{im\phi} \quad \text{for} \quad |\rho| \leq a. \tag{4}$$

The circular cylindrical symmetry can be incorporated into the problem by expressing both $G(\bar{x}, \bar{x}')$ and $E_1(\bar{x})$ in terms of their complex angle representations. This is effected by making the change of integration variable $t = k_1 \cos \psi$ in equations (2) and (3) to obtain

$$G(\bar{x}, \bar{x}') = \frac{i}{4} H_0^{(1)}(k_1 | \bar{x} - \bar{x}'|) - \frac{i}{4\pi} \cdot \int_c h(\Psi) e^{-ik_1 \rho' \cos(\Psi - \phi')} \times e^{ik_1 \rho \cos(\Psi + \phi)} d\Psi, \tag{5}$$

where

$$h(\Psi) = \frac{k_1 \sin \Psi - (k_0^2 - k_1^2 \cos^2 \Psi)^{\frac{1}{2}}}{k_1 \sin \Psi + (k_0^2 - k_1^2 \cos^2 \Psi)^{\frac{1}{2}}} e^{ik_1 h \sin \Psi}$$

and

$$\rho = (x^2 + y^2)^{\frac{1}{2}}, \qquad \rho' = (x'^2 + y'^2)^{\frac{1}{2}},$$

$$\cos \phi' = \frac{x'}{\rho'}, \qquad \sin \phi' = \frac{y'}{\rho'}, \tag{6}$$

$$\cos \phi = x/\rho, \qquad \sin \phi = y/\rho.$$

The contour c is a simple open curve in the complex Ψ plane which comes from $-i\infty$ in the strip $\delta < \text{Re}(\psi) < \pi + \delta$ and recedes to $+i\infty$ in the strip $\delta - \pi < \text{Re}(\psi) < \delta$, where $\delta = \arg(k_1)$. Similarly,

$$E_1(\bar{x}) = \int_c g(\bar{x}_0, \Psi) e^{-ik_1 \rho \cos(\Psi - \phi)} d\Psi, \tag{7}$$

$$g(\bar{x}_0, \Psi) = -\frac{ik_1}{2\pi} \cdot \frac{e^{ik_1 \rho_0 \cos(\Psi - \phi_0)} \sin \Psi}{(k_0^2 - k_1^2 \cos^2 \Psi)^{\frac{1}{2}} + k_1 \sin \Psi},$$

$$\rho_0 = [(h/2)^2 + x_T^2]^{\frac{1}{2}},$$

$$\cos \phi_0 = x_T/\rho_0, \tag{8}$$

$$\sin \phi_0 = h/2\rho_0,$$

and ϕ is defined in (6).

The singular term in $G(\bar{x}, \bar{x}')$ can be expanded using the addition theorem for cylinder functions.

$$H_0^{(1)}(k_1 | \bar{x} - \bar{x}' |) = \sum_{l=-\infty}^{+\infty} H_l^{(1)}(k_1\rho_>) J_l(k_1\rho_<) e^{il(\phi-\phi')}, \quad (9)$$

where $\rho_> = \max(\rho, \rho')$, $\rho_< = \min(\rho, \rho')$.

Because the integration with respect to Ψ in the nonsingular part of $G(\bar{x}, \bar{x}')$ converges uniformly with respect to $\bar{x}$ and $\bar{x}'$, provided $y+y' < h$, and, similarly, the sum in (9) converges uniformly in $\bar{x}$ and $\bar{x}'$, the order of integration in the former and integration and summation in the latter can legitimately be interchanged. Hence, in particular, we have

$$\begin{aligned} \frac{i}{4}\int_0^{2\pi} d\phi' \int_0^a \rho' d\rho' E_2(\bar{x}') H_0^{(1)}(k_1 | \bar{x} - \bar{x}' |) \\ = \frac{i\pi}{2} \sum_{m=-\infty}^{+\infty} a_m e^{im\phi} \Big\{ H_m^{(1)}(k_1\rho) \\ \cdot \int_0^{\rho} \rho' J_m(k_1\rho') J_m(k_2\rho') d\rho' \\ + J_m(k_1\rho) \\ \cdot \int_{\rho}^a \rho' J_m(k_1\rho') H_m^{(1)}(k_2\rho') d\rho' \Big\}. \end{aligned} \quad (10)$$

This becomes, after doing the integrations and simplifying,

$$\begin{aligned} \frac{i}{4}\int_0^{2\pi} d\phi' \int_0^a d\rho' \rho' E_2(\bar{x}') H_0^{(1)}(k_1 | \bar{x} - \bar{x}' |) \\ = \frac{1}{k_2^2 - k_1^2} \sum_{m=-\infty}^{+\infty} a_m e^{im\phi} \\ \cdot \Big\{ J_m(k_2\rho) + \frac{i\pi}{2} J_m(k_1\rho) Q_m \Big\}, \end{aligned} \quad (11)$$

where

$$\begin{aligned} Q_m = a[k_2 J_{m+1}(k_2 a) H_m^{(1)}(k_1 a) \\ - k_1 J_m(k_2 a) H_{m+1}^{(1)}(k_1 a)]. \end{aligned} \quad (12)$$

The angle integration over the nonsingular term in the Green's function can be effected using the result (Gröbner and Hofreiter, 1961)

$$\begin{aligned} \int_0^{2\pi} e^{-ik_1\rho' \cos(\Psi-\phi') + im\phi'} d\phi' \\ = 2\pi e^{im(\Psi - \pi/2)} J_m(k_1\rho') \end{aligned} \quad (13)^1$$

to obtain

$$\begin{aligned} -\frac{i}{4\pi}\int_0^a d\rho' \rho' \int_0^{2\pi} d\phi' E_2(\bar{x}') \\ \cdot \int_c h(\Psi) e^{-ik_1\rho' \cos(\Psi-\phi') + ik_1\rho\cos(\Psi+\phi)} d\Psi \\ = -\frac{i}{2(k_2^2 - k_1^2)} \sum_{m=-\infty}^{+\infty} a_m K_m e^{-im\pi/2} \\ \int_c h(\Psi) e^{ik_1\rho\cos(\Psi+\phi) + im\Psi} d\Psi, \end{aligned} \quad (14)$$

where

$$\begin{aligned} K_m = a[k_2 J_{m+1}(k_2 a) J_m(k_1 a) \\ - k_1 J_m(k_2 a) J_{m+1}(k_1 a)]. \end{aligned} \quad (15)$$

Combining results (11) and (14) yields, for the second term in the right-hand side of (1),

$$\begin{aligned} i\omega(\epsilon_1' - \epsilon_2')(i\omega\mu_0) \\ \cdot \int_0^{2\pi} d\phi' \int_0^a \rho' d\rho' E_2(\bar{x}') G(\bar{x}, \bar{x}') \\ = \sum_{m=-\infty}^{+\infty} a_m \Big\{ e^{im\phi}[J_m(k_2\rho) + i\pi/2 J_m(k_1\rho) Q_m] \\ - \frac{i}{2} K_m e^{-im(\pi/2)} \\ \cdot \int_c h(\Psi) e^{ik_1\rho\cos(\Psi+\phi) + im\Psi} d\Psi \Big\}. \end{aligned} \quad (16)$$

Substituting (4) for the left-hand side of (1) and (16) for the first and second terms on the right-hand side of (1) results in a matrix equation for the coefficients a_m. [Note that the first term on the right-hand side of (16) cancels the unknown $E_2(x)$.] We have

$$\begin{aligned} 0 = \int_c g(\bar{x}_0, \Psi) e^{-ik_1\rho\cos(\Psi-\phi)} d\Psi \\ + \frac{i}{2} \sum_{m=-\infty}^{+\infty} a_m \Big[\pi e^{im\phi} Q_m J_m(k_1\rho) - K_m e^{-im(\pi/2)} \end{aligned} \quad (17)$$

[1] It is not difficult to show that this relation is valid for arbitrary complex Ψ.

$$\cdot \int_c h(\Psi) e^{ik_1\rho \cos(\Psi+\phi)+im\Psi} d\Psi \Big].$$

To proceed, multiply both sides of (17) by $e^{-in\phi}$ and integrate ϕ from 0 to 2π. Note that all of the pertinent integrals needed were discussed in the steps that lead to (16). Factoring the common factor $J_n(k_2\rho)$ which results in each term gives

$$e^{-i3n(\pi/2)} \int_c g(\bar{x}_0, \Psi) e^{-in\Psi} d\Psi + i\frac{\pi}{2} a_n Q_n - \frac{i}{2} \sum_{m=-\infty}^{+\infty} a_m K_m e^{i(n-m)\pi/2} \times \int_c h(\Psi) e^{i(n+m)\Psi} d\Psi = 0.$$

This, upon slight manipulation, becomes

$$\sum_{m=-\infty}^{+\infty} L_{nm} a_m = T_n, \quad n = 0, \pm 1, \pm 2, \cdots, \quad (18)$$

where

$$L_{nm} = (\pi Q_m \delta_{nm} - K_m e^{i(n-m)\pi/2} I_{nm}), \quad (19)$$

and where

$$Q_m = [k_2 a J_{m+1}(k_2 a) H_m^{(1)}(k_1 a) - k_1 a J_m(k_2 a) H_{m+1}^{(1)}(k_1 a)]$$

and

$$K_m = [k_2 a J_{m+1}(k_2 a) J_m(k_1 a) - k_1 a J_m(k_2 a) J_{m+1}(k_1 a)].$$

In (18) I_{nm} and T_n are integrals which must be evaluated numerically. In the quasi-static regime (i.e., when displacement currents can be neglected), T_n is given by

$$T_n = \frac{2i}{\pi} e^{-i3\pi n/4} (H_0)^n \cdot \int_0^\infty \frac{e^{-(s^2 - iH_0^2)^{\frac{1}{2}}}}{s + (s^2 - iH_0^2)^{\frac{1}{2}}} \cdot [\cos(X_0 s) g_e^{-n}(s) + i \sin(X_0 s) g_0^{-n}(s)] ds, \quad (20)$$

where $H_0 = (\sigma_1 \mu_0 \omega)^{\frac{1}{2}} h/2$, $X_0 = 2x_T/h$,

$$g_e^n(s) = \tfrac{1}{2}\{[s + (s^2 - iH_0^2)^{\frac{1}{2}}]^n + [-s + (s^2 - iH_0^2)^{\frac{1}{2}}]^n\},$$

and

$$g_0^n(s) = \tfrac{1}{2}\{[s + (s^2 - iH_0^2)^{\frac{1}{2}}]^n - (-s + (s^2 - iH_0^2)^{\frac{1}{2}}]^n\}.$$

Similarly, we find that

$$I_{nm} = \frac{2ie^{-i(m+n)\pi/4}}{(H_0)^{m+n}} \cdot \int_0^\infty \frac{ds e^{-2(s^2 - iH_0^2)^{\frac{1}{2}}}}{(s^2 - iH_0^2)^{\frac{1}{2}}} \cdot \frac{(s^2 - iH_0^2)^{\frac{1}{2}} - s}{(s^2 - iH_0^2)^{\frac{1}{2}} + s}^{m+n} g_e^{m+n}(s). \quad (21)$$

An interesting limiting case of (18) is the limit when $k_0 \to k_1$ [note here that the terms in (18) must not be interpreted in their quasi-static forms]. In this limit the interface vanishes; then $I_{nm} = 0$ and the matrix equation becomes diagonal. Furthermore, T_n in this limit becomes

$$\lim_{k_0 \to k_1} T_n = -\tfrac{1}{2} e^{-in\phi_0} H_n^{(1)}(k_1 \rho_0),$$

where

$$\rho_0 = [x_T^2 + (h/2)^2]^{\frac{1}{2}}, \quad \phi_0 = \tan^{-1} \frac{h}{(2x_T)}.$$

It follows that

$$\lim_{k_0 \to k_1} a_n = -\frac{e^{-in\phi_0} H_n^{(1)}(k_1 \rho_0)}{2\pi Q_n}.$$

This is, in fact, the classical solution for the line source excitation of a lossy cylinder (Wait, 1959).

In general, the matrix equation for the coefficients in (18) is not diagonal and must be solved by truncating and then inverting the complex matrix L_{nm}. For electrically small cylinders such that $|k_1 a| \lesssim 1$ (but with no restriction on $k_2 a$), only a few terms in the multipole field expansion (4) are required. Since the matrix L_{nm} is almost diagonally dominant, the truncation process is not critical. This physically means that the modes do not couple strongly. Numerically, this is borne out

in calculations which show that, for $|k_1 a| < 1$, the coefficients a_n, as obtained from a 5×5 and 9×9 matrix, agree to five significant figures.

Another check which was performed was to see if the electric field is continuous at the cylinder boundary. The results show that the continuity is good to within 5 percent of the incident field strength evaluated on the boundary.

FIELD EXPRESSIONS

We now assume the coefficients a_n are known. The electric field at any point in the lower half-space ($y < h/2$) is then determined from (1). Thus, we find the total electric field E_2 is

$$E_2(\bar{x}) = E_1(\bar{x}) + E_1^s(\bar{x}) + E_2^s(\bar{x}). \quad (22)$$

Now, $E_1(\bar{x})$, the z component of the field in the absence of the cylinder, is given by

$$E_1(\bar{x}) = \frac{1}{\pi}\int_0^\infty \frac{\cos(X_1 s)e^{-(s^2-iH_1^2)^{\frac{1}{2}}}}{s+(s^2-iH_1^2)^{\frac{1}{2}}}\,ds, \quad (23)$$

where $H_1 = (\sigma_1\mu_0\omega)^{\frac{1}{2}}(h/2-y)$, $X_1 = (x_T - x)/(h/2-y)$. The term E_1^s, which can be interpreted as the contribution to the scattered field that is independent of interface interactions, is

$$E_1^s(\bar{x}) = i\frac{\pi}{2}\sum_{m=-\infty}^{+\infty} a_m K_m H_m^{(1)}(k_1\rho)e^{im\phi}, \quad (24)$$

where

$$K_m = [k_2 a J_{m+1}(k_2 a)J_m(k_1 a) - k_1 a J_m(k_2 a)H_{m+1}^{(1)}(k_1 a)].$$

The term E_2^s, which accounts for multiple interface interactions and combines with E_1^s to properly match the boundary conditions at the interface, is given by[2]

$$E_2^s = -\frac{i}{2}\sum_{m=-\infty}^{+\infty} a_m K_m e^{im\pi/2}\,{}^s\epsilon_m$$

where

$${}^s\epsilon_m = \frac{2ie^{-i\pi m/4}}{(H_2)^m}\int_0^\infty \frac{e^{-(s^2-iH_2^2)^{\frac{1}{2}}}}{(s^2-iH_2^2)^{\frac{1}{2}}}\left[\frac{(s^2-iH_2^2)^{\frac{1}{2}}-s}{(s^2-iH_2^2)^{\frac{1}{2}}+s}\right]$$

$$\times [\cos(X_2 s)g_e^m(s) + i\sin(X_2 s)g_0^m(s)]ds$$

and

$$g_{e,0}^m(s, H_2) = \tfrac{1}{2}\{[s-(s^2-iH_2^2)^{\frac{1}{2}}]^m \pm [-s-(s^2-iH_2^2)^{\frac{1}{2}}]^m\},$$

where $H_2 = (\sigma_1\mu_0\omega)^{\frac{1}{2}}(h-y)$, $X_2 = x/(h-y)$.

Similar results apply to the magnetic field components. Thus, from (22), and Maxwell's equations, the x component is

$$H_x = H_{x_1} + H_{x_1}^s + H_{x_2}^s, \quad (25)$$

where

$$H_{x_1} = \frac{i}{\pi\omega\mu_0\left(\frac{h}{2}-y\right)}\int_0^\infty \frac{\cos(X_1 s)e^{-(s^2-iH_1^2)^{\frac{1}{2}}}(s^2-iH_1^2)^{\frac{1}{2}}}{s+(s^2-iH_1^2)^{\frac{1}{2}}}\,ds \quad (26)$$

and

$$H_{x_1}^s = \frac{\pi}{2}\sum_{m=-\infty}^{+\infty} a_m K_m e^{im\phi}\left[\frac{im\cos\phi}{\omega\mu_0\rho}H_m^{(1)}(k_1\rho) + Y_1\sin\phi H_m^{(1)\prime}(k_1\rho)\right], \quad (27)$$

where

$$Y_1 = \frac{k_1}{k_0 Z_0}, \quad Z_0 = \left(\frac{\mu_0}{\epsilon_0}\right)^{\frac{1}{2}} \cong 120\pi \text{ ohms}$$

and

$$H_{x_2}^s = -iY_1\sum_{m=-\infty}^{+\infty}\frac{a_m K_m e^{i(m-1)\pi/4}}{(H_2)^{m+1}}\,h_{mx}^s,$$

where

$$h_{mx}^s = \int_0^\infty e^{-(s^2-iH_2^2)^{\frac{1}{2}}}\frac{[s-(s^2-iH_2^2)^{\frac{1}{2}}]}{[s+(s^2-iH_2^2)^{\frac{1}{2}}]} \cdot [\cos(X_2 s)g_e^m(s, H_2) + i\sin(X_2 s)g_0^m(s, H_2)]ds. \quad (28)$$

The analogous results for the y components are

$$H_y = H_{y_1} + H_{y_1}^s + H_{y_2}^s, \quad (29)$$

[2] This decomposition of the scattered field is mainly of heuristic significance; the coefficients a_m also depend upon the interface.

where

$$H_{y_1} = \frac{-i}{\pi\omega\mu_0\left(\frac{h}{2} - y\right)} \cdot \int_0^\infty \frac{\sin(X_1 s)e^{-(s^2 - iH_1^2)^{\frac{1}{2}}}}{s + (s^2 - iH_1^2)^{\frac{1}{2}}} ds, \tag{30}$$

$$H_{y_1}^s = -\frac{\pi}{2}\sum_{m=-\infty}^{+\infty} a_m K_m e^{im\phi}\left[\frac{im\sin\phi}{\omega\mu_0\rho} H_m^{(1)}(k_1\rho) + Y_1 \sin\phi H_m^{(1)\prime}(k_1\rho)\right], \tag{31}$$

$$H_{y_2}^s = -Y_1 \sum_{m=-\infty}^{+\infty} \frac{a_m K_m e^{i(m-1)\pi/4}}{(H_2)^{m+1}} h_{my}^s, \tag{32}$$

$$h_{my}^s = -\int_0^\infty \frac{se^{-(s^2 - iH_2^2)^{\frac{1}{2}}}(s - [s^2 - iH_2^2)^{\frac{1}{2}}]}{(s^2 - iH_2^2)^{\frac{1}{2}}(s + [s^2 - iH_2^2)^{\frac{1}{2}}]} \cdot [\cos(X_2 s)g_0^m(s, H_2) + i\sin(X_2 s)g_e^m(s, H_2)]ds. \tag{33}$$

This completes the description of the field components.

NUMERICAL RESULTS

In certain suggested location schemes (Wait and Spies, 1971), the ratio of horizontal to vertical magnetic fields (H_x/H_y for both amplitude and phase) is of interest. Both amplitude and phase of H_x/H_y are measurable quantities if the observer has a crossed magnetic loop antenna. The basic model to be considered consists of the symmetric case $x_T = -h/2$ $y = -h/2$ (refer to Figure 1b) for a range of $x = -3h$ to $3h$. The figures are defined in terms of numerical distances $H = (\sigma_1\mu_0\omega)^{\frac{1}{2}}h$, $X = x/h$, $A = (\sigma_1\mu_0\omega)^{\frac{1}{2}}a$, and the conductivity contrast $K = \sigma_2/\sigma_1$. The abscissa in each case is X. The ordinate for Figures 2a, 3a, and 4a is the amplitude of H_x/H_y, while the ordinate of Figures 2b, 3b, and 4b is the phase of H_x/H_y in degrees. In each figure, the homogeneous case $A = 0$ is included for comparison. In Figures 2a and 2b, the numerical parameters are $H = 0.1$, $A = 0.01$, and $K = 10^7$. These numbers give an induction number of 31.7. Both the present integral equation ap-

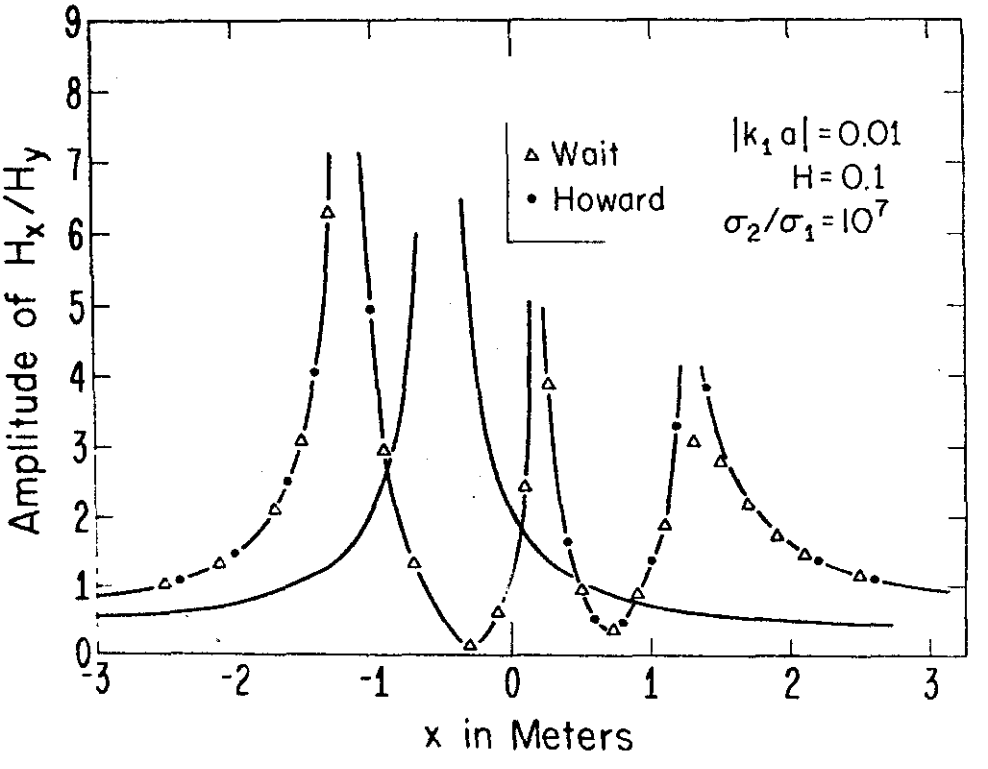

FIG 2a. Amplitude comparison for ratio of horizontal to vertical magnetic fields versus X for $H = 0.1$, $K = 10^7$, and $A = 0.01$.

proach and Wait's method (mentioned above) are plotted. Note that in this case the two methods are coincident. These figures correspond to the situation arising from the occurrence of a metallic pipe or track in the vicinity of the EM link. The remaining figures use $H=2.0$ and $K=10^8$. This corresponds to a receiver $\sqrt{2}$ skin depths below the surface. These cases are suitable for considering the field modification due to a larger naturally occurring inhomogeneity. Figures 3a and 3b apply to the case $A=0.1$. The isotropic scatter term ($n=0$) is still seen to be the only significant contribution. Figures 4a and 4b consider the case $A=0.5$. The inhomogeneity is now large enough to require the excitation of the nonisotropic modes, which explains the discrepancy in amplitude (the corresponding phase is not plotted).

The first thing to note in the figures is the singularity in each instance for $X=-\frac{1}{2}$ for the homogeneous case. This corresponds to $x=x_T$; i.e., the point directly under the source where, according to (17), H_{y_1} vanishes. Similarly, at this point the phase of the ratio (H_x/H_y) in the homogeneous case shifts by 180 degrees [see (15) and (17)]. The oscillation(s) to the right of the first peak in the amplitude plots is related to the vanishing of the isotropic term in $H^s_{y_1}$ in (17) at $X=0$ where it changes sign. This effect is thus more pronounced when the inhomogeneity is large (for larger values of A).

The horizontal coordinate of an inhomogeneity for the examples considered can be inferred by a steep gradient in the amplitude ratio and an extremum in the corresponding phase ratio.

In all figures, the integral equation method was truncated such that $|n|, |m| \leq N=2$ (5 modes). In a case identical to the data for Figures 4a and 4b, except that $A=0.5$, the calculation was also run for $N=4$. The coefficients a_m changed at most in the fifth significant figure. The mode amplitudes $a_{\pm 1}$ were in this case approximately 30 percent of the magnitude of a_0 (hence the discrepancy in amplitude—the corresponding phase is not plotted). The truncation error is less critical than

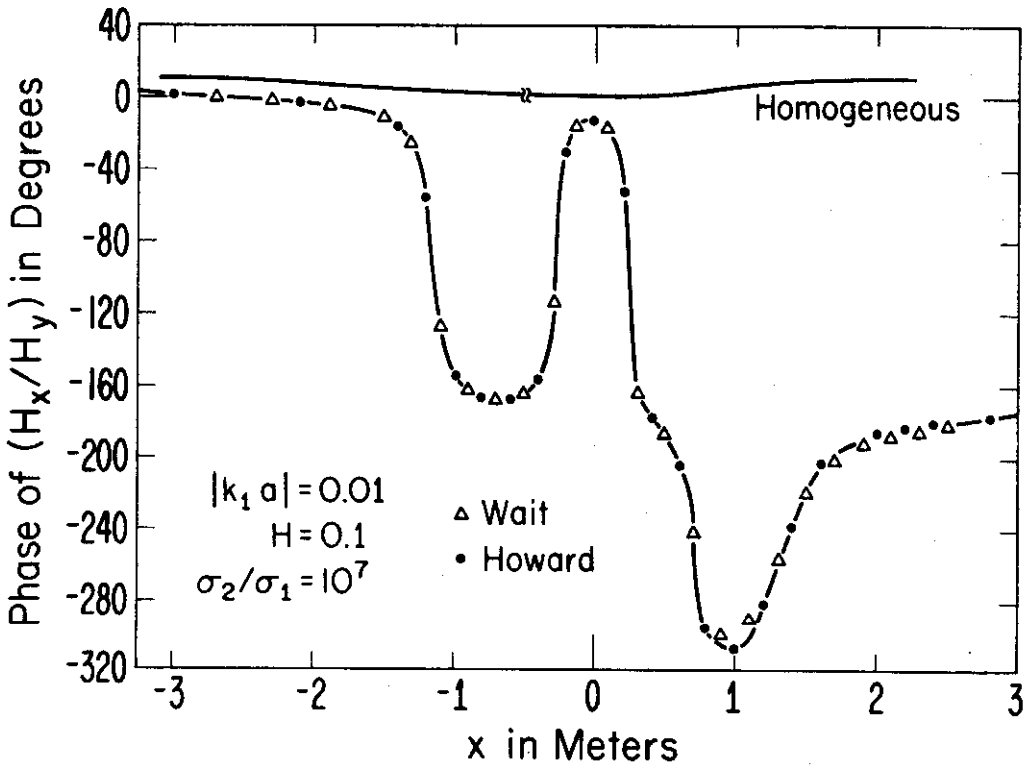

FIG. 2b. Phase comparison for ratio of horizontal to vertical magnetic fields versus X for $H=0.1$, $K=10^7$, and $A=0.01$.

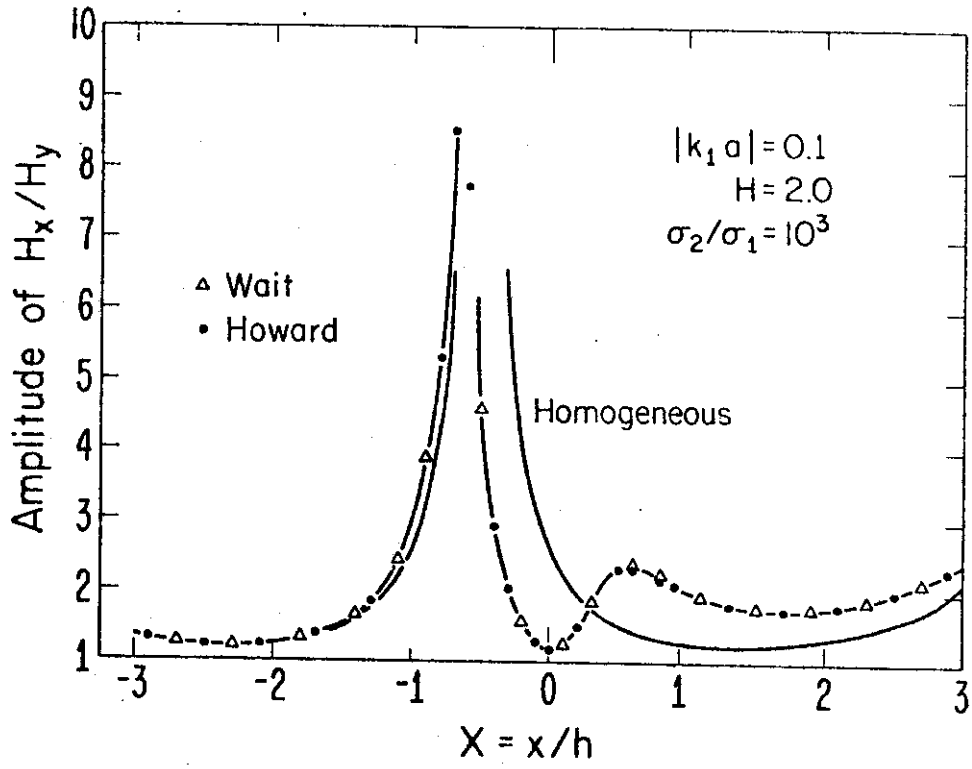

FIG. 3a. Amplitude comparison for ratio of horizontal to vertical magnetic fields versus X for $H=2$, $K=10^3$, and $A=0.1$.

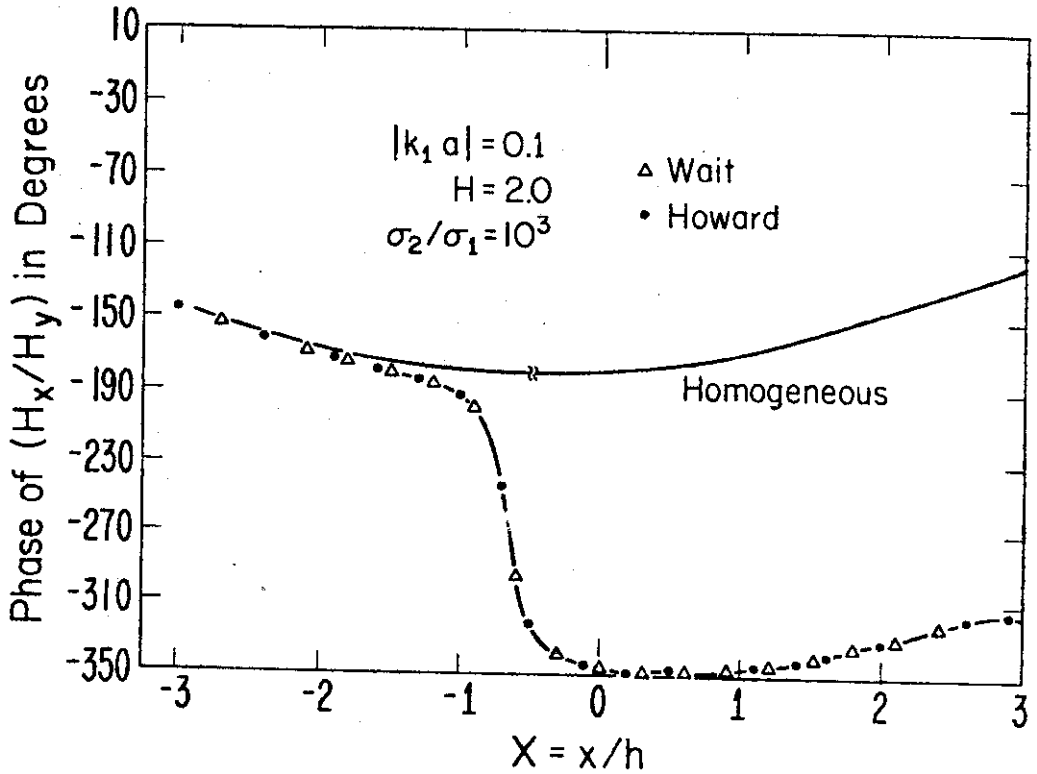

FIG. 3b. Phase comparison for ratio of horizontal to vertical magnetic fields versus X for $H=2$, $K=10^3$, and $A=0.1$.

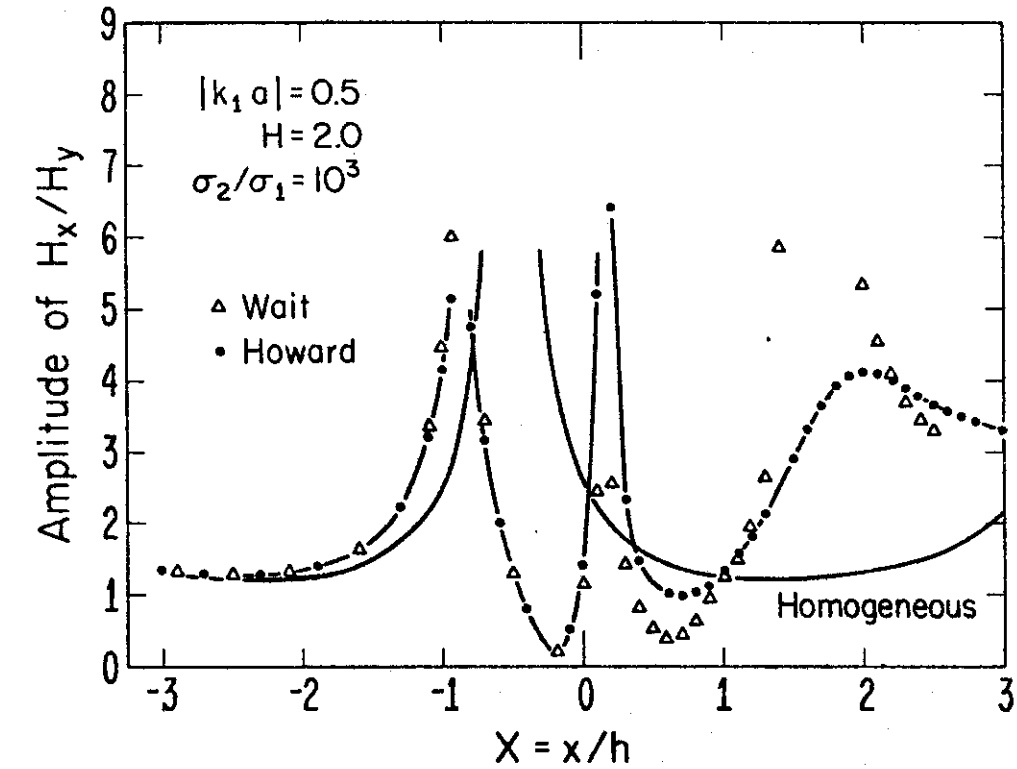

FIG. 4a. Amplitude ratio of horizontal to vertical magnetic fields versus X for $H=2$, $K=10^3$, and $A=0.5$.

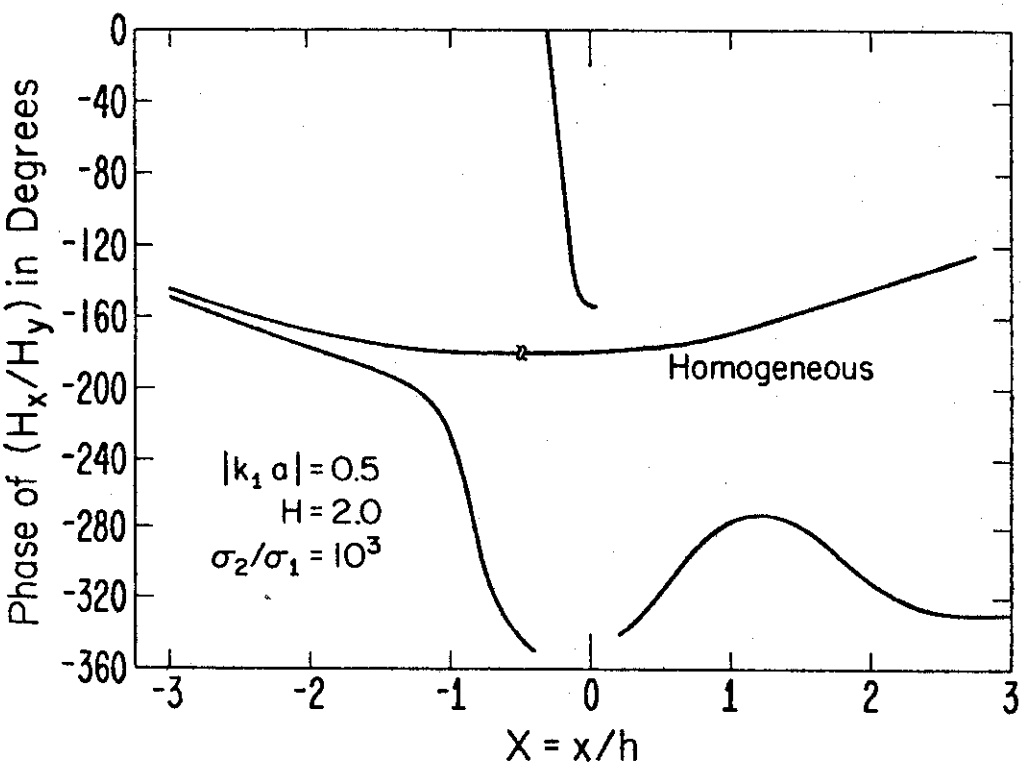

FIG. 4b. Phase ratio of horizontal to vertical magnetic fields versus X for $H=2$, $K=10^3$, and $A=0.5$.

in problems that have edge singularities. This is because the neglected terms for $|m| > N$, $|n| \leq N$ in (5), where N is the truncation integer, are small if $N \gg |k_1 a|$. [See Appendix A (Howard, 1972).]

CONCLUSION

A modified mode-match method in conjunction with an integral equation has been shown to be effective in dealing with the problem of scattering from a buried cylindrical inhomogeneity. The method of Wait (1970), which treats the case of small inhomogeneities in a much more direct manner, has been demonstrated to be in complete agreement with the mode-match treatment. The success of the latter can be attributed to the fact that all but one of the integrations occurring in the formalism, including the singular component in the kernel of the integral equation, can be done in closed form. Application of the mode-match method to scattering from penetrable objects results in a matrix equation for the mode amplitudes. The number of modes required in the Fourier Bessel series description of the scattered field depends on the argument of the Bessel functions occurring therein. Since the Bessel functions of the first kind are maximum where the order is approximately equal to the argument, the number of terms needed in the mode series is proportional to $|k_1 a|$, where a is the radius of the inhomogeneity. Thus, the mode-match matrix for good solution must have approximately $|k_1 a|^2$ elements. In contrast, for two-dimensional problems, the point-match technique requires the field to be matched at a number of points proportional to the cross-sectional area of the inhomogeneity, and, thus, the matrix for the point-match method is of order $|k_1 a|^4$. The reduction of the matrix size is clearly an advantage in reducing computation time. Also important in reducing computer time was the factoring of the matrix elements. The semianalytic approach also yields well-behaved matrices in contrast to the problems which sometimes occur in point-matching schemes.

ACKNOWLEDGMENTS

The author thanks Dr. J. R. Wait for suggesting the problem and for helpful discussion in the course of this research. This research was sponsored in part by the United States Bureau of Mines.

REFERENCES

D'Yakonov, B. P., 1959, The diffraction of electromagnetic waves by a circular cylinder in a homogeneous half-space: Bull. Acad. Sci. U.S.S.R., Geophys. Ser., No. 9, p. 950–955.

Gröbner, W., and Hofreiter, N., 1961, Integraltatè, Zweiterteil, Bestimmte Integrale: Vienna, Springer-Verlag, p. 65.

Hohmann, G. W., 1971, Electromagnetic scattering by conductors in the earth near a line source of current: Geophysics v. 36, no. 1, p. 101–131.

Howard, A. Q., Jr., 1972. Mode match solutions to electromagnetic scattering problems in a conducting half-space environment: University of Colorado, Ph.D. thesis.

Parry, J. R., and Ward, S. H., 1971, Electromagnetic scattering from cylinders of arbitrary cross section in a conductive half-space: Geophysics, v. 36, no. 1, p. 67–120.

Wait, J. R., 1959, Electromagnetic radiation from cylindrical structure: Pergamon Press, Oxford.

——— 1972, The effect of a buried conductor on the sub-surface fields for line source excitation: Radio Science, v. 7, no. 5, p. 587–591.

Wait, J. R., and Spies, K. P., 1971, Sub-surface electromagnetic fields of a line source on a conducting half-space: Radio Sci., v. 6, no. 8/9, p. 781–786.

Ward, S. H., and Morrison, H. F., (Editors), 1971, Special issue on Electromagnetic Scattering: Geophysics, v. 36, no. 1.

Reprint from the Review
PURE AND APPLIED GEOPHYSICS (PAGEOPH)
Formerly 'Geofisica pura e applicata'
Vol. 95, 1972/III BIRKHÄUSER VERLAG BASEL Pages 150–156

The Sub-Surface Magnetic Fields Produced by a Line Current Source on a Non-Flat Earth [1])

By JAMES R. WAIT[2]) and R. E. WILKERSON[2])

Summary – A simple cylindrical model is employed to estimate the effect of non-flatness of the ground on the sub-surface electromagnetic field from a current-carrying cable on the surface. It is shown that, if the surface curvature is sufficiently small, the fields in the cylinder model are very similar to those for the conducting half-space model of the earth employed earlier. The results can be used to provide estimates of expected errors in electromagnetic direction-finding of a buried receiving terminal.

1. Introduction

In a previous communication [1][3]), we reported on the analysis and calculations of the sub-surface fields in a conducting half-space produced by a line current located on the surface. Similar calculations have since been brought to my attention [2], [3]. In our work, we were interested in the application of the basic Green's function to scattering from inhomogeneities such as longitudinal conductors. The latter can be expected to have a major effect on modifying the structure of the received field at the buried terminal. This could pose a serious limitation on the direction-finding capability of a simple crossed loop receiving device.

Here, we would like to consider an alternative and much simpler approach that should give needed insight to the effect of non-flatness on the ground surface. Thus, we adopt a cylindrical model chosen so that the curvature of the surface is matched to the local topography rather than the mean curvature of the earth (for present purposes, the latter is zero!).

2. A classical preliminary problem

The basic prototype problem is the classical one of a uniform line current source located outside an infinitely long homogeneous cylinder of radius R_0 [4]. The situation

[1]) The research reported here was supported in part by the Mine Safety Center, U.S. Bureau of Mines.

[2]) Institute for Telecommunication Sciences, Office of Telecommunications, Boulder, Colorado, 80302, U.S.A.

[3]) Numbers in brackets refer to References, page 156.

is illustrated in Figure 1 where we have chosen a cylindrical coordinate system (ϱ, ϕ, z). The external medium $\varrho > R_0$ is free space with permittivity ε_0 and the internal medium $\varrho < R_0$ has a conductivity σ and permittivity ε. The line source with current I amps, located at (ϱ_0, ϕ_0, z), varies harmonically as $\exp(i\,\omega\,t)$ where $\varrho_0 \geqq R_0$.

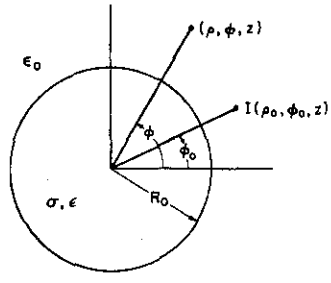

Figure 1
The prototype cylinder problem

For $\varrho > R_0$, we have only a z-component of the total electric field that can be written

$$E_z = E_z^p + E_z^s \tag{1}$$

as a sum of a primary and secondary parts. We know that [4]

$$E_z^p = -\frac{i\,\mu_0\,\omega\,I}{2\,\pi} K_0[\gamma_0[\varrho^2 + \varrho_0^2 - 2\,\varrho\,\varrho_0 \cos(\phi - \phi_0)]^{1/2}] \tag{2}$$

where $\gamma_0 = i(\varepsilon_0\,\mu_0)^{1/2}\,\omega$ and $\mu_0 = 4\,\pi \times 10^{-7}$. Using a standard addition theorem for modified Bessel functions, this, for $R_0 < \varrho < \varrho_0$, can be written

$$E_z^p = -\frac{i\,\mu_0\,\omega\,I}{2\,\pi} \sum_{m=0}^{\infty} \varepsilon_m\, K_m(\gamma_0\,\varrho_0)\, I_m(\gamma_0\,\varrho) \cos m(\phi - \phi_0) \tag{3}$$

where $\varepsilon_m = 1$ for $m = 0$, $= 2$ for $m = 1, 2, 3, \ldots$. Then, it follows that the secondary field for $\varrho > R_0$ will have the form

$$E_z^s = -\frac{i\,\mu_0\,\omega\,I}{2\,\pi} \sum_{m=0}^{\infty} \varepsilon_m\, A_m\, K_m(\gamma_0\,\varrho) \cos m(\phi - \phi_0) \tag{4}$$

where A_m is a coefficient yet to be determined.

The next step is to write down a suitable form for the total internal field. Thus, for the sourceless region $\varrho < R_0$, we have

$$E_z = -\frac{i\,\mu_0\,\omega\,I}{2\,\pi} \sum_{m=0}^{\infty} \varepsilon_m\, B_m\, I_m(\gamma\varrho) \cos m(\phi - \phi_0) \tag{5}$$

where $\gamma = (i\,\sigma\,\mu_0\,\omega - \varepsilon\,\mu_0\,\omega^2)^{1/2}$ and where B_m is also an unknown coefficient.

The boundary conditions for the present problem requires that E_z and $\partial E_z/\partial\varrho$ be continuous at $\varrho = R_0$. This leads to the system

$$K_m(\gamma_0\,\varrho_0)\,I_m(\gamma_0\,R_0) + A_m\,K_m(\gamma_0\,R_0) = B_m\,I_m(\gamma\,R_0) \tag{6}$$

$$K_m(\gamma_0\,\varrho_0)\,\gamma_0\,I'_m(\gamma_0\,R_0) + A_m\,\gamma_0\,K'_m(\gamma_0\,R_0) = B_m\,\gamma\,I'_m(\gamma\,R_0) \tag{7}$$

where the prime indicates differentiation with respect to the argument of the Bessel function. On eliminating A_m from (6) and (7), we get

$$B_m = -\frac{K_m(\gamma_0\,\varrho_0)}{\gamma_0\,R_0}\,\frac{1}{[I_m(\gamma\,R_0)\,K'_m(\gamma_0\,R_0) - (\gamma/\gamma_0)\,I'_m(\gamma\,R_0)\,K_m(\gamma_0\,R_0)]} \tag{8}$$

where we have used the Wronskian relation

$$K_m(x)\,I'_m(x) - K'_m(x)\,I_m(x) = 1/x\,.$$

Letting $\varrho_0 \to R_0$, we see that

$$B_m = -\left[I_m(\gamma\,R_0)\left(\frac{\gamma_0\,R_0\,K'_m(\gamma_0\,R_0)}{K_m(\gamma_0\,R_0)}\right) - \gamma\,R_0\,I'_m(\gamma\,R_0)\right]^{-1}. \tag{9}$$

This constitutes a statement of the exact solution of the problem.

For the present application, we can exploit the condition $|\gamma_0\,R_0| \ll 1$. Then, using the fact that for $x \ll 1$, $K'_m(x)/K_m(x) \sim -m/x$, (9) reduces to

$$B_m \simeq [m\,I_m(\gamma\,R_0) + \gamma\,R_0\,I'_m(\gamma\,R_0)]^{-1}. \tag{10}$$

Inserting this into (5), we have the following explicit expression for the internal fields for a line source on the surface of the cylinder

$$E_z = -\frac{i\,\mu_0\,\omega\,I}{2\,\pi}\sum_{m=0}^{\infty}\varepsilon_m\,\frac{I_m(\gamma\,\varrho)\cos m(\phi - \phi_0)}{m\,I_m(\gamma\,R_0) + \gamma\,R_0\,I'_m(\gamma\,R_0)}. \tag{11}$$

Corresponding expressions for the magnetic fields are

$$H_\varrho = -\frac{1}{i\,\mu_0\,\omega\,\varrho}\,\frac{\partial E_z}{\partial\phi} = \frac{I}{2\,\pi\,\varrho}\sum_{m=0}^{\infty}\varepsilon_m\,\frac{m\,I_m(\gamma\,\varrho)\sin m(\phi - \phi_0)}{m\,I_m(\gamma\,R_0) + (\gamma\,R_0)\,I'_m(\gamma\,R_0)} \tag{12}$$

and

$$H_\phi = \frac{1}{i\,\mu_0\,\omega}\,\frac{\partial E_z}{\partial\varrho} = \frac{I}{2\,\pi\,\varrho}\sum_{m=0}^{\infty}\varepsilon_m\,\frac{(\gamma\,\varrho)\,I'_m(\gamma\,\varrho)\cos m(\phi - \phi_0)}{m\,I_m(\gamma\,R_0) + (\gamma\,R_0)\,I'_m(\gamma\,R_0)}. \tag{13}$$

3. Application to a topographic feature

We now apply the prototype solution to the situation depicted in Figure 2. A Cartesian coordinate system (x, y, z) is chosen with the line source I located at the origin. The observer at P has coordinates (x, y, z) in the Cartesian system, and coordinates (ϱ, ϕ, z) in the cylindrical system where the latter has an origin at Q. The line Q is the center of curvature of the cylindrical surface, and it has Cartesian coordinates (x_0, y_0, z). [Note that the z-axes of the two coordinate systems are coincident but in opposite directions.]

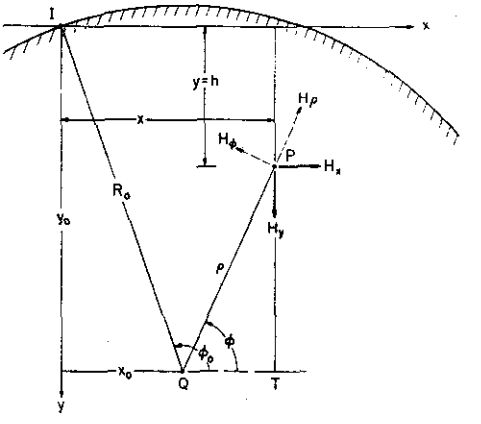

Figure 2
Geometry for a line current source on the cylindrical surface and the observer at buried location P

The quantities of interest are the orthogonal components of the magnetic field at the observer P expressed in the Cartesian system. Clearly, these are obtained as follows:

$$H_x = H_\varrho \cos\phi - H_\phi \sin\phi \tag{14}$$

$$H_y = -H_\varrho \sin\phi - H_\phi \cos\phi \tag{15}$$

where H_ϱ and H_ϕ are given by (12) and (13). For numerical work and comparisons with earlier studies (e.g. [1]), it is desirable to define two dimensionless field parameters A and B as follows:

$$A = -\frac{2\pi h}{I} H_x = A_\varrho \cos\phi - A_\phi \sin\phi \tag{16}$$

and

$$B = \frac{2\pi h}{I} H_y = A_\varrho \sin\phi + A_\phi \cos\phi \tag{17}$$

where

$$A_\varrho = -(2\pi h/I) H_\varrho \quad \text{and} \quad A_\phi = -(2\pi h/I) H_\phi$$

From (12) and (13), the latter are given explicitly as follows:

$$A_\varrho = -\left(\frac{h}{\varrho}\right) \sum_{m=0}^{\infty} \varepsilon_m \frac{m\, I_m(\gamma\, \varrho) \sin m(\phi - \phi_0)}{m\, I_m(\gamma\, R_0) + (\gamma\, R_0)\, I'_m(\gamma\, R_0)} \tag{18}$$

and

$$A_\phi = -\left(\frac{h}{\varrho}\right) \sum_{m=0}^{\infty} \varepsilon_m \frac{(\gamma\, \varrho)\, I'_m(\gamma\, \varrho) \cos m(\phi - \phi_0)}{m\, I_m(\gamma\, R_0) + (\gamma\, R_0)\, I'_m(\gamma\, R_0)} \tag{19}$$

where

$$I_m(\gamma\, R_0) = \sum_{n=0}^{\infty} \frac{(\gamma\, R_0)^{m+2n}}{n!(m+n)!\, 2^{m+2n}} \tag{20}$$

is the power series definition of the modified Bessel function. Of course, (18) and (19) are only valid if $\varrho \leqq R_0$.

In the case where displacement currents in the earth are negligible (i.e., where $\varepsilon\, \omega \ll \sigma$), we see that $\gamma \simeq (i\, \sigma\, \mu_0\, \omega)^{1/2}$. Then the modified Bessel functions of order m can be expressed in terms of Thompson's ber and bei function of order m. Specifically, $I_m(Z\, e^{i\pi/4}) = e^{-i(\pi/2)m}\, (\mathrm{ber}_m\, Z + i\, \mathrm{bei}_m\, Z)$ where $Z \cong |\gamma\, R_0| \simeq (\sigma\, \mu_0\, \omega)^{1/2}\, R_0$ is real.

Some needed geometrical relations follow immediately from Figure 2. First, we note that $y_0 = (R_0^2 - x_0^2)^{1/2}$, then $P\, T = y_0 - h$ and $Q\, T = x - x_0$. Consequently

$$\tan\phi = \frac{P\, T}{Q\, T} = \frac{(R_0^2 - x_0^2)^{1/2} - h}{x - x_0} \tag{21}$$

or

$$\phi = \arctan\left\{\frac{[(R_0/h)^2 - (x_0/h)^2]^{1/2} - 1}{(x/h) - (x_0/h)}\right\}. \tag{22}$$

Also, it is seen that

$$\varrho = [(P\, T)^2 + (Q\, T)^2]^{1/2}$$

and thus

$$\gamma\, \varrho = (\gamma\, h)\left\{\left[\left[\left(\frac{R_0}{h}\right)^2 - \left(\frac{x_0}{h}\right)^2\right]^{1/2} - 1\right]^2 + \left(\frac{x}{h} - \frac{x_0}{h}\right)^2\right\}^{1/2} \tag{23}$$

where $\gamma\, h \simeq e^{i\pi/4}\, H$ and $H = (\sigma\, \mu_0\, \omega)^{1/2}\, h$. Furthermore, because P is an interior point, $\varrho < R_0$ and (23) tells us that $(x - x_0)^2 \leqq R_0^2 - (h - y_0)^2$.

4. Discussion of some typical numerical results

Numerical calculations of the normalized field functions A and B have been carried for a range of the dimensionless parameters $H = |\gamma\, h|$, $R = |\gamma\, R_0|$, $X = x/h$ and $X_0 = x_0/h$. In order to illustrate the results here, we plot $|A|$ and $|B|$ as a function of the dimensionless distance parameter $X = x/h$ for $R = 5$, 10, and ∞. For the curves in Figure 3a,

we have $x_0=0$ and $H=0.2$, in Figure 3b, we have $x_0=0.5h$ and $H=0.2$, and in Figure 3c, we have $x_0=0$ and $H=1.0$. The qualitative behavior of the curves is very similar in all three cases. The effect of finite curvature of the air-ground interface is to increase the level of the normalized horizontal field (i.e., $|A|$), while the maximum response of the vertical field (i.e., $|B|$) is lowered somewhat. Actually, the curves designated $R=\infty$ are based on the results for the conducting half-space or flat earth model as described before [1]. As we see, if the radius of curvature of the surface is sufficiently large, it

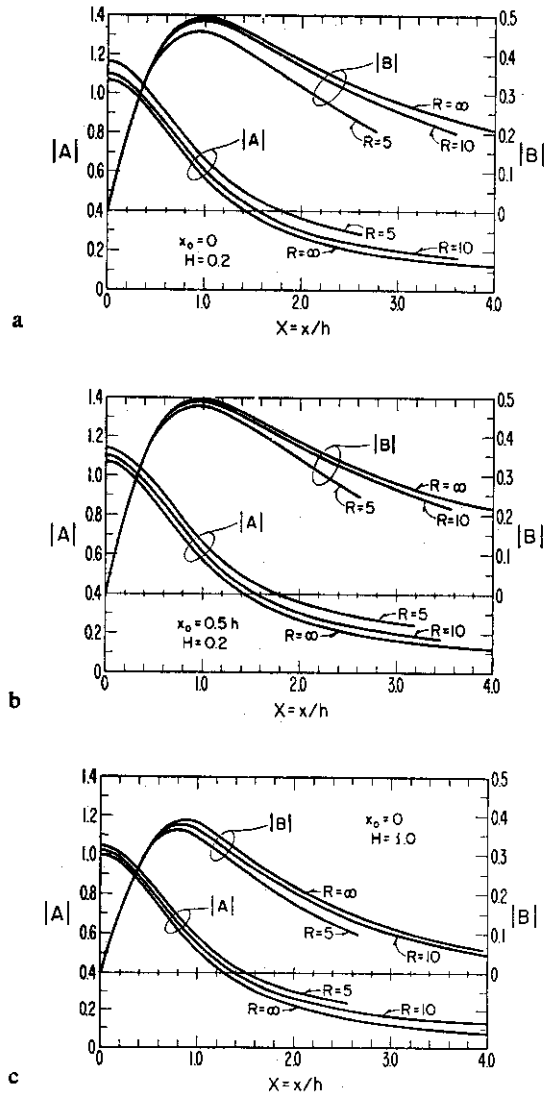

Figures 3, a, b and c
Normalized magnetic fields as a function of horizontal distance for geometry of Figure 2

appears that the conducting cylinder results approach those for the half-space. This is a reassuring check on the numerical data, since the method of calculation is vastly different in the two cases.

To deal with a specific example, we choose the ground conductivity σ to be 1 millimho/m and the operating frequency to be 100 Hz. Then the parameter $H=0.20$ if the observer depth $h=225$ m, while the parameter $H=1.0$ if $h=1.12$ km. Thus, if $R=10$, the radius of curvature R_0 of the surface is 11.2 km, while if $R=5$, we have $R_0=5.6$ km. These correspond to moderately rough terrain features.

The theory and the numerical data available for this problem should be useful for making various estimates of the expected errors introduced by the non-flatness of the ground on the direction of the magnetic field at a buried observer. In particular, the phase angle between the complex phasors A and B at the observer position will also depend on the radius of curvature R_0. This factor and other interesting questions are reserved for future work on this subject.

References

[1] J. R. Wait and K. P. Spies, *Sub-surface electromagnetic fields of a line source on conducting half-space*, Radio Sci. *6* (August–September 1971), 781-786.

[2] D. B. Large, Private communication (Westinghouse Georesearch Laboratory, Boulder, Colo. Jan. 1971).

[3] G. W. Hohmann, *Electromagnetic scattering by conductors in the earth near a line source of current*, Geophys. *36*, No. 1 (1971).

[4] J. R. Wait, *Electromagnetic radiation from cylindrical structures* (Pergamon Press, Oxford, England, 1959).

(Received 26th July 1971)

Electronics Letters, Vol. 7, No. 23
18 November 1971

INFLUENCE OF EARTH CURVATURE ON THE SUBSURFACE ELECTROMAGNETIC FIELDS OF A LINE SOURCE

Indexing terms: Electromagnetic fields and waves, Geophysics

The subsurface magnetic field produced by an oscillating line source of current on the Earth's surface is considered. Particular attention is given to evaluating the effect of non-flatness of the ground on the structure of the field at the buried receiving point. It is indicated that the wave-tilt ratio will still be a useful parameter in contemplated schemes for direction-finding in mine rescue operations.

There are a number of problems in applied geophysics[1] where an electromagnetic source field is set up by a long insulated cable carrying an alternating current. Most recently, an array of such cables has seen proposed as a mechanism to provide a modulated field at a subsurface point for reception by trapped miners.[2] If the structure of the subsurface field can be predicted, there is a good possibility, with a simple receiving device, that the location of personnel following a mine disaster can be ascertained. We have undertaken to examine this question from a theoretical point of view. In the present letter, the specific problem of the influence of local earth curvature is taken up. This is an extension of an earlier study where the subsurface field of a cable on a homogeneous flat earth was treated.[3]

A general solution for the electromagnetic fields of a line current source on a nonflat, homogeneous earth is not available. On the other hand, certain 2-dimensional configurations are amenable to numerical treatment as discussed in an excellent paper by Hohmann.[4] We use a similar model

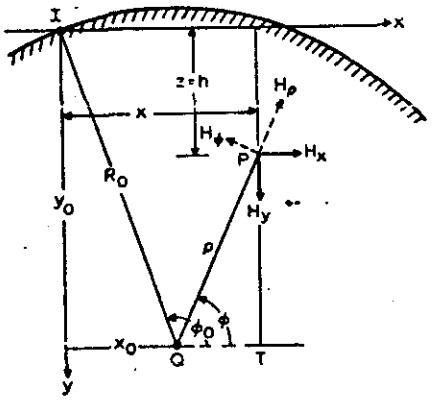

Fig. 1 *Geometry of the 2-dimensional model for a current line source on the surface of a locally cylindrical topographic feature*

here which has the virtue of relative simplicity. Specifically, we consider a current line source on the surface of a homogeneous earth that has the local characteristics of a circular cylinder. The situation is illustrated in Fig. 1, where we have designated the line source by I and the subsurface receiving point by P. The quantities of interest are the magnetic-field components H_x and H_y at P, in the Cartesian frame (x, y, z), for a uniform source current $I \exp(i\omega t)$.

To obtain a tractable solution, we assume that the essence of the problem can be preserved if we adopt the solution for a uniform line source parallel to a 'large' homogeneous cylinder of conductivity σ. The radius of the cylinder is R_0, and it is centred at Q with co-ordinates (x_0, y_0). Also, we can achieve some further simplicity by neglecting all displacement currents both in the air and in the conducting earth. Clearly, this will be valid when all significant dimensions are small compared with a free-space wavelength. The solution for this problem and the underlying assumptions were described previously,[5] and it is convenient, as an intermediate step, to express the results for the magnetic fields at P in terms of cylindrical co-ordinates (ρ, ϕ, z) centred at Q. Thus

$$H_\rho = \frac{I}{\pi\rho} \sum_{m=1}^{\infty} \frac{m I_m(\gamma\rho) \sin m(\phi - \phi_0)}{\gamma R_0 I_{m-1}(\gamma R_0)} \quad \ldots \quad (1)$$

and

$$H_\phi = \frac{I}{2\pi\rho} \frac{\gamma\rho I_1(\gamma\rho)}{\gamma R_0 I_1(\gamma R_0)} + \frac{I}{\pi\rho} \sum_{m=1}^{\infty} \frac{\gamma\rho I_{m-1}(\gamma\rho) - m I_m(\gamma\rho)}{\gamma R_0 I_{m-1}(\gamma R_0)} \cos m(\phi - \phi_0) \quad (2)$$

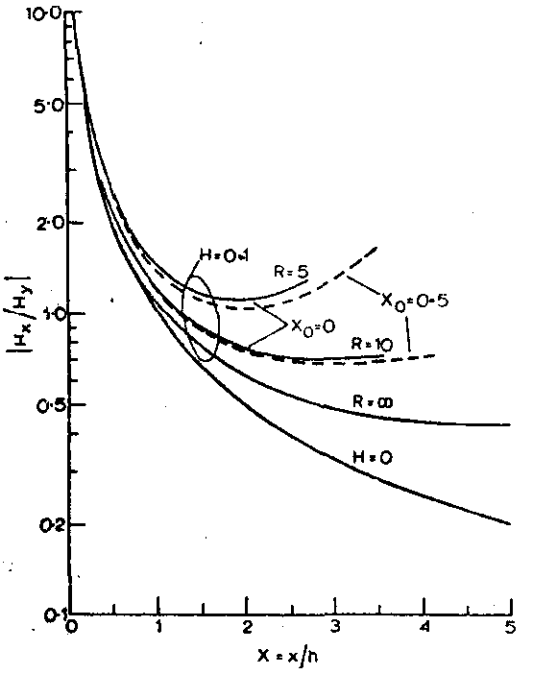

Fig. 2 *Magnetic-wave tilt produced by the line source at the subsurface point P for various values of the parameters $R = |\gamma R_0|$ and $X_0 = x/h$, as a function of $X = x/h$, for $H = |\gamma h| = 0{\cdot}1$*

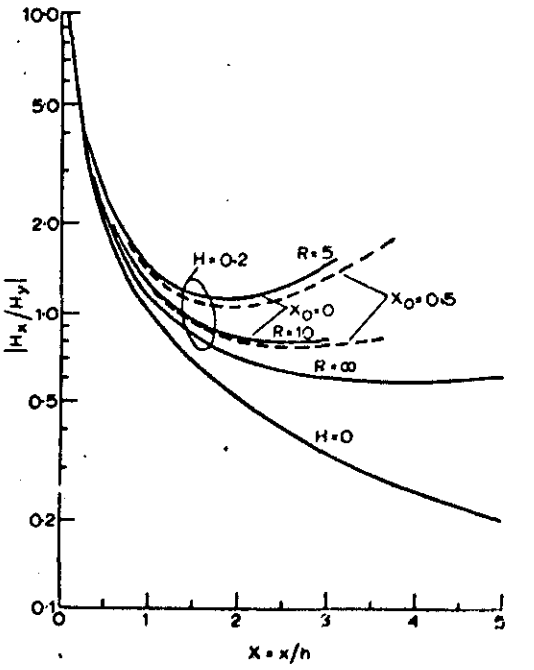

Fig. 3 *Wave tilt for $H = 0{\cdot}2$*

where $\gamma = (i\sigma\mu_0\omega)^{\frac{1}{2}}$, $\mu_0 = 4\pi \times 10^{-7}$ and $I_m(Z)$ is the modified Bessel function of integer order m and (complex) argument Z.

The desired Cartesian components are now obtained from

$$H_x = H_\rho \cos\phi - H_\phi \sin\phi \quad . \quad . \quad . \quad . \quad . \quad . \quad . \quad (3)$$

and

$$H_y = -H_\rho \sin\phi - H_\phi \cos\phi \quad . \quad . \quad . \quad . \quad . \quad . \quad . \quad (4)$$

Of particular interest is the wave-tilt ratio $|H_x/H_y|$. This is a quantity which can be measured easily by a single rotatable loop antenna at P. Using eqns. 1, 2, 3 and 4, this ratio is calculated and plotted in Figs. 2, 3 and 4 as a function of the parameter $X = x/h$ for fixed values of the parameters

$$H = |\gamma h| = (\sigma\mu_0\omega)^{\frac{1}{2}} h \qquad X_0 = x_0/h$$

and

$$R = |\gamma R_0| = (\sigma\mu_0\omega)^{\frac{1}{2}} R_0$$

On each Figure, we show the 'ideal' response function for $H = 0$ corresponding to free-space conditions. Also, using the earlier results[3] for a halfspace or flat earth, the response functions for $R = \infty$ are shown in Figs. 2, 3 and 4. In addition, the relative location of the centre curvature of the cylindrical air–earth interface is specified by the ratio $X_0 = x_0/h$. As indicated, this parameter is either 0 or 0·5. Finally, we note that the parameter $H = |\gamma h|$ determines the electrical depth of the observer beneath the level of the line source. For a typical operating frequency of 100 Hz and a ground conductivity $\sigma = 10^{-3}$ S/m, we easily calculate that the values $H = 0{\cdot}1$, 0·2 and 1·0 correspond to actual depths of 113, 225 and 1125 m, respectively. Under the same conditions, the assigned values $R = 5$ and 10 correspond to actual radii of curvature of 5·6 and 11·3 km. The latter correspond to moderately rough terrain features.

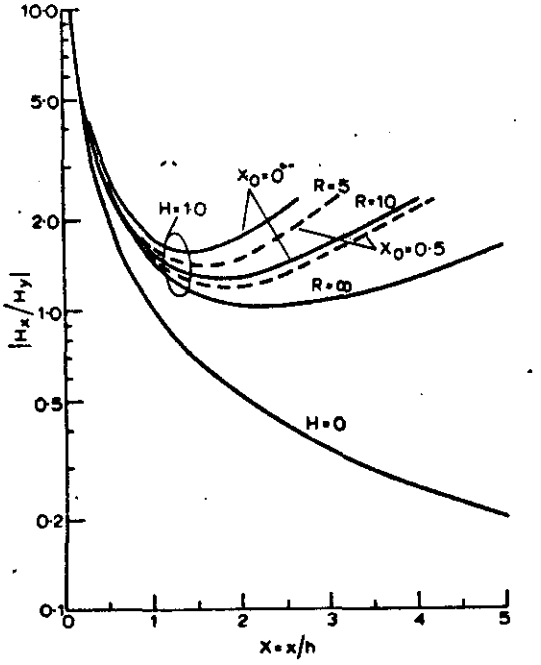

Fig. 4 *Wave tilt for $H = 1{\cdot}0$*

The results shown in Figs. 2, 3 and 4 indicate that the wave-tilt ratio is influenced not only be the finite conductivity of the overburden, but also by the curvature of the air–earth interface. The departures from the ideal response function (i.e. for $H = 0$) increase progressively with the electrical depth parameter H. Also, such departures are emphasised by the finite curvature of the surface. These facts should be borne in mind when contemplating the use of electromagnetic waves for a detection scheme in mine rescue operations.

Further work on the subject should allow for the 3-dimensional nature of the problem by considering curvature in both principal planes. Also, without formal mathematical difficulty, stratification of the overburden could be treated. These are worthy subjects for further analytical study if the scope of electromagnetic techniques in mine rescue operations is to be fully realised.

I am extremely grateful to R. E. Wilkerson for performing the numerical calculations of the wave tilt for finite values of R.

JAMES R. WAIT

25th October 1971

Institute for Telecommunications Sciences
US Department of Commerce
Boulder, Colo. 80302, USA

References

1 GRANT, F. S., and WEST, G. F.: 'Interpretation theory in applied geophysics' (McGraw-Hill, 1966)
2 WAIT, J. R.: 'Array technique for electromagnetic positional determination of a buried receiving point', *Electron. Lett.*, 1971, 7, pp. 186–187
3 WAIT, J. R., and SPIES, K. P.: 'Sub-surface electromangetic fields of a line source on a conducting half-space', *Radio Sci.*, 1971, 6
4 HOHMANN, G. W.: 'Electromagnetic scattering by conductors in the earth near a line source of current', *Geophysics*, 1971, 36, pp. 101–131
5 WAIT, J. R.: 'The cylindrical ore body in the presence of a cable carrying an oscillating current', *ibid.*, 1952, 17, pp. 378–386 [In eqn. 13 replace μ_2/μ_1 by $\kappa\mu_2/\mu_1$, and in eqn. 14 replace $(k \pm n)$ by $n(k \pm 1)$]

Radio Science, Volume 8, Numbers 8, 9, pages 805–810, August-September 1973

Subsurface electromagnetic fields of a line source on a two-layer earth

James R. Wait and Kenneth P. Spies

Institute for Telecommunication Sciences, Office of Telecommunications, US Department of Commerce, Boulder, Colorado 80302

(Received January 22, 1973; revised January 29, 1973.)

A previous analysis for a line source on a homogeneous half-space model of the earth is extended to allow for the presence of stratification. The formal integral solution is reduced to a form suitable for numerical integration. Also, a number of special cases and limiting forms are considered. It is shown that the subsurface field has a structure that can be significantly modified when the half-space is no longer homogeneous. The results have application to the design of electromagnetic techniques in mine rescue operations.

INTRODUCTION

Communication from a surface-based transmitter and an observer buried in the earth must be established following mine disasters. Because telephone wires and other normal means of communication can be interrupted, it is desirable that the electromagnetic signals propagate directly through the earth medium. In such situations, a desirable transmitting facility consists of a long insulated cable excited by an audio-frequency electric current. The fields at a subsurface point can be detected either by a multiturn loop or by the voltage induced in wire connecting two electrodes. The latter may be metal roof bolts or other metal probes that have good contact with the host rock.

If the length of the transmitter cable is much greater than all other physical dimensions, we can assume, for purposes of analysis, that the subsurface fields are the same as those for an infinite line source of uniform current. In other words, the resultant fields are those produced by induction rather than by conduction. Unfortunately, the situation is complicated by the presence of the inhomogeneous overburden that both attenuates and distorts the subsurface fields. In a previous investigation, *Wait and Spies* [1971] considered a homogeneous conducting half-space model that permitted an explicit calculation of the fields for a time-harmonic source current. Also, *Wait* [1971] advocated the use of such cable fields in a direction-finding scheme. This would permit as subsurface observer to determine his location relative to the surface-based transmitter. In such cases, it may be necessary to employ an array of such cables with a capability to allow a subsurface point to be scanned in a regular sequence.

A fundamental limitation to any down-link communication or subsurface location scheme is imposed by the conductive inhomogeneous over-burden. With this motivation in mind, we extend our earlier analysis to a two-layer half-space. In particular, we are interested in how the structure of the subsurface field is modified when the conductivity of the upper layer differs from the conductivity of the lower layer. Such a condition is typical in most environments in the vicinity of coal mines, although we admit that the model is still highly idealized.

THE INTEGRAL FORMULATION

With reference to the rectangular coordinate system shown in Figure 1, a layered nonmagnetic half-space consists of a homogeneous slab of conductivity σ_1 occupying the region $0 < y < h_1$, and a semi-infinite homogeneous medium of conductivity σ_2 occupying the region $y > h_1$, while a uniform line-source current I coincides with the z axis. If the fields vary with time as $\exp(i\omega t)$, and the frequency is sufficiently low that displacement currents are negligible compared with conduction currents, the nonvanishing field components at a subsurface point (x, h) are given by

$$H_x = \begin{cases} -\frac{I}{\pi}\int_0^\infty \frac{u_1}{u_1+\lambda}\left[\frac{\exp(-u_1 h) - R\exp[-u_1(2h_1-h)]}{1-RR_0\exp(-2u_1h_1)}\right]\cos\lambda x\, d\lambda & 0 < h \le h_1 \\ -\frac{I}{\pi}\int_0^\infty \frac{u_1}{u_1+\lambda}\left[\frac{(1-R)\exp(-u_1h_1)\exp[-u_2(h-h_1)]}{1-RR_0\exp(-2u_1h_1)}\right]\cos\lambda x\, d\lambda & h_1 \le h \end{cases} \quad (1)$$

$$H_y = \begin{cases} \frac{I}{\pi}\int_0^\infty \frac{\lambda}{u_1+\lambda}\left[\frac{\exp(-u_1 h) + R\exp[-u_1(2h_1-h)]}{1-RR_0\exp(-2u_1h_1)}\right]\sin\lambda x\, d\lambda & 0 < h \le h_1 \\ \frac{I}{\pi}\int_0^\infty \frac{\lambda}{u_1+\lambda}\left[\frac{(1+R)\exp(-u_1h_1)\exp[-u_2(h-h_1)]}{1-RR_0\exp(-2u_1h_1)}\right]\sin\lambda x\, d\lambda & h_1 \le h \end{cases} \quad (2)$$

$$E_z = \begin{cases} -\frac{i\mu_0\omega I}{\pi}\int_0^\infty \frac{1}{u_1+\lambda}\left[\frac{\exp(-u_1 h) + R\exp[-u_1(2h_1-h)]}{1-RR_0\exp(-2u_1h_1)}\right]\cos\lambda x\, d\lambda & 0 < h \le h_1 \\ -\frac{i\mu_0\omega I}{\pi}\int_0^\infty \frac{1}{u_1+\lambda}\left[\frac{(1+R)\exp(-u_1h_1)\exp[-u_2(h-h_1)]}{1-RR_0\exp(-2u_1h_1)}\right]\cos\lambda x\, d\lambda & h_1 \le h \end{cases} \quad (3)$$

where

$$R = (u_1 - u_2)/(u_1 + u_2)$$

$$R_0 = (u_1 - \lambda)/(u_1 + \lambda)$$

where

$$u_j = (\lambda^2 + \gamma_j^2)^{1/2}$$

$$\gamma_j^2 = i\sigma_j\mu_0\omega$$

$$j = 1, 2$$

The relevant formal theory for this layered geometry is available [*Wait*, 1970]. We remark here that (a) the field components satisfy the appropriate Helmholtz equation in the layers, (b) the field components are all continuous at the interface $y = h_1$, (c) the fields all decay exponentially as $y \to \infty$, and (d) the fields reduce to those for a uniform half-space if $h_1 \to \infty$ and/or if $\sigma_1 \to \sigma_2$.

For numerical work, it is convenient to express these components in terms of the following dimensionless parameters:

$$X = x/h$$

$$H = (\sigma_1\mu_0\omega)^{1/2}h$$

$$D = (\sigma_1\mu_0\omega)^{1/2}h_1$$

$$K = \sigma_2/\sigma_1$$

Also, as indicated below, we change the variable of integration to a dimensionless $s = \lambda h$. Then, the fields may be written as

$$H_x = -(I/2\pi h)A \quad (4)$$

$$H_y = (I/2\pi h)B \quad (5)$$

$$E_z = -(i\mu_0\omega I/2\pi)F \quad (6)$$

where A, B, and F are dimensionless field functions that conform to an earlier analysis for the homogeneous half-space model. For the configuration being considered here, we see that

$$A = \int_0^\infty a(s)\cos Xs\, ds \quad (7)$$

$$B = \int_0^\infty b(s)\sin Xs\, ds \quad (8)$$

and

$$F = \int_0^\infty f(s)\cos Xs\, ds \quad (9)$$

where

$$a(s) = \begin{cases} \frac{2(s^2+iH^2)^{1/2}}{(s^2+iH^2)^{1/2}+s}\,\frac{\exp[-(s^2+iH^2)^{1/2}] - R\exp[-(2D/H-1)(s^2+iH^2)^{1/2}]}{1-RR_0\exp[-2(D/H)(s^2+iH^2)^{1/2}]} & 0 \le H \le D \\ \frac{2(s^2+iH^2)^{1/2}}{(s^2+iH^2)^{1/2}+s}\,\frac{(1-R)\exp[-(D/H)(s^2+iH^2)^{1/2} - (1-D/H)(s^2+iKH^2)^{1/2}]}{1-RR_0\exp[-2(D/H)(s^2+iH^2)^{1/2}]} & D \le H \end{cases} \quad (10)$$

$$b(s) = \begin{cases} \dfrac{2s}{(s^2 + iH^2)^{1/2} + s} \dfrac{\exp[-(s^2 + iH^2)^{1/2}] + R \exp[-(2D/H - 1)(s^2 + iH^2)^{1/2}]}{1 - RR_0 \exp[-2(D/H)(s^2 + iH^2)^{1/2}]} \\ \qquad 0 \le H \le D \qquad (11) \\ \dfrac{2s}{(s^2 + iH^2)^{1/2} + s} \dfrac{(1 - R)\exp[-(D/H)(s^2 + iH^2)^{1/2} - (1 - D/H)(s^2 + iKH^2)^{1/2}]}{1 - RR_0 \exp[-2(D/H)(s^2 + iH^2)^{1/2}]} \\ \qquad D \le H \end{cases}$$

$$f(s) = [b(s)]/s = \begin{cases} \dfrac{2}{(s^2 + iH^2)^{1/2} + s} \dfrac{\exp[-(s^2 + iH^2)^{1/2}] + R \exp[-(2D/H - 1)(s^2 + iH^2)^{1/2}]}{1 - RR_0 \exp[-2(D/H)(s^2 + iH^2)^{1/2}]} \\ \qquad 0 < H \le D \qquad (12) \\ \dfrac{2}{(s^2 + iH^2)^{1/2} + s} \dfrac{(1 + R)\exp[-(D/H)(s^2 + iH^2)^{1/2} - (1 - D/H)(s^2 + iKH^2)^{1/2}]}{1 - RR_0 \exp[-2(D/H)(s^2 + iH^2)^{1/2}]} \\ \qquad D \le H \end{cases}$$

$$R = \frac{(s^2 + iH^2)^{1/2} - (s^2 + iKH^2)^{1/2}}{(s^2 + iH^2)^{1/2} + (s^2 + iKH^2)^{1/2}} \qquad (13)$$

$$R_0 = \frac{(s^2 + iH^2)^{1/2} - s}{(s^2 + iH^2)^{1/2} + s} \qquad (14)$$

Our task is to calculate A, B, F, where X, H, D/H, and K are given.

SPECIAL CASES AND LIMITING FORMS

First of all, we note that if $K = 1$ (i.e., if $\sigma_1 = \sigma_2$), then $R = 0$ and

$$a(s) = \frac{2(s^2 + iH^2)^{1/2}}{(s^2 + iH^2)^{1/2} + s} \exp[-(s^2 + iH^2)^{1/2}] \qquad (15)$$

$$b(s) = sf(s)$$

$$= \frac{2s}{(s^2 + iH^2)^{1/2} + s} \exp[-(s^2 + iH^2)^{1/2}] \qquad (16)$$

thus, A, B, and F reduce, as they should, to the forms for a homogeneous half-space (1). On the other hand, if $H = 0$ corresponding to the frequency tending to 0, then $R = R_0$ and

$$a(s) = b(s) = \exp(-s) \qquad (17)$$

$$f(s) = [\exp(-s)]/s \qquad (18)$$

Therefore

$$A = \int_0^\infty [\exp(-s)] \cos Xs\, ds = 1/(1 + X^2) \qquad (19)$$

$$B = \int_0^\infty [\exp(-s)] \sin Xs\, ds = X/(1 + X^2) \qquad (20)$$

In this static limit, the integral for F does not converge, since the integrand behaves as $1/s$, near the origin. In this case, however, it is not difficult to show that

$$E_s \propto \lim_{\omega \to 0} (\omega \log \omega) \to 0$$

Another special case that is useful for checking the numerical data given below is to let $h_1 \to 0$. Thus, we should recover the results for a homogeneous half-space with conductivity σ_2. For example, if we use the functional notation $A = A(H, X, K, D)$ for the general two-layer case, we see that

$$A(H, X, K, 0) = A(K^{1/2}H, X) \qquad (21)$$

where

$$A(H, X) = 2\int_0^\infty \frac{(s^2 + iH^2)^{1/2}}{(s^2 + iH^2)^{1/2} + s} \cdot \{\exp[-(s^2 + iH^2)^{1/2}]\} \cos sX\, ds \qquad (22)$$

This is one of the integrals considered before (1) for the homogeneous half-space. The same identity applies to the field functions B and F.

A limiting case of the two-layer formulation oc-

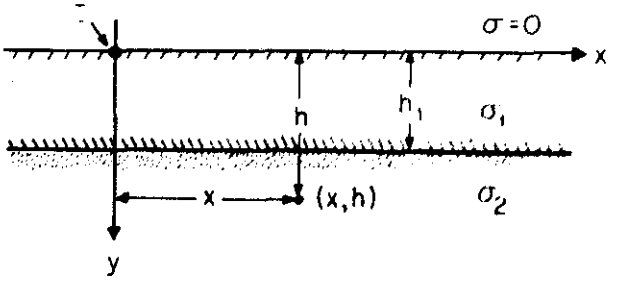

Fig. 1. Two-layer model of the earth for excitation by a uniform line current on the surface.

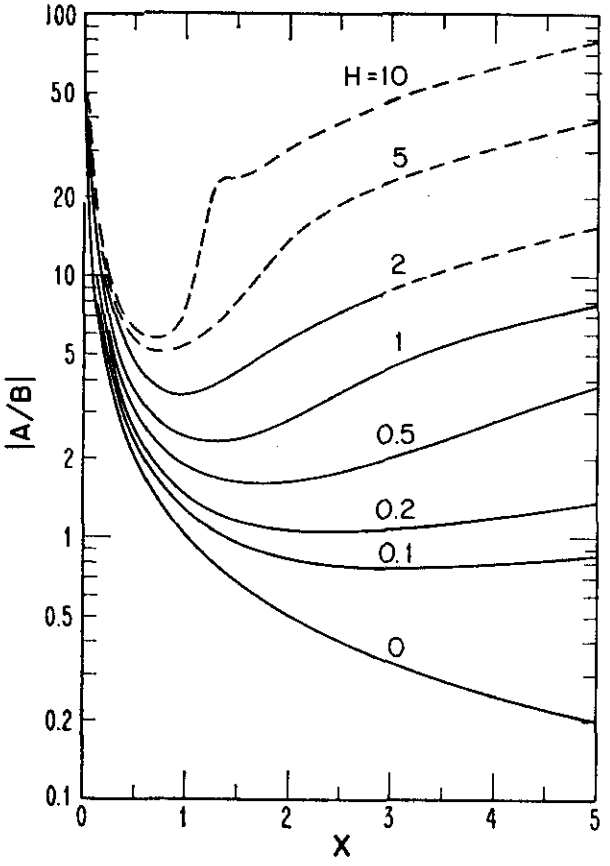

Fig. 2. Ratio between the horizontal and the vertical components of the magnetic field at a subsurface observing point located in the lower stratum of a two-layer earth. For this figure and for the succeeding ones, $X = x/h$, $H = (\sigma_1 \mu_0 \omega)^{1/2} h$, $D/H = h_1/h$, and $K = \sigma_2/\sigma_1$. For this figure $D/H = 0.5$, and $K = 10$.

curs when $x \to \infty$ [*Wait*, 1970]. In this high-frequency limit, the electric field E_z varies as $x^{-3/2} \exp(-i k_0 x)$, where k_0 is the free-space wave number. This fact emerges from a general asymptotic development for the far-zone fields of a line source on a stratified half-space (3). Provided $|k_0 x| \ll 1$, being consistent with the neglect of displacement currents, E_z varies simply as x^{-2} in this quasi-static asymptotic range. Some results for this case were given by *Bannister* [1968], who was specifically interested in the application to the measurement of the conductivity of the sea bed. In his case, the parameters equivalent to $|\gamma_1 x|$ and $|\gamma_2 x|$ were very large so that the fields could be described by their quasi-static asymptotic forms. In our contemplated application to mine rescue procedures, we would seldom be working in a frequency or distance range where these asymptotic results could be used. Nevertheless, they do serve as an excellent check on the numerical integration results discussed below.

In the notation used here, the quasi-static asymptotic results are valid if both HX and $K^{1/2}HX$ are sufficiently large (i.e., greater than about 5). Then we find that

$$A \simeq 2QP/(i^{1/2} H X^2) \tag{23}$$

$$B \simeq 2Q^2 G/(iH^2 X^3) \tag{24}$$

and

$$F \simeq 2Q^2 G/(iH^2 X^2) \tag{25}$$

where Q is the commonly encountered wave-tilt factor [*Wait*, 1970] given by

$$Q = [1 + r \exp(-2i^{1/2} D)]/[1 - r \exp(-2i^{1/2} D)] \tag{26}$$

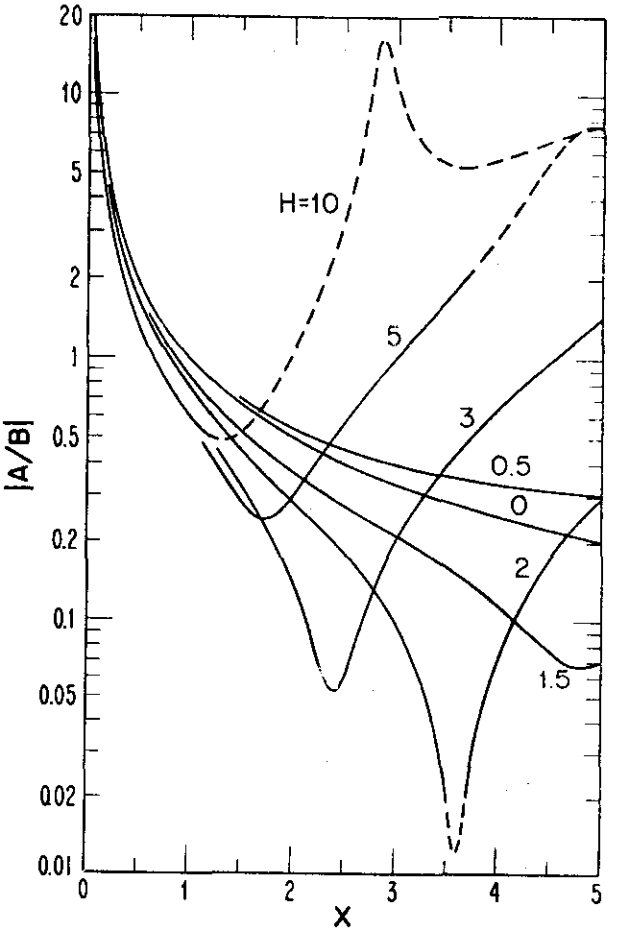

Fig. 3. Ratio between the horizontal and the vertical components of the magnetic field at a subsurface observing point located in the lower stratum of a two-layer earth. $D/H = 0.5$; $K = 0.1$.

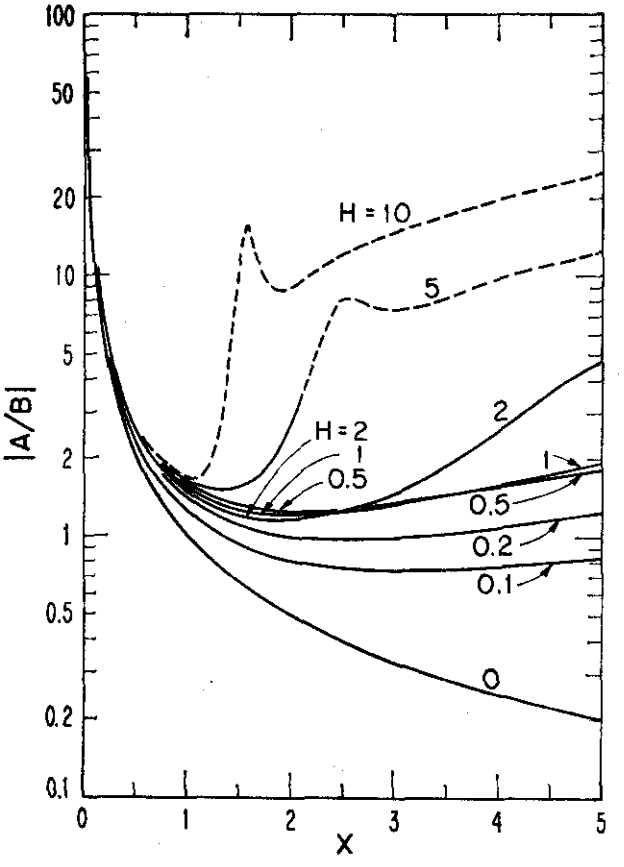

Fig. 4. Ratio of the field components when the observing point is within the upper stratum. $D/H = 2$; $K = 10$.

and r is a reflection coefficient defined by

$$r = \lim_{\epsilon \to 0} R = (1 - K^{1/2})/(1 + K^{1/2}) \quad (27)$$

Here, G and P are depth-gain functions that correspond to the ratio of the field at depth H to that at the surface. These are found to have the form

$$G = [\exp(-i^{1/2}H) + r \cdot \exp(-2i^{1/2}D + i^{1/2}H)]/[1 + r\exp(-2i^{1/2}D)] \quad (28)$$

$$P = [\exp(-i^{1/2}H) - r \cdot \exp(-2i^{1/2}D + i^{1/2}H)]/[1 - r\exp(-2i^{1/2}D)] \quad (29)$$

for $0 < H \leq D$. The corresponding forms in the lower region are

$$G = \{(1 + r)/[1 + r\exp(-2i^{1/2}D)]\} \cdot \exp[-i^{1/2}D - i^{1/2}(H - D)K^{1/2}] \quad (30)$$

$$P = \{(1 - r)/[1 - r\exp(-2i^{1/2}D)]\} \cdot \exp[-i^{1/2}D - i^{1/2}(H - D)K^{1/2}] \quad (31)$$

for $H \geq D$.

DISCUSSION OF RESULTS

Using numerical integration as discussed before [*Wait and Spies*, 1971], A, B, and F have been evaluated for a selected range of the parameters X, H, K, and D. These results are available on request from the authors in tabulated form for a range of X from 0 to 5 and for all combinations of the following values of the parameters: $H = 0.1$, 0.2, 0.5, 1.0, 1.5, 0.2, 0.5, 1.0, 2.0; $D/H = h_1/h = 0.5$, 1.0, 2.0; $K = 0.1$, 10. Also, some values of A, B, and F were obtained for $K = 0.01$ and 100 for a restricted range of the other parameters.

A derived quantity of special interest is the magnitude of the ratio H_x/H_y at the sub-surface observer point. As we mentioned before (1), this ratio, equal to $|A/B|$, can be measured by two crossed

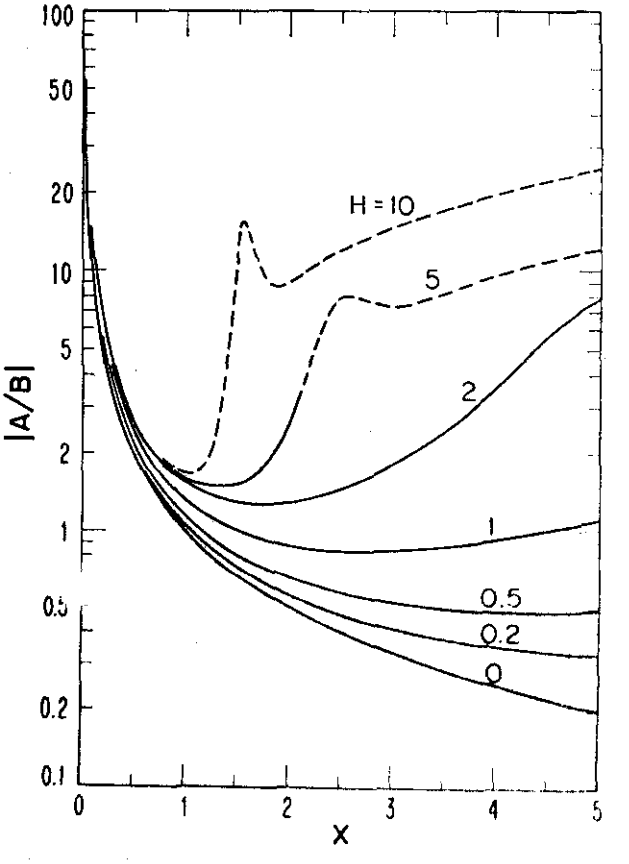

Fig. 5. Ratio of the field components when the observing point is within the upper stratum. $D/H = 2$; $K = 0.1$.

loops or by a single loop rotatable about an axis. Using the numerical data for A and B, this ratio is plotted in Figures 2 and 3 as a function of the displacement X for $K = 0.1$ and $K = 10$, respectively, for $D/H = 0.5$, and a range of H values. Here and in the figures that follow, the curves are broken whenever $|A|$ and/or $|B|$ is less than 10^{-3} (i.e., < -60 db). These results in Figures 2 and 3 correspond to locating the observer within the substratum. The corresponding results for the case in which the observer is within the upper layer are shown in Figures 4 and 5, where we choose $D/H = 2.0$.

The effect of varying the conductivity contrast $K(= \sigma_2/\sigma_1)$ is illustrated in Figures 6 and 7, where we choose $D/H = 0.5$ and 2, respectively, and fix $H = 1$ (i.e., $D = 0.5$ and 2).

In general, $|A/B|$ always has a pronounced peak at $X = 0$ corresponding to the observer directly beneath the source cable. On examining the curves in Figures 2, 3, 4, 5, 6, and 7 we see that the peak may be obscured to some extent by the presence of the stratification in the overburden. No doubt this behavior should be taken into account in any feasibility studies of source-location techniques that utilize subsurface magnetic-field measurements.

An important and nontrivial extension of the present analysis is to allow for the nonuniformity of the thickness of the upper layer. This subject is being currently investigated by using a wave-optical technique.

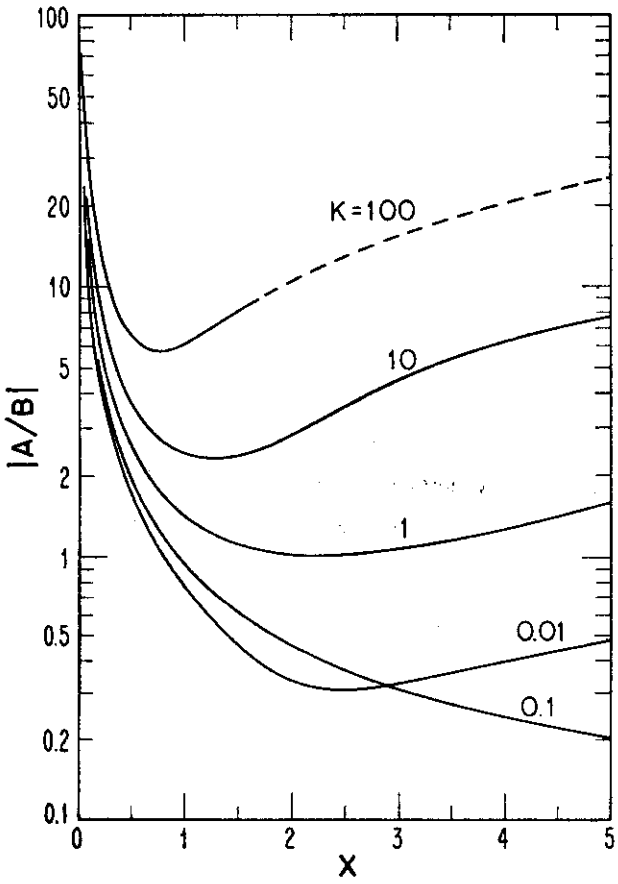

Fig. 6. Ratio of the field components illustrating the effect of conductivity contrast between the layers. $H = 1$; D/H = 0.5.

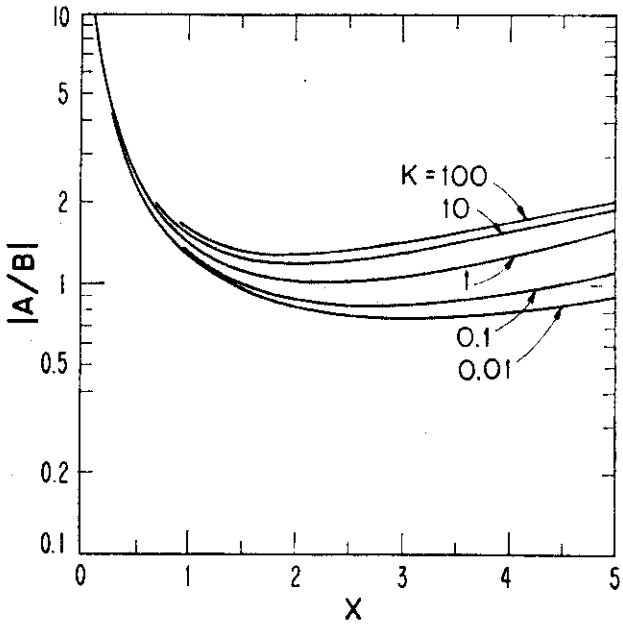

Fig. 7. Ratio of the field components illustrating the effect of conductivity contrast between the layers. $H = 1$; $D/H = 2.0$.

Acknowledgments. We would like to thank Dr. R. G. Geyer of the Colorado School of Mines for suggesting this problem, and Mrs. Loys Gappa for her help in preparing the manuscript. The research was supported by the US Bureau of Mines.

REFERENCES

Bannister, P. R. (1968) Electromagnetic fields within a a stratified earth produced by a long horizontal line source, *Radio Sci.*, *3*(4), 387–390.

Wait, J. R. (1970), *Electromagnetic Waves in Stratified Media*, 2nd ed., chap. 2, pp. 8–63, Pergamon, New York.

Wait, J. R. (1971), Array technique for electromagnetic positional determination of a buried receiving point, *Electron. Lett.*, *7*(8), 186–187.

Wait, J. R., and K. P. Spies (1971), Subsurface electromagnetic fields of a line source on a conducting half-space, *Radio Sci.*, *6*(8/9), 781–786.

IEEE Trans. AP, Vol. 22, No. 1, 145-146, 1974.

COMMUNICATIONS

Diffusion of Electromagnetic Pulses into the Earth from a Line Source

DAVID A. HILL AND JAMES R. WAIT

***Abstract*—The subsurface electromagnetic fields of a line source with a delta function current are considered. All displacement currents are neglected. The time-dependent electric and magnetic fields at the buried observer are illustrated. The resulting waveforms all have a leading spike followed by a slowly decaying tail of opposite polarity. The results have possible application to downlink signaling in mine rescue work.**

Manuscript received May 17, 1973.

D. A. Hill is with the Institute for Telecommunication Sciences, Office of Telecommunications, U.S. Department of Commerce, Boulder, Colo. 80302.

J. R. Wait is with the Cooperative Institute for Research in Environmental Sciences, University of Colorado, Boulder, Colo. 80302, and Consultant to the Institute for Telecommunication Sciences, Office of Telecommunications, U.S. Department of Commerce, Boulder, Colo. 80302.

Introduction

Expressions for the subsurface electric field of a line source with an impulsive current were derived previously [1]. However, in application to downlink communication and signaling, the time-dependent voltages induced in small loop receiving antennas are also of interest. These voltage waveforms are proportional to the time derivatives of the appropriate magnetic field components. Here, we consider these response waveforms and obtain numerical results for all the field components for any location of the observer within the lower half-space.

Electric Field

The line source carries an impulsive current $I_0\delta(t)$ and is coincident with the z axis. The subsurface observer is located at $(x, -h)$ in the earth ($y < 0$), as shown in Fig. 1. If all displacement currents are neglected, the inverse transform of the known time-harmonic solution for the electric field [2] can be readily evaluated. This impulse response [1] for $t > 0$ is given by

$$e_z(t) = \frac{I_0}{\pi\sigma}\int_0^\infty \cos\lambda x\left(\frac{\partial}{\partial h}+\lambda\right)\left[\frac{(\mu_0\sigma)^{1/2}h}{2(\pi t^3)^{1/2}}\exp\left(-\frac{\lambda^2 t}{\mu_0\sigma}-\frac{\mu_0\sigma h^2}{4t}\right)\right]d\lambda \tag{1}$$

where σ is the conductivity of the half space, and μ_0 is permeability of free space.

In order to evaluate (1), we consider integrals of the type

$$I_0 = \int_0^\infty \exp(-\alpha\lambda^2)\cos\lambda x\, d\lambda \tag{2}$$

$$I_1 = \int_0^\infty \lambda\exp(-\alpha\lambda^2)\cos\lambda x\, d\lambda \tag{3}$$

where

$$\alpha = \frac{t}{(\mu_0\sigma)}.$$

The first integral is well known, and the second can be written in a convenient summation form [3]. Thus

$$I_0 = \frac{(\pi)^{1/2}\exp(-x^2/4\alpha)}{2\alpha^{1/2}} \tag{4}$$

$$I_1 = \frac{1}{2\alpha} - \frac{x}{4\alpha^{3/2}}\sum_{k=0}^{\infty}\frac{(-1)^k k!}{(2k+1)!}(x\alpha^{-1/2})^{2k+1}. \tag{5}$$

By substituting (4) and (5) into (1) and carrying out the differentiation, we obtain

$$e_z(t) = \frac{I_0}{4\pi\sigma l^2(\sigma\mu_0 h^2)}E_z(D,T) \tag{6}$$

where the normalized electric-field waveform is given by

$$E_z(D,T) = \exp\left(-\frac{1}{4T}\right)\left\{(T^{-2}-\tfrac{1}{2}T^{-3})\exp\left(-\frac{D^2}{4T}\right)+\pi^{-1/2}T^{-5/2}\cdot\left[1-\frac{D}{2T^{1/2}}\sum_{k=0}^{\infty}\frac{(-1)^k k!}{(2k+1)!}(DT^{-1/2})^{2k+1}\right]\right\} \tag{7}$$

where $D = x/h$, and $T = t/(\sigma\mu_0 h^2)$. Here, I_0 has units of charge, while E_z, D, and T are dimensionless.

Actually, (6) is equivalent to that of Wait's [1] whose result contains the tabulated Dawson's integral [4] rather than an infinite sum, and also T is defined differently. Here, we choose the summation form because it is relatively convenient to evaluate on a computer and also it yields the asymptotic expansion for large T directly.

Waveforms of E_z for various values of D are shown in Fig. 2. Note that E_z is attenuated and stretched out as D is increased.

Magnetic Field

The time derivatives of the two magnetic field components h_x and h_y can be obtained from Maxwell's equations:

$$\frac{\partial h_x(t)}{\partial t} = \frac{1}{\mu_0}\frac{\partial e_z(t)}{\partial h} \tag{8}$$

$$\frac{\partial h_y(t)}{\partial t} = \frac{1}{\mu_0}\frac{\partial e_z(t)}{\partial x}. \tag{9}$$

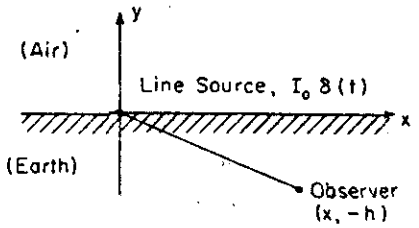

Fig. 1. Conducting half space with line source on surface and subsurface observer.

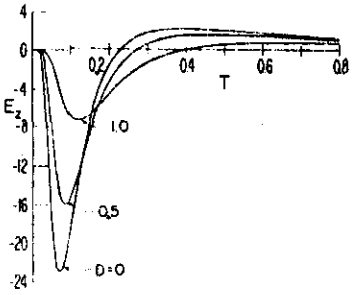

Fig. 2. Normalized electric field waveforms as function of position.

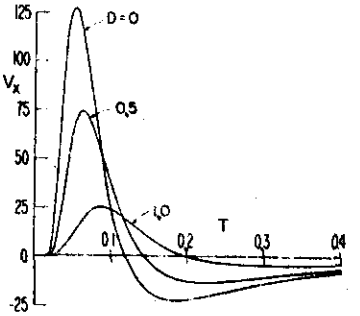

Fig. 3. Normalized voltage waveform for loop with horizontal axis as function of position.

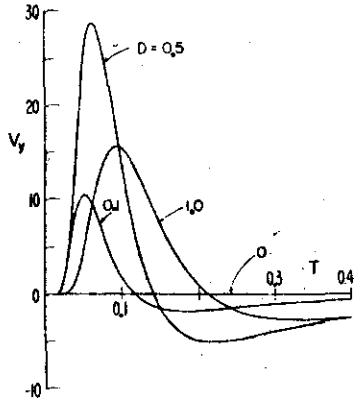

Fig. 4. Normalized voltage waveform for loop with vertical axis as function of position.

Consequently, the voltages induced in small loops with either x- or y- directed axes (v_x or v_y) are given by

$$v_x(t) = AN\frac{\partial e_z(t)}{\partial h} \tag{10}$$

$$v_y(t) = AN\frac{\partial e_z(t)}{\partial x} \tag{11}$$

where A is the loop area and N is the number of turns.

By substituting (6) into (10) and (11), and carrying out the differentiations, we obtain the voltage waveforms

$$\left.\begin{matrix} v_x(t) \\ v_y(t) \end{matrix}\right\} = \frac{I_0AN}{4\pi\sigma h^3(\sigma\mu_0h^2)}\left\{\begin{matrix} V_x(D,T) \\ V_y(D,T) \end{matrix}\right. \tag{12, 13}$$

where

$$V_x(D,T) = \frac{\exp(-1/4T)}{T^3}\left\{\left(-\tfrac{3}{2}+\frac{1}{4T}\right)\exp\left(-\frac{D^2}{4T}\right)+\left(1-\frac{1}{2T}\right)\cdot\frac{T^{1/2}}{\pi^{1/2}}\left[1-\frac{D}{2T^{1/2}}\sum_{k=0}^{\infty}\frac{(-1)^k k!}{(2k+1)!}(DT^{-1/2})^{2k+1}\right]\right\} \tag{14}$$

and

$$V_y(D,T) = \frac{-\exp(-1/4T)}{T^3}\left[\frac{D}{2}\left(1-\frac{1}{2T}\right)\exp\left(-\frac{D^2}{8T}\right)+\frac{1}{\pi^{1/2}}\sum_{k=0}^{\infty}\frac{(-1)^k(k+1)!}{(2k+1)!}(DT^{-1/2})^{2k+1}\right] \tag{15}$$

where $D = x/h$, and $T = t/(\sigma\mu_0h^2)$.

As defined, V_x and V_y are dimensionless, while v_x and v_y are proportional to h^{-3}. In the important special case of the observer directly below the source ($D = 0$), V_y is zero and V_x simplifies to

$$V_x(0,T) = \exp\left(-\frac{1}{4T}\right)\left[\pi^{-1/2}T^{-5/2}-\frac{3}{2}T^{-3}-\frac{1}{2}\pi^{-1/2}T^{-7/2}+\frac{1}{4}T^{-4}\right]. \tag{16}$$

The response functions V_x and V_z, for arbitrary D, were computed from (12) and (13), and are shown in Figs. 3 and 4. As indicated, the waveforms are stretched out as D increases. The peak of V_x decreases with increasing D while V_y increases from zero for small D before decreasing for larger D.

Concluding Remarks

While the results given here pertain to a delta function current, the response for an arbitrary current can be obtained by convolution. All waveforms shown have a spike followed by a slow tail, and the length of the tail could be a determining factor in pulsewidths and repetition frequencies for downlink communications [5]. On the other hand, the dependence of pulse shape on position could be useful in source location for a buried observer.

Acknowledgment

We wish to thank Dr. Geyer, Colorado School of Mines, for his suggestions and for the opportunity to exchange unpublished material.

References

[1] J. R. Wait, "Transient excitation of the earth by a line source of current," *Proc. IEEE* (lett.), vol. 59, pp. 1287–1288, Aug. 1971.
[2] ——, *Electromagnetic Waves in Stratified Media*, 2nd ed. Oxford, England: Pergamon, 1970.
[3] I. M. Ryshik and I. S. Gradstein, *Tables of Series, Products, and Integrals*. Berlin, Germany: Veb Deutscher Verlag der Wissenschaften, 1963, p. 180.
[4] A. Abramowitz and J. A. Stegun, Eds., *Handbook of Mathematical Functions*. Washington, D.C.: National Bureau of Standards, 1964, p. 319.
[5] D. B. Large, L. Ball, and A. J. Farstad, "Radio transmission to and from underground coal mines—theory and measurement," *IEEE Trans. Commun.*, vol. COM 21, pp. 194–202, Mar. 1973.

ARRAY TECHNIQUE FOR ELECTROMAGNETIC POSITIONAL DETERMINATION OF A BURIED RECEIVING POINT

Indexing terms: Telecommunication links, Safety

We describe a scheme to locate personnel in a coal mine following a disaster. The method, while not yet tested, would require only that the trapped miner be equipped with a loop receiving device. Operating frequencies in the low audio range are called for.

There is more than a casual interest in exploiting electromagnetic waves to locate miners following a disaster. The possibility that all conventional means of communication are eliminated should not be ruled out. However, if the miners are equipped with a simple receiving device, it is feasible for them to perceive an audio-frequency electromagnetic signal from a surface transmitter. Such a downlink communication scheme has been demonstrated by the Georesearch Laboratory of the Westinghouse Electric Corporation. They also envisage an uplink scheme using seismic signals generated by hammer blows. A technique for utilising the seismic signals for direction finding and/or source location has also been considered (as described orally by D. B. Large of Westinghouse). Here, we would like to suggest that there may be some direction-finding capability using a scanning array of electromagnetic line sources on the surface. If such a method is to be feasible, the receiving terminal must be simple. We outline a possible scheme to achieve this goal.

The simplest scheme which we envisage is a parallel pair of long current-carrying cables on the earth's surface. If the

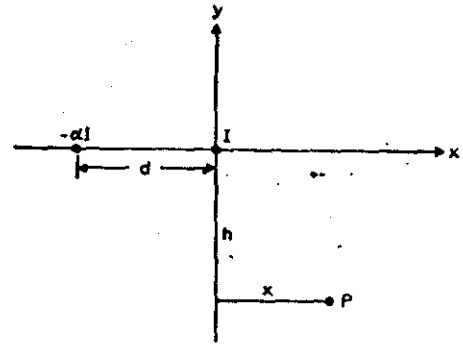

Fig. 1 *Cross-sectional view of situation*

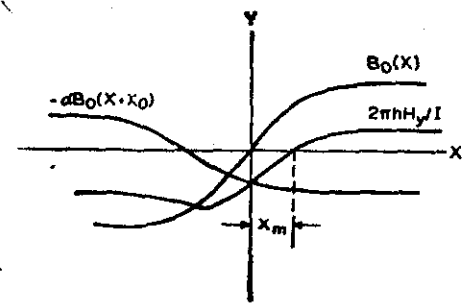

Fig. 2 *Illustrating superposition of 2-cable fields*

earthed endpoints of these cables are sufficiently far away, the fields in the vicinity may be imagined to emanate from infinite line sources.

The configuration is illustrated in Fig. 1, which is a cross-sectional view of the situation. As indicated, a current I amperes flows in one cable, while a current $-\alpha I$ amperes flows in the other cable. Here α is a factor which can be varied by the operator on the surface. The two cables are separated by a distance d, which is kept constant for a given test.

We now choose a rectangular co-ordinate system (x, y, z) so that the Earth's surface is the plane $y = 0$ and the first cable is coincident with the z axis. Then, the second cable is located at $x = -d$ and $y = 0$. The receiving location is a depth $y = -h$, but its location relative to the cable pair is not known; i.e. we wish to determine the x co-ordinate of the subsurface point P indicated in Fig. 1.

A relatively simple quantity to detect at the subsurface point P is the vertical component of the resultant magnetic field. If the frequency of the alternating current in the cables is sufficiently low, the fields at P can be estimated from static theory. As discussed elsewhere, this calls for operating frequencies of the order of 100 Hz or less, and limits the depths to less than several hundred metres for moderately conducting overburdens. For purposes of this discussion, we will employ the static theory, even though there is a more refined analysis available[1, 2].

Under the conditions stated, the vertical magnetic-field component H_y at P is given by a simple adaptation of the Biot–Savart law. Thus,

$$H_y = \frac{I}{2\pi h}\left\{\frac{X}{1+X^2} - \alpha\frac{X+X_0}{1+(X+X_0)^2}\right\} \quad . \quad . \quad (1)$$

where $X = x/h$ and $X_0 = d/h$. If the observer is equipped with a rudimentary horizontal loop (i.e. vertical axis) and voltage detector, he is able to note by a seismic hammer blow when the signal has a maximum or a minimum. For example, if α is varied in some systematic pattern by the surface operator (e.g. a saw-tooth scan of one minute), there will be a point in time when H_y vanishes. For a fixed and known value of X_0, one can then determine X from eqn. 1 by setting the term in braces equal to zero. In general, this leads to the cubic equation

$$X(1+(X+X_0)^2) = \alpha(1+X^2)(X+X_0) \quad . \quad . \quad . \quad (2)$$

which can be solved explicitly for the desired root X_m.

A graphical interpretation of the results is useful at this stage. To this end, we write eqn. 1 in the form

$$H_y = \{I/(2\pi h)\}\{B_0(X) - \alpha B_0(X+X_0)\} \quad . \quad . \quad . \quad (3)$$

where $B_0(X) = X(1+X^2)^{-1} = (X+X^{-1})^{-1}$. The normalised field of the current I in the main cable is $B_0(X)$ and the normalised field of the current $-\alpha I$ in the secondary cable is $-\alpha B_0(X+X_0)$. These functions are sketched in Fig. 2. As indicated, the sum of these is the resultant normalised field $2\pi h H_y/I$. The latter is obviously zero at some point $X = X_m$ where $X_m > 0$, provided that $0 < \alpha < 1$.

It is easy to see from eqn. 2 that, if both X and $X_0 \ll 1$, the solution for the root is particularly simple. Then

$$X_m = \alpha X_0/(1-\alpha) .$$

It is also evident that the resolving power of the scheme is only satisfactory when X_m and X_0 are not too large.

As mentioned above, the simple analysis given here is only valid when eddy currents induced in the overburden are negligible. At sufficiently low frequencies, this will always be the case. Of course, this imposes a difficulty with the receiving equipment, which needs to be more sensitive as the frequency is lowered. Actually, the principle of the detection scheme is still applicable when eddy currents are not negligible. It then becomes necessary to assume a half-space model of the earth and replace the field function $B_0(x)$ by its more general form $B(X, H)$. The latter is a complex function of both X and $H = \sqrt{2}\,h/\delta$ where δ is the electrical skin depth of the overburden. Tables of $B(X, H)$ are given elsewhere.[1] In principle, they can be used to devise a detection scheme for the general case of a conductive overburden.

The discussion has considered a 2-dimensional configuration involving parallel-line sources. In a single application of the technique, it is only possible to deduce the value of the x co-ordinate of the observer. The procedure, however, can be repeated for current line sources parallel to the x axis, in which case the z co-ordinate of the observer could be determined.

Other possibilities include the use of arrays of line sources

operating either at the same frequency or at multiple frequencies. The feasibility of such schemes should be investigated at the earliest opportunity.

J. R. WAIT

9th March 1971

Institute for Telecommunication Sciences
Office of Telecommunications
Boulder, Colo. 80302, USA

References

1 WAIT, J. R., and SPIES, K. P.: 'Sub-surface electromagnetic fields of a line source on a conducting half-space', *Radio Sci.*, 1971, 6
2 WAIT, J. R.: 'Electromagnetic waves in stratified media' (Pergamon, 1962), chap. 2

Electronic Letters, Vol. 9, No. 15,
26th July 1973

LOW-FREQUENCY IMPEDANCE OF A CIRCULAR LOOP OVER A CONDUCTING GROUND

Indexing terms: Antenna theory, loop antennas, Electrical impedance

Using a quasistatic approach, the input impedance of a circular wire loop is calculated for the case where the Earth is represented as a homogeneous conducting halfspace. It is shown that the input resistance is only proportional to the ground conductivity when the loop radius is small compared with the electrical skin depth.

In various technical applications, one is interested in transmitting useful power from a ground-based loop antenna. For example, in proposed mine-rescue techniques,[1] it is desired to communicate with a subsurface observer via a transmission path through the overburden. In a previous analytical study,[2] we considered the subsurface fields for an insulated circular loop of wire on or just above the Earth's surface. We did not, however, consider the power required to maintain the specified uniform current I in the wire loop. In this letter, we consider this problem.

As before, the frequency is assumed to be sufficiently low for the current round the loop to be uniform. Alternatively, the feed points are sufficiently numerous for an adequately uniform current to be maintained, even for higher frequencies. The quantity of interest here is the self impedance Z, which is defined by $Z = V/I$, where V is the total voltage integrated round the loop.

The geometry is indicated in Fig. 1, where the Earth is taken to be a homogeneous halfspace of conductivity σ for $z < 0$ with respect to a cylindrical-co-ordinate system (ρ, ϕ, z). The loop of radius a is located at $z = h_0$ in the vacuum region for $z > 0$. The single-turn wire making up the loop has a radius c, where $c \ll a$. The wire itself is assumed to be perfectly conducting.

For the model adopted, the electric field E_ϕ in the space $z > 0$ can be derived from $E_\phi = \partial F/\partial \rho$, where F is a scalar function of ρ and z. Under quasistatic conditions, the latter is given by[2]

$$F = \frac{i\mu_0 \omega a^2 I}{2} \int_0^\infty \frac{2J_1(\lambda a)}{\lambda a} J_0(\lambda \rho) \times [\exp(-\lambda|z-h_0|) + (\lambda-u)(\lambda+u)^{-1} \exp\{-\lambda(z+h_0)\}]d\lambda \quad . \quad . \quad . \quad (1)$$

where $u = (\lambda^2 + i\sigma\mu_0\omega)^{\frac{1}{2}}$. The time factor adopted is $\exp(i\omega t)$, and the angular frequency ω is assumed to be sufficiently low for all the displacement currents to be negligible. The magnetic permeability of the whole space is taken to be $\mu_0 (= 4\pi \times 10^{-7}$ H/m).

The self impedance Z is now calculated from

$$Z = \left[\frac{-2\pi a E_\phi}{I}\right]_{\substack{\rho=a \\ z=h_0+c}} \quad . \quad . \quad . \quad . \quad . \quad . \quad . \quad . \quad . \quad (2)$$

If we now write

$$Z = i\mu_0 \omega a (P + S) \quad . \quad . \quad . \quad . \quad . \quad . \quad . \quad . \quad . \quad (3)$$

it easily follows that

$$P = \pi \int_0^\infty (J_1(x))^2 \exp(-B_0 x)\, dx \quad . \quad . \quad . \quad . \quad (4)$$

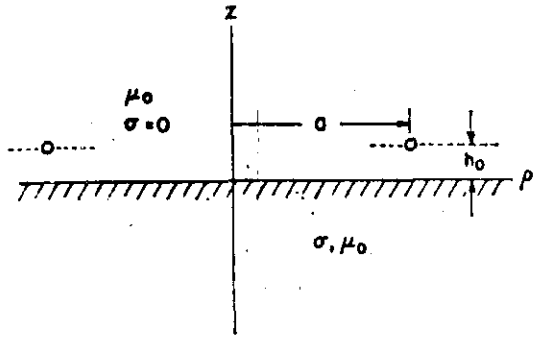

Fig. 1 *Side view of circular loop over the conducting halfspace model of the ground*

and

$$S = \pi \int_0^\infty (J_1(x))^2 \frac{x - (x^2 + i2A^2)^{\frac{1}{2}}}{x + (x^2 + i2A^2)^{\frac{1}{2}}} \exp(-Bx)\, dx \quad (5)$$

where

$$A = \frac{a}{\delta} = \frac{\text{loop radius}}{\text{skin depth}} \qquad \delta = \left(\frac{2}{\sigma\mu_0\omega}\right)^{\frac{1}{2}}$$

$$B_0 = \frac{c}{a} = \frac{\text{wire radius}}{\text{loop radius}}$$

and

$$B = \frac{2h_0 + c}{a} \simeq \frac{2h_0}{a} = \frac{2 \times \text{loop height}}{\text{loop radius}}$$

Here, of course, P is the (normalised) primary inductance of the loop, and can be expressed in terms of the complete elliptic integrals as follows:

$$P = \frac{2}{k_0}\left\{\left(1 - \frac{k_0^2}{2}\right) K(k_0) - E(k_0)\right\} \quad . \quad . \quad . \quad . \quad (6)$$

where $k_0 = 2(B_0^2 + 4)^{-\frac{1}{2}}$. Here, following standard notation,

$$K(k) = \int_0^{\pi/2} \frac{d\theta}{(1 - k^2 \sin^2\theta)^{\frac{1}{2}}}$$

and

$$E(k) = \int_0^{\pi/2} (1 - k^2 \sin^2\theta)^{\frac{1}{2}}\, d\theta$$

In the general case, it appears that the secondary influence characterised by S must be evaluated by numerical methods. For small values of A, we can write

$$S \simeq -if(B)A^2 \quad . \quad . \quad . \quad . \quad . \quad . \quad . \quad . \quad . \quad . \quad (7)$$

where

$$f(B) = \frac{\pi}{2} \int_0^\infty \frac{(J_1(x))^2}{x^2} \exp(-Bx)\, dx \quad . \quad . \quad . \quad (8)$$

If, in addition, $B \ll 1$, we can replace the exponential by $1 - Bx$ in eqn. 8, yielding standard integrals.[3] Then

$$f(B) \simeq \frac{2}{3} - \frac{\pi}{4} B \quad . \quad . \quad . \quad . \quad . \quad . \quad . \quad . \quad . \quad . \quad (9)$$

The other limiting case is when A is very large. To illustrate this case, we first note that

$$S = S_\infty + \Delta S \quad . \quad . \quad . \quad . \quad . \quad . \quad . \quad . \quad . \quad . \quad (10)$$

where

$$S_\infty = S|_{A=\infty} = -\frac{2}{k}\left\{\left(1 - \frac{k^2}{2}\right) K(k) - E(k)\right\} \quad (11)$$

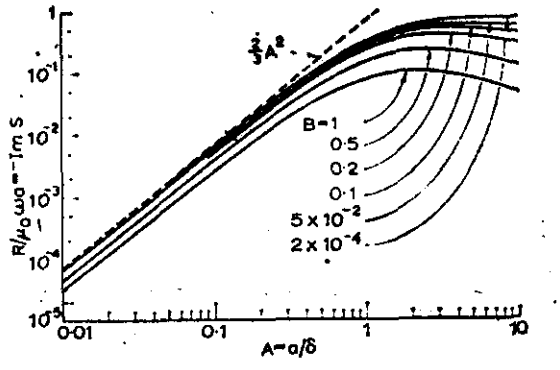

Fig. 2A *Normalised input resistance of the loop as a function of the loop radius for several elevations*

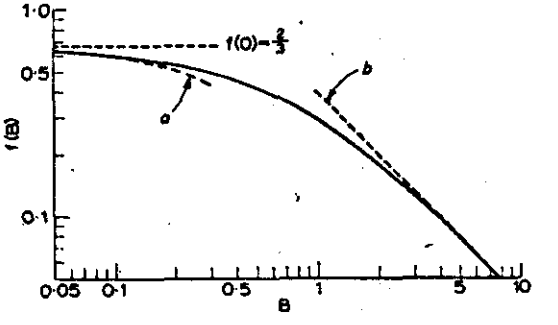

Fig. 2B *Function f(B) showing its limiting behaviour for small and large B values*
a Small-*B* approximation, $f(B) \simeq 2/3 - (\pi/4)B$
b Large-*B* approximation, $f(B) \simeq \pi/8B$

where $k = 2(B^2+4)^{-\frac{1}{2}}$, and

$$\Delta S = \pi \int_0^\infty \frac{2x}{x + (x^2 + i2A^2)^{\frac{1}{2}}} \{J_1(x)\}^2 \exp(-Bx)\, dx \quad (12)$$

If A is sufficiently large, we see that

$$\Delta S \simeq \left(\frac{2}{i}\right)^{\frac{1}{2}} \frac{\pi}{A} \int x \exp(-Bx)\{J_1(x)\}^2\, dx \quad . \quad . \quad (13)$$

is the leading term in an expansion in inverse powers of A. This integral has been given by Luke;[4] thus

$$\Delta S \simeq \left(\frac{2}{i}\right)^{\frac{1}{2}} \frac{Bk}{2A(1-k^2)} \times \left\{\left(1 - \frac{k^2}{2}\right) E(k) - (1-k^2) K(k)\right\}$$

It appears this is only a valid correction if the product AB is very large compared with 1.

Numerical values of P from eqn. 6 were obtained for several values of B_0 as follows:

$B_0 = 10^{-6}$; $P = 13{\cdot}89$

$B_0 = 10^{-5}$; $P = 11{\cdot}59$

$B_0 = 10^{-4}$; $P = 9{\cdot}29$

The corresponding values of the inductance L of the loop in free space are then $L = \mu_0 aP$ henrys.

Using numerical integration, the complex quantity S was evaluated* from eqn. 5 for various values of B and A. Of particular interest is the resistive component $R = \mathrm{Re}\,Z = \mu_0 \omega a(-\mathrm{Im}\,S)$ ohms. The normalised quantity $R/\mu_0 \omega a$ is plotted in Fig. 2A as a function of A for various values of B. As indicated, R varies linearly with A^2 for A less than about 0·2. In this range, for the B values indicated, the approximation $S \simeq -iF(B)A^2$ is applicable. To aid the user, a plot of the function $F(B)$ is shown in Fig. 2B, along with the limiting asymptotes.

The limiting value of R for a/δ tending towards infinity is rather interesting. If B is sufficiently small, we see that the ordinate in Fig. 2A approaches $\pi/4$. This is entirely consistent with the concept that the resistance of the loop is equivalent to $2\pi a \times (\mu_0 \omega/8)$ ohms. The factor $\mu_0 \omega/8$ is identical to the resistance per unit length of an infinitely long current-carrying wire lying on or just above the surface of a conducting halfspace.[6]

The present result can be used in estimating the total power requirements for a downlink communication system. For example, if we choose $a = 0{\cdot}5$ km, $f = 100$ Hz and $\sigma = 10^{-2}$ S/m, we see from Fig. 2A that $-\mathrm{Im}\,S \simeq 0{\cdot}25$ and that the corresponding value of the resistance R is $0{\cdot}10\,\Omega$. This is comparable to the ohmic resistance of the loop itself if, for example, we selected a single-turn copper wire with a radius of the order of 1·4 cm.

J. R. WAIT
K. P. SPIES

Institute for Telecommunication Sciences
Office of Telecommunications
US Department of Commerce
Boulder, Colo. 80302, USA

3rd July 1973

* Numerical tables available on request from the authors

References

1 LARGE, D. B., BALL, L., and FARSTAD, A. J.: 'Radio transmission to and from underground coal mines—theory and measurement', *IEEE Trans.*, 1973, COM-21, pp. 194–202
2 WAIT, J. R., and SPIES, K. P.: 'Subsurface electromagnetic fields of a circular loop of current located above ground', *ibid.*, 1972, AP-20, pp. 520–522
3 WHEELON, A. D.: 'Tables of summable series and integrals involving Bessel functions' (Holden-Day, 1968) (e.g. see formulas 11.308 and 11.204)
4 LUKE, Y. L.: 'Integrals of Bessel functions', (McGraw-Hill, 1962), p. 316, no. 20
5 WAIT, J. R.: 'On the impedance of a long wire suspended over the ground', *Proc. Inst. Radio Eng.*, 1961, 49, p. 1429. (Note that the 3 in the denominator of the second term in the two equations for ΔR should be 3π)

Canadian Journal of Physics, Vol. 51, No. 14,
1534-1540, 1973

Subsurface Electromagnetic Fields of a Grounded Cable of Finite Length[1]

DAVID A. HILL AND JAMES R. WAIT

Institute for Telecommunication Sciences, Office of Telecommunications, U.S. Department of Commerce and Cooperative Institute for Research in Environmental Sciences, University of Colorado, Boulder, Colorado 80302

Received March 15, 1973

The subsurface fields of a finite line source or current-carrying cable are examined. Some special cases, such as the low-frequency limit, are treated analytically, and some simple working formulas are obtained. The general field expressions are reduced to single integrals with finite limits that are evaluated numerically. It is shown that if the source cable is sufficiently long, the fields are approximated by those for an infinite cable. The results have possible application to downlink communication and radio location of trapped miners.

On étudie les champs produits sous la surface du sol par une source constituée par une portion rectiligne finie d'un câble transportant du courant. Certains cas spéciaux, par exemple, la limite aux basses fréquences, sont traités analytiquement, et quelques formules directement applicables sont obtenues. Les expressions générales des composantes de champ sont réduites à des intégrales simples avec des limites finies, et ces intégrales sont évaluées numériquement. On montre que si le câble source est suffisamment long, les champs sont approximativement les mêmes que ceux d'un câble infini. Les résultats ont des applications pour les communications souterraines et la localisation par radio de mineurs emprisonnés.

[Traduit par le journal]

Can. J. Phys., 51, 1534 (1973)

Introduction

The subsurface fields of an infinite line source on a conducting half-space have been examined by Wait and Spies (1971). In any real communication link from the surface to an underground terminal, the line source or current-carrying cable is of finite length. Here, we examine the subsurface fields of a finite line source with the purpose of determining what cable length is sufficient, and when the infinite line source is a good approximation. The earth is taken to be a homogeneous conducting half-space, and the current in the cable is assumed to be constant. The latter assumption is well justified at audio frequencies when an insulated cable is terminated by grounded electrodes that are separated by distances small compared with a free-space wavelength (Wait 1952; Sunde 1968).

Formulation

The geometry of the line source of length $2l$ located on the half-space, and the observer in the half-space, are as shown in Fig. 1. The observer is located at (x, y, z), and the x-directed source current I runs from $-l$ to l on the x axis. The current varies as $\exp(i\omega t)$, and the angular frequency ω is sufficiently low that all displacement currents are negligible. The Hertz vector contains both x and z components (Π_x and Π_z) and the contribution from an incremental source of length dx' located at x' is given by Wait (1961) and Banos (1966):

$$d\Pi_x = \frac{I\,dx'}{2\pi\sigma}\int_0^\infty \frac{e^{uz}}{u+\lambda} J_0(\lambda\rho)\lambda\,d\lambda$$

$$d\Pi_z = \frac{I\,dx'}{2\pi\sigma}\frac{\partial}{\partial x}\int_0^\infty \frac{e^{uz}}{u+\lambda} J_0(\lambda\rho)\,d\lambda \qquad [1]$$

where

$$u = (\lambda^2 + \gamma^2)^{1/2}, \quad \gamma^2 = i\omega\mu_0\sigma,$$

$$\rho = [y^2 + (x - x')^2]^{1/2}$$

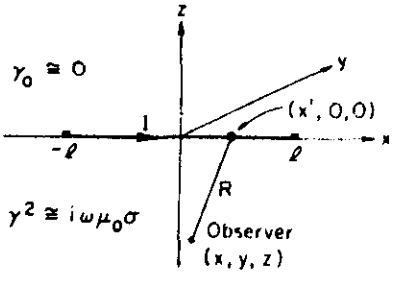

FIG. 1. Finite line source on a homogeneous half-space.

[1]The research reported here was supported by the U.S. Bureau of Mines, Pittsburgh Mining and Safety Research Center.

μ_0 is the permeability of free space, and σ is the conductivity of the half-space. Here, and in what follows, we restrict the observer to the subsurface region $z < 0$.

Since a numerical integration on x' will be required, it is desirable to eliminate the λ integration. For this quasi-static situation, Wait (1961) has shown that the λ integration can be performed to yield the result

$$d\Pi_x = \frac{I\,dx'}{2\pi\sigma\gamma^2}\left(\frac{\partial^2 P}{\partial z^2} - \frac{\partial^3 N}{\partial z^3} + \gamma^2\frac{\partial N}{\partial z}\right)$$

[2]
$$d\Pi_z = \frac{I\,dx'}{2\pi\sigma\gamma^2}\left(\frac{\partial^3 N}{\partial x\partial z^2} - \frac{\partial^2 P}{\partial x\partial z}\right)$$

where $N = I_0[(\gamma/2)(R + z)]K_0[(\gamma/2)(R - z)]$, $P = R^{-1}\exp(-\gamma R)$, $R = (\rho^2 + z^2)^{1/2}$, and I_0 and K_0 are modified Bessel functions of order zero. The magnetic field components are derived from the curl of the Hertz vector

[3] $$d\boldsymbol{H} = \sigma\,\text{curl}\,d\boldsymbol{\Pi}$$

By carrying out the curl operation in [3], and utilizing the fact that N satisfies the wave equation, $(\nabla^2 - \gamma^2)N = 0$, the magnetic field components are obtained:

$$dH_x = \frac{I\,dx'}{2\pi\gamma^2}\left(\frac{\partial^4 N}{\partial x\partial y\partial z^2} - \frac{\partial^3 P}{\partial x\partial y\partial z}\right)$$

[4]
$$dH_y = \frac{I\,dx'}{2\pi\gamma^2}\left(\frac{\partial^3 P}{\partial z^3} + \frac{\partial^3 P}{\partial x^2\partial z} + \frac{\partial^4 N}{\partial z^2\partial y^2}\right)$$

$$dH_z = \frac{I\,dx'}{2\pi\gamma^2}\left(\frac{\partial^4 N}{\partial y\partial z^3} - \gamma^2\frac{\partial^2 N}{\partial y\partial z} - \frac{\partial^3 P}{\partial y\partial z^2}\right)$$

The electric field components have been given by Wait (1961):

$$dE_x = \frac{-I\,dx'}{2\pi\sigma}\left(\frac{\partial^2 P}{\partial z^2} + \frac{\partial^3 N}{\partial y^2\partial z}\right)$$

[5]
$$dE_y = \frac{I\,dx'}{2\pi\sigma}\frac{\partial^3 N}{\partial y\partial x\partial z}$$

$$dE_z = \frac{I\,dx'}{2\pi\sigma}\frac{\partial^2 P}{\partial x\partial z}$$

To obtain the resultant fields for the finite-length cable, we integrate [4] and [5] over the range of x' from $-l$ to l.

The components of interest here are H_y, H_z, and E_x, since all other components vanish in the vertical plane $x = 0$. Also, these are the only nonzero components everywhere if the line source is of infinite length. For normalization purposes, it is useful to write the fields in the manner

$$H_y = \frac{I}{2\pi h}A(H, Y, X, L)$$

[6]
$$H_z = \frac{I}{2\pi h}B(H, Y, X, L)$$

$$E_x = \frac{-i\omega\mu_0 I}{2\pi}F(H, Y, X, L)$$

where $H = (\omega\mu_0\sigma)^{1/2}h$, $Y = y/h$, $X = x/h$, and $L = l/h$ and $h(= -z)$ is the observer depth. Note that A, B, and F are dimensionless. For the case of the infinite line source ($L = \infty$), these quantities have been tabulated (Wait and Spies 1971). By comparing [4] and [5] with [6], the following integral forms are found for A, B, and F:

$$A(H, Y, X, L) = \frac{h}{\gamma^2}\int_{-l}^{l}\left(\frac{\partial^3 P}{\partial z^3} + \frac{\partial^3 P}{\partial x^2\partial z} + \frac{\partial^4 N}{\partial z^2\partial y^2}\right)dx'$$

[7]
$$B(H, Y, X, L) = \frac{h}{\gamma^2}\int_{-l}^{l}\left(\frac{\partial^4 N}{\partial y\partial z^3} - \gamma^2\frac{\partial^2 N}{\partial y\partial z} - \frac{\partial^3 P}{\partial y\partial z^2}\right)dx$$

$$F(H, Y, X, L) = \frac{1}{\gamma^2}\int_{-l}^{l}\left(\frac{\partial^2 P}{\partial z^2} + \frac{\partial^3 N}{\partial y^2\partial z}\right)dx'$$

The specific expressions for the partial derivatives of P and N in [7] are given in the Appendix.

Low-Frequency Limit

The low-frequency limit is useful both as a check on the numerical work and as a simple means of determining trends at low frequencies. If the frequency approaches zero, then γ approaches zero and the Hertz components are given by

$$d\Pi_x = \frac{I\,dx'}{4\pi\sigma}\int_0^\infty e^{\lambda z}J_0(\lambda\rho)\,d\lambda = \frac{I\,dx'}{4\pi\sigma}\frac{1}{R}$$

[8]
$$d\Pi_z = \frac{-I\,dx'}{4\pi\sigma}\frac{(x - x')}{\rho}\int_0^\infty e^{\lambda z}J_1(\lambda\rho)\,d\lambda$$

$$= \frac{-I\,dx'}{4\pi\sigma}\frac{(x - x')}{\rho^2}(1 + z/R)$$

where we make use of the integrals listed by Wheelon (1968). It is important to note that $d\Pi_z$ does not vanish in this limit. This is consistent with the notion that the electric fields can be derived from a scalar potential Φ that is given by

$$\Phi = -\left(\frac{\partial \Pi_x}{\partial x} + \frac{\partial \Pi_z}{\partial z}\right) = \frac{-I\,dx'}{2\pi\sigma}\frac{\partial}{\partial x}\left(\frac{1}{R}\right)$$

for the static limit.

The magnetic field components are obtained from the curl operation in [3]. Thus

$$dH_z = \frac{I\,dx'}{4\pi}\frac{y}{R^3}$$

$$dH_y = \frac{I\,dx'}{4\pi}\left\{\frac{-z}{R^3} + \frac{\partial}{\partial x}\left[\frac{x-x'}{\rho^2}\left(1+\frac{z}{R}\right)\right]\right\} \quad [9]$$

There is also an x component which is not of interest here. The quantities in [9] can be integrated from $x' = -l$ to $x' = +l$ to obtain the total fields

$$H_y = \frac{I}{4\pi}\left\{\frac{-z}{y^2+z^2}\left[\frac{l-x}{[(l-x)^2+y^2+z^2]^{1/2}} + \frac{l+x}{[(l+x)^2+y^2+z^2]^{1/2}}\right] + \frac{l-x}{(l-x)^2+y^2}\left[1+\frac{z}{[(l-x)^2+y^2+z^2]^{1/2}}\right] + \frac{l+x}{(l+x)^2+y^2}\left[1+\frac{z}{[(l+x)^2+y^2+z^2]^{1/2}}\right]\right\}$$

$$H_z = \frac{I}{4\pi}\frac{y}{y^2+z^2}\left[\frac{l-x}{[(l-x)^2+y^2+z^2]^{1/2}} + \frac{l+x}{[(l+x)^2+y^2+z^2]^{1/2}}\right] \quad [10]$$

From [10], the normalized quantities A and B, as defined in [6], are found to be

$$A(0, Y, X, L) = \frac{-1}{2(1+Y^2)}\left[\frac{L-X}{[(L-X)^2+1+Y^2]^{1/2}} + \frac{L+X}{[(L+X)^2+1+Y^2]^{1/2}}\right] + \frac{(L-X)/2}{(L-X)^2+Y^2}\left[1-\frac{1}{[(L-X)^2+1+Y^2]^{1/2}}\right] + \frac{(L+X)/2}{(L+X)^2+Y^2}\left[1-\frac{1}{[(L+X)^2+1+Y^2]^{1/2}}\right]$$

$$B(0, Y, X, L) = \frac{Y/2}{1+Y^2}\left[\frac{L-X}{[(L-X)^2+1+Y^2]^{1/2}} + \frac{L+X}{[(L+X)^2+1+Y^2]^{1/2}}\right] \quad [11]$$

As L approaches ∞, the following results are obtained:

$$A(0, Y, X, \infty) = \frac{1}{1+Y^2}, \quad B(0, Y, X, \infty) = \frac{Y}{1+Y^2} \quad [12]$$

The results are of course independent of X and agree with infinite line source results (Wait and Spies 1971).

Results for finite L are shown in Figs. 2 and 3 for $X = 0$. Note that A in Fig. 2 overshoots its final value and that $L = 1$ is sufficient to obtain a horizontal magnetic field equal to that of the infinite line source. However, the B values in Fig. 3 approach their final values quite slowly, particularly for larger Y. Consequently, a fairly large value of L is required to obtain a vertical magnetic field nearly equal to that of the infinite line source.

High-Frequency Limit

The other useful limiting case is for high frequencies where $|\gamma y|$ is large. In this case, terms involving P are negligible, and N is asymptotically given by (Wait 1961)

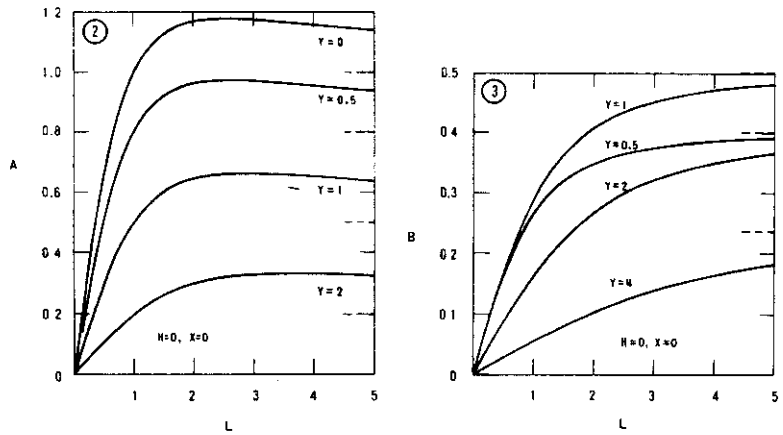

FIG. 2. Low-frequency limit of the horizontal magnetic field as a function of Y and L. Final values are dashed.
FIG. 3. Low-frequency limit of the vertical magnetic field as a function of Y and L. Final values are dashed.

[13] $$N \sim \frac{e^{\gamma z}}{\gamma \rho} \quad \text{for} \quad z \leqslant 0$$

Consequently, dE_x and dH_y are given by

[14] $$dE_x \sim -\frac{I\,dx'}{2\pi\sigma} e^{\gamma z} \frac{\partial^2}{\partial y^2}\left(\frac{1}{\rho}\right) \quad \text{and} \quad dH_y \sim -\frac{I\,dx'}{2\pi\gamma} e^{\gamma z} \frac{\partial^2}{\partial y^2}\left(\frac{1}{\rho}\right)$$

In order to determine dH_z, we must include higher-order terms in N. If this is done, the result is

[15] $$dH_z \sim -\frac{I\,dx'}{2\pi\gamma^2} e^{\gamma z} \frac{\partial}{\partial y}\left(\frac{1}{\rho^3}\right)$$

The x' integrations can be done in [14] and [15] to yield the total fields:

$$E_x \sim -\frac{I}{2\pi\sigma} e^{\gamma z} \frac{\partial^2}{\partial y^2} \{\ln [l - x + [(l - x)^2 + y^2]^{1/2}] - \ln [-(l + x) + [(l + x)^2 + y^2]^{1/2}]\}$$

[16] $$H_y \sim -\frac{I}{2\pi y} e^{\gamma z} \frac{\partial^2}{\partial y^2} \{\ln [l - x + [(l - x)^2 + y^2]^{1/2}] - \ln [-(l + x) + [(l + x)^2 + y^2]^{1/2}]\}$$

$$H_z \sim -\frac{I}{2\pi\gamma^2} e^{\gamma z} \frac{\partial}{\partial y}\left\{\frac{1}{y^2}\left[\frac{l - x}{[(l - x)^2 + y^2]^{1/2}} + \frac{l + x}{[(l + x)^2 + y^2]^{1/2}}\right]\right\}$$

If l approaches ∞, then [16] reduces to

[17] $$E_x|_{l=\infty} \sim \frac{-I}{\pi\sigma} \frac{e^{\gamma z}}{y^2}, \quad H_y|_{l=\infty} \sim \frac{I}{\pi\gamma} \frac{e^{\gamma z}}{y^2}, \quad H_z|_{l=\infty} \sim \frac{2I}{\pi\gamma^2} \frac{e^{\gamma z}}{y^3}$$

Thus, the normalized quantities A, B, and F are given by

$$A(H, Y, X, \infty) \sim \frac{2}{i^{1/2} H Y^2} \exp(-i^{1/2} H)$$

[18] $$B(H, Y, X, \infty) \sim \frac{4}{iH^2 Y^3} \exp(-i^{1/2} H)$$

$$F(H, Y, X, \infty) \sim \frac{2}{iH^2 Y^2} \exp(-i^{1/2} H)$$

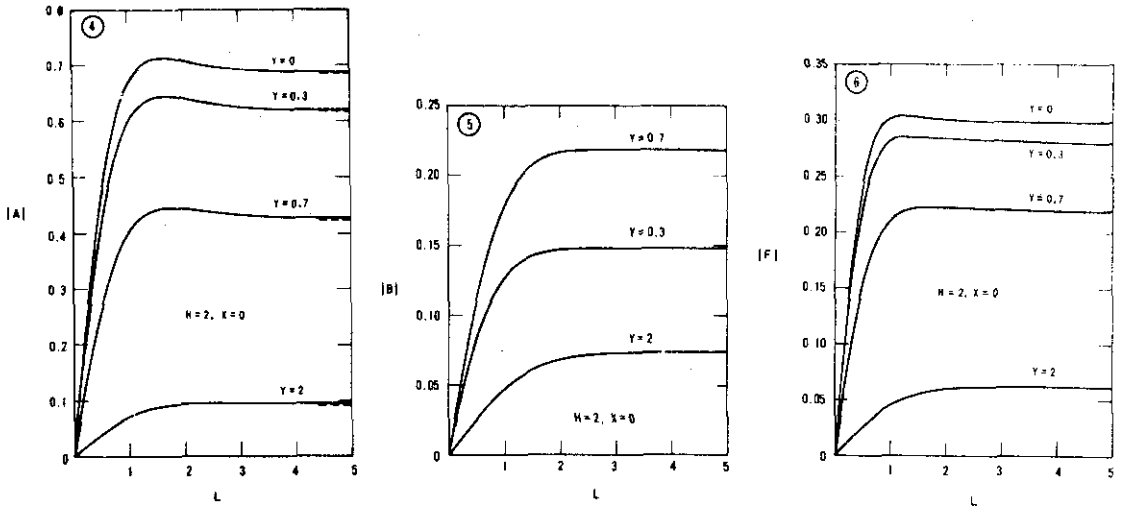

FIG. 4. Magnitude of the horizontal magnetic field as a function of Y and L.
FIG. 5. Magnitude of the vertical magnetic field as a function of Y and L.
FIG. 6. Magnitude of the horizontal electric field as a function of Y and L.

These results agree with those of the infinite line source (Wait and Spies 1971).

We stress that the "high-frequency" limit solutions discussed in this section are applicable when the horizontal distance, ρ, is much *greater* than a skin depth in the earth, and much *less* then the free-space wavelength. Thus, the formulas are of limited applicability, although they are useful for checking the results of the numerical integration.

General Numerical Results

For general values of H, a numerical integration over finite limits of the expressions in [7] is required. Even though the integrands are quite complicated, they are well behaved numerically. Consequently, the computer program for A, B, and F is quite fast, and the influence of the various parameters can be studied easily. Here, we illustrate some of the important features in graphical form.

Results for $H = 2$ and $X = 0$ are shown in Figs. 4, 5, and 6. For large L, all quantities approach those of the infinite line source (Wait and Spies 1971) which is reassuring. Although A, B, and F are now complex, only the magnitudes are plotted since the phases are relatively constant with L.

We note that $|A|$ in Fig. 4 still has a slight overshoot before settling down to its final value for large L. A similar trend for $|F|$ is shown in Fig. 6. In both cases, L greater than about 1 is sufficient to yield field strengths nearly equal to that of the infinite line source. However, a larger value of L would be required to reach a nearly maximum value of $|B|$ as shown in Fig. 5. Consequently, if the vertical magnetic field is important, a value for L in the neighborhood of 2 might be more appropriate, if we wish to simulate an infinitely long cable. This could be a crucial factor in designing a subsurface location scheme that makes use of the well-defined structure of the magnetic fields produced by an infinite line source.

Concluding Remarks

Analytical expressions for the subsurface fields of a finite line source have been derived for high-frequency and low-frequency limits. For the general case, a single numerical integration along the source is required. Although a constant current distribution has been assumed, an arbitrary distribution would present no problem since the source integration is done numerically. Also, multiple grounding of the source cable and arrays of such cables could be treated by simple extensions of the present formulation.

Results for low and medium frequencies indicate that the finite line source fields approach those of an infinite line source quite quickly. For instance, $L \simeq 1$ appears to be sufficient for the horizontal electric and magnetic fields, and $L \simeq 2$ is sufficient for the vertical magnetic field.

It is important to realize that the finite line source excites currents in the earth by induction and by conduction. The effect of the latter vanishes in the limit of an infinitely long cable when the magnetic field is measured at the subsurface point. The results shown in Figs. 2–6 for finite L implicitly account for the effect of the conduction currents injected at the electrodes.

In a sequel to this work, we plan to consider the fields produced by a finite source cable located within a coal mine.

Appendix

There are four terms in derivatives of P which are required in [7]. The differentiation is straightforward, and the resultant forms are

$$\frac{\partial^2 P}{\partial z^2} = \frac{e^{-\gamma R}}{R^2}\left[\frac{1}{R}\left(-1+\frac{3z^2}{R^2}\right)+\gamma\left(-1+\frac{3z^2}{R^2}\right)+\frac{\gamma^2 z^2}{R}\right]$$

$$\frac{\partial^3 P}{\partial z^3} = \frac{z\, e^{-\gamma R}}{R^3}\left[\frac{3}{R^2}\left(3-\frac{5z^2}{R^2}\right)+\frac{3\gamma}{R}\left(3-\frac{5z^2}{R^2}\right)+3\gamma^2\left(1-\frac{2z^2}{R^2}\right)-\frac{\gamma^3 z^2}{R}\right]$$

[19]
$$\frac{\partial^3 P}{\partial y \partial z^2} = \frac{y\, e^{-\gamma R}}{R^3}\left[\frac{3}{R^2}\left(1-\frac{5z^2}{R^2}\right)+\frac{3\gamma}{R}\left(1-\frac{5z^2}{R^2}\right)+\gamma^2\left(1-\frac{6z^2}{R^2}\right)-\frac{\gamma^3 z^2}{R}\right]$$

$$\frac{\partial^3 P}{\partial x^2 \partial z} = \frac{z\, e^{-\gamma R}}{R^3}\left\{\frac{3}{R^2}\left[1-\frac{5(x-x')^2}{R^2}\right]+\frac{3\gamma}{R}\left[1-\frac{5(x-x')^2}{R^2}\right]+\gamma^2\left[1-\frac{6(x-x')^2}{R^2}\right]-\frac{\gamma^3(x-x')^2}{R}\right\}$$

The four terms in derivatives of N can be simplified by replacing the derivatives of the modified Bessel functions by Bessel functions of zero and first order. This procedure, used previously by Wait and Campbell (1953*a*, *b*), yields the following expressions which are quite suitable for numerical evaluation.

[20]
$$\frac{\partial^2 N}{\partial y \partial z} = \frac{\gamma y}{2}[A_{00} I_0 K_0 + A_{11} I_1 K_1 + A_{01} I_0 K_1 + A_{10} I_1 K_0]$$

where

$$A_{00} = \frac{\gamma z}{R^2}, \quad A_{11} = -\frac{\gamma z}{R^2}, \quad A_{01} = \frac{1}{R^2}\left(-1+\frac{z}{R}\right), \quad A_{10} = -\frac{1}{R^2}\left(1+\frac{z}{R}\right)$$

$$\frac{\partial^3 N}{\partial y^2 \partial z} = \frac{\gamma}{2}[B_{00} I_0 K_0 + B_{11} I_1 K_1 + B_{01} I_0 K_1 + B_{10} I_1 K_0]$$

where

$$B_{00} = \frac{\gamma z}{R}\left(1-\frac{3y^2}{R^2}\right), \quad B_{11} = \frac{\gamma z}{R^2}\left(-1+\frac{3y^2}{R^2}+\frac{2y^2}{\rho^2}\right)$$

$$B_{01} = \frac{1}{R^2}\left[-1+\frac{z(1-\gamma^2 y^2)}{R}+\frac{3y^2}{R^2}-\frac{3y^2 z}{R^3}\right], \quad B_{10} = \frac{1}{R^2}\left[-1-\frac{z(1-\gamma^2 y^2)}{R}-\frac{3y^2}{R^2}+\frac{3y^2 z}{R^3}\right]$$

$$\frac{\partial^4 N}{\partial y^2 \partial z^2} = \frac{\gamma}{2}[C_{00} I_0 K_0 + C_{11} I_1 K_1 + C_{01} I_0 K_1 + C_{10} I_1 K_0]$$

where

$$C_{00} = \frac{\gamma z^2}{R^4}\left[-3+\gamma^2 y^2+\frac{15y^2}{R^2}\right]$$

$$C_{11} = \frac{\gamma}{R^2}\left[-2+\frac{z^2(3-\gamma^2 y^2)}{R^2}+\frac{6y^2}{R^2}-\frac{15y^2 z^2}{R^4}+\frac{2y^2(R^2-2z^2)}{\rho^2 R^2}\right]$$

$$C_{01} = \frac{1}{R^3}\left[\frac{z(3-\gamma^2\gamma^2)}{R} - \gamma^2(y^2+z^2) - \frac{3z^2(1-2\gamma^2y^2)}{R^2} - \frac{15zy^2}{R^3} + \frac{15y^2z^2}{R^4} + \frac{\gamma^2y^2z(R+z)}{\rho^2}\right]$$

$$C_{10} = \frac{1}{R^3}\left[\frac{z(3-\gamma^2y^2)}{R} + \gamma^2(y^2+z^2) + \frac{3z^2(1-2\gamma^2y^2)}{R^2} - \frac{15zy^2}{R^3} - \frac{15y^2z^2}{R^4} + \frac{\gamma^2y^2z(R-z)}{\rho^2}\right]$$

$$\frac{\partial^4 N}{\partial y \partial z^3} = \frac{\gamma y}{2}\left[D_{00}I_0K_0 + D_{11}I_1K_1 + D_{01}I_0K_1 + D_{10}I_1K_0\right]$$

where

$$D_{00} = \frac{\gamma z}{R^4}\left(-3 + \frac{15z^2}{R^2} + \gamma^2z^2\right), \quad D_{11} = \frac{\gamma z}{R^4}\left(13 - \frac{15z^2}{R^2} - \gamma^2z^2\right)$$

$$D_{01} = \frac{1}{R^2}\left(\frac{3}{R^2} - \frac{3z}{R^3} - \frac{15z^2}{R^4} + \frac{15z^3}{R^5} - \gamma^2 - \frac{3\gamma^2z}{R} - \frac{\gamma^2z^2}{R^2} + \frac{6\gamma^2z^3}{R^3}\right)$$

$$D_{10} = \frac{1}{R^2}\left(\frac{3}{R^2} + \frac{3z}{R^3} - \frac{15z^2}{R^4} - \frac{15z^3}{R^5} - \gamma^2 + \frac{3\gamma^2z}{R} - \frac{\gamma^2z^2}{R^2} - \frac{6\gamma^2z^3}{R^3}\right)$$

The argument of I_0 and I_1 is $(\gamma/2)(R+z)$, and the argument of K_0 and K_1 is $(\gamma/2)(R-z)$.

Acknowledgments

We wish to thank Dr. R. G. Geyer, of the Colorado School of Mines, for his suggestions, and Mrs. Loys A. Gappa for her assistance in preparing the manuscript.

BANOS, A. 1966. Dipole radiation in the presence of a conducting half-space (Pergamon Press, New York).

SUNDE, E. D. 1968. Earth conduction effects in transmission systems (Dover Publications, New York), Chap. V, pp. 140–172.

WAIT, J. R. 1952. Can. J. Phys. **30**, 512.

——— 1961. Can. J. Phys. **39**, 1017.

WAIT, J. R. and CAMPBELL, L. L. 1953*a*. J. Geophys. Res. **58**, 21.

——— 1953*b*. J. Geophys. Res. **58**, 167.

WAIT, J. R. and SPIES, K. P. 1971. Radio Sci. **6**, 781.

WHEELON, A. D. 1968. Tables of summable series and integrals involving Bessel functions (Holden-Day, San Francisco), p. 72.

Pure and Applied Geophysics, Vol. 111,
2324-2332, (1973/X)

Subsurface Electric Fields of a Grounded Cable of Finite Length for both Frequency and Time Domain

By DAVID A. HILL[1]) and JAMES R. WAIT[2])

Summary – The subsurface electric fields of a current-carrying cable are examined for both steady-state and transient situations. Closed form expressions are obtained for two of the electric field components, and a numerical integration is used to obtain the third component. Waveforms for a step-function current excitation are displayed. The results have possible application to pulsed downlink communication in mine rescue operations.

1. Introduction

The time harmonic subsurface fields of a finite length line source or current-carrying cable on a conducting half-space have been examined by HILL and WAIT [1]. The emphasis was on examining the effects of finite cable length on the subsurface magnetic fields. Here we consider the electric field; also we extend the analysis to the time domain by treating a step-function current. The nature of the build-up of the subsurface electric field is of importance. This rise time dictates what pulse width and pulse repetition frequency can be used in a downlink communication system.

The half-space is taken to be homogeneous, and the current in the cable is assumed to be uniform. This is justified for an insulated cable with grounded ends for sufficiently low frequencies [4, 3, 8]. Actually, related problems of the transient subsurface fields of an infinitesimal horizontal dipole and transient coupling between surface cables have been treated by Wait [5]. The techniques employed here are similar.

2. Frequency domain solution

The line source extends from $-l$ to l on the x-axis, and the observer in the half-space ($z < 0$) is located at (x,y,z) as shown in Fig. 1. The x-directed current is $I\exp(i\omega t)$, and the angular frequency ω is sufficiently low that displacement currents are negligible

[1]) Institute for Telecommunication Sciences, Office of Telecommunications, U.S. Department of Commerce, Boulder, Colorado 80302.

[2]) Cooperative Institute for Research in Environmental Sciences, University of Colorado.

everywhere. Under these conditions, the electric field components from an incremental source of length dx' located at $(x',0,0)$ are given by [6]

$$dE_x = \frac{-I\,dx'}{2\pi\sigma}\left(\frac{\partial^2 P}{\partial z^2} + \frac{\partial^3 N}{\partial y^2\,\partial z}\right),$$

$$dE_y = \frac{I\,dx'}{2\pi\sigma}\frac{\partial^3 N}{\partial y\,\partial x\,\partial z},$$

$$dE_z = \frac{I\,dx'}{2\pi\sigma}\frac{\partial^2 P}{\partial x\,\partial z}, \tag{1}$$

where

$$P = r^{-1}\exp(-\gamma r),$$
$$N = I_0[(\gamma/2)(r+z)]\,K_0[(\gamma/2)(r-z)],$$
$$r = [(x-x')^2 + y^2 + z^2]^{1/2},$$
$$\gamma = (i\omega\mu_0\sigma)^{1/2},$$

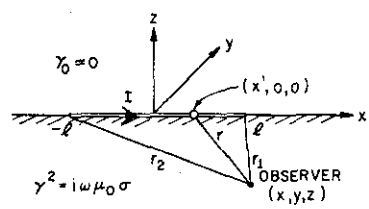

Figure 1
Finite line source on a homogeneous half-space with a subsurface observation point

σ is the conductivity of the half-space, μ_0 is the permeability of free space, and I_0 and K_0 are zero-order modified Bessel functions. To obtain the fields of the cable, we integrate (1) on x' from $-l$ to l.

Since dE_y and dE_z contain $\partial/\partial x\,(=-\partial/\partial x')$, the integration can be performed easily to yield

$$E_y = \frac{-I}{2\pi\sigma}\frac{\partial^2}{\partial y\,\partial z}(N_1 - N_2),$$

$$E_z = \frac{-I}{2\pi\sigma}\frac{\partial}{\partial z}(P_1 - P_2), \tag{2}$$

where

$$N_{\frac{1}{2}} = N|_{r=r_{\frac{1}{2}}},$$
$$P_{\frac{1}{2}} = P|_{r=r_{\frac{1}{2}}},$$

and

$$r_{\frac{1}{2}} = [(x \mp l)^2 + y^2 + z^2]^{1/2}.$$

After carrying out the differentiation, E_z can be written in the following convenient form

$$E_z = -[I/(2\pi\sigma h^2)]\, E_{zn}(W, L, X, Y), \tag{3}$$

where

$$E_{zn} = R_1^{-3} \exp[-(iW)^{1/2} R_1][1 + (iW)^{1/2} R_1] - R_2^{-3} \exp[-(iW)^{1/2} R_2][1 + (iW)^{1/2} R_2],$$

$$W = \omega\mu_0 \sigma h^2, \qquad L = l/h, \qquad X = x/h, \qquad Y = y/h,$$

$$R_{\frac{1}{2}} = r_{\frac{1}{2}}/h = [(X \mp L)^2 + Y^2 + 1]^{1/2},$$

and h ($= -z$) is the observer depth. Note that E_{zn}, W, L, X, and Y are all dimensionless and that W can be considered a normalized frequency since it is proportional to ω. The dependence of $|E_{zn}|$ on W is illustrated in Fig. 2 for $L = 1$ and various values of X and Y. In a typical example with $\sigma = 10^{-2}$ mhos/m and $h = 100$ m, the frequency f is given by

$$f = W/(2\pi\sigma\mu_0 h^2) = 1266W \text{ Hz}. \tag{4}$$

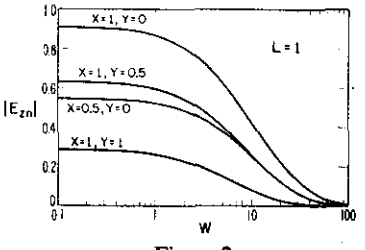

Figure 2
Frequency dependence of $|E_{zn}|$ for various observation points

Consequently, the frequency range in Fig. 2 is 126.6 Hz to 126.6 kHz for the above values of σ and h. The phase of E_{zn} is a generally decreasing function of W.

In order to express E_y in a convenient form, the differentiations in (2) are carried out and derivatives of the modified Bessel functions are replaced by zero- and first-order functions. The resultant E_y in normalized form is

$$E_y = -[I/(2\pi\sigma h^2)]\, E_{yn}(W, L, X, Y), \tag{5}$$

where

$$\begin{aligned} E_{yn} = \frac{(iW)^{1/2} Y}{2} \Bigg\{ & \left[\frac{(iW)^{1/2}}{R_1^2} (I_1 K_1 - I_0 K_0) \right|_{R=R_1} \\ & - \left(\frac{1}{R_1^3} + \frac{1}{R_1^2} \right) (I_0 K_1) \Big|_{R=R_1} + \left(\frac{1}{R_1^3} - \frac{1}{R_1^2} \right) (I_1 K_0) \Big|_{R=R_1} \Bigg] \\ & - \left[\frac{(iW)^{1/2}}{R_2^2} (I_1 K_1 - I_0 K_0) \right|_{R=R_2} - \left(\frac{1}{R_2^3} + \frac{1}{R_2^2} \right) (I_0 K_1) \Big|_{R=R_2} \\ & + \left(\frac{1}{R_2^3} - \frac{1}{R_2^2} \right) (I_1 K_0) \Big|_{R=R_2} \Bigg] \Bigg\}, \end{aligned}$$

the argument of I_0 and I_1 is $(iW)^{1/2}(R-1)/2$, and the argument of K_0 and K_1 is $(iW)^{1/2}(R+1)/2$. The dependence of $|E_{yn}|$ on W is illustrated in Fig. 3 for $L=1$ and various values of X and Y. The phase of E_{yn} is again a decreasing function of W.

The integration for E_x must be done numerically, and some results have been given [1]. However, here we wish to normalize in the following form

$$E_x = -[I/(2\pi\sigma h^2)]\, E_{xn}(W, L, X, Y), \tag{6}$$

where

$$E_{xn} = h^2 \int_{-t}^{t} \left(\frac{\partial^2 P}{\partial z^2} + \frac{\partial^3 N}{\partial y^2\, \partial z}\right) dx',$$

$$\frac{\partial^2 P}{\partial z^2} = \frac{\exp(-\gamma r)}{r^3}\left[\left(\frac{3z^2}{r^2} - 1\right) + \gamma r\left(\frac{3z^2}{r^2} - 1\right) + \gamma^2 z^2\right],$$

$$\frac{\partial^3 N}{\partial y^2\, \partial z} = \frac{\gamma}{2}[B_{00} I_0 K_0 + B_{11} I_1 K_1 + B_{01} I_0 K_1 + B_{10} I_1 K_0],$$

$$B_{00} = \frac{\gamma z}{r^2}\left(1 - \frac{3y^2}{r^2}\right),$$

$$B_{11} = \frac{\gamma z}{r^2}\left[-1 + \frac{3y^2}{r^2} + \frac{2y^2}{r^2 - z^2}\right],$$

$$B_{01} = \frac{1}{r^2}\left[-1 + \frac{3y^2}{r^2} + \frac{z(1 - \gamma^2 y^2)}{r} - \frac{3zy^2}{r^3}\right],$$

$$B_{10} = \frac{1}{r^2}\left[-1 + \frac{3y^2}{r^2} - \frac{z(1 - \gamma^2 y^2)}{r} + \frac{3zy^2}{r^3}\right],$$

the argument of I_0 and I_1 is $\gamma(r+z)/2$, and the argument of K_0 and K_1 is $\gamma(r-z)/2$. The x' integration was done numerically, and the resultant dependence of $|E_{xn}|$ on W for $L=1$ and various values of X and Y is illustrated in Fig. 4. It is interesting that the curves peak near $W=5$ before falling off for large W. As in the previous cases, the phase is a decreasing function of W.

A simple special case is the low frequency limit, where the electric field is given by the gradient of a scalar potential [6]. Thus

$$d\mathbf{E}^{dc} = \frac{I dx'}{2\pi\sigma}\nabla\frac{\partial}{\partial x}\left(\frac{1}{r}\right),$$

$$\mathbf{E}^{dc} = \frac{-I}{2\pi\sigma}\nabla\left(\frac{1}{r_1} - \frac{1}{r_2}\right). \tag{7}$$

Consequently, the normalized components are given by

$$E_{xn}^{dc} = (L - X)R_1^{-3} + (L + X)R_2^{-3},$$

$$E_{yn}^{dc} = -Y(R_1^{-3} - R_2^{-3}),$$

$$E_{zn}^{dc} = R_1^{-3} - R_2^{-3}. \tag{8}$$

All computed results in Figs. 2–4 agree with these limits as $W \to 0$. These limits are important because they are the final values of the step responses that are computed in the following section.

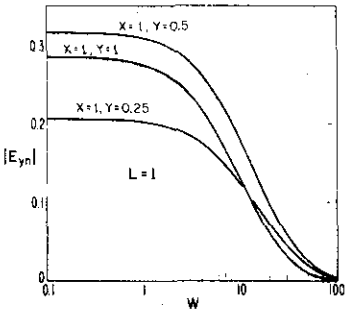

Figure 3
Frequency dependence of $|E_{yn}|$ for various observation points

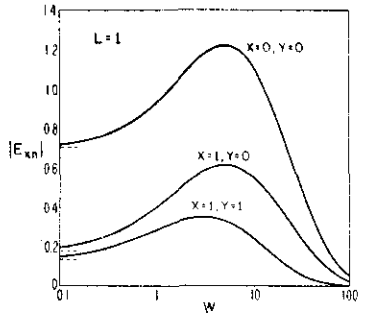

Figure 4
Frequency dependence of $|E_{xn}|$ for various observation points

3. *Step response*

In this case, the cable current is given by $IU(t)$ where $U(t)$ is the unit step function at $t = 0$. The step responses are given by the following inverse Fourier transform:

$$\begin{Bmatrix} \tilde{E}_x^s(t) \\ \tilde{E}_y^s(t) \\ \tilde{E}_z^s(t) \end{Bmatrix} = \frac{1}{2\pi} \int_{-\infty}^{\infty} \frac{\exp(i\omega t)}{i\omega} \begin{Bmatrix} E_x \\ E_y \\ E_z \end{Bmatrix} d\omega \tag{9}$$

where E_x, E_y, and E_z are given in the previous section.

The following standard inverse Fourier (or Laplace) transform is useful in obtaining $\tilde{E}_z^s$

$$\mathfrak{F}^{-1}[\exp(-a(i\omega)^{1/2})/(i\omega)] = \operatorname{erfc}[a/(2t^{1/2})]\, U(t), \tag{10}$$

where

$$\operatorname{erfc}(x) = \frac{2}{\pi^{1/2}} \int_x^\infty e^{-y^2}\, dy$$

is the complement of the error function for real argument x. By applying (10) to (2), we obtain

$$\tilde{E}_z^s(t) = \frac{-I}{2\pi\sigma} \frac{\partial}{\partial z} \{r_1^{-1} \operatorname{erfc}[(r_1/2)(\mu_0\sigma/t)^{1/2}] - r_2^{-1} \operatorname{erfc}[(r_2/2)(\mu_0\sigma/t)^{1/2}]\} \tag{11}$$

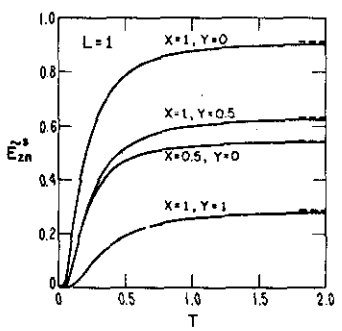

Figure 5
Step response $\tilde{E}_{zn}^s$ for various observation points

The unit step $U(t)$ has been omitted in (11), and it is understood from hereon that all time responses are zero for negative time. We now write (11) in the normalized form

$$\tilde{E}_z^s(t) = -[I/(2\pi\sigma h^2)]\, \tilde{E}_{zn}^s(T, L, X, Y), \tag{12}$$

where

$$\tilde{E}_{zn}^s = \frac{\operatorname{erfc}[(R_1/2)\,T^{-1/2}]}{R_1^3} - \frac{\exp[-R_1^2/(4T)]}{(\pi T)^{1/2} R_1^2} - \frac{\operatorname{erfc}[(R_2/2)\,T^{-1/2}]}{R_2^3} + \frac{\exp[-R_2^2/(4T)]}{(\pi T)^{1/2} R_2^2}$$

and $T = t/(\sigma\mu_0 h^2)$.

Curves of $\tilde{E}_{zn}^s$ vs. T are given in Fig. 5 for $L = 1$ and various values of X and Y. Note that, at $T = 2$, $\tilde{E}_{zn}^s$ has nearly reached its static limit as given by (8). For typical values of σ ($= 10^{-2}$ mhos/m) and h ($= 100$ m), the quantity $\sigma\mu_0 h^2$ is 0.1258 msec. Consequently, $T = 1$ corresponds to $t = 0.1258$ msec. The quantity $\sigma\mu_0 h^2$ has also appeared as the effective time constant for the transient fields of a pulsed loop [7].

In determining $\tilde{E}_y^s$, the following inverse Fourier (or Laplace) transform is useful [2]:

$$\mathfrak{F}^{-1}\{I_0[a(i\omega)^{1/2}]\, K_0[b(i\omega)^{1/2}]\} = \frac{\exp[-(a^2+b^2)/(4t)]}{2t} \cdot I_0\left(\frac{ab}{2t}\right). \tag{13}$$

Application of (13) to (2) allows the expression of the impulse response in closed form. Consequently, the step response can be written as an integral of the step response:

$$\tilde{E}_y^s(t) = -[I/(2\pi\sigma h^2)]\, \tilde{E}_{yn}^s(T, L, X, Y), \tag{14}$$

where

$$\tilde{E}_{yn}^s(T, L, X, Y) = \int_0^T \tilde{E}_{yn}^i(T', L, X, Y)\, dT'$$

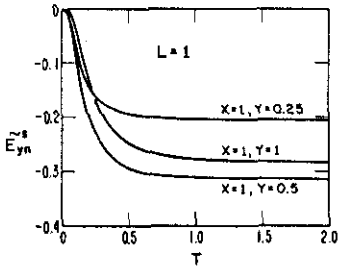

Figure 6
Step response $\tilde{E}_{yn}^s$ for various observation points

and

$$\tilde{E}_{yn}^i = \frac{Y}{16T^3}\left\{\exp\left(-\frac{R_1^2+1}{8T}\right)\left[I_1\left(\frac{R_1^2-1}{8T}\right) - I_0\left(\frac{R_1^2-1}{8T}\right)\right]\right.$$
$$\left. - \exp\left(\frac{R_2^2+1}{8T}\right)\left[I_1\left(\frac{R_2^2-1}{8T}\right) - I_0\left(\frac{R_2^2-1}{8T}\right)\right]\right\}.$$

The integration in (14) was done numerically, and the resultant step responses for $L = 1$ and various values of X and Y are shown in Fig. 6. Again, the final values as given by (8) have essentially been reached at $T = 2$.

In order to determine $\tilde{E}_x^s$, the inverse Fourier transform was done numerically as follows:

$$\tilde{E}_x^s(t) = -[I/(2\pi\sigma h^2)]\, \tilde{E}_{xn}^s(T, L, X, Y), \tag{15}$$

where

$$\tilde{E}_{xn}^s(T, L, X, Y) = \frac{1}{2\pi}\int_{-\infty}^{\infty} \frac{E_{xn}(W, L, X, Y)}{iW} \exp(iWT)\, dW,$$

and E_{xn} is given by (6). The resultant curves of $\tilde{E}^s_{xn}$ vs. T are shown in Fig. 7 for $L = 1$ and various values of X and Y. These waveforms, unlike those for $\tilde{E}^s_{zn}$ and $\tilde{E}^s_{yn}$, contain an overshoot and a slow recovery to the final value.

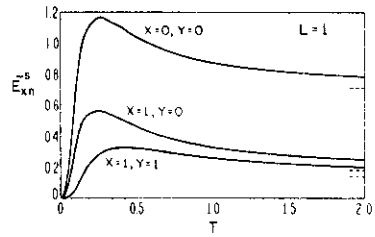

Figure 7
Step response $\tilde{E}^s_{xn}$ for various observation points

4. Concluding remarks

Both the time-harmonic and the transient subsurface electric field for a finite length cable carrying a step function current have been examined. Closed form expressions have been obtained for the y and z components, whereas numerical integration was required for the x component. The time-domain waveforms are fairly simple and the final values can be obtained from a scalar potential. However, the waveforms for the x component do contain an overshoot. The time constant of the waveforms is roughly $\sigma\mu_0 h^2$ which is consistent with previous results for loop sources.

Acknowledgements

We thank Dr. RICHARD G. GEYER for his useful suggestions, Drs. H. PARKINSON and J. POWELL for their encouragement, and their organization, the U.S. Bureau of Mines, for its support, and Mrs. LOYS GAPPA for her help in preparing the manuscript.

REFERENCES

[1] D. A. HILL and J. R. WAIT, *Subsurface Electromagnetic Fields of a Grounded Cable of Finite Length*, unpublished report, January 1973.
[2] G. E. ROBERTS and H. KAUFMAN, *Table of Laplace Transforms* (W. B. Saunders Co., Philadelphia 1966), 311 pp.
[3] E. D. SUNDE, *Earth Conduction Effects in Transmission Systems* (Dover Publications, New York 1968), pp. 140–172.
[4] J. R. WAIT, *Electromagnetic fields of current-carrying wires in a conducting medium*, Can. J. Phys. *30* (1952), 512–523.

[5] J. R. WAIT, *Propagation of electromagnetic pulses in a homogeneous conducting earth*, Appl. Sci. Res. *8B* (1960), 213–253.
[6] J. R. WAIT, *The electromagnetic fields of a horizontal dipole in the presence of a conducting half-space*, Can. J. Phys. *39* (1961), 1017–1028.
[7] J. R. WAIT and D. A. HILL, *Transient signals from a buried dipole*, J. Appl. Phys. *42* (10) (1971), 3866–3869.
[8] J. R. WAIT, *Electromagnetic wave propagation along a buried insulated wire*, Can. J. Phys. *50* (1972), 2402–2409.

(Received 29th March 1973)

Journal of Applied Physics, Vol. 44, No. 12, 5275-5279, December 1973

Electromagnetic surface fields of an inclined buried cable of finite length

David A. Hill

Institute for Telecommunication Sciences, Office of Telecommunications, U. S. Department of Commerce, Boulder, Colorado 80302

(Received 5 July 1973; in final form 17 August 1973)

The magnetic fields on the surface produced by a buried current-carrying cable of finite length are considered. A homogeneous half-space model of the earth and quasistatic conditions are assumed. The cable is grounded at its end points and oriented at an arbitrary angle to the interface. While, in general, numerical integration is required, the low-frequency limit may be treated analytically. Small cable tilts are shown to modify the direction of the surface field but not the magnitude. The results have possible application to uplink communication and radio location of trapped miners.

I. INTRODUCTION

The subsurface fields of both infinite-length[1,2] and finite-length[3] line sources have been examined for the source located at the surface. Here, we examine the fields of a buried finite-length cable which makes an arbitrary angle with the interface. This case is of practical interest because either the cable may be tilted or the earth surface may not be level.

The earth is taken to be a homogeneous half-space, and the current in the cable is assumed to be constant. The constant-current assumption is valid at sufficiently low frequencies when an insulated cable is grounded at the end points.[4,5] Since we are primarily interested in reception at the surface with loop antennas, the desired quantities are the three magnetic field components evaluated at the interface.

II. FORMULATION

The geometry of the buried cable of length $2l$ carrying a current $I\exp(i\omega t)$ is shown in Fig. 1, and the angular frequency ω is sufficiently low that all displacement currents are negligible. The cable is located in the xz plane and makes an angle α with the $z=0$ plane. Its center is on the z axis at $z=-h$, and a general source point on the cable has Cartesian coordinates $(x',0,-h')$. We introduce s as the distance from the cable center to the source point. Consequently, the source coordinates are given by

$$x'=s\cos\alpha \quad \text{and} \quad h'=h-s\sin\alpha. \tag{1}$$

The Hertz vector has both x and z components (Π_x and Π_z), and in deriving the contribution from an incremental source of length ds it is convenient to resolve the current into x and z (horizontal and vertical) components. The contribution from the vertical component is given by Wait[4] and Banos[6]:

$$d\Pi_z^v=(I\,ds\,\sin\alpha/4\pi\sigma)[R_0^{-1}\exp(-\gamma R_0)-R^{-1}\exp(-\gamma R)], \tag{2}$$

where

$$\gamma=(i\omega\mu_0\sigma)^{1/2}, \quad R_0=[(x-x')^2+y^2+(z+h')^2]^{1/2},$$
$$R=[(x-x')^2+y^2+(z-h')^2]^{1/2}, \quad z<0, \quad h'>0,$$

μ_0 is the permeability of free space, and σ is the conductivity of the half-space. Although (2) applies to the case of both source and observer in the conducting half-space, it is useful for evaluation of the magnetic field at the surface ($z=0^-$), since the magnetic field is continuous across the interface. However, the limit of $d\Pi_z^v$ as z approaches zero is seen to be zero. Since the x and y derivatives are also zero, the curl is zero and the magnetic field is zero. Consequently, the vertical component of the buried source does not contribute to the surface magnetic field (within the quasistatic approximation).

The contribution from the horizontal component of current is given by Wait[7]:

$$d\Pi_x^h=(I\,ds\cos\alpha/4\pi\sigma)[R_0^{-1}\exp(-\gamma R_0)-R^{-1}\exp(-\gamma R)$$
$$+2\int_0^\infty (u+\lambda)^{-1}\exp[u(z-h')]J_0(\lambda\rho)\lambda\,d\lambda],$$
$$d\Pi_z^h=\frac{I\,ds\cos\alpha}{2\pi\sigma}\frac{\partial}{\partial x}\int_0^\infty (u+\lambda)^{-1}\exp[u(z-h')]J_0(\lambda\rho)\,d\lambda, \tag{3}$$

where

$$u=(\lambda^2+\gamma^2)^{1/2} \quad \text{and} \quad \rho=[(x-x')^2+y^2]^{1/2}.$$

Wait[7] has shown that the λ integrations can be carried out to yield

$$d\Pi_x^h=\frac{I\,ds\cos\alpha}{4\pi\sigma}\left[R_0^{-1}\exp(-\gamma R_0)-P+2\gamma^{-2}\right.$$
$$\left.\times\left(\frac{\partial^2 P}{\partial z^2}-\frac{\partial^2 N}{\partial z^2}+\gamma^2\frac{\partial N}{\partial z}\right)\right],$$
$$d\Pi_z^h=\frac{I\,ds\cos\alpha}{2\pi\sigma\gamma^2}\left(\frac{\partial^2 N}{\partial x\,\partial z^2}-\frac{\partial^2 P}{\partial x\,\partial z}\right), \tag{4}$$

where

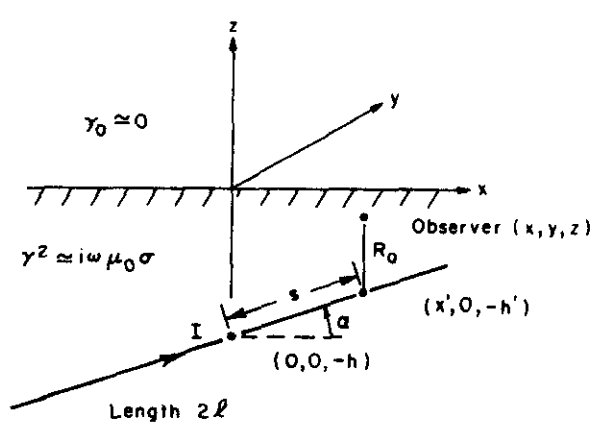

FIG. 1. Tilted line source in a homogeneous half-space.

$$N = I_0[(\gamma/2)(R + z - h')]K_0[(\gamma/2)(R - z + h')],$$

$$P = R^{-1}\exp(-\gamma R),$$

and I_0 and K_0 are modified Bessel functions of order zero. The magnetic field components are derived from the curl of the Hertz vector:

$$d\mathbf{H} = \sigma\,\mathrm{curl}\,d\boldsymbol{\Pi}. \tag{5}$$

Since we are interested in evaluating the magnetic field at the interface, the following relationships are useful:

$$R_0\big|_{z=0} = R\big|_{z=0} \quad \text{and} \quad \frac{\partial R_0}{\partial z}\bigg|_{z=0} = -\frac{\partial R}{\partial z}\bigg|_{z=0}. \tag{6}$$

By substituting (4) into (5) and utilizing (6) as well as the fact that both N and P satisfy the wave equation $[(\nabla^2 - \gamma^2)N = (\nabla^2 - \gamma^2)P = 0]$, the magnetic field components at the interface ($z = 0$) are obtained:

$$dH_x = \frac{I\,ds\cos\alpha}{2\pi\gamma^2}\left(\frac{\partial^4 N}{\partial x\,\partial y\,\partial z^2} - \frac{\partial^3 P}{\partial x\,\partial y\,\partial z}\right),$$

$$dH_y = \frac{I\,ds\cos\alpha}{2\pi\gamma^2}\left(\frac{\partial^4 N}{\partial y^2\,\partial z^2} - \frac{\partial^3 P}{\partial y^2\,\partial z}\right), \tag{7}$$

$$dH_z = \frac{I\,ds\cos\alpha}{2\pi\gamma^2}\left(\frac{\partial^4 N}{\partial y\,\partial z^3} - \gamma^2\frac{\partial^2 N}{\partial y\,\partial z} - \frac{\partial^3 P}{\partial y\,\partial z^2}\right).$$

To obtain the resultant magnetic field of the cable, we integrate (7) over the range of s from $-l$ to l. For normalization purposes, it is convenient to write the fields in the following manner:

$$H_x = (I/2\pi h)H_{xn}(H, Y, X, L, \alpha),$$

$$H_y = (I/2\pi h)H_{yn}(H, Y, X, L, \alpha), \tag{8}$$

$$H_z = (I/2\pi h)H_{zn}(H, Y, X, L, \alpha),$$

where $H = (\omega\mu_0\sigma)^{1/2}h$, $Y = y/h$, $X = x/h$, and $L = l/h$. Note that H_{xn}, H_{yn}, and H_{zn} are dimensionless. By comparing (7) and (8), the following forms are found for H_{xn}, H_{yn}, and H_{zn}:

$$H_{xn} = \frac{h\cos\alpha}{\gamma^2}\int_{-l}^{l}\left(\frac{\partial^4 N}{\partial x\,\partial y\,\partial z^2} - \frac{\partial^3 P}{\partial x\,\partial y\,\partial z}\right)ds,$$

$$H_{yn} = \frac{h\cos\alpha}{\gamma^2}\int_{-l}^{l}\left(\frac{\partial^4 N}{\partial y^2\,\partial z^2} - \frac{\partial^3 P}{\partial y^2\,\partial z}\right)ds, \tag{9}$$

$$H_{zn} = \frac{h\cos\alpha}{\gamma^2}\int_{-l}^{l}\left(\frac{\partial^4 N}{\partial y\,\partial z^3} - \gamma^2\frac{\partial^2 N}{\partial y\,\partial z} - \frac{\partial^3 P}{\partial y\,\partial z^2}\right)ds.$$

The specific expressions for the partial derivatives of P and N in (9) are given in the Appendix. Although the electric field components are not of major interest here, similar expressions in P and N can be derived.

III. LOW-FREQUENCY LIMIT

The low-frequency limit is useful both as a check on the numerical work and as a means of determining trends at low frequencies. For γ approaching zero, the Hertz components in (3) reduce to

$$d\Pi_x^h = \frac{I\,ds\cos\alpha}{4\pi\sigma}\left\{R_0^{-1} - R^{-1} + \int_0^\infty \exp[-\lambda(h' - z)]J_0(\lambda\rho)\,d\lambda\right\}$$

$$= \frac{I\,ds\cos\alpha}{4\pi\sigma R_0}, \tag{10}$$

$$d\Pi_z^h = \frac{-I\,ds\cos\alpha}{4\pi\sigma}\,\frac{(x - x')}{\rho}\int_0^\infty \exp[-\lambda(h' - z)]J_1(\lambda\rho)\,d\lambda$$

$$= \frac{-I\,ds\cos\alpha}{4\pi\sigma}\,\frac{(x - x')}{\rho^2}[1 + (z - h')R^{-1}],$$

where we have made use of integrals listed by Wheelon.[8]

In order to simplify the discussion, we now consider the cable to be level ($\alpha = 0$). The magnetic field components are obtained from the curl of (10). Evaluated at the interface ($z = 0$), they become

$$dH_x = \frac{-I\,ds}{4\pi}\,\frac{\partial}{\partial y}\left[\frac{x - s}{\rho^2}(1 - hR^{-1})\right],$$

$$dH_y = \frac{I\,ds}{4\pi}\left\{\frac{-h}{R^3} + \frac{\partial}{\partial x}\left[\frac{x - s}{\rho^2}(1 - hR^{-1})\right]\right\}, \tag{11}$$

$$dH_z = \frac{I\,ds}{4\pi}\,\frac{y}{R^3}.$$

The total field of the cable is obtained by integrating (11) from $-l$ to l. The resulting integrals can be done in closed form and can be simplified to yield

$$H_x = \frac{Iy}{4\pi}[\rho_1^{-2} - \rho_2^{-2} - h(R_1^{-1}\rho_1^{-2} - R_2^{-1}\rho_2^{-2})],$$

$$H_y = \frac{I}{4\pi}\left(\frac{-h}{y^2 + h^2}[(l - x)R_1^{-1} + (l + x)R_2^{-1}]\right.$$

$$\left. + (l - x)\rho_1^{-2}(1 - hR_1^{-1}) + (l + x)\rho_2^{-2}(1 - hR_2^{-1})\right), \tag{12}$$

$$H_z = \frac{I}{4\pi}\left(\frac{y}{y^2 + h^2}[(l - x)R_1^{-1} + (l + x)R_2^{-1}]\right),$$

where

$$R_{\frac{1}{2}} = [(x \mp l)^2 + y^2 + h^2]^{1/2}$$

and

$$\rho_{\frac{1}{2}} = [(x \mp l)^2 + y^2]^{1/2}.$$

In the limit of an infinite cable ($l \to \infty$), (12) reduces to

$$H_x \to 0,$$

$$H_y \to \frac{-I}{2\pi}\,\frac{h}{h^2 + y^2}, \tag{13}$$

$$H_z \to \frac{I}{2\pi}\,\frac{y}{h^2 + y^2}.$$

These limits agree with those of the infinite line source,[1] and graphical results for arbitrary length are presented later.

IV. HIGH-FREQUENCY LIMIT

Another useful limiting case is for high frequencies where $|\gamma\rho|$ is large. At the interface ($z = 0$), terms involving P are then negligible and N is asymptotically given by[7]

$$N \approx (\gamma\rho)^{-1}\exp(-\gamma h'). \tag{14}$$

Consequently, dH_x and dH_y are given by

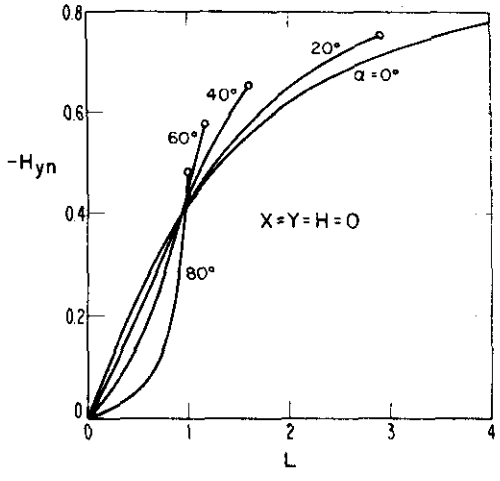

FIG. 2. Low-frequency behavior of H_{yn} as a function of L and α for observer directly above source. Circles indicate the intersection of the cable with the interface.

$$dH_x \approx \frac{I\,ds\cos\alpha}{2\pi\gamma}\exp(-\gamma h')\frac{\partial^2}{\partial x\,\partial y}(\rho^{-1}),$$

$$dH_y \approx \frac{I\,ds\cos\alpha}{2\pi\gamma}\exp(-\gamma h')\frac{\partial^2}{\partial y^2}(\rho^{-1}). \tag{15}$$

In order to determine dH_z, we must include higher order terms in N, and the result is

$$dH_z \approx -\frac{I\,ds\cos\alpha}{2\pi\gamma^2}\exp(-\gamma h')\frac{\partial}{\partial y}(\rho^{-3}). \tag{16}$$

In order to simplify the discussion, we again treat the case of the level cable ($\alpha = 0$). In this case, the s integrations can be performed to yield the total cable fields:

$$H_x \approx \frac{-I\exp(-\gamma h)}{2\pi\gamma}\frac{\partial^2}{\partial x\,\partial y}[\ln(l-x+\rho_1)-\ln(-l-x+\rho_2)],$$

$$H_y \approx \frac{-I\exp(-\gamma h)}{2\pi\gamma}\frac{\partial^2}{\partial y^2}[\ln(l-x+\rho_1)-\ln(-l-x+\rho_2)], \tag{17}$$

$$H_z \approx \frac{-I\exp(-\gamma h)}{2\pi\gamma^2}\frac{\partial}{\partial y}\left[\frac{1}{y^2}\left(\frac{l-x}{\rho_1}+\frac{l+x}{\rho_2}\right)\right].$$

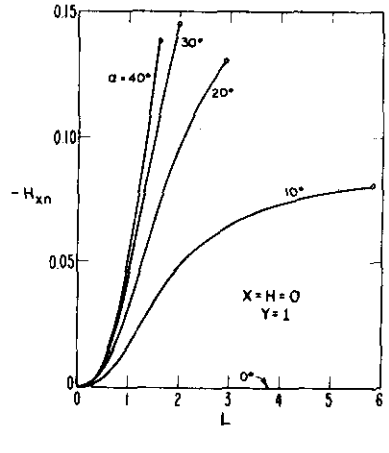

FIG. 3. Low-frequency behavior of H_{xn} as a function of L and α.

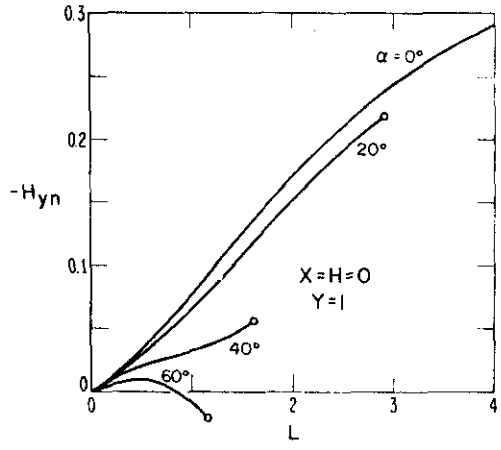

FIG. 4. Low-frequency behavior of H_{yn} as a function of L and α.

If the cable becomes infinite ($l \to \infty$), then (17) reduces to

$$H_x \to 0,$$

$$H_y \to I\exp(-\gamma h)/\pi\gamma y^2, \tag{18}$$

$$H_z \to 2I\exp(-\gamma h)/\pi\gamma^2 y^3.$$

These limits are identical to those for an infinite cable at the surface for a subsurface observer.[3]

The "high-frequency" solutions are actually valid only for a range where the horizontal distance is large compared to a skin depth in the earth and small compared to a free-space wavelength. However, even though this solution is somewhat restricted, it is quite useful in checking the general numerical results.

V. GENERAL NUMERICAL RESULTS

For general values of the various parameters, a numerical integration of the expressions as given in (9) is required. Even though the integrands appear quite complicated, they are well behaved numerically, and the resultant computer program for H_{xn}, H_{yn}, and H_{zn} is quite fast. Consequently, the influence of the parameters (H, Y, X, L, α) can be studied easily.

Results for the static case ($H = 0$) with the observer directly above the cable center ($X = Y = 0$) are shown as a function of L for various cable angles α in Fig. 2. Only the y component H_{yn} is nonzero in this case, and

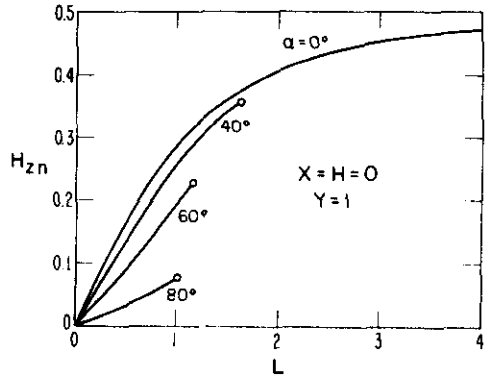

FIG. 5. Low-frequency behavior of H_{zn} as a function of L and α.

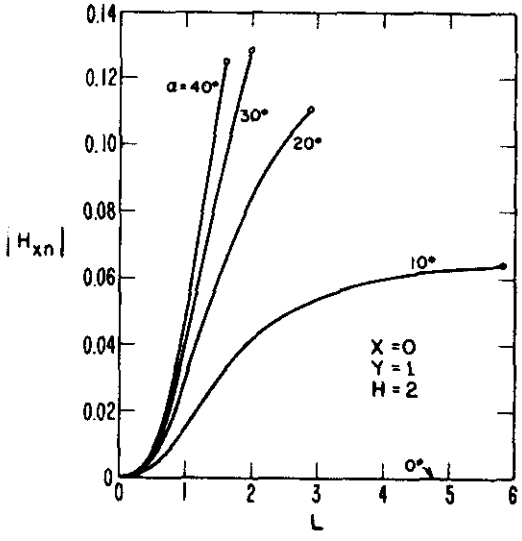

FIG. 6. Behavior of $|H_{xn}|$ as a function of L and α for $H=2$.

the final value for the level case ($\alpha=0°$) is -1. Consequently, even at $L=4$, the level cable does not approximate an infinite cable. By examining the curves for small L, it is possible to determine where the short dipole approximation fails—that is, the point where the curves are no longer linear in L. Examination of the curves shows that the linear behavior ends in the vicinity of $L=0.3$. The various curves terminate at values of L where the cable would intersect the surface. The curves indicate that small tilts ($\alpha<20°$) do not strongly influence the results. However, further increases in α can change the results considerably.

Results for a different observation point ($X=0$, $Y=1$) are shown in Figs. 3–5. As α is increased, H_{zn} in Fig. 3 becomes nonzero. For this component, the dipole approximation is always invalid because it gives zero for H_{zn}. H_{yn} in Fig. 4 is seen to approach its infinite-line-source value of -0.5 quite slowly. H_{xn} in Fig. 5 is seen to approach its final value of 0.5 somewhat more rapidly. Figures 4 and 5 reveal that fairly large values of α are again required to significantly change the results from those of the level case. The crossover in the curve for $\alpha=60°$ in Fig. 4 is a result of a strong negative contribution from the end of the cable near the interface. Such behavior has been found in both H_{yn} and

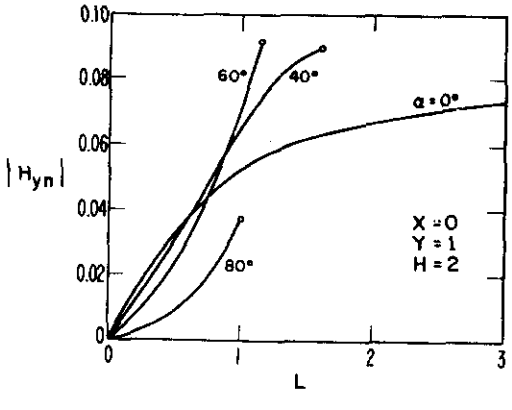

FIG. 7. Behavior of $|H_{yn}|$ as a function of L and α for $H=2$.

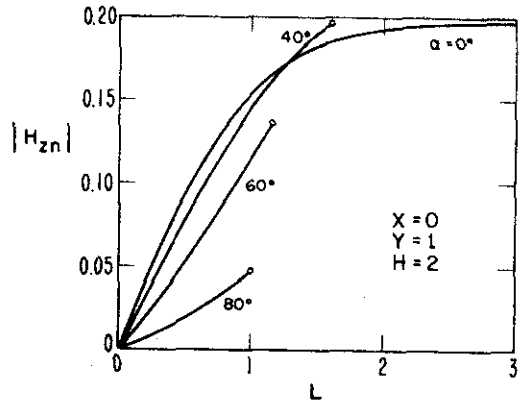

FIG. 8. Behavior of $|H_{zn}|$ as a function of L and α for $H=2$.

H_{zn} for other observation points when α becomes large.

Results for $H=2$ at the same observation point are shown in Figs. 6–8. The tilt again introduces nonzero values of $|H_{zn}|$ in Fig. 6. However, $|H_{yn}|$ and $|H_{xn}|$ are again relatively unaltered by small values of α. The dipole approximation again fails in the neighborhood of $L=0.3$. The phases are not shown since they remain fairly constant with changing L.

VI. CONCLUDING REMARKS

Analytical expressions for the surface fields of a buried finite line source have been derived for the high and low-frequency limits when the source is level. For the general case, a single numerical integration along the source is required. A constant current distribution has been assumed, but arbitrary distributions or cable arrays could be handled, since the source integration is done numerically.

Results for low and medium frequencies indicate that the infinite-cable result is achieved only for very long cables ($L>5$). The infinite-cable result is reached for much shorter cables when the cable is at the interface.[3] At the other extreme, the short dipole approximation appears to be valid for only very short cables ($L<0.3$). Consequently, a large range exists where the general formulation is required. When the cable is tilted, the short dipole approximation becomes even worse. For instance, the x components of the magnetic field, shown in Figs. 3 and 6, are predicted to be zero.

The effect of cable tilt is shown to be small for the y and z components for tilts less than 20°. However, the tilt does strongly alter the normally small x component. Consequently, small cable tilts can be expected to produce only small changes in the surface field strength, but they may considerably alter the direction of the field.

ACKNOWLEDGMENTS

The author would like to thank Dr. J.R. Wait and Dr. R.G. Geyer for their useful comments.

APPENDIX

There are three terms in derivatives of P which are required in (9), and the resultant forms evaluated at the interface ($z=0$) are

$$\frac{\partial^3 P}{\partial x\,\partial y\,\partial z} = (x-x')yh'R^{-4}\exp(-\gamma R)(\gamma^3 + 6\gamma^2 R^{-1} + 15\gamma R^{-2} + 15R^{-3}),$$

$$\frac{\partial^3 P}{\partial y^2\,\partial z} = h'R^{-3}\exp(-\gamma R)[-\gamma^3 + \gamma(\gamma^2 y^2 - 3)R^{-1} + 3(2\gamma^2 y^2 - 1)R^{-2} + 15\gamma y^2 R^{-3} + 15y^2 R^{-4}],$$

$$\frac{\partial^3 P}{\partial y\,\partial z^2} = yR^{-3}\exp(-\gamma R)[\gamma^3 + 3\gamma R^{-1} + 3R^{-2} + h'^2(-\gamma^3 R^{-1} - 6\gamma^2 R^{-2} - 15\gamma R^{-3} - 15R^{-4})].$$

The four terms in derivatives of N can be simplified by replacing the derivatives of the modified Bessel functions by Bessel functions of zero and first order.[9,10] This procedure yields the following expressions at the interface ($z=0$), which are quite suitable for numerical evaluation:

$$\frac{\partial^4 N}{\partial x\,\partial y\,\partial z^2} = \frac{\gamma y(x-x')}{2}[A_{00}I_0K_0 + A_{11}I_1K_1 + A_{01}I_0K_1 + A_{10}I_1K_0]$$

where

$$A_{00} = \gamma h'^2 R^{-4}(\gamma^2 + 15R^{-2}),$$

$$A_{11} = \gamma R^{-3}\{4R^{-1} - \gamma^2 h'^2 R^{-1} - 15h'^2 R^{-3} - (3h'^2 R^{-2} - 2)[(R+h')^{-1} + (R-h')^{-1}]\},$$

$$A_{01} = R^{-3}[-\gamma^2 + 6\gamma^2 h'^2 R^{-2} + 12h'R^{-3} + 15h'^2 R^{-4} - (R+h')^{-1}(-\gamma^2 h'^2 R^{-1} - 3h'R^{-2} - 3h'^2 R^{-3})],$$

$$A_{10} = R^{-3}[\gamma^2 - 6\gamma^2 z^2 R^{-2} + 12h'R^{-3} - 15h'^2 R^{-4} - (R-h')^{-1}(\gamma^2 h'^2 R^{-1} - 3h'R^{-2} + 3h'^2 R^{-3}];$$

$$\frac{\partial^2 N}{\partial y\,\partial z} = \frac{\gamma y}{2}[B_{00}I_0K_0 + B_{11}I_1K_1 + B_{01}I_0K_1 + B_{10}I_1K_0],$$

where

$$B_{00} = -\gamma h'R^{-2}, \quad B_{11} = \gamma h'R^{-2},$$
$$B_{01} = -R^{-2}(1 + h'R^{-1}), \quad B_{10} = -R^{-2}(1 - h'R^{-1});$$

$$\frac{\partial^4 N}{\partial y^2\,\partial z^2} = \frac{\gamma}{2}[C_{00}I_0K_0 + C_{11}I_1K_1 + C_{01}I_0K_1 + C_{10}I_1K_0],$$

where

$$C_{00} = \gamma h'^2 R^{-4}(-3 + \gamma^2 y^2 + 15y^2 R^{-2}),$$

$$C_{11} = \gamma R^{-2}[-2 + h'^2 R^{-2}(3 - \gamma^2 y^2) + 6y^2 R^{-2} - 15y^2 h'^2 R^{-4} + 2y^2 \rho^{-2} R^{-2}(R^2 - 2h'^2)],$$

$$C_{01} = R^{-3}[h'R^{-1}(\gamma^2 y^2 - 3) - \gamma^2(y^2 + h'^2) - 3h'^2 R^{-2}(1 - 2\gamma^2 y^2) + 15h'y^2 R^{-3} + 15y^2 h'^2 R^{-4} - \gamma^2 y^2 h'\rho^{-2}(R - h')],$$

$$C_{10} = R^{-3}[h'R^{-1}(\gamma^2 y^2 - 3) + \gamma^2(y^2 + h'^2) + 3h'^2 R^{-2}(1 - 2\gamma^2 y^2) + 15h'y^2 R^{-3} - 15y^2 h'^2 R^{-4} - \gamma^2 y^2 h'\rho^{-2}(R + h')];$$

$$\frac{\partial^4 N}{\partial y\,\partial z^3} = \frac{\gamma y}{2}[D_{00}I_0K_0 + D_{11}I_1K_1 + D_{01}I_0K_1 + D_{10}I_1K_0],$$

where

$$D_{00} = \gamma h'R^{-4}(3 - 15h'^2 R^{-2} - \gamma^2 h'^2),$$
$$D_{11} = \gamma h'R^{-4}(-13 + 15h'^2 R^{-2} + \gamma^2 h'^2),$$
$$D_{01} = R^{-2}(3R^{-2} + 3h'R^{-3} - 15h'^2 R^{-4} - 15h'^3 R^{-5} - \gamma^2 + 3\gamma^2 h'R^{-1} - \gamma^2 h'^2 R^{-2} - 6\gamma^2 h'^3 R^{-3}),$$
$$D_{10} = R^{-2}(3R^{-2} - 3h'R^{-3} - 15h'^2 R^{-4} + 15h'^3 R^{-5} - \gamma^2 - 3\gamma^2 h'R^{-1} - \gamma^2 h'^2 R^{-2} + 6\gamma^2 h'^3 R^{-3}).$$

The argument of I_0 and I_1 is $(\gamma/2)(R-h')$, and the argument of K_0 and K_1 is $(\gamma/2)(R+h')$.

[1] J.R. Wait and K.P. Spies, Radio Sci. 6, 781 (1971).
[2] D.B. Large, L. Ball, and A.J. Farstad, IEEE Trans. Commun. COM-21, 194 (1973).
[3] D.A. Hill and J.R. Wait, Can. J. Phys. 51, 1534 (1973).
[4] J.R. Wait, Can. J. Phys. 30, 512 (1952).
[5] E.D. Sunde, *Earth Conduction Effects in Transmission Systems* (Dover, New York, 1968), pp. 140–172.
[6] A. Banos, *Dipole Radiation in the Presence of a Conducting Half-space* (Pergamon, New York, 1966).
[7] J.R. Wait, Can. J. Phys. 39, 1017 (1961).
[8] A.D. Wheelon, *Tables of Summable Series and Integrals Involving Bessel Functions* (Holden-Day, San Francisco, 1968), p. 72.
[9] J.R. Wait and L.L. Campbell, J. Geophys. Res. 58, 21 (1953).
[10] J.R. Wait and L.L. Campbell, J. Geophys. Res. 58, 167 (1953).

Radio Science, Volume 8, Number 12, pages 1169–1176, December 1973

Excitation of a homogeneous conductive cylinder of finite length by a prescribed axial current distribution

James R. Wait

Cooperative Institute for Research in Environmental Sciences, University of Colorado, and Environmental Research Laboratories, National Oceanic and Atmospheric Administration, US Department of Commerce, Boulder, Colorado 80302

David A. Hill

Institute for Telecommunication Sciences, Office of Telecommunications, US Department of Commerce, Boulder, Colorado 80302

(Received June 14, 1973.)

The boundary value problem posed is a truncated cylindrical region excited by a specified distribution of electric current over a concentric cylindrical surface. The end conditions are that the total normal current density is zero. The solution is carried through for excitation by a symmetrically located axial current filament that is adjacent to the cylinder. Numerical results of the resultant magnetic field are given for the quasi-static situation for a perfectly conducting cylinder. It is indicated that the results depend significantly on the length of the cylindrical target. Even for very long cylinders, there is no quantitative similarity with the corresponding two-dimensional model of a cylinder of infinite length.

INTRODUCTION

The theory of the interaction of electromagnetic waves with finite or bounded structures is extremely involved except in a few special cases. For example, the vector wave solution for the sphere is about the only case that is tractable when the incident wave is arbitrary and the body dimensions are comparable with a wavelength. The class of obtainable solutions for scalar wave problems is somewhat broader, but even here we are restricted to separable geometries.

The need for useable results for finite body scattering has motivated many investigators to utilize numerical techniques [*Ward and Morrison*, 1971] such as the moment method [*Harrington*, 1968]. Even here the three-dimensional nature of the problem compounds the usual difficulty of excessive computation time. One well-known alternative to a direct numerical attack is to employ high frequency asymptotic techniques [*Fox*, 1964] such as J. B. Keller's geometrical theory of diffraction.

Here, we should like to point out the possibility of getting useful results from a special form of a truncated conducting cylinder that is excited by a finite axial current element. It is suggested that the results to this problem can provide insight to scattering by finite cylinders and, hopefully, they will be useful as a check on numerical procedures developed for more general three-dimensional structures. Also, we shall utilize the low frequency solutions to show graphically how the magnetic field varies in the vicinity of the cylinder for various positions of the adjacent current element.

FORMULATION

The specific situation of interest is illustrated in Figure 1. A conducting cylinder of conductivity σ and magnetic permeability μ occupies the space $\rho < a$ and $|z| < s$ in terms of a cylindrical coordinate system (ρ, ϕ, z). The region $\rho > a$ external to the cylinder has a conductivity σ_0 and magnetic permeability μ_0. To allow for the existence of displacement currents, we can allow both σ and σ_0 to be complex. Over the concentric cylindrical surface $\rho = \rho_0$, we specify that the axial current density is a known function $K(\phi, z)$ amp m^{-1}. Actually, in Figure 1 we only show the region for $z > 0$.

We now propose to find a solution of the problem under the stipulation that the normal current density is zero at the surface $z = |s|$. This, in turn,

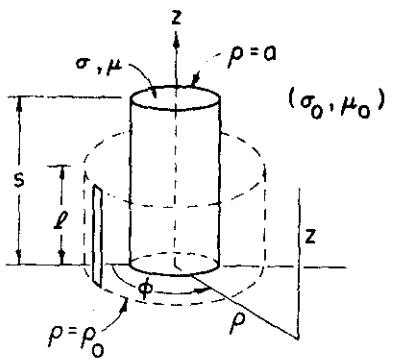

Fig. 1. General configuration showing only region for $z > 0$.

requires that the normal electric field E_z is also zero over this surface. On the other hand, since we are interested mainly in the situation of symmetry about the plane $z = 0$, we can utilize the fact that $E_\rho = 0$ on this plane. Thus, attention may be restricted just to the region $0 < z < s$, if we remember that the solutions for even symmetry are even about $z = 0$. In what follows, we shall adopt a time factor $\exp(i\omega t)$.

We fully appreciate that the posed problem is not directly applicable to an isolated finite cylinder, but we can assert that the solution of this idealized situation should tell us something about the effects of truncating the cylindrical structure. If the latter is relatively thin and highly conducting, it can be expected that the normal current density within the structure tends to vanish at the ends.

FORMAL SOLUTION

To facilitate the analysis of the posed problem, we express the total field in terms of electric and magnetic Hertz vectors that have only z components Π and Π^*, respectively [*Wait*, 1959]. Thus, for the region $\rho < a$, the field components are obtained from

$$E_\rho = (\partial^2 \Pi/\partial\rho\,\partial z) - (i\mu\omega/\rho)(\partial \Pi^*/\partial\phi) \quad (1)$$

$$E_\phi = (1/\rho)(\partial^2 \Pi/\partial\phi\,\partial z) + i\mu\omega(\partial \Pi^*/\partial\rho) \quad (2)$$

$$H_\rho = (-i\gamma^2/\mu\omega\rho)(\partial \Pi/\partial\phi) + (\partial^2 \Pi^*/\partial\rho\,\partial z) \quad (3)$$

$$H_\phi = (i\gamma^2/\mu\omega)(\partial \Pi/\partial\rho) + (1/\rho)(\partial^2 \Pi^*/\partial\phi\,\partial z) \quad (4)$$

$$E_z = [-\gamma^2 + (\partial^2/\partial z^2)]\Pi \quad (5)$$

$$H_z = [-\gamma^2 + (\partial^2/\partial z^2)]\Pi^* \quad (6)$$

where $\gamma = (i\sigma\mu\omega)^{1/2}$ is the propagation constant for the cylinder. The solutions for the region $\rho > a$ have the same form as (1) through (6), but we add a subscript zero where appropriate.

The required forms of the solution for $\rho < a$ are

$$\Pi = \sum_n \sum_m a_{m,n} I_m(v_n\rho) e^{-im\phi} \cos\lambda_n z \quad (7)$$

and

$$\Pi^* = \sum_n \sum_m a_{m,n}^* I_m(v_n\rho) e^{-im\phi} \sin\lambda_n z \quad (8)$$

where $v_n = (\lambda_n^2 + \gamma^2)^{1/2}$. Here, I_m is a modified Bessel function of the first kind that remains finite at $\rho = 0$. For single-valuedness in ϕ, obviously m ranges from $-\infty$ to $+\infty$ through all integers. Also, since $E_z = 0$ at $z = s$, we note that $\lambda_n = (2n + 1)(\pi/2s)$ where $n = 0, 1, 2, 3, \cdots$. In addition, we readily confirm that $E_\rho = 0$ at $z = 0$, in accordance with our assumptions concerning symmetry.

In dealing with the region external to the cylinder, we choose the wave-functions to have the following form, for $a < \rho < \rho_0$,

$$\Pi = \sum_n \sum_m [b_{m,n} I_m(u_n\rho) + c_{m,n} K_m(u_n\rho)] e^{-im\phi} \cos\lambda_n z \quad (9)$$

$$\Pi^* = \sum_n \sum_m c_{m,n}^* K_m(u_n\rho) e^{-im\phi} \sin\lambda_n z \quad (10)$$

and, for $\rho > \rho_0$

$$\Pi = \sum_n \sum_m d_{m,n} K_m(u_n\rho) e^{-im\phi} \cos\lambda_n z \quad (11)$$

$$\Pi^* = \sum_n \sum_m d_{m,n}^* K_m(u_n\rho) e^{-im\phi} \sin\lambda_n z \quad (12)$$

where $u_n = (\lambda^2 + \gamma_0^2)^{1/2}$. Here, K_m is a modified Bessel function of the second kind that assures outgoing waves as $\rho \to \infty$. These forms of the solutions are chosen to allow for a possible discontinuity in H_ϕ at the surface $\rho = \rho_0$, while E_ϕ, E_z, and H_z are continuous. The latter immediately tells us that $c_{m,n}^* = d_{m,n}^*$.

We next express the prescribed current excitation as a double Fourier series in the manner

$$K(\phi, z) = \sum_n \sum_m F_{m,n} e^{-im\phi} \cos\lambda_n z. \quad (13)$$

where $F_{m,n}$ is easily determined. The boundary condition at $\rho = \rho_0$ written as

$$H_\phi|_{\rho_0+0} - H_\phi|_{\rho_0-0} = K(\phi, z) \quad (14)$$

is now easily applied. Using the Wronskian relation $I_m'(Z)K_m(Z) - I_m(Z)K_m'(Z) = 1/Z$, we determine that

$$b_{m,n} = (\eta_0\rho_0/\gamma_0) K_m(u_n\rho_0) F_{m,n} \quad (15)$$

where $\eta_0 = i\mu_0\omega/\gamma_0$. Thus, the coefficient $b_{m,n}$ is determined entirely by the excitation.

The boundary conditions at the surface of the cylinder are that E_z, H_z, E_ϕ, and H_ϕ are continuous at $\rho = a$. Application of these leads to four linear equations to solve for the four unknown coefficients. Omitting algebraic details, this process leads to

$$c_{m,n} = (-b_{m,n}/D)\{[(u^2/v^2) - 1]^2(im\lambda_n/a)^2 I_u K_u - [(\gamma u^2/v)(1/\eta)(I_u I_v'/I_v) - (\gamma_0 u/\eta_0) I_u'] \cdot [(\gamma u^2/v)(\eta I_v'/I_v) K_u - \gamma_0 u \eta_0 K_u']\} \quad (16)$$

and

$$c_{m,n}^* = (-b_{m,n}/D)(im\lambda_n/a^2)[(u^2/v^2) - 1]\gamma_0/\eta_0 \quad (17)$$

where

$$D = [(u^2/v^2) - 1]^2(im\lambda_n/a)^2 K_u^2 - [(\gamma u^2/v)(1/\eta)(K_u I_v'/I_v) - (\gamma_0 u/\eta_0) K_u'] \cdot [(\gamma u^2/v)(\eta I_v'/I_v) K_u - \gamma_0 u \eta_0 K_u'] \quad (18)$$

Here, we have used the following abbreviated notation $I_u = I_m(u_n a)$, $I_v = I_m(v_n a)$, $K_u = K_m(u_n a)$, $u = u_n$, $v = v_n$, and $\eta = i\mu\omega/\gamma$. The two coefficients for the internal fields can be obtained from

$$a_{m,n} = (u^2 b_{m,n} I_u + u^2 c_{m,n} K_u)/v^2 I_v \quad (19)$$

and

$$a_{m,n}^* = u^2 c_{m,n}^* K_u/v^2 I_v \quad (20)$$

To complete the statement of the formal solution of the posed problem, we observe that the Fourier inverse of (13) is

$$F_{m,n} = (1/\pi s)\int_0^s \int_0^{2\pi} K(\phi, z) e^{im\phi}\, d\phi \cos \lambda_n z\, dz \quad (21)$$

If we specialize this to an axial current I amp in a filamental strip of half-length l as indicated in Figure 2, we can replace (21) by

$$F_{m,n} = \int_0^l \cos \lambda_n z\, dz \int_{\phi_0 - \Delta/2}^{\phi_0 + \Delta/2} (I/\rho_0 \Delta) e^{im\phi}\, d\phi \quad (22)$$

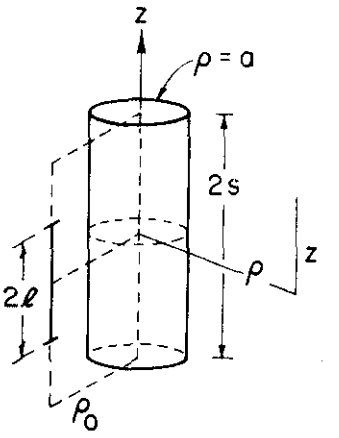

Fig. 2. Specialization to a linear current element adjacent to the conducting cylinder.

where Δ is the angular width of the strip. These elementary integrations yield

$$F_{m,n} = (I/\pi\rho_0)[\sin (m\Delta/2)/(m\Delta/2)] \cdot e^{im\phi_0}(\sin \lambda_n l)/\lambda_n s \quad (23)$$

The corresponding value for $b_{m,n}$ is given by (15). If $\Delta \to 0$ corresponding to a filamental line current, we have

$$b_{m,n} = (I/\pi)(\eta_0/\gamma_0) K_m(u_n \rho_0) e^{im\phi_0}(\sin \lambda_n l)/\lambda_n s \quad (24)$$

The corresponding electric dipole excitation is obtained by regarding $\lambda_n l$ as a small quantity whence

$$b_{m,n} \simeq (Il/\pi s)(\eta_0/\gamma_0) K_m(u_n \rho_0) e^{im\phi_0} \quad (25)$$

where Il is the current moment.

We shall now consider some aspects of the general solution before considering the static limit. Equation 16 can be written

$$c_{m,n} = -b_{m,n}[I_m(u_n a)/K_m(u_n a)]\Lambda_{m,n} \quad (26)$$

where

$$\Lambda_{m,n} = \frac{\left[\frac{\gamma}{v\eta}\frac{I_v'}{I_v} - \frac{\gamma_0}{u\eta_0}\frac{I_u'}{I_u}\right]\left[\frac{\gamma\eta}{v}\frac{I_v'}{I_v} - \frac{\gamma_0\eta_0}{u}\frac{K_u'}{K_u}\right] + \left(\frac{1}{v^2} - \frac{1}{u^2}\right)^2\left(\frac{m\lambda_n}{a}\right)^2}{\left[\frac{\gamma}{v\eta}\frac{I_v'}{I_v} - \frac{\gamma_0}{u\eta_0}\frac{K_u'}{K_u}\right]\left[\frac{\gamma\eta}{v}\frac{I_v'}{I_v} - \frac{\gamma_0\eta_0}{u}\frac{K_u'}{K_u}\right] + \left(\frac{1}{v^2} - \frac{1}{u^2}\right)^2\left(\frac{m\lambda_n}{a}\right)^2} \quad (27)$$

In the case of a perfectly conducting cylinder ($\gamma \to \infty$), we see that $\Lambda_{m,n} = 1$ and, in this case, $c_{m,n}^* = 0$ is a consequence of (17). An important special case of (27) is when $m = 0$. Then, in explicit notation,

$$\Lambda_{0,n} = \{(\gamma/v_n\eta)[I_0'(v_na)/I_0(v_na)] - (\gamma_0/u_n\eta_0)[I_0'(u_na)/I_0(u_na)]\} \div \{(\gamma/v_n\eta)[I_0'(v_na)/I_0(v_na)] - (\gamma_0/u_n\eta_0)[K_0'(u_na)/K_0(u_na)]\} \quad (28)$$

In this case, we also note that $c_{0,n}^* = 0$.

EXPLICIT FIELD EXPRESSIONS

We now consider the explicit forms for the electric Hertz potential Π, since this is of prime interest in calculating the fields in the principal plane $z = 0$. First of all, we note that this function for $\rho > a$ can be split into a primary and secondary portion as follows:

$$\Pi = \Pi_{pr} + \Pi_{sec}$$

The primary component, for $a < \rho < \rho_0$, is

$$\Pi_{pr} = (I/\pi)(\eta_0/\gamma_0) \sum_m \sum_n K_m(u_n\rho_0) I_m(u_n\rho) \cdot e^{im(\phi_0-\phi)}[(\sin \lambda_n l)/\lambda_n s] \cos \lambda_n z \quad (29)$$

For $\rho > \rho_0$, the corresponding expression is obtained by interchanging ρ_0 and ρ. Using a well-known addition theorem for modified Bessel functions, the summation over m is readily performed to yield

$$\Pi_{pr} = (I\eta_0/\pi\gamma_0) \sum_{n=0}^{\infty} K_0(u_n\rho_d) \cdot [(\sin \lambda_n l)/\lambda_n s] \cos \lambda_n z \quad (30)$$

where $\rho_d = [\rho^2 + \rho_0^2 - 2\rho\rho_0 \cos(\phi_0 - \phi)]^{1/2}$ is the radial distance from the observer to the source current element.

The secondary part of the electric Hertz potential in the region $\rho > a$ is conveniently written

$$\Pi_{sec} = -(I\eta_0/\pi\gamma_0) \sum_m \sum_n [K_m(u_n\rho_0)/K_m(u_na)] \cdot I_m(u_na) K_m(u_n\rho) \Lambda_{m,n} e^{im(\phi_0-\phi)} \cos \lambda_n z \quad (31)$$

where there is no apparent further simplicity.

To obtain the magnetic field components, we merely perform the differentiations indicated in (3) and (4). Restricting attention to the plane $z = 0$, it easily follows from (30) that the primary magnetic fields are

$$H_\rho^{pr} = [I\rho_0 \sin(\phi_0 - \phi)/\pi\rho_d] \cdot \sum_{n=0}^{\infty} K_1(u_n\rho_d)[(\sin \lambda_n l)/\lambda_n s]u_n \quad (32)$$

$$H_\phi^{pr} = \{I[\rho - \rho_0 \cos(\phi_0 - \phi)]\pi\rho_d\} \cdot \sum_{n=0}^{\infty} K_1(u_n\rho_d)[(\sin \lambda_n l)/\lambda_n s]u_n \quad (33)$$

where $\lambda_n = (2n + 1)\pi/2s$. On the other hand, the secondary fields that follow from (31) are

$$H_\rho^{sec} = (I/\pi\rho) \sum_{m=-\infty}^{+\infty} \sum_{n=0}^{\infty} \Lambda_{m,n}[K_m(u_n\rho_0)/K_m(u_na)] \cdot I_m(u_na) K_m(u_n\rho) im e^{im(\phi_0-\phi)}[(\sin \lambda_n l)/\lambda_n s] \quad (34)$$

and

$$H_\phi^{sec} = (I/\pi) \sum_{m=-\infty}^{+\infty} \sum_{n=0}^{\infty} \Lambda_{m,n}[K_m(u_n\rho_0)/K_m(u_na)] \cdot I_m(u_na) u_n K_m'(u_n\rho) e^{im(\phi_0-\phi)}[(\sin \lambda_n l)/\lambda_n s] \quad (35)$$

Using (32) through (35), the total fields are obtained exactly from $H_\rho = H_\rho^{pr} + H_\rho^{sec}$ and $H_\phi = H_\phi^{pr} + H_\phi^{sec}$ in the plane $z = 0$ and for $\rho > a$. The double series expansions in (34) and (35) are rather cumbersome, but the convergence is rapid when $|\gamma a|$, $|\gamma_0 a|$, and $|\gamma_0 s|$ are not excessively large compared with unity.

SOME SPECIFIC RESULTS FOR THE QUASI-STATIC LIMIT

Some simplification is achieved in the low frequency or quasi-static case. For example, if $|\gamma_0 a|$, $|\gamma_0\rho|$, and $|\gamma_0\rho_0|$ are all $\ll 1$, we can effectively replace u_n by λ_n everywhere. However, unless $|\gamma a|$ is also small, we must retain the form for v_n. But, of course, if the cylinder is very highly conducting, such that $|\gamma a| \gg 1$, the complicated factor $\Lambda_{m,n}$ can be replaced by unity in (34) and (35). Thus, in the case of a perfectly conducting cylinder and in the quasi-static limit, we can use (32) through (35) with u_n replaced everywhere by λ_n and $\Lambda_{m,n}$ by unity. Some numerical data for this case are given below. To present these results, the reader is referred to Figure 3, where we have chosen a cartesian co-

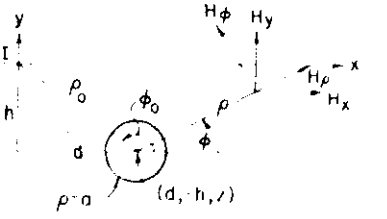

Fig. 3. Cross section (i.e., $z = 0$ plane) of the cylindrical target in the presence of the current cable.

ordinate system (x, y, z) with the current element at the origin. The field components H_x, H_y at the observer are thus obtained from

$$H_x = H_\rho \cos\phi - H_\phi \sin\phi$$

$$H_y = H_\rho \sin\phi + H_\phi \cos\phi$$

We can visualize this situation as the scanning of the resultant fields at the earth's surface $(y = 0)$ for a buried cylindrical target centered at $x = d$ and $y = -h$. In view of our quasi-static assumptions, we have neglected the effects of the induced currents in the region external to the cylinder.

In Figure 4, we plot the normalized horizontal field $2\pi hH_x/I$ as a function of the normalized horizontal coordinate x/h in the transverse plane $z = 0$. Here, we choose $a/h = 0.5$, $d/h = 1$, $l/s = 0.5$, and $s/h = 2$, 10, and ∞. The case $s/h = \infty$ is based on the solution for the corresponding two-dimensional problem of a parallel line source carrying the same current I (see appendix A). The corresponding results for $2\pi hH_y/I$ are illustrated in Figure 5. A similar set of curves is shown in Figures 6 and 7, where the only difference is that $d/h = 0$. This case corresponds to having the cylindrical target located directly beneath the current element.

FINAL REMARKS

The general features of the response curves in Figures 4 through 7 are not surprising. In all cases they have the form expected for a secondary source of current induced in the target that tends to oppose the fields of the primary current. Of particular interest is the fact that the half-lengths of the truncated cylinder must be greater than a factor of 10 of the burial depth h before the magnitude of the response

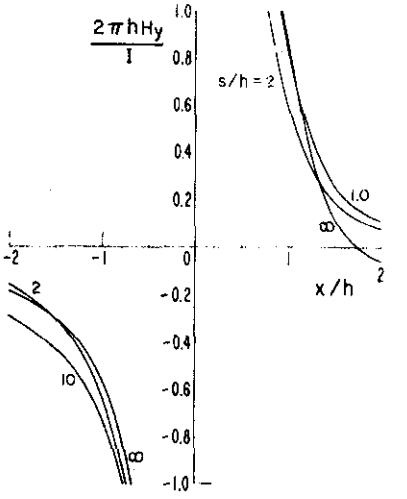

Fig. 5. Normalized vertical magnetic field as a function of the horizontal displacement for a buried and displaced finite cylinder, $a/h = 0.5$, $d/h = 1.0$, $l/s = 0.5$, $y = 0$.

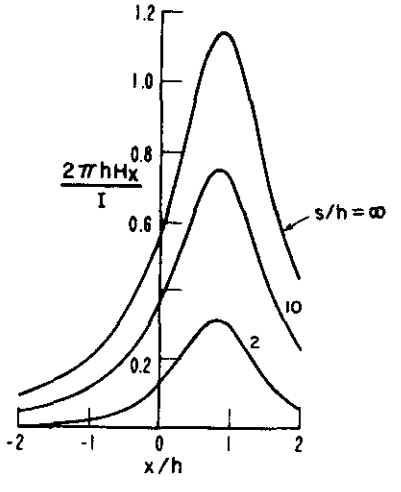

Fig. 4. Normalized horizontal magnetic field as a function of the horizontal displacement for a buried and displaced finite cylinder, $a/h = 0.5$, $d/h = 1.0$, $l/s = 0.5$, $y = 0$.

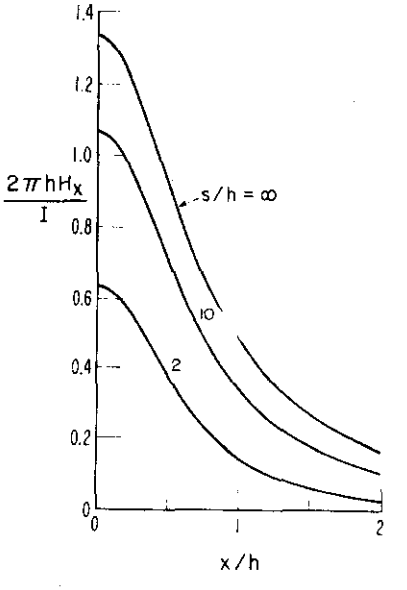

Fig. 6. Horizontal field for a finite cylinder buried directly beneath the source cable, $a/h = 0.5$, $d = 0$, $l/s = 0.5$, $y = 0$.

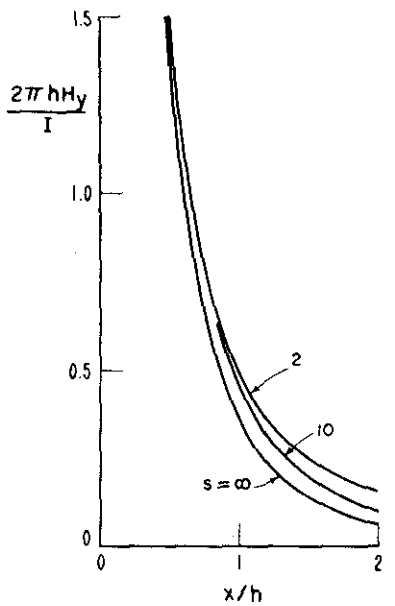

Fig. 7. Vertical field for a finite cylinder buried directly beneath the source cable, $a/h = 0.5$, $d = 0$, $l/s = 0.5$, $y = 0$.

approaches that for an infinite cylinder with the same transverse dimensions. This is an important factor to keep in mind when two-dimensional models are being employed to simulate the scattering from finite structures.

APPENDIX A: TWO-DIMENSIONAL MODEL

For comparison purposes, it is useful to consider the purely two-dimensional problem of a uniform line current parallel to a homogeneous circular cylinder of radius, a, with conductivity σ and permeability μ [*Wait*, 1952 (in equation 13 replace μ_2/μ_1 by $n\mu_2/\mu_1$, and in equation 14 replace $(k \pm n)$ by $n(k \pm 1)$), 1959]. This can be considered as the limit of the finite cylinder configuration as $s \to \infty$.

Using cylindrical coordinates (ρ, ϕ, z), the cylinder is defined by $\rho < a$ for $-\infty < z < \infty$. The line source is located at $\rho = \rho_0$ and $\phi = \phi_0$ where $\rho_0 > a$. The primary electric field of the line source has only a z component, given by

$$E_z^{pr} = (-i\mu_0\omega I/2\pi) K_0(\gamma_0\rho_d) \tag{A1}$$

where

$$\rho_d = [\rho_0^2 + \rho^2 - 2\rho_0\rho \cos(\phi_0 - \phi)]^{1/2} \tag{A2}$$

The corresponding magnetic field components are

$$H_\phi^{pr} = (1/i\mu_0\omega)(\partial E_z^{pr}/\partial\rho)$$

$$= \{I[\rho - \rho_0 \cos(\phi_0 - \phi)]/2\pi\rho_d\}\gamma_0 K_1(\gamma_0\rho_d) \tag{A3}$$

$$H_\rho^{pr} = (-1/\rho i\mu_0\omega)(\partial E_z^{pr}/\partial\phi)$$

$$= [+I\rho_0 \sin(\phi_0 - \phi)/2\pi\rho_d]\gamma_0 K_1(\gamma_0\rho_d) \tag{A4}$$

In the quasi-static case where $|\gamma_0\rho_d| \ll 1$, these are expressible in the simpler form

$$H_\phi^{pr} \simeq I[\rho - \rho_0 \cos(\phi_0 - \phi)]/2\pi\rho_d^2 \tag{A5}$$

and

$$H_\rho^{pr} \simeq I\rho_0 \sin(\phi_0 - \phi)/2\pi\rho_d^2 \tag{A6}$$

Using a previously known solution, we can write down the corresponding forms for the secondary fields external to the cylinder. The exact expressions for the two magnetic field components for the region $\rho > a$ are [*Wait*, 1952]

$$H_\phi^{sec} = -(I/2\pi\rho) \sum_{m=-\infty}^{+\infty} q_m[K_m(\gamma_0\rho_0)/K_m(\gamma_0 a)] \cdot I_m(\gamma_0 a)e^{-im(\phi-\phi_0)}\gamma_0\rho_0 K_m'(\gamma_0\rho) \tag{A7}$$

and

$$H_\rho^{sec} = -(I/2\pi\rho) \sum_{m=-\infty}^{+\infty} q_m[K_m(\gamma_0\rho_0)/K_m(\gamma_0 a)] \cdot I_m(\gamma_0 a)e^{-im(\phi-\phi_0)} im K_m(\gamma_0\rho) \tag{A8}$$

where

$$q_m = \{-(1/\eta)[I_m'(\gamma a)/I_m(\gamma a)] + (1/\eta_0)[I_m'(\gamma_0 a)/I_m(\gamma_0 a)]\}/\{(1/\eta)[I_m'(\gamma a)/I_m(\gamma a)] - (1/\eta_0)[K_m'(\gamma_0 a)/K_m(\gamma_0 a)]\} \tag{A9}$$

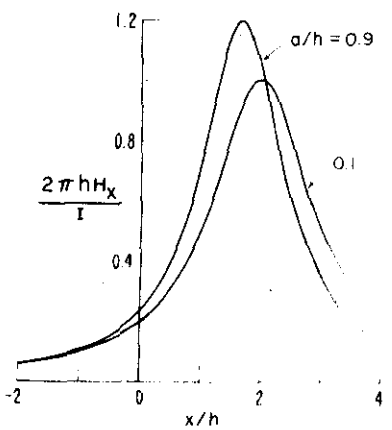

Fig. A1. Normalized field as a function of the horizontal displacement for a buried infinite cylinder, $d/h = 2$, $y = 0$.

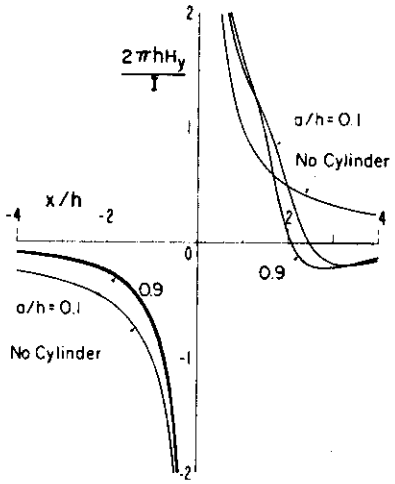

Fig. A2. Normalized field as a function of the horizontal displacement for a buried infinite cylinder, $d/h = 2$, $y = 0$.

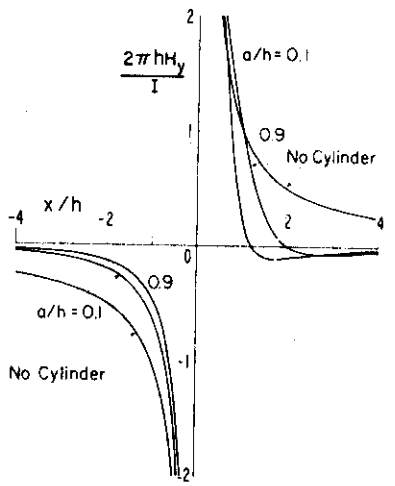

Fig. A4. Normalized field as a function of the horizontal displacement for a buried infinite cylinder, $d/h = 1$, $y = 0$.

The quasi-static forms for the secondary fields are then found to be

$$H_\phi^{sec} \simeq (I/2\pi\rho) \sum_{m=1}^{\infty} q_m (a^{2m}/\rho_0{}^m \rho^m) \cdot \cos m(\phi - \phi_0) + H_{0\phi}^{sec} \quad \text{(A10)}$$

and

$$H_\rho^{sec} \simeq (-I/2\pi\rho) \sum_{m=1}^{\infty} q_m (a^{2m}/\rho_0{}^m \rho^m) \cdot \sin m(\phi - \phi_0) \quad \text{(A11)}$$

where

$$H_{0\phi}^{sec} \simeq (I/2\pi\rho) q_0 \ln (0.89\gamma_0\rho_0)/\ln (0.89\gamma_0 a) \quad \text{(A12)}$$

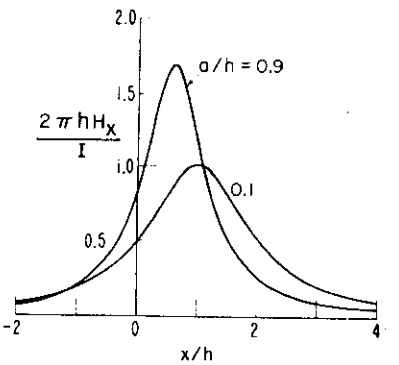

Fig. A3. Normalized field as a function of the horizontal displacement for a buried infinite cylinder, $d/h = 1$, $y = 0$.

In the limiting case where we let $\gamma_0 \to 0$, we see that $q_m = -1$ and $q_0 = -1$, and $H_{0\phi}{}^{sec} \simeq -I/(2\pi\rho)$. Then (A10) and (A11) can be summed as geometric series to give

$$H_\phi^{sec} = (-I/2\pi\rho) \cdot [1 - (a^2/\rho_0\rho) \cos (\phi - \phi_0)]/[1 - 2(a^2/\rho_0\rho) \cdot \cos (\phi - \phi_0) + (a^2/\rho_0\rho)^2] \quad \text{(A13)}$$

and

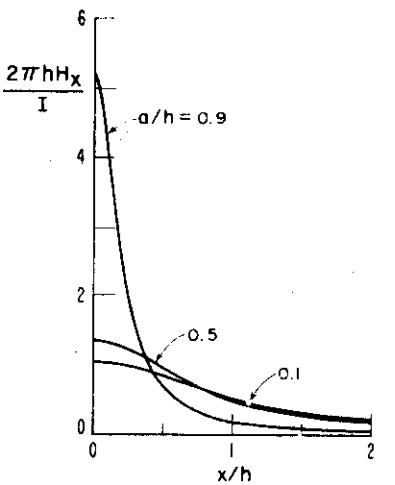

Fig. A5. Normalized field as a function of the horizontal displacement for a buried infinite cylinder, $d/h = 0$, $y = 0$.

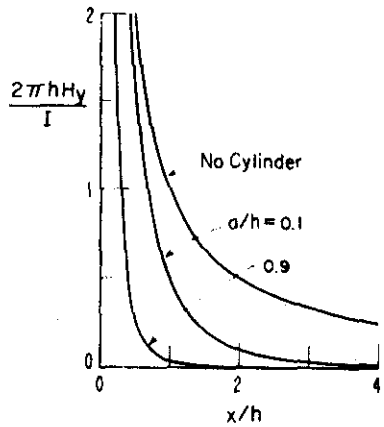

Fig. A6. Normalized field as a function of the horizontal displacement for a buried infinite cylinder, $d/h = 0$, $y = 0$.

$$H_\rho^{sec} = (I/2\pi\rho) \cdot [(a^2/\rho_0\rho)\sin(\phi - \phi_0)]/[1 - 2(a^2/\rho_0\rho) \cdot \cos(\phi - \phi_0) + (a^2/\rho_0\rho)^2] \quad \text{(A14)}$$

Again, referring to Figure 3, we consider the total H_x and H_y components in the plane $y = 0$, where now the buried cylinder (of perfect conductivity) is of infinite length. In Figure A1 we show a plot of $2\pi hH_x/I$ as a function of x/h for $d/h = 2$, for $a/h = 0.9$, and $a/h = 0.1$. The corresponding results for $2\pi hH_y/I$ are shown in Figure A2. Similar curves are shown in Figures A3 and A4, where $d/h = 1$, and finally in Figures A5 and A6 where $d/h = 0$.

REFERENCES

Fox, J. (Ed.) (1964), *Quasi-Optics*, pp. 1–25, Polytechnic, New York.

Harrington, R. F. (1968), *Field Computation by Moment Methods*, pp. 82–102, Macmillan, New York.

Wait, J. R. (1952), A cylindrical ore body in the presence of a cable carrying an oscillating current, *Geophys.*, *17*(2), 378–386.

Wait, J. R. (1959), *Electromagnetic Radiation from Cylindrical Structures*, pp. 182–183, Pergamon, New York.

Ward, S. H., and H. F. Morrison (Eds.) (1971), Special Issue on Electromagnetic Scattering, *Geophys.*, *36*(1), 1–183.

Geofisica Internacional, Vol. 12, No. 4,
245-266, October 1972

(Received from publisher - June 1974)
(Submitted - October 1973)

GEOFISICA
INTERNACIONAL

REVISTA DE LA UNION GEOFISICA MEXICANA, AUSPICIADA POR EL INSTITUTO DE GEOFISICA DE LA UNIVERSIDAD NACIONAL AUTONOMA DL MEXICO

Vol. 12 México, D. F., 1o. de octubre de 1972 Núm. 4

ELECTROMAGNETIC RESPONSE OF A CONDUCTING CYLINDER OF FINITE LENGTH

DAVID A. HILL* and
JAMES R. WAIT**

RESUMEN

Los campos electromagnéticos se calculan para un cilindro finito, excitado por una fuente circular y, para propósitos de comparación, mediante excitación de una fuente lineal. Estos resultados también se comparan con los del caso del cilindro infinito. Se encuentra que la importancia relativa de la componente con simetría acimutal de la corriente disminuye cuando el cilindro es finito. Este artículo ha sido motivado por las convincentes sugerencias de S. K. Singh relativas a la posible importancia de la corriente con simetría acimutal inducida en cuerpos alargados de minerales, por algunas configuraciones de fuentes electromagnéticas utilizadas en la exploración geofísica.

ABSTRACT

The electromagnetic fields are calculated for a truncated cylinder excited by a loop source and, for comparision, for excitation by a line source. These results are also compared with the infinite cylinder case. It is found that the relative importance of the azimuthally symmetric component of the current is diminished when the cylinder is truncated. This paper is prompted by the cogent suggestions of S. K. Singh concerning the possible importance of the symmetrical current induced in elongated ore bodies by certain electromagnetic source configurations used in geophysical exploration.

* *Institute for Telecommunication Sciences, Office of Telecommunications*
** *Cooperative Institute for Research in Environmental Sciences University of Colorado, National Oceanic and Atmospheric Administration U.S. Department of Commerce, Boulder, Colorado.*

INTRODUCTION

In a previous analysis (Wait and Hill 1973), we formulated the boundary value problem of a truncated cylindrical region excited by a specified distribution of electric current over a concentric cylindrical surface. Preliminary numerical results were given for excitation by an electric line source of finite length. Here we consider the extension for excitation by a long slender loop. Also we examine the importance of the azimuthally symmetric component of the current induced in the cylinder. The effect of truncation and type of excitation on the azimuthally symmetric current component provides insight to the scattering mechanism for scatterers of finite length.

Quantitative information on this subject is important from the standpoint of determining the performance of electromagnetic source location schemes in mine rescue operations. For example, we can anticipate major distortions of the surface fields for a buried source if metallic conductors, such as pipes and rails, are in the vicinity. It is also possible that the truncated cylinder could serve as a convenient model for an elongated sulphide metallic body that is to be detected by a grounded or non-grounded e.m. exploration technique.

FORMULATION

For the sake of simplicity, we consider a perfectly conducting cylinder excited by a finite line source as shown in Figure 1. The cylinder occupies the space $\rho < a$ and $|z| < s$, and the region external to the cylinder ($\rho > a$) has conductivity σ, and magnetic permeability μ_o. The problem is made tractable by requiring that the normal current density be zero at the two horizontal surfaces where $|z| = s$. This condition requires that the normal electric field is also zero at $|z| = s$. Because of this cor ition, we are not actually treating an isolated finite cylinder, but we expect the solution to tell us something about the effects of truncation.

If we excite the cylinder with a z-directed line current, I exp ($i\omega t$),

from $z = -\ell$ to $z = +\ell$, then the solution is even about $z = 0$. The primary magnetic field components, H_ρ^{pr} and H_ϕ^{pr}, are given by (Wait and Hill, 1973).

$$H_\rho^{pr} = \frac{I\rho_o \sin(\phi_o - \phi)}{\pi\rho_d} \sum_{n=0}^{\infty} K_1(u_n\rho_d) \frac{\sin\lambda_n\ell}{\lambda_n s} u_n \cos\lambda_n z, \qquad (1)$$

$$H_\phi^{pr} = \frac{I[\rho - \rho_o\cos(\phi_o - \phi)]}{\pi\rho_d} \sum_{n=0}^{\infty} K_1(u_n\rho_d) \frac{\sin\lambda_n\ell}{\lambda_n s} u_n \cos\lambda_n z$$

Where $\rho_d = [\rho^2 + \rho_o^2 - 2\rho\rho_o\cos(\phi_o - \phi)]^{1/2}$,

$$\lambda_n = (2n+1)\pi/(2s), \quad u_n = [\lambda_n^2 + \gamma_o^2]^{1/2},$$

$$\gamma_o^2 = i\omega\mu_o\sigma,$$

and K_m is a modified Bessel function of the second kind. The secondary magnetic fields, H_ρ^{sec} and H_ϕ^{sec}, are given by

$$H_\rho^{sec} = \frac{I}{\pi\rho} \sum_{m=-\infty}^{\infty} \sum_{n=0}^{\infty} \frac{I_m(u_n a)}{K_m(u_n a)} K_m(u_n\rho_o) K_m(u_n\rho) im \ldots$$

$$\exp[im(\phi_o - \phi)] \frac{\sin\lambda_n\ell}{\lambda_n s} \cos\lambda_n z, \qquad (2)$$

$$H_{\phi}^{sec} = \frac{I}{\pi} \sum_{m=-\infty}^{\infty} \sum_{n=0}^{\infty} \frac{I_m(u_n a)}{K_m(u_n a)} K_m(u_n \rho_o)\, u_n K'_m(u_n \rho) \ldots$$

$$\exp[im(\phi_o - \phi)] \frac{\sin \lambda_n \ell}{\lambda_n s} \cos \lambda_n z,$$

where I_m is a modified Bessel function of the first kind. The general expressions for the secondary fields of a cylinder of finite conductivity are given by Wait and Hill (1973).

If we consider two oppositely directed line sources to approximate a long slender loop source, then the line source solutions for the primary and secondary fields are directly applicable. If the positive line source is located at (ρ_o^+, ϕ_o^+) and the negative line source is located at (ρ_o^-, ϕ_o^-), then the secondary fields for loop excitation, $H_{\rho}^{\ell,sec}$, are given by

$$H_{\rho}^{\ell,sec} = H_{\rho}^{sec}\Big|_{\substack{\rho_o = \rho_o^+ \\ \phi_o = \phi_o^+}} - H_{\rho}^{sec}\Big|_{\substack{\rho_o = \rho_o^- \\ \phi = \phi_o^-}}$$

$$H_{\phi}^{\ell,sec} = H_{\phi}^{sec}\Big|_{\substack{\rho_o = \rho_o^+ \\ \phi_o = \phi_o^+}} - H_{\phi}^{sec}\Big|_{\substack{\rho_o = \rho_o^- \\ \phi_o = \phi_o^-}}$$

where H_{ρ}^{sec} and H_{ϕ}^{sec} are given by (2).

Since we are particularly interested in the behavior of the azimuth-

ally symmetric (m = 0) term of the secondary field, it is useful to examine the behavior of this term analytically as the loop width w goes to zero. For the case of broadside excitation ($\rho_o^+ = \rho_o^-$) the loop width w is equal to $\rho\,\Delta$, where Δ is the angular separation of the two line sources. We examine only the ϕ component, since the ρ component of the secondary field has no m = 0 term. The limit of $H_\phi^{\ell,sec}$ as w (or Δ) goes to zero is

$$H_\phi^{\ell,\,sec} = H_\phi^{sec}\Big|_{\phi_o = \phi_o + \frac{\Delta}{2}} - H_\phi^{sec}\Big|_{\phi_o = \phi_o - \frac{\Delta}{2}} \simeq \frac{w}{\rho_o}\,\frac{\partial H_\phi^{sec}}{\partial \phi_o} \qquad (4)$$

By noting that $\partial/\partial\,\phi_o$ introduces a factor im in (2), we conclude that the m = 0 term is not excited by broadside excitation.

For the case of end-on excitation ($\phi_o^+ = \phi_o^-$), we again examine the result as w goes to zero. In this case, the limit of $H_\phi^{\ell,sec}$ is given by

$$H_\phi^{\ell',sec} = H_\phi^{sec}\Big|_{\rho_o = \rho_o + \frac{w}{2}} - H_\phi^{sec}\Big|_{\rho_o = \rho_o - \frac{w}{2}} \simeq w\,\frac{\partial H_\phi^{sec}}{\partial \rho_o} \qquad (5)$$

By Examing (5) and (2), we note that the m = 0 term is excited by end-on excitation.

Since the effect of truncation on the secondary fields is of interest, it is useful to examine the limit of an infinite cylinder. If we let $\ell = s$ and let s approach ∞, then u_m approaches γ_o and λ_n approaches zero. Consequently, the n summation in (2) reduces to

$$\sum_{n=0}^{\infty} \frac{\sin \lambda_n s}{\lambda_n s} \rightarrow \frac{2}{\pi} \sum_{n=0}^{\infty} \frac{(-1)^n}{2n+1} = \frac{1}{2}, \qquad (6)$$

where a summation formula by Wheelon (1968) has been used. By applying (6) to (12), the secondary fields for an infinite cylinder, $H_\rho^{sec,\infty}$ and $H_\phi^{sec,\infty}$, are found to be

$$H_\rho^{sec,\infty} = \frac{I}{2\pi\rho} \sum_{m=-\infty}^{\infty} \frac{I_m(\gamma_o a)}{K_m(\gamma_o a)} K_m(\gamma_o \rho_o) K_m(\gamma_o \rho) \text{ im} \ldots$$

$$\exp [\text{im}(\phi_o - \phi)], \qquad (7)$$

$$H_\phi^{sec,\infty} = \frac{I}{2\pi} \sum_{m=-\infty}^{\infty} \frac{I_m(\gamma_o a)}{K_m(\gamma_o a)} K_m(\gamma_o \rho_o) \gamma_o K'_m(\gamma_o \rho) \ldots$$

$$\exp [\text{im}(\phi_o - \phi)]$$

The results in (7) agree with the known two dimensional result (Wait, 1952; 1959).

NUMERICAL RESULTS FOR LINE SOURCE EXCITATION

It is useful to examine some numerical results for line source excitation before examining loop excitation. The special geometry for numerical results is shown in Figure 2 with the line source at the origin of a cartesian coordinate system x, y, z. The magnetic field components H_x and H_y are obtained from

$$H_x = H_\rho \cos\phi - H_\phi \sin\phi \qquad (8)$$

$$H_y = H_\rho \sin\phi + H_\phi \cos\phi$$

All results are computed for an observer on the x-axis. Consequently, the situation could involve scanning the vertical and horizontal magnetic fields (H_y and H_x) at the earth's surface ($y = 0$) for a buried cylinder centered at $x = d$ and $y = -h$.

In Figure 3, we show the magnitude of the normalized vertical secondary magnetic field $2\pi h\,|H_y^{sec}|/I$ as well as the $m = 0$ term for an infinite cylinder. For all cases in this section, we choose $d = 0$, $a/h = 0.5$, and $|\gamma_0 h| = 0.5$. Since $d = 0$, the curves are symmetrical about $x = 0$. In Figure 4, we show the magnitude of the normalized horizontal magnetic field $2\pi h|H_x^{sec}|/I$ as well as the $m = 0$ term for an infinite cylinder. Results in Figures 3 and 4 are obtained from (7) and (8).

In Figure 5, we show the case similar to that of Figure 3, but for a truncated cylinder with $s/h = 2.0$ and $\ell/s = 0.5$. Note that the relative importance of the $m = 0$ terms is somewhat reduced here due to the truncation of the cylinder. In Figure 6, we show the case similar to that in Figure 4, but again for a truncated cylinder with $s/h = 2.0$ and $\ell/s = 0.5$. Again the relative magnitude of the $m = 0$ term is somewhat reduced due to the truncation. Results in Figures 5 and 6 are obtained from (2) and (8).

NUMERICAL RESULTS FOR LOOP EXCITATION

The geometry for loop excitation is also shown in Figure 2. The positive line source is located on the x-axis at $x = w/2$ and the negative line source is on the x-axis at $x = -w/2$. The required values of ρ_o^+, ρ_o^-, ϕ_o^+, and ϕ_o^- are given by:

$$\rho_o^+ = [h^2 + (d - w/2)^2]^{1/2}, \quad \rho_o^- = [h^2 + (d + w/2)^2]^{1/2}, \ldots$$

$$\phi_o^+ = \tan^{-1}[h/(-d + w/2)], \phi_o^- = \tan^{-1}[h/(-d - w/2)]. \quad (9)$$

The results in this section are obtained from (3) and (8). We again can visualize the situation as scanning the vertical and horizontal magnetic field components at the surface (y = 0) for a buried cylinder with a loop excitation. One possible reason for using a loop is that no grounding of the current-carrying cable is required.

In Figures 7 and 8, we show the magnitudes of the vertical and horizontal secondary normalized components, $2\pi h^2 |H_y^{\ell,sec}|/(w\ I)$ and $2\pi\ h^2 |H_x^{\ell,sec}|/(w\ I)$, for an infinite cylinder. Again we have chosen a/h = 0.5 and $|\gamma_o h| = 0.5$, but we have taken d/h equal to 0.5 so that the m = 0 term will be nonzero. We can see from (4) that the m = 0 term would be zero for d = 0 because ρ_o^+ would equal ρ_o^-. Also, while the m = 0 terms are symmetric about x/h = 0.5, the total secondary fields are not.

In Figures 9 and 10, we show the same cases for a truncated cylinder with s/h = 2.0 and ℓ/s = 0.5, and the results are quite similar to those in Figures 7 and 8. The total field which would be measured includes also a primary vertical component from the loop.

FINAL REMARKS

The results for loop excitation in Figures 7-10 are qualitatively similar to those for line source excitation in Figures 3-6, but they show a reduced importance of the azimuthally symmetric m = 0 term. Of course the primary fields of the loop are quite different and, as a result, the measured vertical component would differ considerably from that of a line source.

Also it has been demonstrated in Figures 5, 6, 9, and 10, that truncation of the cylinder results in a reduced magnitude of the m = 0 term. This is expected on physical reasoning since the symmetric current must be zero at the ends, but other currents could flow up one side of the cylinder and down the other. As pointed out by Singh (1973), it is important to consider the effect of the m = 0

term since it may be very significant. It's effect was ignored in an early paper (Wait 1952) on the subject, although the general theory given there contained it.

The numerical results shown in Figs. 3 to 10 inclusive are restricted to the value $|\gamma_0 h| = 0.5$. This is a typical value of the parameter when the surrounding medium is finitely conducting. As pointed out by Singh (1973), this parameter should not be assumed zero when modelling ore bodies immersed by country rock. However, the conclusions and general nature of our results are not affected by the precise value of $|\gamma_0 h|$. To illustrate this point, we illustrate the effect of finite γ_0 for the infinite cylinder case and for line source excitation only in Figs. 11 and 12 with the pertinent parameters indicated on the figure. Corresponding curves for a truncated cylinder are illustrated in Figs. 13 and 14. Here the case $\gamma_0 = 0$ corresponds to a purely static condition. The general theoretical results given by Wait and Hill (1973) also allow the effect of finite conductivity of the cylinder to be accounted for. We plan to carry out these calculations in the near future.

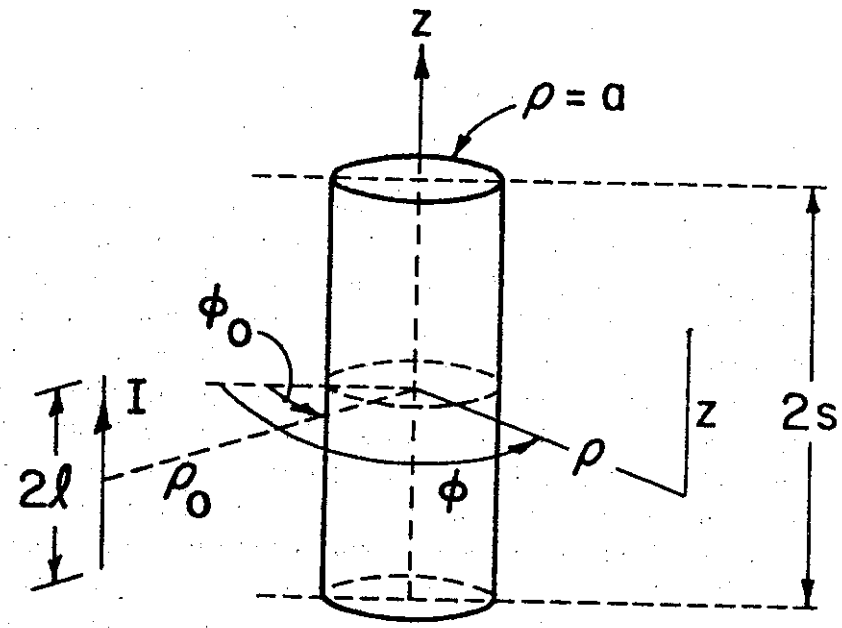

Figure 1. Geometry for a finite length cylinder and line source.

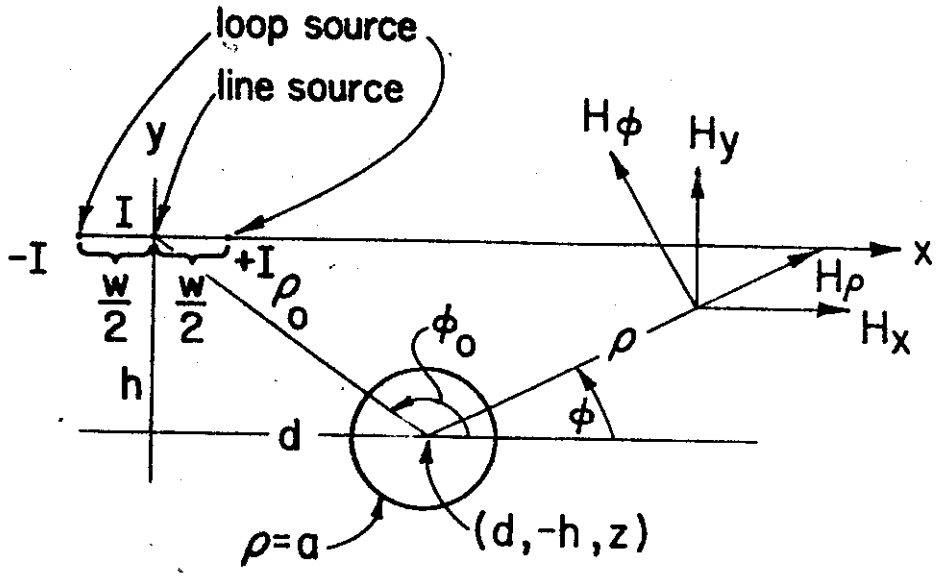

Figure 2. Special geometry for numerical results, both line source and loop excitation.

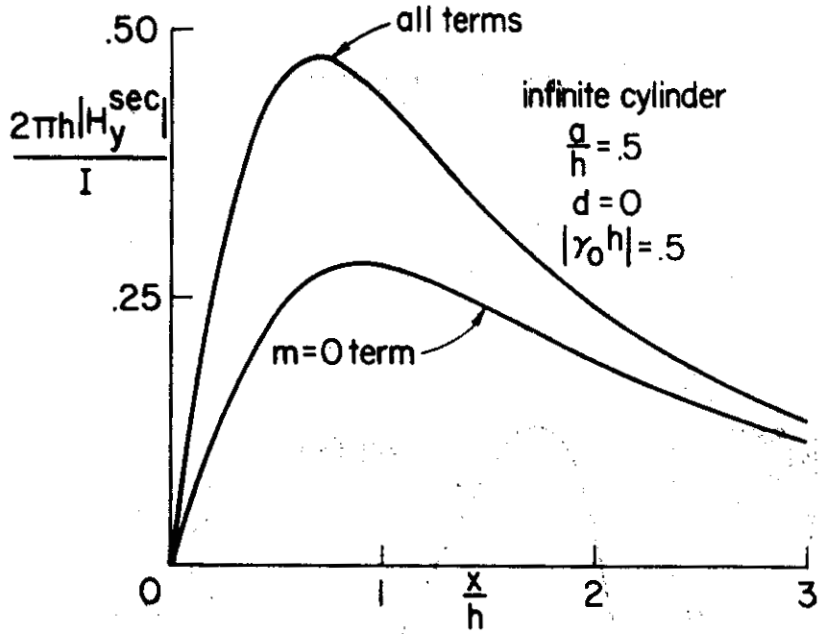

Figure 3. Normalized vertical secondary magnetic field of an infinite cylinder for line source excitation. All numerical results are for y and z equal zero.

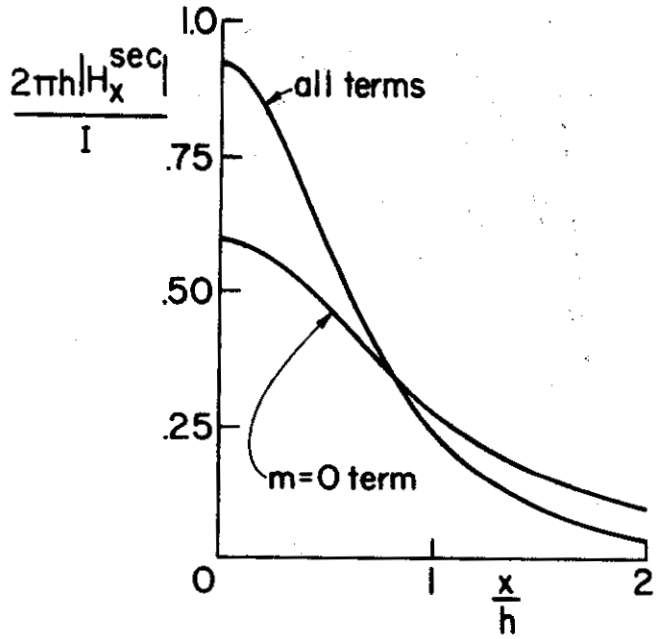

Figure 4. Normalized horizontal secondary magnetic field of an infinite cylinder for line source excitation.

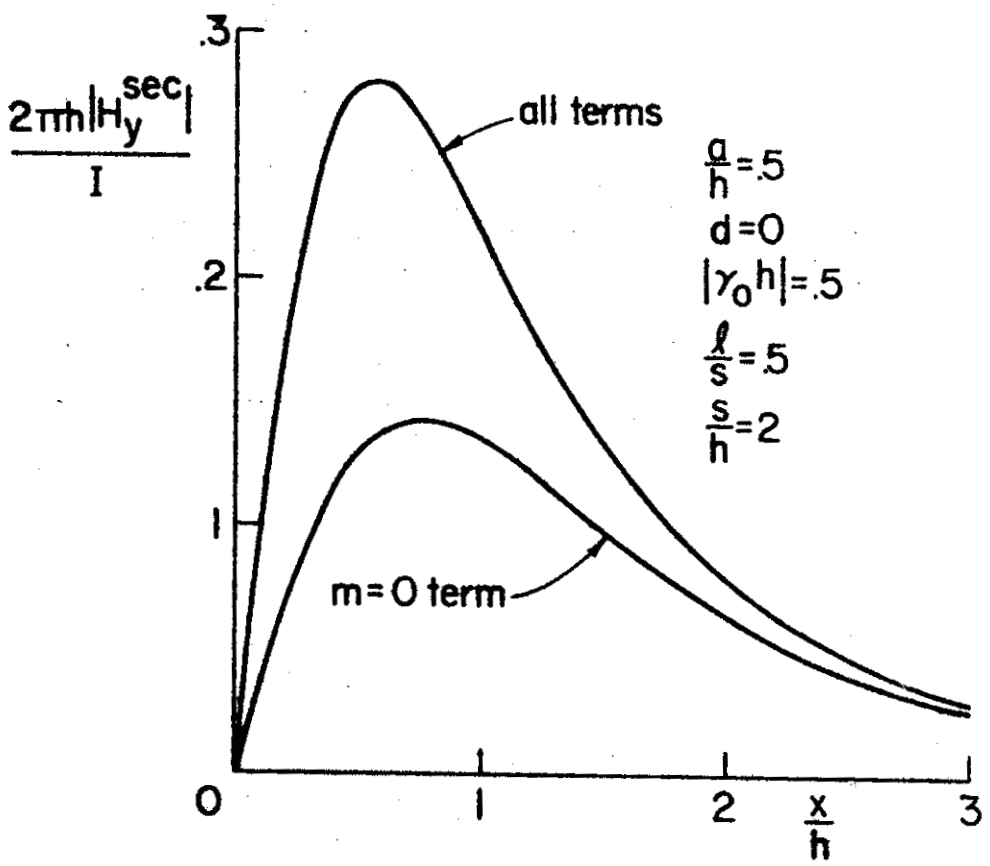

Figure 5. Normalized vertical secondary magnetic field of a truncated cylinder for line source excitation.

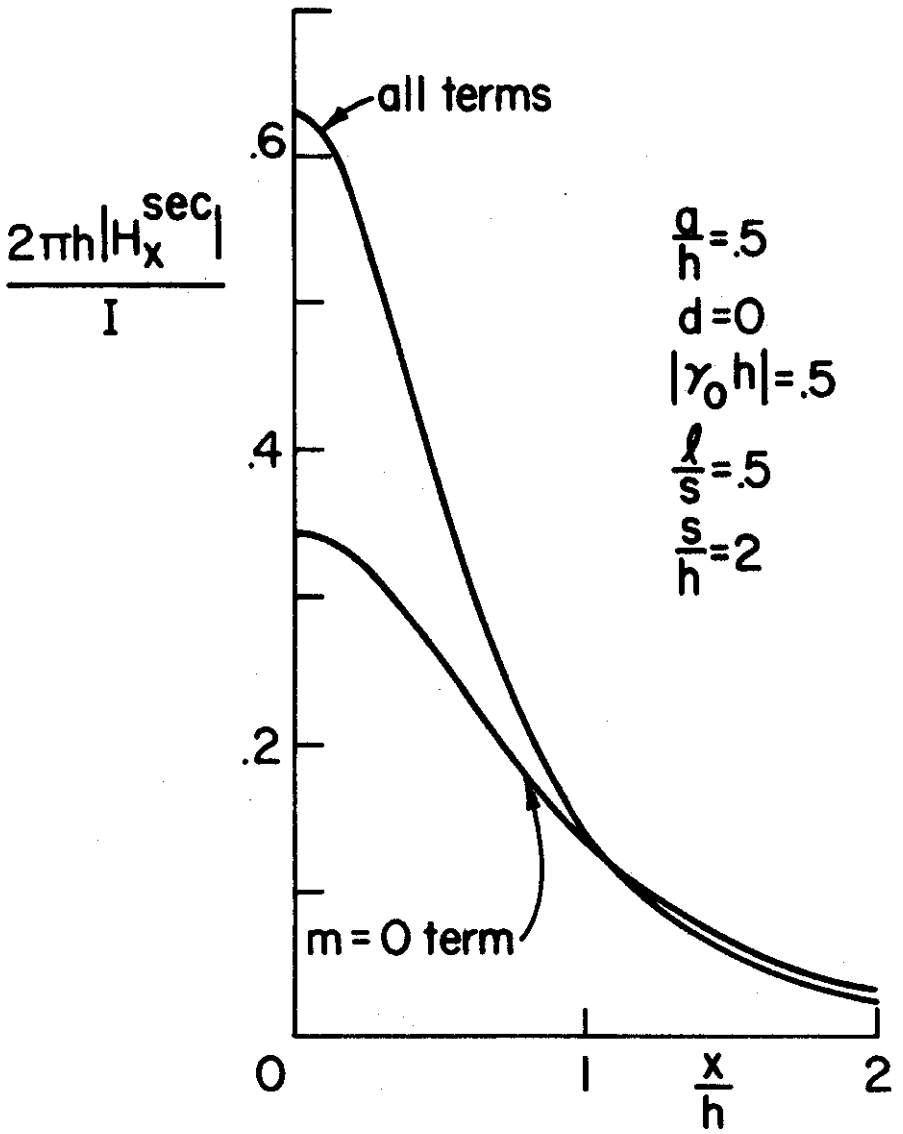

Figure 6. Normalized horizontal secondary magnetic field of a truncated cylinder for line source excitation.

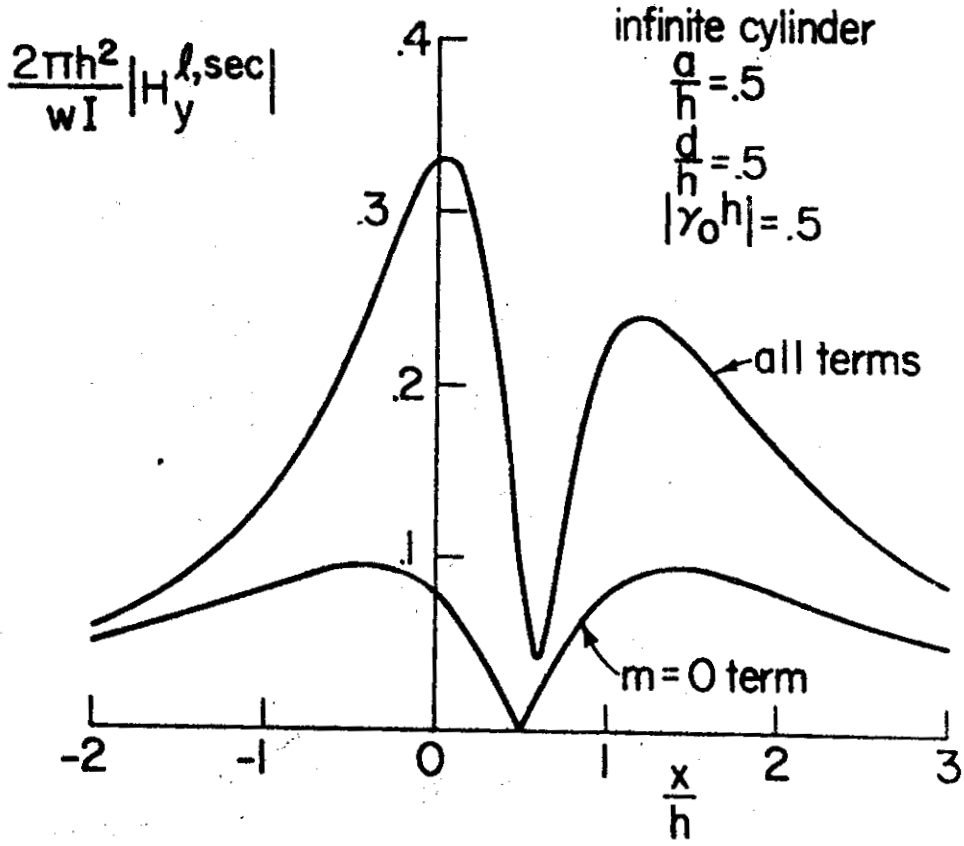

Figura 7. Normalized vertical secondary magnetic field of an infinite cylinder for loop excitation.

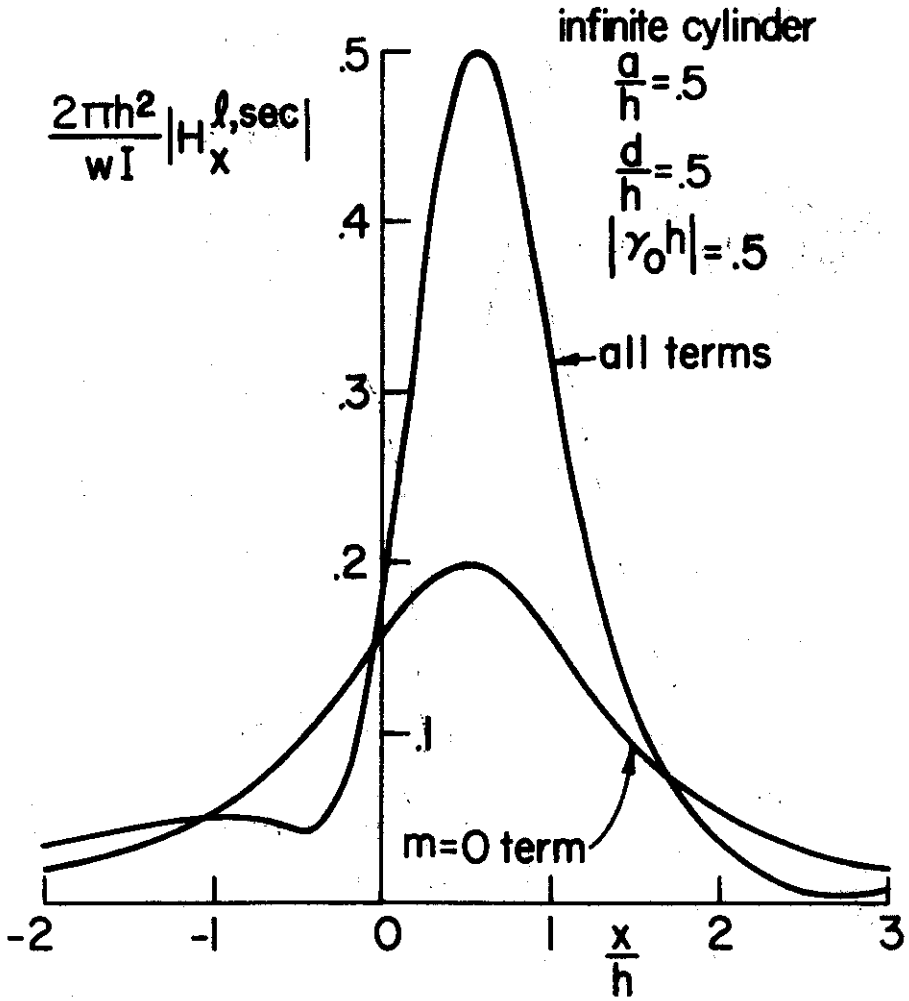

Figure 8. Normalized horizontal secondary magnetic field of an infinite cylinder for loop excitation.

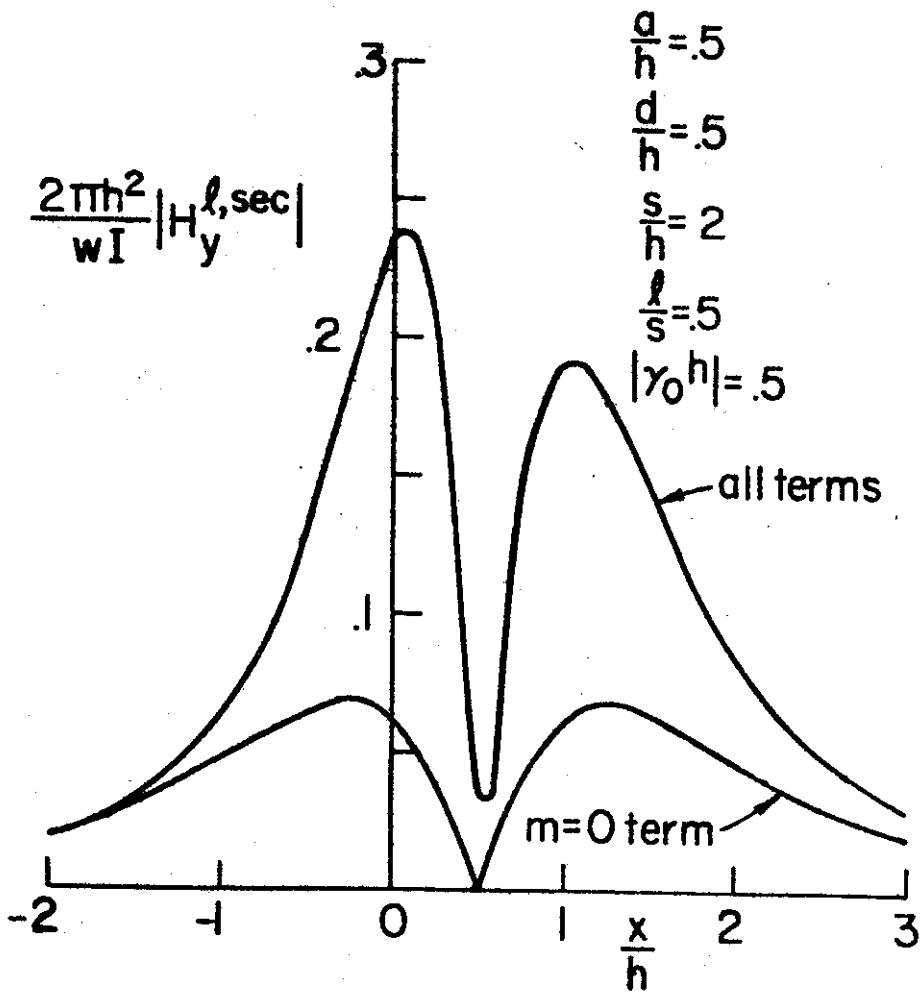

Figure 9. Normalized vertical secondary magnetic field of a truncated cylinder for loop excitation.

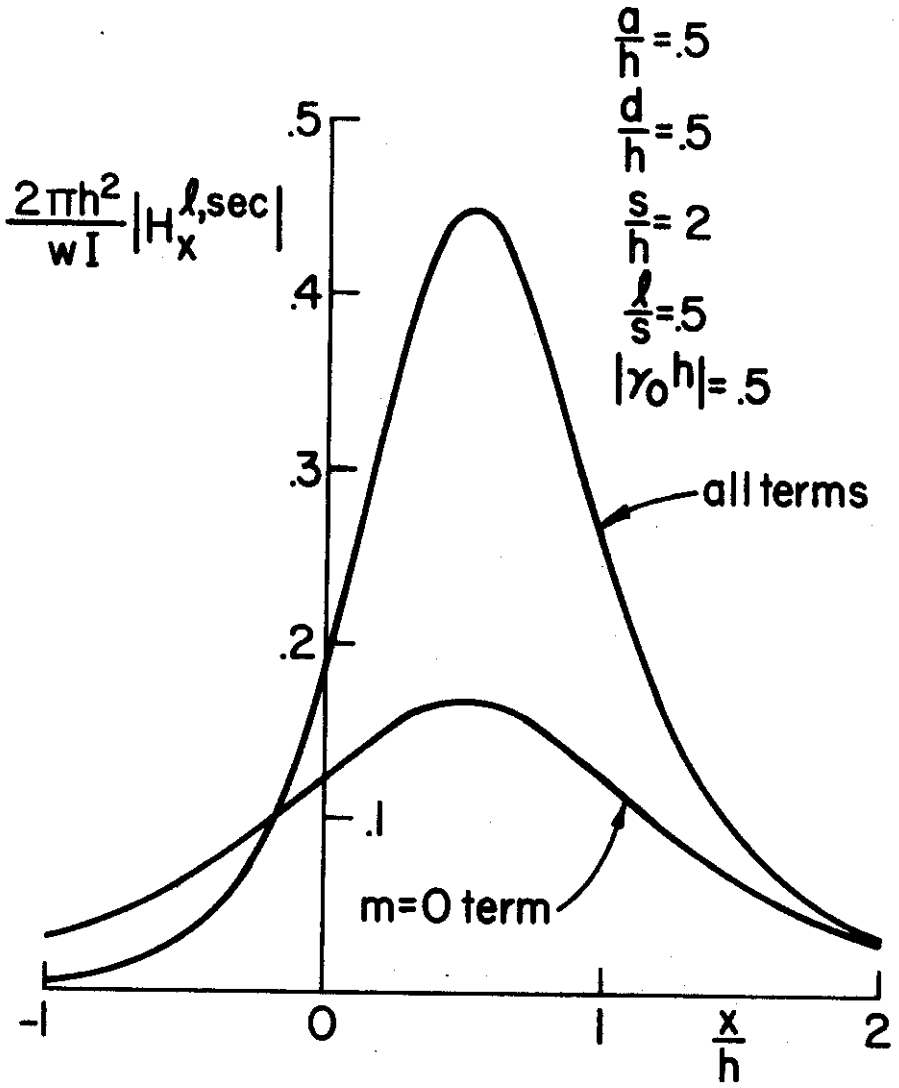

Figure 10. Normalized horizontal secondary magnetic field of a truncated cylinder for loop excitation.

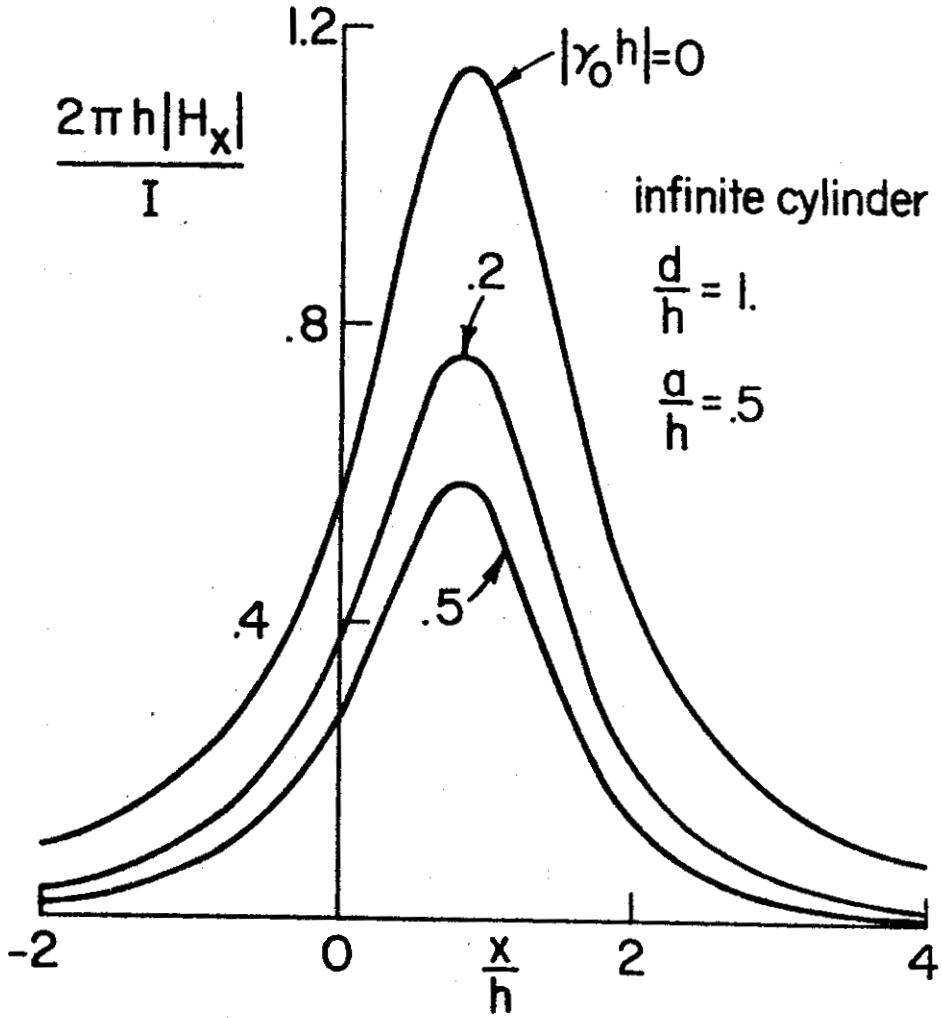

Figure 11. Effect of γ_0 on the horizontal magnetic field for the infinite cylinder case.

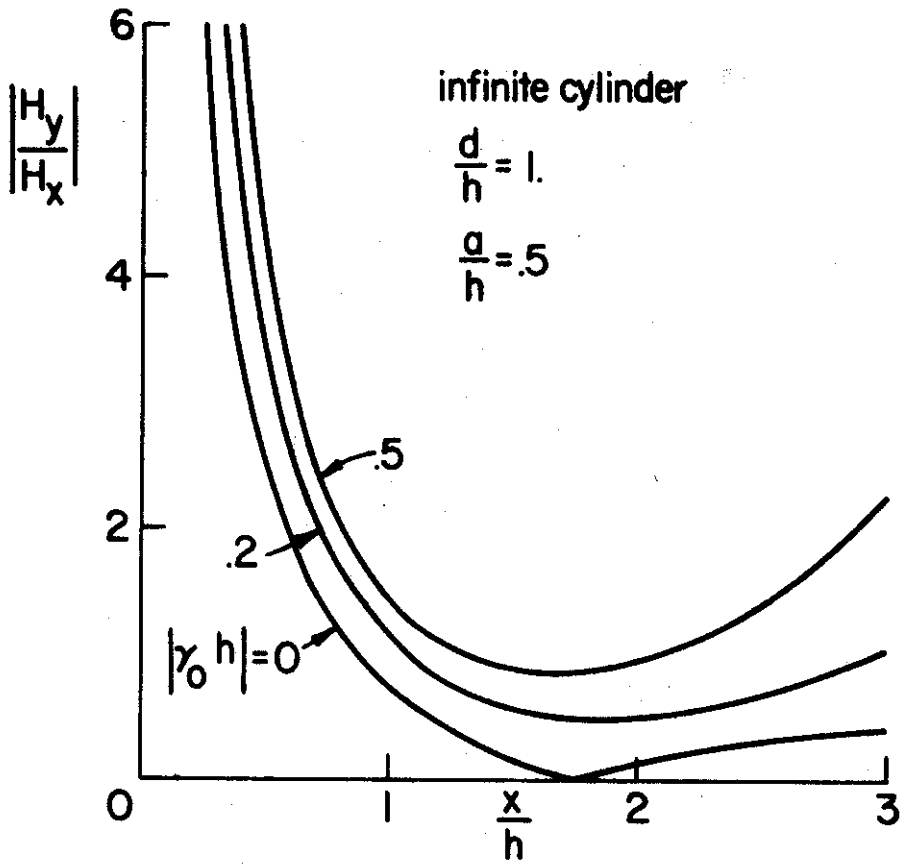

Figure 12. Effect of γ_0 on the magnitude of the ratio of vertical to horizontal magnetic field (infinite cylinder case).

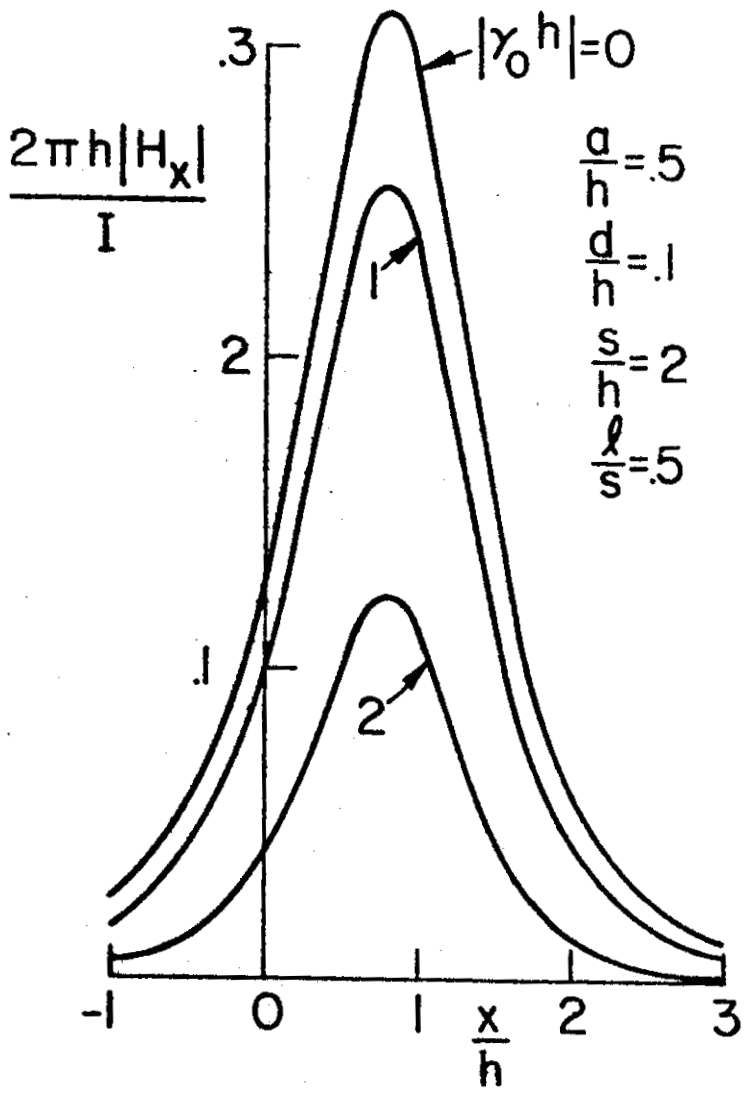

Figure 13. Effect of γ_0 on the horizontal magnetic field for the truncated cylinder case.

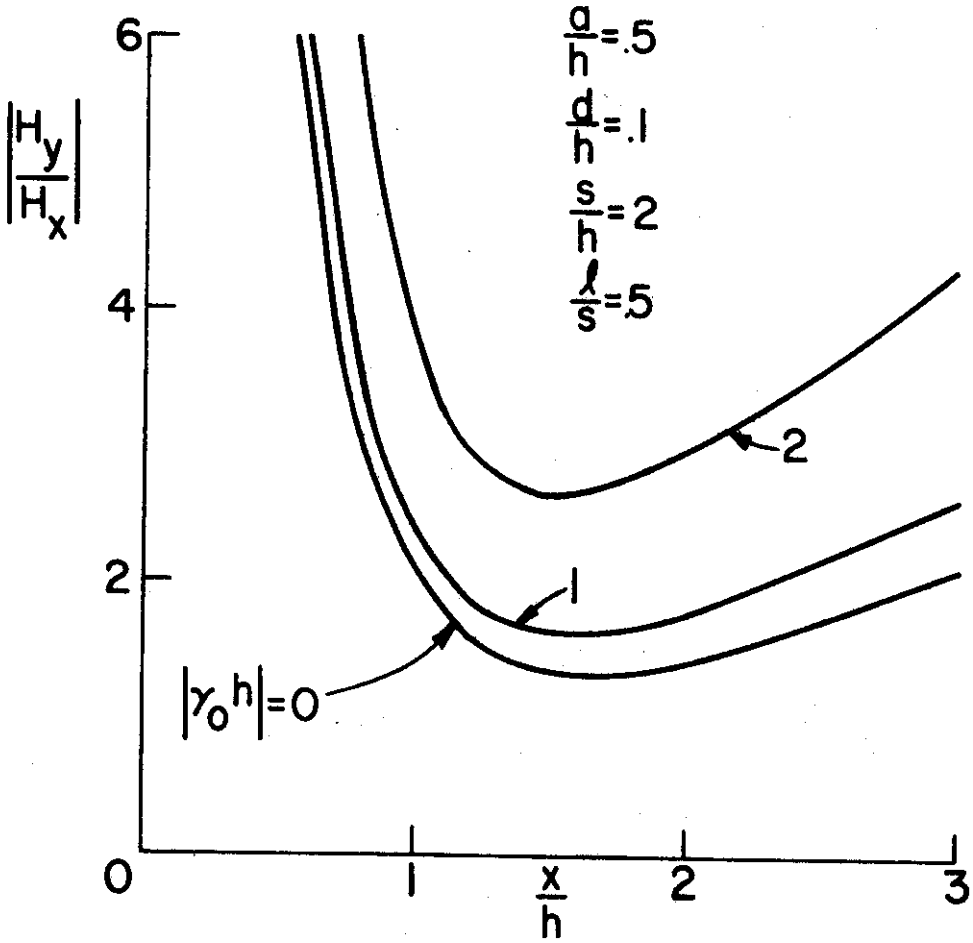

Figure 14. Effect of γ_0 on the magnitude of the ratio of vertical to horizontal magnetic field (truncated cylinder case).

BIBLIOGRAPHY

SINGH, S. K., 1973. On axially symmetric electric current induced in a cylinder under a line source, *Geophysics*, 38:971-974.

WAIT, J. R., 1952. A cylindrical ore body in the presence of a cable carrying an oscillating current, *Geophysics*, 17(2): 378-386.

WAIT, J. R., 1959. *Electromagnetic Radiation from Cylindrical Structures*, Pergamon Press, Oxford, England.

WAIT, J. R. and D. A. HILL, 1973. Excitation of a homogeneous conductive cylinder of finite length by a prescribed axial current distribution, *Radio Science*, 7 October 1973 (in press).

WHEELON, A. D., 1968. *Tables of Summable Series and Integrals Involving Bessel Functions*, Holden-Day, San Francisco, p. 9.

ADDITIONAL BIBLIOGRAPHY

NEGI, J. G., C. P. GUPTA, and U. RAVAL, 1972. Induction anomaly due to an elongated covered ore-zone excited by a long current carrying cable, *Geophys., Prosp., 20:* 193-211.

NEGI, J. G. and U. RAVAL, 1969. Negative electromagnetic screening by a cylindrical conducting cover, *Geophys., 36*(6): 944-957.

SINGH, S. K., 1972. Transient electromagnetic response of a conducting infinite cylinder embedded in a conducting medium, *Geofis. Int. 12*(1): 7-21.

WAIT, J. R., 1973. On electromagnetic induction in elongated ore bodies, *Geophys.* (Letter to the Editor) 38: 984-985.

WAIT, J. R. and R. E. WILKERSON, 1972. The sub-surface fields produced by a line-current source on a non-flat earth (cylindrical model), *Pure and Appl. Geophys. 95*(III): 150-156.

WARD, S. H. and H. F. MORRISON (Eds.) 1972. Special issue on Electromagnetic Scattering, *Geophys., 36*(I): 1-183.

Radio Science, Volume 9, Number 1, pages 71–73, January 1974

Perturbation of magnetic dipole fields by a perfectly conducting prolate spheroid

David A. Hill and James R. Wait

Institute for Telecommunication Sciences, Office of Telecommunications, US Department of Commerce, Boulder, Colorado 80302

(Received September 6, 1973.)

The effect of a perfectly conducting prolate spheroid on the surface fields of a buried vertical magnetic dipole is examined in the quasi-static case. When the spheroid is in the vicinity of the source and near the surface, the errors introduced in source location can be significant. The results have possible application to rescue operations following coal mine disasters and in similar situations.

INTRODUCTION

The feasibility of locating a buried vertical magnetic dipole source (horizontal loop) from surface measurements of the vertical and horizontal magnetic field components has been investigated by *Wait* [1971]. For sufficiently low frequencies the air-earth interface has a negligible effect and a single observation of the complex ratio of the vertical and horizontal field components is sufficient for source location. Inhomogeneities in the earth distort the surface fields and may lead to errors in source location. To provide insight into this problem, the effect of a spherical inhomogeneity has been investigated [*Hill and Wait*, 1973].

Here we examine the effect of a perfectly conducting prolate spheroid for the case where the frequency is sufficiently low that currents in the surrounding medium can be neglected. Consequently, the situation reduces to a magnetostatic problem, and an exact solution is available [*Wait*, 1960]. The prolate spheroid is considered to be a reasonable model to study the influence of a finite or bounded conductor such as a metal pipe, railway conductor, or even an ore vein. At least it is not so idealized as a sphere.

FORMULATION

The geometry of the spheroid and source dipole is shown in Figure 1. The prolate spheroid is centered at the origin of a Cartesian coordinate system (x, y, z), and its major axis is coincident with the z axis. The semiminor axis a, semimajor axis b, and semifocal distance c are related by

$$c = (b^2 - a^2)^{1/2} \tag{1}$$

The prolate spheroidal coordinates are (η, δ, ϕ) and the surface of the spheroid is defined by $\eta = \eta_0$ where

$$\eta_0 = [1 - (a/b)^2]^{-1/2} \tag{2}$$

The boundary condition on the spheroid is that the normal component of the magnetic field must vanish. The resultant solution for the magnetic potential Ω of a magnetic point charge K located at (η', δ', ϕ') is [*Wait*, 1960]:

$$\Omega = (K/4\pi)\left[1/R - \sum_{n=0}^{\infty}\sum_{m=0}^{n} M_{mn} \cdot [P_n^m{}'(\eta_0)/Q_n^m{}'(\eta_0)]Q_n^m(\eta)P_n^m(\delta)\cos m(\phi - \phi')\right] \tag{3}$$

where

$$M_{mn} = [\epsilon_m(-1)^m/c](2n + 1) \cdot [(n - m)!/(n + m)!]^2 Q_n^m(\eta')P_n^m(\delta')$$

$$\epsilon_m = \begin{cases} 1, & m = 0 \\ 2, & m \neq 0 \end{cases}$$

$$R = [(x - x')^2 + (y - y')^2 + (z - z')^2]^{1/2}$$

P_n^m and Q_n^m are associated Legendre functions of degree n and order m of the first and second kind, and prime denotes differentiation with respect to the argument. The definitions of P_n^m and Q_n^m follow those of *Smythe* [1968].

The magnetic field $\mathbf{H}$ of a y-directed magnetic dipole of strength Kdl is given by

$$\mathbf{H} = -dl\nabla(\partial/\partial y')\Omega \tag{4}$$

In order to simplify the results, we restrict both the source and the observer to the equatorial plane ($z = z' = 0$) as shown in Figure 1. Consequently, $H_z = 0$ and H_y is given by [*Wait*, 1960]

$$H_y = (Kdl/4\pi)\Big\{[3(y - y')^2/R^5 - 1/R^3] + (1/c)\sum_{n=0}^{\infty}\sum_{m=0}^{n}\epsilon_m(-1)^m \tag{5}$$
$$(2n+1)[(n-m)!/(n+m)!]^2[P_n^{m\prime}(\eta_0)/Q_n^{m\prime}(\eta_0)] \cdot [P_n^m(0)]^2 V_n^m\Big\}$$

where

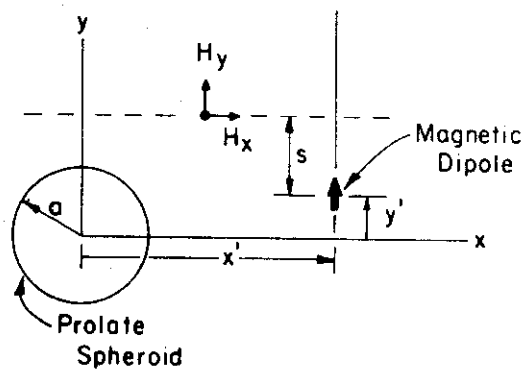

Fig. 1. Geometry for source and observer in the equatorial plane of a prolate spheroid ($z = 0$). The imagined earth-air interface is the plane $y = y' + s$.

$$V_n^m = Q_n^{m\prime}(\eta)Q_n^{m\prime}(\eta')\cos m(\phi - \phi')\{[(\sin\phi)/c](\eta^2 - 1)^{1/2}/\eta\}\{[(\sin\phi')/c][(\eta')^2 - 1]^{1/2}/\eta'\}$$
$$+ Q_n^m(\eta)Q_n^m(\eta')m^2\cos m(\phi - \phi)\{[(\cos\phi)/c](\eta^2 - 1)^{-1/2}\}\{[(\cos\phi')/c][(\eta')^2 - 1]^{-1/2}\}$$
$$- Q_n^m(\eta)Q_n^{m\prime}(\eta')m\sin m(\phi - \phi')\{[(\cos\phi)/c](\eta^2 - 1)^{-1/2}\}\{[(\sin\phi')/c][(\eta')^2 - 1]^{1/2}/\eta'\}$$
$$+ Q_n^{m\prime}(\eta)Q_n^m(\eta')m\sin m(\phi - \phi')\{[(\sin\phi)/c](\eta^2 - 1)^{-1/2}\}\{[(\cos\phi')/c][(\eta')^2 - 1]^{-1/2}\}$$

The following similar expression for H_x can be derived by applying (4) to (3):

$$H_x = (Kdl/4\pi)\Big\{-3(x - x')(y - y')R^{-5} + (1/c)\sum_{n=0}^{\infty}\sum_{m=0}^{n}\epsilon_m(-1)^m$$
$$(2n+1)[(n-m)!/(n+m)!]^2[P_n^{m\prime}(\eta_0)/Q_n^{m\prime}(\eta_0)] \cdot [P_n^m(0)]^2 W_n^m\Big\} \tag{6}$$

where

$$W_n^m = Q_n^{m\prime}(\eta)Q_n^{m\prime}(\eta')\cos m(\phi - \phi')\{[(\cos\phi)/c](\eta^2 - 1)^{1/2}/\eta\}\{[(\sin\phi')/c][(\eta')^2 - 1]^{1/2}/\eta'\}$$
$$- Q_n^m(\eta)Q_n^m(\eta')m^2\cos m(\phi - \phi')\{[(\sin\phi)/c](\eta^2 - 1)^{-1/2}\}\{[(\cos\phi')/c][(\eta')^2 - 1]^{-1/2}\}$$
$$+ Q_n^m(\eta)Q_n^{m\prime}(\eta')m\sin m(\phi - \phi')\{[(\sin\phi)/c](\eta^2 - 1)^{-1/2}\}\{[(\sin\phi')/c][(\eta')^2 - 1]^{1/2}/\eta'\}$$
$$+ Q_n^{m\prime}(\eta)Q_n^m(\eta')m\sin m(\phi - \phi')\{[(\cos\phi)/c](\eta^2 - 1)^{1/2}/\eta\}\{[(\cos\phi')/c][(\eta')^2 - 1]^{1/2}\}$$

The prolate spheroidal coordinates required in (5) and (6) are related to the Cartesian coordinates by:

$$\phi = \tan^{-1}(y/x),\ \eta = (1/c)(x^2 + y^2 + c^2)^{1/2} \tag{7}$$
$$\phi' = \tan^{-1}(y'/x'),\ \eta' = (1/c)[(x')^2 + (y')^2 + c^2]^{1/2}$$

NUMERICAL RESULTS

For the interesting case when both the source and observer are reasonably close to the observer, a large number of terms are required to achieve convergence of the summations in (5) and (6). Consequently, a computer subroutine was written for P_n^m which utilizes forward recurrence in n and m, and a subroutine was written for Q_n^m which utilizes backward recurrence in n and forward recurrence in m. The derivatives $P_n^{m\prime}$ and $Q_n^{m\prime}$ are easily obtained in terms of P_n^m and Q_n^m. Computed values for P_n^m, Q_n^m, $P_n^{m\prime}$, and $Q_n^{m\prime}$ checked exactly with tabulated six-figure values [*National Bureau of Standards*, 1945]. A computer program for H_x and H_y in (5) and (6) was then written and checked by requiring that the boundary condition was satisfied at the surface of the spheroid ($\eta = \eta_0$).

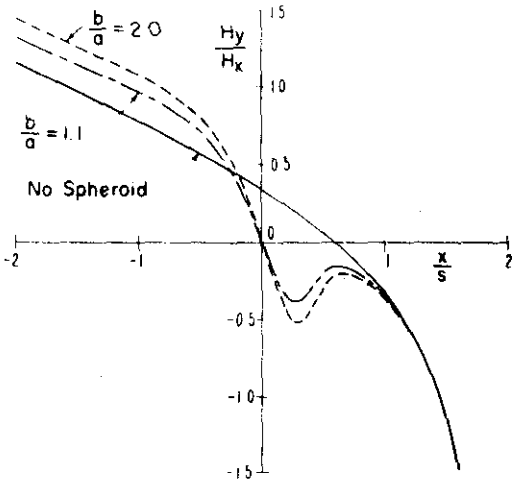

Fig. 2. Ratio of vertical to horizontal magnetic field component for a prolate spheroid which is tangent to the interface; $x'/s = 2$, $y'/s = -0.5$, and $a/s = 0.5$.

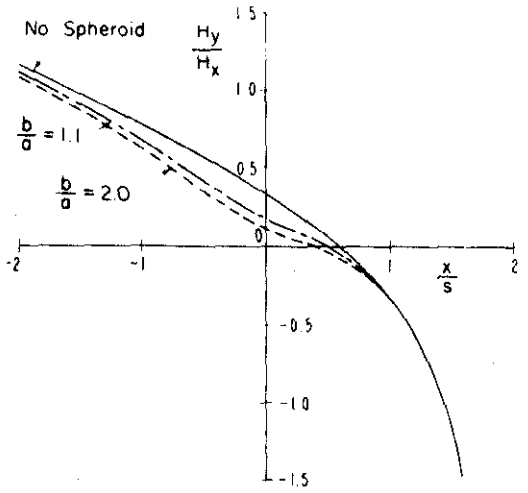

Fig. 3. Ratio of vertical to horizontal magnetic field component for a buried prolate spheroid; $x'/s = 2$, $y' = 0$, $a/s = 0.5$.

If we imagine that the earth-air interface is located at $y = s + y'$ as shown in Figure 1, then H_y and H_x are the vertical and horizontal magnetic field components that would be measured in a source location scheme. Since the ratio of vertical to horizontal components has been suggested as a useful quantity [*Wait*, 1971], the ratio H_y/H_x is shown as a function of x in Figure 2 for $a/s = 2$, $y'/s = -0.5$, and $x'/s = 2$. Since the spheroid is tangent to the interface at $x = 0$, the vertical component H_y is zero at $x = 0$. Note that a slightly larger anomaly occurs for the longer spheroid ($b/a = 2$). Results for the same case with the spheroid buried ($y' = 0$) are shown in Figure 3. The anomaly in H_y/H_x is somewhat weaker, but it occurs over a larger horizontal range.

CONCLUDING REMARKS

The exact quasi-static solution for a magnetic dipole in the presence of a perfectly conducting prolate spheroid has been used to calculate the perturbation of magnetic field components. Results in Figures 2 and 3 indicate that significant errors in source location could result when the spheroid is in the vicinity of the source and close to the interface.

REFERENCES

Hill, D. A., and J. R. Wait (1973), The electromagnetic response of a buried sphere for buried dipole excitation, *Radio Sci.*, *8*(8), in press.

National Bureau of Standards (1945), *Tables of Associated Legendre Functions*, 300 pp., Columbia University Press, New York.

Smythe, W. R. (1968), *Static and Dynamic Electricity*, 3rd ed., pp. 144–152, McGraw-Hill, New York.

Wait, J. R. (1960), Some solutions for electromagnetic problems involving spheroidal, spherical, and cylindrical bodies, *J. Res. Nat. Bur. Stand.*, *64B*(1), 15–32. (In this reference, in equation 12 and the following equations $-\partial/\partial y'$ should be $+\partial/\partial y'$ for a dipole in the positive y direction.)

Wait, J. R. (1971), Criteria for locating an oscillating magnetic dipole in the earth, *Proc. IEEE*, *59*(16), 1033–1035.

Rivista Italiana di Geofisica, Vol. XXII, N. 5/6,
pp. 421-424 (1973)

Perturbation of Magnetic Dipole Field by a Finitely Conducting Circular Cylinder

by David A. Hill & James R. Wait (*)

Introduction.

Location of a buried vertical magnetic dipole source (horizontal loop) from surface measurements of the vertical and horizontal magnetic field components has been investigated by Wait [1]. The air-earth interface has a negligible effect at sufficiently low frequencies, and the source locations can be determined from a single observation of the complex ratio of vertical and horizontal magnetic field components. However, inhomogeneities in the earth distort the surface fields and cause errors in source location. Effects of spherical [Hill & Wait [2]] and prolate spheroidal [Hill & Wait [3]] inhomogeneities have been investigated.

Here we examine the effect of a finitely conducting circular cylinder for the case where the frequency is sufficiently low that currents in the surrounding medium can be neglected. The circular cylinder should be a reasonable model for long conductors such as metal pipes, metal tracks, or even ore veins. Also, the comparison with the prolate spheroid is of interest in determining the effect of finite length of the scatterer. Also, of course, this comparison serves as an excellent check on the numerical calculations since the two representations are basically different.

Formulation.

The geometry of the cylinder and source dipole are shown in Fig. 1. The axis of the cylinder coincides with the z axis of a Cartesian coordinate system (x, y, z). The cylinder has conductivity σ and permeability μ while the external region has permeability μ_0. All displacement currents are neglected.

The fields inside the cylinder are a solution of the wave equation, and the exterior fields are a solution of Laplace's equation. The boundary conditions are that the normal flux and the tangential fields are continuous at the cylinder boundary. The resultant solution for the magnetic potential Ω of a magnetic point charge K located at (x', y', z') for both source and observer outside the cylinder is [Wait [4]]:

$$\Omega = \frac{K}{4\pi}\left\{\frac{1}{R} + \frac{1}{\pi}\sum_{m=-\infty}^{\infty}\int_{-\infty}^{\infty} A_m(h)\, K_m(|h|\rho')\, K_m(|h|\rho)\exp[-ih(z-z')]\, dh \exp[-im(\phi-\phi')]\right\},$$

where

$$R = [(x-x')^2 + (y-y')^2 + (z-z')^2]^{1/2},$$

$$(1)\qquad A_m(h) = -\frac{\left\{\tilde{I}_m(|h|a) - (\mu/\mu_0)\left[\tilde{I}_m(\alpha a) + \frac{m^2\gamma^2}{\alpha^4 h^2 a^4}\,\frac{1}{\tilde{I}_m(\alpha a)}\right]\right\}}{\left\{\tilde{K}_m(|h|a) - (\mu/\mu_0)\left[\tilde{I}_m(\alpha a) + \frac{m^2\gamma^2}{\alpha^4 h^2 a^4}\,\frac{1}{\tilde{I}_m(\alpha a)}\right]\right\}}\,\frac{I_m(|h|a)}{K_m(|h|a)}$$

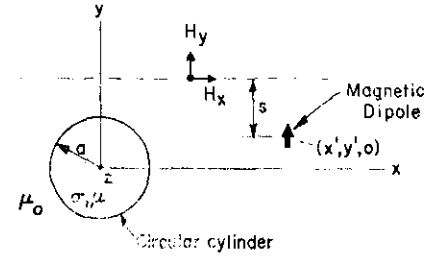

Fig. 1 - *Geometry for source and observer in the plane z = o. The imagined earth-air interface is the plane y = y' = s.*

and

$$\alpha = (\gamma^2 + h^2)^{1/2}, \qquad \gamma = (i\omega\mu\sigma)^{1/2},$$

$$\tilde{I}_m(\alpha) = \frac{I'_m(\alpha)}{\alpha I_m(\alpha)}, \qquad \tilde{K}_m(\alpha) = \frac{I'_m(\alpha)}{\alpha K_m(\alpha)}.$$

Here ρ and ϕ are standard cylindrical coordinates, and I_m and K_m are modified Bessel functions of order m. A time dependence $\exp(i\omega t)$ is assumed. Note that for a perfectly conducting cylinder ($|\gamma|a \to \infty$),

(*) Institute for Telecommunication Sciences, Office of Telecommunications, U. S. Department of Commerce, *Boulder*, Colorado 80302, USA.

$A_m(h)$ reduces to

$$A_m(h)\Big|_{\gamma a \to \infty} = -\frac{I'_m(|h|a)}{K'_m(|h|a)}. \tag{2}$$

The magnetic field $\vec{H}$ of a y- directed magnetic dipole of strength Kdl for $\rho > a$, is given by

$$\vec{H} = -dl\,\nabla\frac{\partial}{\partial y'}\Omega\,. \tag{3}$$

In order to simplify the results, we restrict both the source and observer to the equatorial plane ($z = z' = 0$). Consequently, $H_z = 0$ and H_y is given by [WAIT (4)]:

$$H_y = \frac{K\,dl}{4\pi}\left\{\left[\frac{3(y-y')^2}{R^5} - \frac{1}{R^3}\right] - \frac{1}{\pi}\sum_{m=-\infty}^{\infty}\int_{-\infty}^{\infty} A_m(h)\left[|h|K'_m(|h|\rho)\sin\phi - \frac{im}{\rho}K_m(|h|\rho)\cos\phi\right]\times\right.$$
$$\left.\times\left[|h|K'_m(|h|\rho')\sin\phi' + \frac{im}{\rho'}K_m(|h|\rho')\cos\phi'\right]dh\exp[-im(\phi-\phi')]\right\}. \tag{4}$$

The following similar expression can be derived by applying (3) to (1):

$$H_x = \frac{K\,dl}{4\pi}\left\{\frac{3(y-y')(x-x')}{R^5} - \frac{1}{\pi}\sum_{m=-\infty}^{\infty}\int_{-\infty}^{\infty} A_m(h)\left[|h|K'_m(|h|\rho)\cos\phi + \frac{im}{\rho}K_m(|h|\rho)\sin\phi\right]\times\right.$$
$$\left.\times\left[|h|K'_m(|h|\rho')\sin\phi' + \frac{im}{\rho'}K_m(|h|\rho')\cos\phi'\right]dh\exp[-im(\phi-\phi')]\right\}. \tag{5}$$

Numerical results.

For the interesting case where both the source and observer are close to the cylinder, a large number of terms are required in the m summations in (4) and (5); also the h integration must be performed numerically. Consequently, the computer time can become excessive. Fortunately, the m summation can be converted to run over positive values only by using the following relationships:

$$I_{-m}(\alpha) = I_m(\alpha),\quad K_{-m}(\alpha) = K_m(\alpha),\quad A_{-m}(h) = A_m(h)\,. \tag{6}$$

Also, the h integral can be taken over just positive values of h since the integrands are even in h. A further saving is made possible by interchanging the order of summation and integration since the modified Bessel functions required in the summation are quickly generated by recurrence (forward for K_m and backward for I_m). The remaining h integral is well behaved. The integrand approaches a constant as h approaches zero and decays exponentially as h becomes large as long as the source and observer are not both on the cylinder.

A computer program was written to evaluate H_y and H_x in (4) and (5) with the time-saving features described above. The case of a perfectly conducting cylinder was checked by requiring that the normal magnetic field was zero at the cylinder boundary ($\rho = a$). A partial check was obtained for finite γa by checking $A_m(h)$ with previous values [WAIT (4)].

If we imagine that the earth-air interface is located at $y = s + y'$ as shown in Figure 1, then H_y and H_x are the vertical and horizontal magnetic field components which would be measured in a source location scheme. Since the ratio of vertical and horizontal components has been suggested as a useful quantity [WAIT (1)], H_y/H_x is shown as a function of x in Figure 2 for $|\gamma|a = \infty$, $a/s = 2$, $y'/s = -0.5$, and $x'/s = 2$. Also shown are results for a prolate spheroid of axial ratio b/a with the major axis coincident with the z-axis [HILL & WAIT (3)]. Both the spheroids and the cylinder are tangent to the interface at $x = 0$,

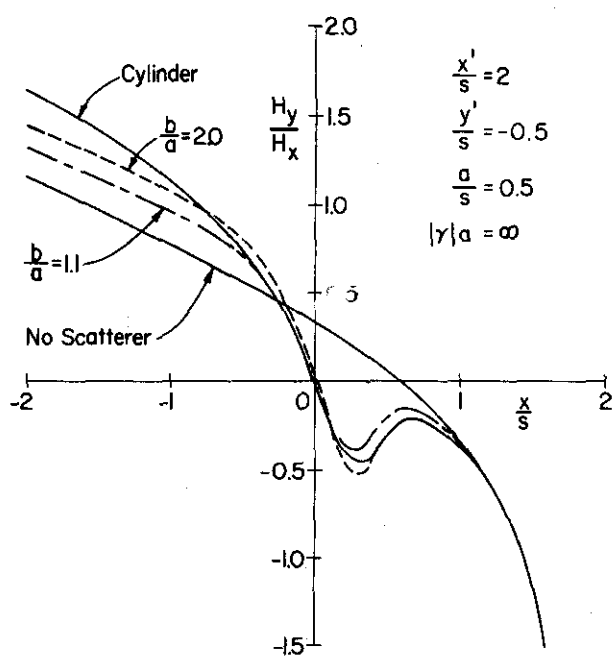

Fig. 2 – *Ratio of vertical to horizontal magnetic field for a scatterer (cylinder or prolate spheroid) which is tangent to the interface.*

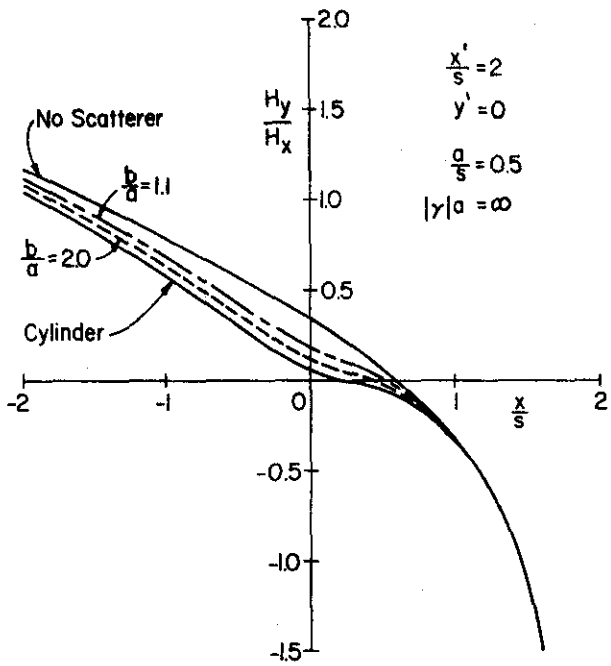

Fig. 3 – *Ratio of vertical to horizontal magnetic field for a buried scatterer (cylinder or prolate spheroid).*

and the vertical component is zero. Results for the same case with the scatterer buried ($y' = 0$) are shown in Figure 3, and the anomaly in H_y/H_x is somewhat weaker.

The effect of finite $|\gamma|a$ for $\mu = \mu_0$ is illustrated in Figure 4 for the same geometry as in Figure 2. Note that a cylinder with $|\gamma|a = 10$ looks nearly

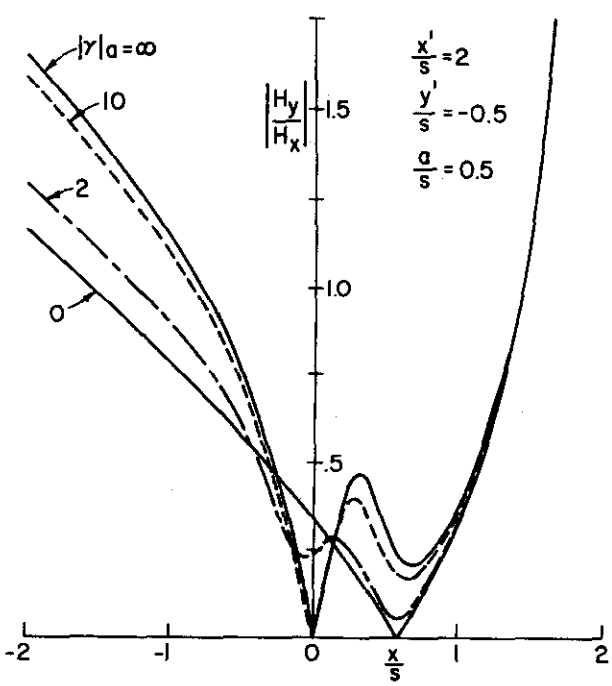

Fig. 4 – *Ratio of vertical to horizontal magnetic field for a finitely conducting cylinder which is parallel to the interface.*

perfectly conducting. The field components are real for $|\gamma|a = 0$ where no scattering occurs and for $|\gamma|a = \infty$ where the scattered field is in phase with the primary field. For general $|\gamma|a$, the scattered field is complex, and the nulls in the total field are partly filled in. This could make source location more difficult.

Concluding remarks.

The exact quasi-static solution for a magnetic dipole in the presence of a finitely conducting circular cylinder has been use to calculate the perturbation of magnetic field components. Results in Figures 2, 3, and 4 indicate that significant errors could result in source location when the spheroid is in the vicinity of the source and close to the interface.

Comparison of the anomalies caused by cylinders and prolate spheroids in Figures 2 and 3, indicates that the infinite cylinder is a fairly good model for finite length scatterers when the magnetic dipole source and the observer are in the equatorial plane. Such was not the case for a finite electric line source excitation [WAIT & HILL (5)].

The effect of conduction currents in the overburden (but not the interface effect) could be included by using the general dyadic Green's function [TAI (6)]. The effect of the interface is difficult to compute even for the two dimensional problem of line source excitation [WAIT (7); HOWARD (8)]. However, for thin cylinders, HOWARD (9) has indicated that the interface effect in the three dimensional problem might be best handled by an interaction technique in transform space with the resultant solution given by a double fast Fourier transform.

REFERENCES

(1) J. R. WAIT: *Criteria for locating an oscillating magnetic dipole in the earth*, Proc. IEEE, 59, (16), (1971), 1033-1035. — (2) D. A. HILL & J. R. WAIT: *The electromagnetic response of a buried sphere for buried dipole excitation*, Radio Science, 8, (8), (1973), 813-818. — (3) D. A. HILL & J. R. WAIT: *Perturbation of magnetic dipole fields by a perfectly conducting prolate spheroid*, Radio Science, 9, (1), (1974), 71-73. — (4) J. R. WAIT: *Some solutions for electromagnetic problems involving spheroidal, spherical and cylindrical bodies*, Jour. Res. Nat'l Bureau of Standards, 64B, No. 1, Jan/Mar (1960), 15-32 (Note that the arguments ha and $h\rho$ of the Bessel functions should be $|ha|$ and $|h\rho|$). — (5) J. R. WAIT & D. A. HILL: *Excitation of a homogeneous conductive cylinder of finite length by a prescribed axial current distribution*, Radio Science, 8, (12), (1973) 1169-1176. — (6) C. T. TAI: *Dyadic Green's functions in electromagnetic theory*, Intext Educational Publishers, Scranton, Ch. 7, (1971). — (7) J. R. WAIT: *The effect of a buried conductor on the sub-surface fields for line source excitation*, Radio Science, 7, (5), (1972), 587-591. — (8) A. Q. HOWARD, Jr.: *The electromagnetic fields of a subterranean cylindrical inhomogeneity excited by a line source*, Geophysics, 37, (6), (1972), 975-984. — (9) A. Q. HOWARD, Jr.: *Fields of a magnetic dipole excited buried cylinder*, presented at the Thru-

The-Earth Electromagnetics Workshop, Golden, Colorado, August 15 (1973).

Summary — The effect of a finitely conducting circular cylinder on the surface fields of a buried vertical magnetic dipole is examined in the quasi-static regime. Results are compared with previous results for the prolate spheroid. When the cylindrical conductor is near the surface in the vicinity of the source, significant errors can result in source location. The results have possible application to rescue operations following mine disasters.

Paper presented at Symposium on Electromagnetic Wave Theory, International Union of Radio Science, London, 9-12 July 1974.

Propagation Under the Earth's Surface (A Review)

by

James R. Wait
Cooperative Institute for Research in Environmental Sciences
University of Colorado
Boulder, Colorado 80302

In this paper we review theoretical model concepts in through-the-earth transmission of electromagnetic waves. While the subject is very broad in its defined scope, we will be conscious of the specific applications to mine rescue and emergency telecommunications in coal mine environments. Without pretending to be entirely impartial we include a critique of the limitations of the available analytical models.

The central problem is to calculate the steady state mutual impedance of a four-terminal network that is the black box characterizing the through-the-earth path. Problems of secondary importance include the determination of the input impedances of the two pairs of terminals and the associated transient responses.

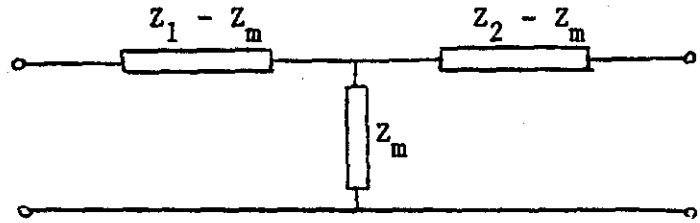

The simple equivalent circuit given tells us a lot about the problem that we are seeking a solution for. The mutual impedance Z_m describes the propagation phenomena involved in transmission from input (source) to the output (receiver). Z_1 and Z_2, on the other hand, are the input impedances. Clearly the latter are needed in a total systems study since we have only a finite amount of power available at the source and the receiver must be matched in some sense to the output terminals of the receiving antenna.

Most of the past literature deals with the calculation or merely the derivation of the mutual impedance Z_m for some highly idealized geometrical configuration. For example, the source for an ungrounded loop is a magnetic dipole that is assigned a fixed magnetic moment. In the most extreme case this magnetic dipole is an infinitesimally small loop (of area dA) with a total circulating current I amps. The moment is IdA! Now we can still use this concept for a multi-turn loop if I is the total azimuthal current and provided the uniform current assumption is valid. Also, of course, we recognize that the finite size of the loop needs to be accounted for in some cases.

In some of the earliest work the fields of this dipole were calculated as if the conduction currents in the earth were negligible. Of course, this is a useful beginning. The next refinement was to correct these magneto-static fields by assuming that we need only multiply them by $\exp(-s/\delta)$ where s was the transmission range and δ was the skin-depth in the earth for the operating frequency being adopted. With the benefit of hindsight we can criticize this correction as being grossly pessimistic for many cases of interest to mine rescue or to communication to a receiving station above or below the source loop.

By using the correct electrodynamic forms of the magnetic dipole fields in an homogeneous conductive medium of infinite extent, we can obtain a better estimate of the relevant value of Z_m. For example, if we are transmitting between two small coaxial loops, we can easily show that $Z_m = Z_o(1 + \Gamma s)\exp(-\Gamma s)$ where $\Gamma = (1 + i)\delta^{-1}$ and Z_o is the static or D.C. coupling limit.

Now usually the transmission takes place from the earth's surface to a buried receiving terminal. Or the converse situation may exist if we are dealing with up-link communication. In both cases the air-earth interface must be considered. Here we can immediately call attention to the classical formulation of Arnold Sommerfeld that dates back to 1909 in its earliest version. This was used as the basis of many analyses in later years but the interest was mainly for the case where the range exceeded a free-space wavelength. Here we are interested in the near zone where the significant distances are small compared with the wavelength in the air but such distances (i.e. depth or offset) may be comparable with the wavelength in the earth. This is "quasi-statics" in the vernacular of the current workers. To obtain field estimates we now have to perform some integrations. Fortunately it was found that identities in Bessel function theory, recognized by mathematicians of the late 19th Century, were ripe for the picking. Thus some closed form field expressions were obtained and published in the 1950's for a fairly broad class of such problems. Numerical results required the manipulation of modified Bessel functions whose arguments were complex. Fortunately for cases of interest, the phase angles were near $\pi/4$ radians so that the tabulated Thomson's functions could be used. These are sometimes called the Kelvin functions and denoted ber, bei, kei, etc.

With the ready availability of high speed computers, the use of intricate closed form field formulas is giving way to direct numerical integration of the Sommerfeld integrals. This is satisfactory provided the programmer has some limiting checks or if he can refer back to some of the earlier work where the more elegant closed-form expressions in terms of special functions are used. Also, as has been indicated recently for finite-length source elements, the special function representations for the dipole source is a convenient starting point. Otherwise double numerical integration is needed!

As mentioned above, the air-earth interface problem is treated by regarding the overburden as a homogeneous half-space. A rather straight-forward extension is the stratified half-space wherein the intermediate interfaces are plane and parallel to the air-earth interface. Further extensions involve electric dipoles rather than magnetic dipoles. These are appropriate when dealing with grounded electrodes connected by insulated cables. No new basic difficulties are encountered here.

In the class of problems discussed above, all three of the impedance elements Z_m, Z_1 and Z_2, are determinable. Thus, in principle, a complete determination or prediction of the system performance is possible. This includes down-link communication efficiency and estimates of source location accuracy for the models assumed.

Traditionally, the source current is assumed to vary harmonically in time. For dealing with transient excitation or in estimating signalling rate we need to understand the time-domain behavior of the system. Formally this is obtained by Fourier or Laplace transform inversion of the preceding transfer functions. In general, this is not a trivial task. However, some rather interesting closed-form results can be obtained if the original spatial wave number integration be deferred until after the Laplace transforms are inverted.

Now that the homogeneous and stratified half-space models have been exhausted, it is appropriate to consider more realistic situations. For example, the earth's surface is not always flat. One approach to allow for this situation, is to adapt cylindrical and spherical boundaries. In such cases, the local radius of curvature is chosen to match roughly the local topography. Results of calculations from such models indicated that transmission ranges were not markedly affected but that source location errors could be significant. An even simpler method conceptually was to retain the uniform half-space model but to allow the plane interference to be tilted at such an angle that the local slope of the terrain was matched. Further analytical work on such models is justified since much insight can be gained without excessive numerical effort. Unfortunately, formally exact solutions for such models are strictly limited. One class of boundary that could be treated for line source excitation is a parabolic or hyperbolic interface. The three dimensional version involving dipoles in the presence of a paraboliodal interface is extremely intricate but it may be worth doing.

One must clearly recognize that the overburden is not a homogeneous slab whether it be bounded by plane or uniformly curved interfaces. Thus, the influence of omnipresent inhomogeneities needs to be understood. An extreme case is when metallic cracks and pipes are in the vicinity of the normal transmission path. To treat such configurations, two dimensional models have been used. An example is the line source excited buried cylinder of infinite length. This is not a trivial problem if one considers the inter-actions between the buried cylindrical inhomogeneity and the air-earth interface. Two specific analytical techniques have been used to get numerical results for this problem. One is essentially a perturbation procedure that involves successive reflections between the cylinder and the plane interface, while the other is a sophisticated integral equation procedure. The results between those methods agree in a common region of validity. The extension to three dimensional versions of these problems is nontrivial. Some progress has been made, however, in using perturbation procedures. An example is the buried sphere in the presence of a surface based dipole source. Some work has also been done on cylinders of finite length where certain assumptions were made about the nature of the axial induced current flow at the ends of the cylinder. Among other things, this analysis showed that predictions based on infinite cylinders may be quite misleading.

Within the scope of these analytical techniques, we encompass both active and passive location concepts. In the active method, of course, the unknown source is energized by the to-be-rescued party. On the other hand, in the passive method, the target to be located is typically a loop of wire or a similar configuration. Various geometries, for such problems, have been considered in both the frequency and the time domain.

The foregoing account of theoretical analyses of electromagnetic induction problems is, by no means, claimed to be exhaustive. The selection has been based mainly on work that the author is familar with. Many of the source papers are to be found in *Radio Science*, the Journal of the U.S. National Committee of URSI.

Some recent offerings on this and related subjects from this writer and his colleagues are:

* *"Array technique for electromagnetic positional determination of a buried receiving point"*, J.R. Wait, Electronic Letters, Vol. 7, No. 8, 186-187, 22 April 1971.

* *"Criteria for locating an oscillating magnetic dipole buried in the earth"*, J.R. Wait, Proc. IEEE (Letters), Vol. 59, No. 6, 1033-1035, June 1971.

"Electromagnetic-pulse propagation in a simple dispersive medium", Electronic Letters, Vol. 7, No. 11, 285-286, 3 June 1971, J.R. Wait.

"Transient excitation of the earth by a line source of current", J.R. Wait, Proc. IEEE (Letters), Vol. 59, No. 8, 1287-1288, August 1971.

* *"Electromagnetic induction technique for locating a buried source"*, J.R. Wait, IEEE Trans. Geosci. Elect., Vol. GE-9, No. 2, 95-98, April 1971.

* *"Transient signals from a buried magnetic dipole"*, J.R. Wait and D.A. Hill, J. Appl. Phys., Vol. 42, No. 10, 3866-3869, September 1971.

"In situ measurements of the complex propagation constant in rocks for frequencies from 1 MHz to 10 Mhz", R.N. Grubb and J.R. Wait, Elect. Letters, Vol. 7, No. 17, 506-507, 26 August 1971.

* *"Subsurface electromagnetic fields of a line source on a conducting half-space"*, Radio Sci., Vol. 6, Nos. 8-9, 781-786, Aug.-Sept. 1971, J.R. Wait and K.P. Spies.

* *"Electromagnetic fields of a small loop buried in a stratified earth"*, J.R. Wait and K.P. Spies, IEEE Trans., Vol. AP-19, No. 5, 717-718, September 1971.

"On radio propagation through the earth", J.R. Wait and J.A. Fuller, IEEE Trans., Vol. AP-19, No. 6, 796-798, November 1971.

"Analytical investigations of electromagnetic wave propagation in the earth's crust", J.R. Wait, in The Structure and Physical Properties of the Earth's Crust, (ed. J.G. Heacock), pp. 315-324 (Geophys. Mono Series, Vol. 14, AGU, Washington, D.C., 1971.

* *"Influence of earth curvature on the subsurface electromagnetic fields of a line source"*, J.R. Wait, Elect. Letters, Vol. 7, No. 23, 697-699, 18 November 1971.

"Subsurface electromagnetic telecommunication - A review", R. Gabillard, P. Degauque, and J.R. Wait, IEEE Trans., Vol. COM-19, No. 6, 1217-1228, December 1971.

"Transient dipole radiation in a conducting medium", J.R. Wait, Revista Brasileira de Tecnologia, Vol. 3, No. 1, 29-37, March 1972.

* *"The effect of a buried conductor on the subsurface fields for line source excitation"*, J.R. Wait, Radio Science, Vol. 7, No. 5, 587-591, May 1972.

"On the theory of transient electromagnetic sounding over a stratified earth", J.R. Wait, Can. J. Phys., Vol. 50, No. 11, 1055-1061, 1 June 1972.

* *"The sub-surface magnetic fields produced by a line current source on a non-flat earth"*, J.R. Wait and R.E. Wilkerson, PAGEOPH, Vol. 95, No. III, 150-156, 1972.

"On calculating transient electromagnetic fields of a small current-carrying loop over a homogeneous earth", J.R. Wait and R.H. Ott, PAGEOPH, Vol. 95, No. III, 157-162, 1972.

"Absorption mode for ELF electromagnetic propagation in the earth-crust waveguide", J.R. Wait, Elect. Letters, Vol. 8, No. 11, 292-294, 1 June 1972.

* *"Transient magnetic fields produced by a step-function-excited loop buried in the earth"*, J.R. Wait and D.A. Hill, Electronic Letters, Vol. 8, No. 11, 294-295, 1 June 1972.

* *"Subsurface electromagnetic fields of a circular loop of current located above ground"*, J.R. Wait and K.P. Spies, IEEE Trans., Vol. AP-20, No. 4, 520-522, July 1972.

"Electromagnetic pulse transmission in homogeneous dispersive rock", J.A. Fuller and J.R. Wait, IEEE Trans., Vol. AP-20, No. 4, 530-533, July 1972.

"Attenuation of electromagnetic waves in the earth-crust waveguide from ELF to VLF", J.R. Wait and K.P. Spies, Radio Science (Letters), Vol. 7, No. 6, 689-690, June 1972.

"EM Coupling of coaxial and coplanar loops in uniform dissipative media", J.A. Fuller and J.R. Wait, Proc. IEEE (Letters), Vol. 60, No. 8, 993-994, August 1972.

* *"Locating an oscillating magnetic dipole in the earth"*, J.R. Wait, Electronic Letters, Vol. 8, No. 16, 404-406, 10 August 1972.

"Theory of electromagnetic reflection from a parallel grid of dielectric coated wires buried in the earth", J.R. Wait, Can. J. Phys., Vc . 50, No. 18, 2149-2157, September 1972.

* *"Electromagnetic surface fields produced by a pulse-excited loop buried in the earth"*, J.R. Wait and D.A. Hill, J. Appl. Phys., Vol. 43, No. 10, 3988-3991, October 1972.

"Electromagnetic wave propagation along a buried insulated wire", J.R. Wait, Can. J. Phys., Vol. 50, No. 20, 2402-2409, 15 October 1972.

Argand representations of the mutual electromagnetic coupling of loops on a two-layer earth", J.R. Wait and J.A. Fuller, Geoexplor., Vol. 10, 221-227, 1972.

* *"Transient electromagnetic fields of a finite circular loop in the presence of a conducting half-space"*, J.R. Wait and D.A. Hill, J. Appl. Phys., Vol. 43, No. 11, 4532-4534, November 1972.

"Electromagnetic transient response of a small wire loop buried in a conducting earth, D.A. Hill and J.R. Wait, Pure and Appl. Geophys., 105(IV), 869-878, 1973.

"Dipole excitation of ultralow-frequency electromagnetic waves in the earth crust wave guide", J.R. Wait and K.P. Spies, JGR, Vol. 77, No. 35, 7118-7120, 10 Dec. 1972.

"High frequency electromagnetic coupling between small coplanar loops over an inhomogeneous ground", J.A. Fuller and J.R. Wait, Geophys., Vol. 37, No. 6, 997-1004, December 1972.

"Electromagnetic propagation in an idealized earth crust waveguide, Part II", J.R. Wait and K.P. Spies, PAGEOPH, Vol. 101, No. IX, 188-193, 1972.

"Resistance of earth electrodes", J.R. Wait, Elect. Letters, Vol. 9, No. 4, 90-91, 22 February 1973.

"Mutual electromagnetic coupling of coaxial loops in a borehole", J.A. Fuller and J.R. Wait, Radio Science, Vol. 8, No. 5, 453-457, May 1973.

"Transmission line theory for an insulated linear antenna in a fluid-or-air-filled borehole", J.R. Wait and J.A. Fuller, Appl. Phys., Vol. 1, 311-316, June 1973.

* *"Subsurface electromagnetic fields of a grounded cable of finite length"*, Can. Journ. of Phys., Vol. 51, No. 14, 1534-1540, 1973, D.A. Hill and J.R. Wait.

* *"Low-frequency impedance of a circular loop over a conducting ground"*, J.R. Wait and K.P. Spies, Electronics Letters, Vol. 9, No. 15, 346-348, 26th July 1973.

* *"Electromagnetic transient response of a small wire loop buried in a homogeneous conducting earth"*, D.A. Hill and J.R. Wait, PAGEOPH, Vol. 105, 869-878, 1973/IV.

* *"The electromagnetic response of a buried sphere for buried-dipole excitation"*, D.A. Hill and J.R. Wait, Radio Science, Vol. 8, Nos. 8-9, 813-818, August-Sept. 1973.

* *"Subsurface electromagnetic fields of a line source on a two-layer earth"*, J.R. Wait and K.P. Spies, Radio Science, Vol. 8, Nos. 8-9, 805-810, August-Sept. 1973.

"Range dependence of the surface impedance for a line-source excited two-layer earth", J.R. Wait and K.P. Spies, IEEE Trans., AP-21, No. 6, Nov. 1973.

* *"Excitation of a homogeneous cylinder of finite length by a prescribed axial current distribution"*, J.R. Wait and D.A. Hill, Radio Science, Vol. 8, No. 12, December 1973.

* *"Sub-surface electric fields of a grounded cable of finite length for both frequency and time domain"*, D.A. Hill and J.R. Wait, Pure and Applied Geophysics, (in press).

* *"Electromagnetic response of a conducting cylinder of finite length"*, D.A. Hill and J.R. Wait, Geofisica Internacional (Mexico) (in press).

"ELF propagation along a horizontal wire located above or buried in the earth", D.C. Chang and J.R. Wait, IEEE Trans., CS (in press).

* *Perturbation of magnetic dipole field by a finitely conducting circular cylinder*, D.A. Hill and J.R. Wait, Rivista Italian. di Geofisica, Vol. 22, No. 5/6, 391-394, 1973.

Those marked with an asterik are included in this reprint collection.

LISTING OF PRELIMINARY REPORTS TO
U.S. BUREAU OF MINES ON CONTRACT NO. H0122061
THAT RELATE TO EM LOCATION AND DOWN-AND UP-LINK COMMUNICATION

Electromagnetic transient response of a small wire loop buried in a homogeneous conducting earth, D.A. Hill and J.R. Wait, 1 July 1972.

Locating an oscillating magnetic dipole in the earth, J.R. Wait, 10 August 1972.

Electromagnetic surface fields produced by a pulse-excited loop buried in the earth, J.R. Wait and D.A. Hill, October 1972.

Transient magnetic fields produced by a step-function excited loop buried in the earth, J.R. Wait and D.A. Hill, October 1972.

The electromagnetic response of a buried sphere for buried dipole excitation, David A. Hill and James R. Wait, 15 January 1973.

Subsurface electromagnetic fields of a grounded cable of finite length, David A. Hill and James R. Wait, 7 February 1973.

Sub-surface electromagnetic fields of a line source on a two-layer earth, J.R. Wait and K.P. Spies, (including Special Report of same title with Numerical Tables), 22 February 1973.

Subsurface electric fields of a grounded cable of finite length for both frequency and time domain, David A. Hill and James R. Wait, 15 March 1973.

Note on the surface impedance and wave tilt for a line source excited two-layer earth, James R. Wait, 6 April 1973.

Electromagnetic surface fields of an inclined buried cable of finite length, David A. Hill, 20 April 1973.

Diffusion of electromagnetic pulses into the earth from a line source, D.A. Hill and J.R. Wait, 11 May 1973.

Low frequency impedance of a circular loop over a conducting ground, James R. Wait and Kenneth P. Spies, 18 June 1973.

Supplementary tables relating to low frequency impedance of a circular loop over a conducting ground, James R. Wait and Kenneth P. Spies, 7 July 1973.

Excitation of a homogeneous conductive cylinder of finite length by a prescribed axial current distribution, James R. Wait and David A. Hill, 10 July 1973.

State of knowledge of analytical techniques for thru-the-earth electromagnetic wave problems relevant to mine rescue, James R. Wait, 16 July 1973.

Electromagnetic response of a conducting cylinder of finite length, David A. Hill and James R. Wait, 1 August 1973.

Perturbation of magnetic dipole fields by a perfectly conducting prolate spheroid, David A. Hill and James R. Wait, 22 August 1973.

Calculations of sub-surface grounded cable and loop sources for comparison with forthcoming experimental data, James R. Wait and David A. Hill, 19 September 1973.

Perturbation of magnetic dipole fields by a finitely conducting circular cylinder, David A. Hill and James R. Wait, 23 November 1973.

Effect of a spherical scatterer on EM source location, David A. Hill, 14 January 1974.

NOTE: Issuances prior to 1 July 1972 are not listed here.